



Evaluating and Miniziming Water Use by Greenhouse Evaporative Cooling Systems in a Semi-Arid Climate

Item Type	text; Electronic Dissertation
Authors	Sabeh, Nadia Christina
Publisher	The University of Arizona.
Rights	Copyright © is held by the author. Digital access to this material is made possible by the University Libraries, University of Arizona. Further transmission, reproduction or presentation (such as public display or performance) of protected items is prohibited except with permission of the author.
Download date	04/01/2021 19:01:01
Link to Item	http://hdl.handle.net/10150/194527

EVALUATING AND MINIMIZING WATER USE BY GREENHOUSE
EVAPORATIVE COOLING SYSTEMS IN A SEMI-ARID CLIMATE

by

Nadia Christina Sabeh

Copyright © Nadia Christina Sabeh 2007

A Dissertation Submitted to the Faculty of the
DEPARTMENT OF AGRICULTURAL AND BIOSYSTEMS ENGINEERING

In Partial Fulfillment of the Requirements
For the Degree of

DOCTOR OF PHILOSOPHY

In the Graduate College

THE UNIVERSITY OF ARIZONA

2007

THE UNIVERSITY OF ARIZONA
GRADUATE COLLEGE

As members of the Dissertation Committee, we certify that we have read the dissertation prepared by Nadia Christina Sabeh entitled Evaluating and Minimizing Water Use by Greenhouse Evaporative Cooling Systems in a Semi-Arid Climate and recommend that it be accepted as fulfilling the dissertation requirement for the Degree of Doctor of Philosophy

Gene Giacomelli, Professor, ABE

Date: 5/24/07

Chieri Kubota, Associate Professor, ABE

Date: 5/24/07

Christopher Choi, Professor, ABE/PLS

Date: 5/24/07

Kurtis Thome, Associate Professor, OPTICS

Date: 5/24/07

Final approval and acceptance of this dissertation is contingent upon the candidate's submission of the final copies of the dissertation to the Graduate College.

I hereby certify that I have read this dissertation prepared under my direction and recommend that it be accepted as fulfilling the dissertation requirement.

Dissertation Director: Gene Giacomelli

Date: 5/24/07

STATEMENT BY AUTHOR

This dissertation has been submitted in partial fulfillment of requirements for an advanced degree at the University of Arizona and is deposited in the University Library to be made available to borrowers under rules of the Library.

Brief quotations from this dissertation are allowable without special permission, provided that accurate acknowledgement of source is made. Requests for permission for extended quotation from or reproduction of this manuscript in whole or in part may be granted by the copyright holder.

SIGNED: Nadia Christina Sabeh

ACKNOWLEDGEMENTS

Firstly, thank you to my advisor, Dr. Gene Giacomelli, for giving me the flexibility and resources to develop and pursue a project that I cared deeply about. Thank you for the opportunity to help shape the research foundation and directives (and landscaping) of the Controlled Environment Agriculture Center. And finally thank you for fostering my communication and people skills into a valuable network of persons and companies that will no doubt be key to my future success.

Thank you to Dr. Chieri Kubota, for recognizing and facilitating my passion to teach and become a strong independent researcher. Our discussions (and disagreements) on the value and validity of my data always challenged me to examine my work with a different perspective and with increased rigor.

Thank you to my other committee members, including Dr. Chris Choi for helping me increase my knowledge of heat and mass transfer and providing me the opportunity to learn Fluent's Computational Fluid Dynamics program, even if I wasn't able to use it for my dissertation. And thank you to my Remote Sensing committee members, Dr. Kurt Thome and Dr. Alfredo Huete. I truly enjoyed learning remote sensing applications and hope to use it more in future endeavors.

Thank you to all my fellow CEAC graduate students – Jennifer Nelkin, Armando Suarez, Paula Costa, Efren Fitz, Wan Lovichit, Hope Jones, Chris Pagliarulo, Myles Lewis, Jason Licamele – who inspired me, debated with me, and helped me become a better researcher. A special thank you to Jenn Nelkin, who not only encouraged me to come to the University of Arizona, but pretty much convinced me that this is where I belonged. I will forever be grateful for your persistence and your friendship. Together we're gonna change the world!

A very special thank you to Shingo Yokoi, for helping me set up all my sensors, challenging me with the intellectual discussions I craved, and for having a family who so graciously opened their home to me in Tokyo, Japan.

Thank you to Steve Kania for helping me set up my sensors and control systems. With your help I became self-sufficient with Campbell dataloggers and Argus Control System.

A very special thank you to the farm crew at the Campus Agriculture Center. Thank you especially to Todd Ruhl, who installed the new fog lines in my greenhouse and was instrumental in keeping my evaporative cooling systems functional. Thank you so much for being prompt with your repairs, keeping me updated on progress, and returning to CEAC after work hours to fix my fog system!

Thank you to ValCo and Gene Parsons for donating the evaporative cooling systems I used for my experiments, and providing more materials when I redesigned the high-

pressure-fog system. And also thank you to PolyTex and Robert Moore for providing CEAC the two greenhouses I used for my experiments. This project wouldn't have been possible without the two of you and your companies.

Thank you Kathryn Hahne, and other members of Cooperative Extension, for helping me put our Evaporative Cooling Workshop together. And thank you to Chuck George for highlighting my project on KOLD 13 News and publicizing my Workshop, which would achieve a 75-person attendance!

Thank you Mom and Dad for encouraging me to follow my bliss, telling me to not worry about the world (and worrying for me), and loving me in every step of my journey. And thank you for teaching me that by facing challenges with global perspective, human compassion, and a joy for life is the true path to saving the world. I love you!

I also want to thank my sister Janan Sabeh, whose independent spirit and human compassion inspire me every day to leave my comfort zone and pursue a path that makes this world a better place. I'm going to miss you next year.

Finally, but absolutely not lastly, thank you Marcia Lane Overton. You made sure I took time to play and enjoy life outside the constraints of research and writing my dissertation. Thank you for coloring my world with joy, laughter, love...and toys from Mrs. Tiggy-Winkles! I love you.

I'd also like to thank my cats, Monsieur Jacque Box and Shaniqua, for waking up with me early every morning, cuddling on my lap while I wrote my dissertation, and checking on me when I was still writing late at night.

Thank you to everyone else who inspired me, encouraged me, pushed me, and believed in my ability to pursue my interests and follow my dreams.

CEAC Paper # T-125933-01-07. Supported by CEAC, the Controlled Environment Agricultural Center, College of Agriculture and Life Sciences, The University of Arizona. Financial support also provided by the United State Department of Agriculture, National Needs Fellowship (3 years) and the United States Department of Interior, Bureau of Reclamation, Water Conservation Field Services Program – Phoenix Area Office (1 year).

DEDICATION

This work is dedicated to my parents, who taught me that following my dreams is not always easy, but in the end will be the most important decision I ever make for myself. I also dedicate this to my sister, who is courageously following her own dreams, as they take her across the world.

“When you follow your dream, all the Universe conspires to help you.”

- The King, *The Alchemist*

“Vision without action is just a dream.

Action without vision is just passing time.

Vision with action can change the world.”

- Joel Barker

TABLE OF CONTENTS

LIST OF FIGURES	16
LIST OF TABLES	24
ABSTRACT	28
1. INTRODUCTION.....	30
2. LITERATURE REVIEW	35
2.1 Energy and Water Balance on the Greenhouse	35
2.1.1 Energy Balance	35
2.1.2 Water Vapor Balance	36
2.2 Greenhouse Cooling.....	37
2.2.1 Ventilation.....	38
2.2.1.1 Mechanical Ventilation.....	38
2.2.1.2 Natural Ventilation	39
2.2.1.3 Ventilation Effects on Greenhouse Climate.....	39
2.2.2 Evaporative Cooling	40
2.2.2.1 Pad-and-Fan Cooling.....	40
2.2.2.2 High-Pressure-Fog Cooling	43
2.2.3 Shading	44
2.3 Water Use for Tomato Crop Production.....	44
2.3.1 Water Use for Field Tomato Crop Production.....	44
2.3.2 Water Use for Greenhouse Crop Production	45

TABLE OF CONTENTS - *Continued*

2.3.2.1 Irrigation Water Use.....	45
2.3.2.2 Evaporative Cooling Water Use.....	46
2.4 Plant Responses to Greenhouse Climate	47
2.4.1 Plant Responses	48
2.4.1.1 Environmental Effects on E_T	48
2.4.1.2 Environmental Effects on T_{Leaf}	49
2.4.2 Measuring Plant Responses	50
2.4.2.1 E_T Measurement Methods.....	50
2.4.2.2 T_{Leaf} Measurement Methods.....	51
2.5 Wind Tunnel Modeling with Particle Image Velocimetry (PIV) Measurements	52
2.6 State of the Art	53
3. OBJECTIVES	55
4. METHODS AND MATERIALS	57
4.1 Greenhouse used for Experiments	57
4.1.1 Evaporative Cooling Pad	58
4.1.2 High-Pressure-Fog System	59
4.1.2.1 Multiple Inlet Fog Nozzle Lines.....	59
4.1.2.2 Single Inlet Fog Nozzle Line.....	60
4.1.2.3 Central, Overhead Fog Nozzle Line	60
4.1.2.4 Side Wall Gutter Fog Nozzle Lines.....	61

TABLE OF CONTENTS - *Continued*

4.1.3 Ventilation System	61
4.1.4 Statistics	63
4.2 Experimental Procedures for Pad-and-Fan and High-Pressure-Fog Tests	64
4.2.1 Operation of the Evaporative Cooling Systems	64
4.2.1.1 Operation of the Pad-and-Fan System – Initial 30-minute tests	64
4.2.1.2 Operation of the Pad-and-Fan System – Final 9-Hour Experiments	65
4.2.1.3 Operation of the High-Pressure-Fog System for Initial Studies on Fog Nozzle Locations	65
4.2.1.4 Operation of the High-Pressure-Fog System – Final 9-Hour Experiments	66
4.2.2 Tomato Plants and Irrigation	66
4.2.3 Measurements and Calculations	67
4.2.3.1 Environmental Conditions	67
4.2.3.2 Cooling Efficiency of the Pad	69
4.2.3.3 Water Use by the Pad-and-Fan System	69
4.2.3.4 Water Use by the High-Pressure-Fog System	71
4.2.3.5 Tomato Plant Water Use and Yield	72
4.2.3.6 Water Use Efficiency.....	73
4.2.3.7 Plant Transpiration.....	74
4.2.3.8 Leaf Temperature.....	74

TABLE OF CONTENTS - *Continued*

4.3 Experimental Procedures for <i>WUE</i> of Greenhouse Tomato Production	75
4.3.1 Tomato Plants and Irrigation	75
4.3.2 Operation of Pad-and-Fan Cooling System	75
4.3.3 Water Use Efficiency (<i>WUE</i>).....	78
4.3.4 Outside and Greenhouse Conditions.....	80
4.4 Energy Balance Equations Used to Estimate Evaporative Cooling Water Use and Inside Air Temperatures for a Greenhouse in Semi-Arid Conditions	80
4.4.1 Energy Balance Equations	80
4.4.2 Estimating Evaporative Cooling Water Use	82
4.4.3 Estimating Inside Air Temperature.....	83
4.5 Experimental Procedures for Testing the Effects of Buoyancy and Wind Direction on Airflow and Temperature Distribution in the Naturally-Ventilated Greenhouse Using a Wind Tunnel Model and Using the Full-Scale Greenhouse	85
4.5.1 Description of Wind Tunnel and Model Greenhouse	86
4.5.2 Temperature Distribution.....	87
4.5.3 Particle Image Velocimetry	88
4.5.4 Experimental Procedure.....	89
4.5.4.1 Archimedes Similarity Calculations	89
4.5.4.2 Simulated Conditions	91
4.5.4.3 Dimensionless Temperature and Air Velocity	93
4.5.5 Greenhouse Validation Experiments	93

TABLE OF CONTENTS - *Continued*

5. RESULTS	95
5.1 Initial Water Use Studies of the Pad-and-Fan Cooling System.....	95
5.1.1 Effect of Ventilation Rate on Water Use	95
5.1.2 Effect of Ventilation Rate on Greenhouse Conditions.....	96
5.1.3 Effect of Outside Climate Conditions on Water Use Rate.....	97
5.2 Effect of Pad-and-Fan Cooling on Greenhouse Water Use, Climate Conditions, Plant Transpiration and Leaf Temperatures for a Semi-Arid Climate	99
5.2.1 Outside Environmental Conditions.....	99
5.2.2 Cooling Efficiency of the Pad-and-Fan Cooling System.....	101
5.2.3 Water Use by the Pad-and-Fan Cooling System.....	102
5.2.4 Water Use by Tomato Plants	105
5.2.5 Total Greenhouse Water Use	106
5.2.6 Water Use Efficiency	107
5.2.7 Greenhouse Environmental Conditions	109
5.2.7.1 <i>Mean Greenhouse Conditions</i>	109
5.2.7.2 <i>Temporal Trends in Greenhouse Conditions</i>	111
5.2.7.3 <i>Spatial Uniformity of Greenhouse Conditions</i>	113
5.2.8 Transpiration Rate and Water Use by Tomato Plants.....	118
5.2.9 Leaf Temperature.....	121

TABLE OF CONTENTS - *Continued*

5.3 Initial Studies on the Effect of Nozzle Location for a High-Pressure-Fog Cooling System in a Single-Span Greenhouse in a Semi-Arid Climate.....	124
5.3.1 Fog Nozzle Location at Vent Inlet.....	124
5.3.2 Fog Nozzle Location on Central, Overhead Line	125
5.3.3 Fog Nozzle Location on Central, Overhead Line and at Pad Inlet	127
5.3.4 Fog Nozzle Location on Side Wall Gutter Lines.....	128
5.4 Effect of High-Pressure-Fog Cooling on Greenhouse Water Use, Climate Conditions, Plant Transpiration and Leaf Temperatures for a Semi-Arid Climate	130
5.4.1 Outside Environmental Conditions.....	130
5.4.2 High-Pressure-Fog Operation	131
5.4.3 Water Use by the High-Pressure-Fog System	133
5.4.4 Water Use by Tomato Plants	137
5.4.5 Total Greenhouse Water Use	138
5.4.6 Water Use Efficiency	139
5.4.7 Greenhouse Environmental Conditions	141
5.4.7.1 <i>Mean Greenhouse Conditions</i>	141
5.4.7.2 <i>Fog duration and Greenhouse Conditions</i>	142
5.4.7.3 <i>Temporal Trends in Greenhouse Environmental Conditions</i>	144
5.4.7.4 <i>Spatial Uniformity of Greenhouse Environmental Conditions</i>	149
5.4.8 Transpiration and Water Uptake Rates by the Tomato Plants	153

TABLE OF CONTENTS - *Continued*

5.4.9 Leaf Temperature	156
5.5 Water Use Efficiency for Hydroponic Greenhouse Tomato Production Using Pad-and-Fan Cooling in a Semi-Arid Climate	159
5.5.1 Outside and Greenhouse Environmental Conditions	159
5.5.2 Seasonal Greenhouse Water Use	161
5.5.3 Greenhouse Water Use Efficiency	163
5.5.3.1 Tomato Yields and Greenhouse Water Use	163
5.5.3.2 Water Use Efficiency.....	165
5.6 Using the Energy Balance Equation to Estimate Evaporative Cooling Water Use and Inside Air Temperatures for a Greenhouse in Semi-Arid Conditions..	167
5.6.1 Evaporative Cooling Water Use	167
5.6.1.1 Pad-and-Fan Cooling Water Use	167
5.6.1.2 High-Pressure-Fog Cooling Water Use	168
5.6.2 Greenhouse Air Temperatures	172
5.6.2.1 Pad-and-Fan System.....	172
5.6.2.2 High-Pressure-Fog System	174
5.7 Using a Wind Tunnel to Test the Effects of Buoyancy and Wind Direction on Airflow and Temperature Distribution in a Naturally-Ventilated Greenhouse.	178
5.7.1 Air Movement in the Wind Tunnel Model	178
5.7.1.1 Wind Direction.....	178
5.7.1.2 Buoyancy (ΔT).....	178

TABLE OF CONTENTS - *Continued*

5.7.2 Temperature Distribution in the Wind Tunnel Model	180
5.7.2.1 <i>Wind Direction</i>	180
5.7.2.2 <i>Buoyancy (ΔT)</i>	181
5.7.3 Full-Scale Greenhouse Validation Study	181
5.7.3.1 <i>No Plants, No Fog</i>	182
5.7.3.2 <i>With Fog and With Plants</i>	183
6. DISCUSSION	185
6.1 Greenhouse Water Use and Water Use Efficiency	185
6.1.1 Pad-and-Fan Cooling	185
6.1.2 High-Pressure-Fog Cooling	187
6.2 Greenhouse Environment	189
6.2.1 Pad-and-Fan Cooling	189
6.2.2 High-Pressure-Fog Cooling	192
6.2.2.1 <i>Fog Nozzle Location</i>	192
6.2.2.2 <i>Ventilation Tests with Central, Overhead Line</i>	193
6.3 Plant Responses	195
6.3.1 Pad-and-Fan Cooling	195
6.3.2 High-Pressure-Fog Cooling	197
6.4 Greenhouse Modeling Studies	199
6.4.1 Energy Balance Model.....	199
6.4.2 Wind Tunnel Model	201

TABLE OF CONTENTS - *Continued*

7. RECOMMENDATIONS.....	204
8. CONCLUSIONS	208
REFERENCES.....	210

LIST OF FIGURES

Figure 2.1 Heat transfer in the greenhouse energy balance include radiation (Q_R), conduction and convection across the glazing (Q_G) and the soil (Q_S), ventilation (Q_V), internal greenhouse components such as plants (Q_P), latent heat transfer to water (Q_L), and any operating heating units (Q_H).	36
Figure 2.2 Water vapor transfer in the greenhouse include ventilation (E_V), evaporative cooling systems (E_C), evaporation from the soil and hydroponic system (E_S), and plant transpiration (E_T).	37
Figure 4.1 Schematic of greenhouse used for cooling experiments shows the location of the evaporative cooling pad (north wall), central, overhead high-pressure-fog line (center of greenhouse), exhaust fans (south wall), and natural ventilation openings (east and west walls, and roof).	58
Figure 4.2 Schematic of the pad for the pad-and-fan system, including a 15-cm thick cellulose pad, inlet water, sump return, storage tank, and pump.	59
Figure 4.3 Location of the fog lines – multiple inlet, single inlet, side gutter, and central, overhead fog lines – used during high-pressure-fog tests in relation to the plant zone, inlet vent/cooling pad, and exhaust fans.	61
Figure 4.4 Spatial location of air temperature and relative humidity sensors, relative to pad and fan walls. They were placed 3 m above the floor at canopy height. Mature tomato plants were grown in the “plant zone” area.	68
Figure 4.5 Schematic diagram of the wind tunnel used at the National Institute for Rural Engineering in Tsukuba, Japan.	86
Figure 4.6 A $1/15$ scale model of arched-roof, single-span greenhouse used for wind tunnel experiments.	87
Figure 4.7 Locations of thermocouples along horizontal cross-section of greenhouse model inside wind tunnel.	88
Figure 4.8 Locations where 3-D airflow measurements were monitored in the full-scale greenhouse in Arizona.	94
Figure 5.1 Thirty-minute averages and standard deviations of water use by two equivalent pad-and-fan systems operating simultaneously for five ventilation rates (4.8, 10.2, 14.1, 18.6, and $21.8 \text{ m}^3 \text{ s}^{-1}$).	95

LIST OF FIGURES - *Continued*

- Figure 5.2 Average plant zone air temperatures (\blacktriangle) and average plant zone relative humidity (\blacksquare) levels measured during the simultaneous operation of pad-and-fan cooling for a greenhouse without plants (open symbols) and an identical plant-filled greenhouse (solid symbols) for five ventilation rates (4.8, 10.2, 14.1, 18.6, and $21.8 \text{ m}^3 \text{ s}^{-1}$). Pad-and-fan water use ($\cdots\circ\cdots$) was the average for the two greenhouses with outside conditions $T_{Air,Out} = 38^\circ\text{C}$, $RH_{Out} = 15\%$ 97
- Figure 5.3 Outside VPD (\blacklozenge) during dry summer conditions (—) and more humid, monsoon summer conditions (\cdots) throughout a typical day, and corresponding water use rates by the pad-and-fan system (\bullet) when operated at one ventilation rate ($10.3 \text{ m}^3 \text{ s}^{-1}$) 98
- Figure 5.4 Outside temperature (—) and relative humidity (\circ) during full day tests of the pad-and-fan system for four ventilation rates: $4.5 \text{ m}^3 \text{ s}^{-1}$ (—), $9.4 \text{ m}^3 \text{ s}^{-1}$ (—), $13 \text{ m}^3 \text{ s}^{-1}$ (—), and $16.7 \text{ m}^3 \text{ s}^{-1}$ (—). 99
- Figure 5.5 Outside solar radiation during pad-and-fan cooling under four ventilation rates: $4.5 \text{ m}^3 \text{ s}^{-1}$ (—), $9.4 \text{ m}^3 \text{ s}^{-1}$ (—), $13 \text{ m}^3 \text{ s}^{-1}$ (—), and $16.7 \text{ m}^3 \text{ s}^{-1}$ (—). 100
- Figure 5.6 Rate of water use by the pad-and-fan evaporative cooling system for 09:00-17:00 for four ventilation rates: $4.5 \text{ m}^3 \text{ s}^{-1}$ ($\cdots\bullet\cdots$), $9.4 \text{ m}^3 \text{ s}^{-1}$ ($\text{--}\blacklozenge\text{--}$), $13 \text{ m}^3 \text{ s}^{-1}$ ($\text{--}\blacksquare\text{--}$), and $16.7 \text{ m}^3 \text{ s}^{-1}$ ($\text{--}\Delta\text{--}$). 103
- Figure 5.7 Total pad-and-fan cooling water use measured (—) and modeled using psychrometrics (\cdots) for four ventilation rates: $4.5 \text{ m}^3 \text{ s}^{-1}$ (\bullet), $9.4 \text{ m}^3 \text{ s}^{-1}$ (\diamond), $13 \text{ m}^3 \text{ s}^{-1}$ (\blacksquare), and $16.7 \text{ m}^3 \text{ s}^{-1}$ (Δ) for the period 08:00-17:00. 104
- Figure 5.8 Mean daytime (08:00 – 17:00) plant zone air temperature ($\text{—}\blacksquare\text{—}$), relative humidity ($\text{--}\circ\text{--}$), and vapor pressure deficit ($\cdots*\cdots$). 110
- Figure 5.9 Incoming solar radiation intensity during the pad-and-fan cooling tests for four ventilation rates: $4.5 \text{ m}^3 \text{ s}^{-1}$ (—), $9.4 \text{ m}^3 \text{ s}^{-1}$ (\cdots), $13.0 \text{ m}^3 \text{ s}^{-1}$ (—), and $16.7 \text{ m}^3 \text{ s}^{-1}$ (—). 111
- Figure 5.10 Mean plant zone air temperatures (solid symbols) and relative humidity levels (open symbols) calculated every 30 minutes for four ventilation rates: $4.5 \text{ m}^3 \text{ s}^{-1}$ ($\cdots\bullet\cdots$), $9.4 \text{ m}^3 \text{ s}^{-1}$ ($\text{--}\blacklozenge\text{--}$), $13 \text{ m}^3 \text{ s}^{-1}$ ($\text{--}\blacksquare\text{--}$), and $16.7 \text{ m}^3 \text{ s}^{-1}$ ($\text{—}\blacktriangle\text{—}$). 112
- Figure 5.11 Mean plant zone absolute humidity (open symbols) and vapor pressure deficit (solid symbols) were calculated every 30 minutes for four ventilation rates: $4.5 \text{ m}^3 \text{ s}^{-1}$ ($\cdots\bullet\cdots$), $9.4 \text{ m}^3 \text{ s}^{-1}$ ($\text{--}\blacklozenge\text{--}$), $13 \text{ m}^3 \text{ s}^{-1}$ ($\text{--}\blacksquare\text{--}$), and $16.7 \text{ m}^3 \text{ s}^{-1}$ ($\text{—}\blacktriangle\text{—}$). 112

LIST OF FIGURES - *Continued*

- Figure 5.12 Mean temperatures observed outside the pad and at several greenhouse locations (0, 4, 12, 20, and 28 m from the pad inlet) during pad-and-fan cooling for four ventilation rates: $4.5 \text{ m}^3 \text{ s}^{-1}$ ($\cdots\bullet\cdots$), $9.4 \text{ m}^3 \text{ s}^{-1}$ ($--\diamond--$), $13 \text{ m}^3 \text{ s}^{-1}$ ($--\blacksquare--$), and $16.7 \text{ m}^3 \text{ s}^{-1}$ ($—\Delta—$). Means were calculated from values measured when outside conditions were most stable (11:00 – 17:00). The solid vertical line represents the cooling pad location. 114
- Figure 5.13 Mean relative humidity levels observed outside and at several greenhouse locations (0, 4, 12, 20, and 28 m from the pad inlet) during pad-and-fan cooling for four ventilation rates: $4.5 \text{ m}^3 \text{ s}^{-1}$ ($\cdots\bullet\cdots$), $9.4 \text{ m}^3 \text{ s}^{-1}$ ($--\diamond--$), $13 \text{ m}^3 \text{ s}^{-1}$ ($--\blacksquare--$), and $16.7 \text{ m}^3 \text{ s}^{-1}$ ($—\Delta—$). Means were calculated from values measured when outside conditions were most stable (11:00 – 17:00). The solid vertical line represents the cooling pad location. 114
- Figure 5.14 Mean vapor pressure deficit values observed outside and at several greenhouse locations (0, 4, 12, 20, and 28 m from the pad inlet) during pad-and-fan cooling for four ventilation rates: $4.5 \text{ m}^3 \text{ s}^{-1}$ ($\cdots\bullet\cdots$), $9.4 \text{ m}^3 \text{ s}^{-1}$ ($--\diamond--$), $13 \text{ m}^3 \text{ s}^{-1}$ ($--\blacksquare--$), and $16.7 \text{ m}^3 \text{ s}^{-1}$ ($—\Delta—$). Means were calculated from values measured when outside conditions were most stable (11:00 – 17:00). The solid vertical line represents the cooling pad location. 115
- Figure 5.15 Mean humidity ratio (W) of the air observed at several greenhouse locations (0, 4, 12, 20, and 28 m from the pad inlet) during pad-and-fan cooling for four ventilation rates: $4.5 \text{ m}^3 \text{ s}^{-1}$ ($\cdots\bullet\cdots$), $9.4 \text{ m}^3 \text{ s}^{-1}$ ($--\diamond--$), $13 \text{ m}^3 \text{ s}^{-1}$ ($--\blacksquare--$), and $16.7 \text{ m}^3 \text{ s}^{-1}$ ($—\Delta—$). Means were calculated from values measured when outside conditions were most stable (11:00 – 17:00). The solid vertical line represents the cooling pad location. 115
- Figure 5.16 Transpiration rates of tomato plants for pad-and-fan cooling for four different ventilation rates: $4.5 \text{ m}^3 \text{ s}^{-1}$ ($\cdots\bullet\cdots$), $9.4 \text{ m}^3 \text{ s}^{-1}$ ($--\diamond--$), $13 \text{ m}^3 \text{ s}^{-1}$ ($--\blacksquare--$), and $16.7 \text{ m}^3 \text{ s}^{-1}$ ($—\Delta—$). Each value represents the one-hour mean of transpired water ($\text{g m}^{-2} \text{ s}^{-1}$) from 30-minute measurements using a lysimeter. 119
- Figure 5.17 Transpiration rate (E_T) of tomato plants versus incoming solar radiation (Rad_{in}) during pad-and-fan cooling for four ventilation rates: $4.5 \text{ m}^3 \text{ s}^{-1}$ (\bullet), $9.4 \text{ m}^3 \text{ s}^{-1}$ (\diamond), $13 \text{ m}^3 \text{ s}^{-1}$ (\blacksquare), and $16.7 \text{ m}^3 \text{ s}^{-1}$ (Δ). Linear regression performed on data points (11:00 – 17:00) for all three ventilation rates. 120

LIST OF FIGURES - *Continued*

- Figure 5.18 Mean leaf temperatures and standard deviations of 3 shaded leaves measured with an infrared thermometer during pad-and-fan evaporative cooling for four ventilation rates: $4.5 \text{ m}^3 \text{ s}^{-1}$ ($\cdots\bullet\cdots$), $9.4 \text{ m}^3 \text{ s}^{-1}$ ($--\diamond--$), $13 \text{ m}^3 \text{ s}^{-1}$ ($--\blacksquare--$), and $16.7 \text{ m}^3 \text{ s}^{-1}$ ($—\Delta—$). The shade curtain was used between 11:00-14:00..... 122
- Figure 5.19 Vapor pressure deficit levels over time during continuous high-pressure-fog cooling, with all fog nozzles located inside the greenhouse at the vent inlet, for five mechanical ventilation rates ($q = 4.5, 9.4, 13.0, 16.7$, and $20.3 \text{ m}^3 \text{ s}^{-1}$) and four fog injection rates, ($E_{Fog} = 0.219, 0.249, 0.622$, and $0.808 \text{ g m}^{-2} \text{ s}^{-1}$). VPD measurements were taken at the following five distances from the inlet: 0 m ($-\circ-$), 4 m ($-\Delta-$), 12 m ($-\diamond-$), 20 m ($-\square-$), and 28 m ($-*-$), and outside ($-+-$)..... 125
- Figure 5.20 Vapor pressure deficit levels during VPD-control of high-pressure-fog cooling ($E_{Fog} = 0.287 \text{ g m}^{-2} \text{ s}^{-1}$), with nozzles located along a central, overhead line running from inlet to exhaust, and using mechanical ventilation rates of 3.0, 3.7, and $4.5 \text{ m}^3 \text{ s}^{-1}$. VPD measurements were taken at the following five distances from the inlet: 0 m ($-\circ-$), 4 m ($-\Delta-$), 12 m ($-\diamond-$), 20 m ($-\square-$), and 28 m ($-*-$), and outside ($-+-$). 126
- Figure 5.21 Vapor pressure deficit levels during VPD-control of high-pressure-fog cooling, with nozzles located along the pad inlet and in a central, overhead line running from inlet to fans ($E_{Fog} = 0.523 \text{ g m}^{-2} \text{ s}^{-1}$), and using mechanical ventilation rates of 3.0, 4.5, 9.4, and $16.7 \text{ m}^3 \text{ s}^{-1}$. VPD measurements were taken at the following five distances from the inlet: 0 m ($-\circ-$), 4 m ($-\Delta-$), 12 m ($-\diamond-$), 20 m ($-\square-$), and 28 m ($-*-$), and outside ($-+-$). 128
- Figure 5.22 Vapor pressure deficit versus time during VPD-control of high-pressure-fog cooling, with side wall gutter fog line of nozzles mounted along the length of the east and side walls near to the gutters ($E_{Fog} = 0.90 \text{ g m}^{-2} \text{ s}^{-1}$), and with mechanical ventilation. VPD was measured at 0 m ($-\circ-$), 4 m ($-\Delta-$), 12 m ($-\diamond-$), 20 m ($-\square-$), and 28 m ($-*-$) distances from the inlet, and outside ($-+-$). 129
- Figure 5.23 Outside temperature ($-$) and relative humidity (\circ) during full day tests of the high-pressure-fog system for four ventilation rates: $3.0 \text{ m}^3 \text{ s}^{-1}$ ($-$), $4.5 \text{ m}^3 \text{ s}^{-1}$ ($-$), and $13 \text{ m}^3 \text{ s}^{-1}$ ($-$). 130
- Figure 5.24 Outside solar radiation levels during full day tests of the high-pressure-fog system for four ventilation rates: $3.0 \text{ m}^3 \text{ s}^{-1}$ ($-$), $4.5 \text{ m}^3 \text{ s}^{-1}$ ($-$), and $13 \text{ m}^3 \text{ s}^{-1}$ ($-$). 131

LIST OF FIGURES - *Continued*

- Figure 5.25 On (○) and Off (×) duration versus time of day for the high-pressure-fog system operated with three ventilation rates: $3.0 \text{ m}^3 \text{ s}^{-1}$ (—), $4.5 \text{ m}^3 \text{ s}^{-1}$ (—), and $13 \text{ m}^3 \text{ s}^{-1}$ (—). The shade curtain was used between 11:00 – 14:30..... 133
- Figure 5.26 Total water use by the high-pressure-fog cooling system versus ventilation rate ($3.0 \text{ m}^3 \text{ s}^{-1}$ (*), $4.5 \text{ m}^3 \text{ s}^{-1}$ (●), and $9.4 \text{ m}^3 \text{ s}^{-1}$ (◇)), and linear relationship between water use and On-time (—) and ventilation rate (....) during 08:00 – 17:00 test period. 135
- Figure 5.27 Rate of water use by the high-pressure-fog evaporative cooling system from 08:00-17:00 for three ventilation rates: $3.0 \text{ m}^3 \text{ s}^{-1}$ (—*), $4.5 \text{ m}^3 \text{ s}^{-1}$ (—●—), and $9.4 \text{ m}^3 \text{ s}^{-1}$ (—◇—)..... 137
- Figure 5.28 Fog water injection rates as influenced by greenhouse air temperature for three ventilation rates: $3.0 \text{ m}^3 \text{ s}^{-1}$ (*), $4.5 \text{ m}^3 \text{ s}^{-1}$ (●), and $9.4 \text{ m}^3 \text{ s}^{-1}$ (◇). Seven-minute intervals (420 s) were used to calculate the mean plant zone air temperature values and fog injection rates for the three ventilation rates tested. 143
- Figure 5.29 Plant zone air relative humidity as a function of fog water injection rate. Equations represent the linear regressions of ventilation rates $3.0 \text{ m}^3 \text{ s}^{-1}$ (*), $4.5 \text{ m}^3 \text{ s}^{-1}$ (●), and $9.4 \text{ m}^3 \text{ s}^{-1}$ (◇) from top to bottom. Seven-minute intervals (420 s) were used to calculate the mean plant zone relative humidity levels and fog injection rates for the three ventilation rates tested..... 144
- Figure 5.30 Incoming solar radiation (Rad_{in}) versus time of day during high-pressure-fog cooling for three ventilation rates: $3.0 \text{ m}^3 \text{ s}^{-1}$ (—), $4.5 \text{ m}^3 \text{ s}^{-1}$ (—), and $9.4 \text{ m}^3 \text{ s}^{-1}$ (—). . 145
- Figure 5.31 Greenhouse temperatures and relative humidity versus time of day during high-pressure-fog for three ventilation rates: a) $3.0 \text{ m}^3 \text{ s}^{-1}$, b) $4.5 \text{ m}^3 \text{ s}^{-1}$, and c) $9.4 \text{ m}^3 \text{ s}^{-1}$. Locations at five distances from the inlet were monitored: 0 m (—), 4 m (....), 12 m (—), 20 m (—), and 28 m (—)..... 146
- Figure 5.32 Seven-minute mean plant zone air temperatures and fog On-time percentages versus time of day for three ventilation rates: $3.0 \text{ m}^3 \text{ s}^{-1}$ (....), $4.5 \text{ m}^3 \text{ s}^{-1}$ (—), and $9.4 \text{ m}^3 \text{ s}^{-1}$ (—). Black lines represent plant zone temperatures and gray lines represent Fog On%. 148
- Figure 5.33 Seven-minute mean plant zone relative humidity levels and fog On-time versus time of day percentages for three ventilation rates: $3.0 \text{ m}^3 \text{ s}^{-1}$ (....), $4.5 \text{ m}^3 \text{ s}^{-1}$ (—), and $9.4 \text{ m}^3 \text{ s}^{-1}$ (—). Black lines represent plant zone temperatures and gray lines represent Fog On%..... 148

LIST OF FIGURES - *Continued*

- Figure 5.34 Box plots of temporal variability in (a) air temperature (ΔT) and (b) relative humidity (ΔRH) during the test period at several greenhouse locations (0, 4, 12, 20, and 28 m distance from inlet), presented as differences between each 1-minute measurement for three ventilation rates (3, 4.5, and $9.4 \text{ m}^3 \text{ s}^{-1}$). 149
- Figure 5.35 Air temperature (mean and s.d. for 11:00-17:00) versus distance from the inlet vent representing spatial uniformity during high-pressure-fog cooling for three ventilation rates: $3.0 \text{ m}^3 \text{ s}^{-1}$ ($-*-$), $4.5 \text{ m}^3 \text{ s}^{-1}$ ($\cdots\bullet\cdots$), and $9.4 \text{ m}^3 \text{ s}^{-1}$ ($--\diamond--$). The solid vertical line represents the cooling pad location. 150
- Figure 5.36 Relative humidity (mean and s.d. for 11:00-17:00) versus distance from inlet vent representing spatial uniformity during high-pressure-fog cooling for three ventilation rates: $3.0 \text{ m}^3 \text{ s}^{-1}$ ($-*-$), $4.5 \text{ m}^3 \text{ s}^{-1}$ ($\cdots\bullet\cdots$), and $9.4 \text{ m}^3 \text{ s}^{-1}$ ($--\diamond--$). The solid vertical line represents the cooling pad location. 150
- Figure 5.37 Vapor pressure deficit (mean and s.d. for 11:00-17:00) versus distance from vent inlet representing spatial uniformity during high-pressure-fog cooling for three ventilation rates: $3.0 \text{ m}^3 \text{ s}^{-1}$ ($-*-$), $4.5 \text{ m}^3 \text{ s}^{-1}$ ($\cdots\bullet\cdots$), and $9.4 \text{ m}^3 \text{ s}^{-1}$ ($--\diamond--$). The solid vertical line represents the cooling pad location. 151
- Figure 5.38 Absolute humidity (mean and s.d. for 11:00-17:00) versus distance from inlet vent representing spatial uniformity during high-pressure-fog cooling for three ventilation rates: $3.0 \text{ m}^3 \text{ s}^{-1}$ ($-*-$), $4.5 \text{ m}^3 \text{ s}^{-1}$ ($\cdots\bullet\cdots$), and $9.4 \text{ m}^3 \text{ s}^{-1}$ ($--\diamond--$). The solid vertical line represents the cooling pad location. 151
- Figure 5.39 Transpiration rate of tomato plants versus time of day for high-pressure-fog cooling between 11:00 – 17:00 for three ventilation rates: $3.0 \text{ m}^3 \text{ s}^{-1}$ ($-*-$), $4.5 \text{ m}^3 \text{ s}^{-1}$ ($\cdots\bullet\cdots$), and $9.4 \text{ m}^3 \text{ s}^{-1}$ ($--\diamond--$). 154
- Figure 5.40 Transpiration rate (E_T) of tomato plants versus incoming solar radiation (Rad_{in}) during high-pressure-fogging for three ventilation rates: $3.0 \text{ m}^3 \text{ s}^{-1}$ (*), $4.5 \text{ m}^3 \text{ s}^{-1}$ (●), and $9.4 \text{ m}^3 \text{ s}^{-1}$ (◇). Linear regression performed on data points (11:00 – 17:00) for all three ventilation rates. 155
- Figure 5.41 Mean and standard deviation of leaf temperature versus time of day of three shaded leaves measured with an infrared thermometer during high-pressure-fog cooling for four ventilation rates: $3.0 \text{ m}^3 \text{ s}^{-1}$ ($---*---$), $4.5 \text{ m}^3 \text{ s}^{-1}$ ($\cdots\bullet\cdots$), and $9.4 \text{ m}^3 \text{ s}^{-1}$ ($--\diamond--$). The shade curtain was used between 11:00 – 14:30. 157

LIST OF FIGURES - *Continued*

- Figure 5.42 Mean daytime (08:00 – 16:00) outside air temperature (♦) and relative humidity (■) during 2006. Test periods during the 8-month study period are delineated. 159
- Figure 5.43 Mean daytime (08:00 – 16:00) outside VPD (Δ) and solar radiation (●) during 2006. Test periods during the 8-month study period are delineated..... 160
- Figure 5.44 Mean daytime (08:00 – 16:00) and nighttime (0:00 – 08:00) inside air temperature (♦) and VPD (Δ) during the crop season (March 8 – October 4, 2006). 161
- Figure 5.45 Daily 24-hr water use rates by the pad-and-fan system (—■—), open irrigation system ($\cdots\Delta\cdots$), and closed irrigation systems ($--\blacktriangle--$) from March 8 to October 4, 2006..... 162
- Figure 5.46 Mean and standard deviation of pad-and-fan cooling efficiency (η_{Cool}) during May 12 – 19, 2006, representing dry, summer conditions (■) (upper data) and during August 10 – 15, 2006, representing summer monsoon conditions (\square) (lower data).. 163
- Figure 5.47 Modeled versus measured water use by the pad-and-fan cooling system using data from 11:00 – 17:00 for four ventilation rates: $4.5 \text{ m}^3 \text{ s}^{-1}$ (●), $9.4 \text{ m}^3 \text{ s}^{-1}$ (\diamond), $13 \text{ m}^3 \text{ s}^{-1}$ (■), and $16.7 \text{ m}^3 \text{ s}^{-1}$ (Δ)..... 167
- Figure 5.48 Modeled versus measured water use by the high-pressure-fog cooling system using a) the energy balance model (*Equation 4.27*) and b) the moisture balance (*Equation 4.26*) for data from 11:00 – 17:00 at 20 m location for three ventilation rates: $3.0 \text{ m}^3 \text{ s}^{-1}$ (*), $4.5 \text{ m}^3 \text{ s}^{-1}$ (●), and $9.4 \text{ m}^3 \text{ s}^{-1}$ (\diamond)..... 168
- Figure 5.49 Water use by the high-pressure-fog system (— —) from 11:00-17:00 and the potential water savings (—) calculated as the difference in predicted and measured water use ($E_{Meas} - E_{Pred}$) in 30-minute increments for three ventilation rates: $3.0 \text{ m}^3 \text{ s}^{-1}$ (*), $4.5 \text{ m}^3 \text{ s}^{-1}$ (●), and $9.4 \text{ m}^3 \text{ s}^{-1}$ (\diamond)..... 170
- Figure 5.50 Modeled versus measured inside air temperatures with pad-and-fan cooling at 4 m, 12 m, and 20 m locations using a) T_{Out} and b) T_{x-l} in the energy balance equation for ventilation rates $4.5 \text{ m}^3 \text{ s}^{-1}$ (●), $9.4 \text{ m}^3 \text{ s}^{-1}$ (\diamond), $13 \text{ m}^3 \text{ s}^{-1}$ (■), and $16.7 \text{ m}^3 \text{ s}^{-1}$ (Δ). 173
- Figure 5.51 Modeled versus measured inside air temperatures with high-pressure-fog at 4 m, 12 m, and 20 m locations using a) T_{Out} and b) T_{x-l} in the energy balance equation for ventilation rates of $3.0 \text{ m}^3 \text{ s}^{-1}$ (*), $4.5 \text{ m}^3 \text{ s}^{-1}$ (●), and $9.4 \text{ m}^3 \text{ s}^{-1}$ 175

LIST OF FIGURES - *Continued*

- Figure 5.52 Velocity vector maps, produced by Particle Image Velocimetry (PIV), demonstrate the general airflow patterns observed in the wind tunnel greenhouse model..... 179
- Figure 5.53 Air velocity and direction within the airflow experiments in the full-scale greenhouse for four treatments: i) no plants, no fog; ii) no plants, with fog; iii) with plants, no fog; and iv) with plants, with fog. Bold numbers represent the measured air West-East vertical plane velocity (m s^{-1}), and numbers in parentheses represent three-dimensional air velocity (m s^{-1}). Wind direction measured in a clockwise rotation (azimuth degree angle, $^{\circ}$). 184

LIST OF TABLES

Table 4.1 Ventilation rates as determined by the number of fans in operation. Fan operation and subsequent ventilation rates for the pad-and-fan and high-pressure fog systems are denoted by superscripts “P” and “F,” respectively.....	63
Table 4.2 Ventilation rates produced by the variable speed fan under several percentages of maximum operating speed.	63
Table 4.3 Operation of the components used by the pad-and-fan system (pad pump, variable speed fan (VSF), fixed speed fan (FSF)) using proportional control to provide the cooling capacity demand. The VSF increased speed in proportion to its maximum speed, whereas the pump and FSF were either On or Off. Equivalent ventilation rates produced by the fans are also provided.....	77
Table 4.4 Infrared temperature measurements made of the greenhouse floor and on the ground outside (both gravel) when the ambient outside temperature was 31°C.	91
Table 4.5 Wind tunnel requirements for temperature difference and wind velocity calculated from the similarity principle using Archimedes number and full-scale greenhouse conditions.....	91
Table 4.6 Wind tunnel treatments testing the effects of wind direction and ΔT ($T_{Floor} - T_{out,ambient}$) on air movement and temperature distribution.	92
Table 5.1 Mean outside climate conditions (temperature, relative humidity, and vapor pressure deficit) for the entire experimental period (08:00 – 17:00) and during the part of the day when outside conditions were relatively stable (11:00 – 17:00) for the full day tests of the pad-and-fan system for four ventilation rates.	100
Table 5.2 Mean cooling efficiency (η_{Pad}) for the pad-and-fan system calculated using the equation $\eta_{Pad} = (T_{DB,Out} - T_{DB,PadIn}) / (T_{DB,Out} - T_{WB,Out})$. Standard deviations represent the variability observed during the testing period (08:00-17:00) for each ventilation rate tested (4.5, 9.4, 13.0, and 16.7 m ³ s ⁻¹). Letters represent significantly different values from a Tukey-Kramer HSD test ($p < 0.01$). Mean changes in humidity ratio ($W_{In} - W_{Out}$) and differences in $T_{DB,In}$ and $T_{WB,Out}$ are also presented.	102
Table 5.3 Correlations (r) between WU_{PF} and ventilation rate using multivariate analysis, and outside climate conditions including temperature (T_{Out}), relative humidity (RH_{Out}), vapor pressure deficit (VPD_{Out}), and absolute humidity (W_{Out}). Correlations were also calculated for each ventilation rate: 4.5, 9.4, 13.0, and 16.7 m ³ s ⁻¹	105

LIST OF TABLES - *Continued*

Table 5.4 Total water use for irrigation (WU_I), total plant water uptake (ΣWU_P), and mean plant water uptake rates ($\overline{WU_P}$) during the test period (08:00-17:00) for four ventilation rates: 4.5, and 9.4, 13.0, and 16.7 m ³ s ⁻¹	106
Table 5.5 Total daily water use per floor area by the open irrigation system (WU_I), pad-and-fan system (WU_{PF}), and closed irrigation system (ΣWU_{PU}) for the 9-hour test day (08:00-17:00) for ventilation rates of 4.5, 9.4, 13.0 and 16.7 m ³ s ⁻¹ . Total greenhouse water use with the pad-and-fan system and open irrigation ($\Sigma WU_{S,Open}$) and closed irrigation ($\Sigma WU_{S,Closed}$) systems also presented.	107
Table 5.6 Water use efficiency (WUE) of the greenhouse water systems, including irrigation for open ($WUE_{I,Open}$) and closed ($WUE_{I,Closed}$) systems and the pad-and-fan system (WUE_{PF}) for four ventilation rates, and the resulting system water use efficiency (WUE_S) when water use by both systems is considered. Results are divided for tomato yields obtained in the experimental greenhouse (39 kg day ⁻¹) and those that might be expected in commercial tomato production (49.5 kg day ⁻¹).	109
Table 5.7 Mean plant zone air temperature, relative humidity, vapor pressure deficit, and incoming radiation during one day of testing (08:00 – 17:00) with standard deviations (<i>italics</i>). The values ΔT (T_{GH-Out}), ΔRH (RH_{GH-Out}), and ΔVPD (VPD_{GH-Out}) represent their differences relative to outside conditions averaged over the same period.	110
Table 5.8 Uniformity of greenhouse air temperature, relative humidity, and vapor pressure deficit during pad-and-fan cooling for four ventilation rates (4.5, 9.4, 13.0, and 16.7 m ³ s ⁻¹) is presented as the mean difference between measurements made at different greenhouse locations during the most stable part of the day (11:00-17:00).	116
Table 5.9 Mean plant water uptake rates (WU_{PU}) from 11:00-17:00 for different ventilation rates for pad-and-fan evaporative cooling. Means with significant difference ($p < 0.05$) according to Tukey-Kramer HSD are represented by different letters.	121
Table 5.10 Leaf temperature (T_{Leaf}) at three locations, and average plant zone air conditions for four ventilation rates during specific times of the day. T_{Leaf} was measured with an Infrared thermometer on three plants at different distances from the cooling pad (5.2, 11, 17.7 m) during pad-and-fan cooling. Numbers in <i>italics</i> refers to maximum T_{Leaf} differences observed. Tests of significance performed with Tukey-Kramer HSD. Values with similar letters are not significantly different at $p < 0.01$.	123

LIST OF TABLES - *Continued*

Table 5.11 Mean outside conditions and standard deviations of air temperature, relative humidity, and vapor pressure for the entire experimental period (08:00 – 17:00) and when outside conditions were relatively stable (11:00 – 17:00).....	131
Table 5.12 Mean fraction of fog operation On-time and mean On-time calculated over a 420 s time interval for three ventilation rates (3.0, 4.5, 9.4 m ³ s ⁻¹). The total fogging time during 08:00-17:00 is also included. Significance tests performed with Tukey-Kramer HSD. Data followed by same letter are not significantly different.....	132
Table 5.13 Correlations (r) between fog water use (WU_{HPF}) and ventilation rate, and outside climate conditions including temperature (T_{Out}), relative humidity (RH_{Out}), vapor pressure deficit (VPD_{Out}), and absolute humidity (W_{Out}); and multivariate correlations were also calculated for each ventilation rate (3.0, 4.5, and 9.4 m ³ s ⁻¹). 135	135
Table 5.14 Total water use for irrigation (W_I), total plant water uptake (ΣWU_P), and mean plant water uptake rates ($\overline{WU_P}$) during the test period (08:00-17:00) for three ventilation rates: 3.0, 4.5, and 9.4 m ³ s ⁻¹ . Mean $\overline{WU_P}$ values were calculated from 30-minute measurements during the test period. Letters represent significantly different values ($p < 0.05$).....	138
Table 5.15 Water use by the high-pressure-fog system (WU_{HPF}), open irrigation system (WU_I), closed irrigation system (ΣWU_P), and the resulting total greenhouse system water use for open ($\Sigma WU_{S,Open}$) and closed ($\Sigma WU_{S,Closed}$) irrigation with high-pressure-fog cooling during 08:00-17:00 test period for ventilation rates of 3.0, 4.5, and 9.4 m ³ s ⁻¹	139
Table 5.16 Water use efficiency (WUE) of the greenhouse water systems, including irrigation for open ($WUE_{I,Open}$) and closed ($WUE_{I,Closed}$) systems and the high-pressure-fog system (WUE_{HPF}) for three ventilation rates, and the resulting system water use efficiency (WUE_S) when water use by both systems is considered. Results are divided for tomato yields obtained in the experimental greenhouse (39 kg day ⁻¹) and those that might be expected in commercial tomato production (49.5 kg day ⁻¹).	140
Table 5.17 Mean plant zone air temperature, relative humidity, vapor pressure deficit, and incoming radiation calculated over the entire test period (08:00 – 17:00) with standard deviations (<i>italics</i>). The values ΔT (T_{GH-Out}), ΔRH (RH_{GH-Out}), and ΔVPD (VPD_{GH-Out}) represent their differences relative to outside conditions averaged over the same period. Letters represent significantly different values from a Tukey-Kramer HSD test ($p < 0.01$).....	141

LIST OF TABLES - *Continued*

Table 5.18 Mean plant water uptake rates (WU_{PU}) for the full test period (11:00-17:00), after initial hydration of the plants (11:00-17:00), during shading (13:00-14:00), and after shading (15:00-16:00) for different ventilation rates for high-pressure-fog evaporative cooling. Means with significant difference ($p < 0.05$) according to Tukey-Kramer HSD are represented by different letters.....	156
Table 5.19 Leaf temperatures (T_{Leaf}) and mean plant zone environmental conditions versus time of day of three plants at different distances from the cooling pad (5.2, 11, 17.7 m) during high-pressure-fog cooling at three ventilation rates. T_{Leaf} was measured with an infrared thermometer. The difference in T_{Leaf} between the three locations determined uniformity. Numbers in italics refers to maximum temperature differences observed. Tests of significance performed with Tukey-Kramer HSD. Values with similar letters for a given time are not significantly different at $p < 0.01$	158
Table 5.20 Mean daily tomato yields and water use rates by the pad-and-fan system and the open and closed irrigation systems. Crop totals presented are based on a 222 m ² production floor area for a 209-day crop life cycle.....	164
Table 5.21 Seasonal and total WUE_{PF} , WUE_I , and WUE_S based on 222 m ² growing area for the 209-day production period.....	166
Table 5.22 Total water use measured ($E_{Measured}$) and predicted ($E_{Predicted}$) by the energy balance model for high-pressure-fog cooling at the 20 m greenhouse location between 11:00-17:00, and the total potential savings in water ($E_{Meas} - E_{Pred}$) during the test of three ventilation rates (3.0, 4.5, and 9.4 m ³ s ⁻¹).	170
Table 5.23 Comparison of measured and modeled mean air temperatures for the time period 11:00 – 17:00 at each plant zone location for a given ventilation rate using the energy balance with both the outside air temperature (T_{Out}) and the previous measured air temperature (T_{x-1}) in Equation 4.25. Letters represent values that are significantly different ($p < 0.01$) for a given location based on Tukey-Kramer HSD.	176
Table 5.24 Values for dimensionless velocity in the x-direction, $U(x)$, and y-direction, $V(y)$, calculated from the particle image velocimetry (PIV) system during wind tunnel experiments.	180
Table 5.25 Values for θ_T calculated from temperatures measured at various locations inside the greenhouse model during the tested wind tunnel treatments. $\theta_T = (T_{in} - T_{tunnel}/T_{Pad} - T_{tunnel})$	181

ABSTRACT

Water availability is a common concern in semi-arid regions, such as Southern Arizona, USA. Hydroponic greenhouse crop production greatly reduces irrigation water use, but the study of water use by evaporative cooling has been limited.

This project investigated water use by two evaporative cooling systems: pad-and-fan and high-pressure-fog with fan ventilation. All studies were performed in a double-layer polyethylene film-covered greenhouse (28 x 9.8 x 6.3 m) with mature tomato plants (2.9 plants m⁻²). Water use efficiency (*WUE*, kg yield per m³ water use) was calculated daily according to ventilation rate, as well as for a 6-month cropping period, which used temperature-controlled pad-and-fan cooling.

Pad-and-fan water use was 3.2, 6.4, 8.5, and 10.3 L m⁻² d⁻¹ for ventilation rates of 0.016, 0.034, 0.047, 0.061 m³ m⁻² s⁻¹, respectively. High-pressure-fog water use with a single central, overhead line was 7.9, 7.4, and 9.3 L m⁻² d⁻¹ for ventilation rates of 0.01, 0.016, 0.034 m³ m⁻² s⁻¹, respectively. For pad-and-fan ventilation rates less than 0.034 m³ m⁻² s⁻¹, total greenhouse *WUE* (20 – 33 kg m⁻³) was similar to field drip irrigation. For the temperature-controlled high-pressure-fog system, total greenhouse *WUE* (14 – 17 kg m⁻³) was similar to field sprinkler irrigation.

For the 6-month crop cycle, combining water use by closed irrigation and pad-and-fan systems produced a total *WUE* of 15 kg m⁻³. Pad-and-fan *WUE* increased during monsoon conditions due to lower water use rates.

Evaporative cooling water use and air temperature were well-predicted by the energy balance model. Predictions of air temperature improved when outside climate the

measured conditions at one greenhouse location. Wind tunnel and full-scale studies of natural ventilation demonstrated the value of knowing airflow patterns when designing and operating a high-pressure-fog system

It is possible for greenhouse tomato production to have a higher *WUE* than field production, if ventilation rates are not excessive, if closed irrigation is used, and if control methodologies are improved. Water use can be minimized by knowing how the evaporative cooling system affects greenhouse climate and plant responses.

1. INTRODUCTION

Traditionally used for floriculture and ornamental production in the U.S.A., greenhouses are becoming increasingly popular for food crop production. In 1997, there were 383 ha of greenhouse vegetable production, accounting for 10% of all farms under some structural protection (USDA, 1997). In 2002, the area of land used for vegetable greenhouse production increased to almost 600 ha (USDA, 2002), with more than 330 ha dedicated to fresh tomato production (Cook and Calvin, 2005). Furthermore, greenhouse tomato production in the U.S. now accounts for 37% of the total fresh market (Cook and Calvin, 2005). Although greenhouse acreage accounts for only 0.2% of the total farm acreage for vegetable crops in the state, greenhouse farms can generate \$600,000 per acre in yearly gross returns, 130 times more than average field production (\$4,300 per acre).

In Arizona, large-scale, advanced-technology greenhouses have increased from 20 acres in 1991 to 330 acres in 2007. The increased greenhouse acreage in southern Arizona has occurred primarily because solar radiation levels are high throughout the year, making year-round production viable without the need for supplemental lighting. However, Southern AZ is experiencing population growth, reductions in water supplies due to increased demands, a history of unconstrained water withdrawals, and prolonged drought (Jacobs and Worden, 2004).

Greenhouse crop production has been recognized as a potential solution for reducing the demand on resources such as water (Jensen, 1996). In a world where 70% of fresh water is used for irrigation, finding alternatives to traditional farming and irrigation practices will be essential for earth's growing population (Jongebreur, 2000). In arid and

semi-arid regions around the world, water used for irrigation is as high as 91% in the Middle East and 85% in Asia and Africa (Ragab and Prudhomme, 2002). In those regions of the world, the majority of farms use surface (or flood) irrigation practices, creating huge inefficiencies of water use.

In Arizona, where most farmland is located in semi-arid regions of the state, irrigation accounts for 80% of the state's used freshwater, 15% greater than the national average (USGS, 2004). Although the average irrigation application rate in the United States has decreased 30% since 1950 (with most reductions occurring after 1980), only 52% of total irrigable acres use sprinklers and microirrigation systems (USGS, 2004). Based on these data, there is a real need for creating agricultural practices to decrease water consumption for food production.

Although reducing overall water use for agriculture is important, with increasing world populations, it may become even more critical to increase food productivity with existing water resources, especially in water-starved countries (Qadir *et al.*, 2003). Hydroponic greenhouse production systems are poised to provide solutions to both water conservation and food productivity issues. Hydroponic systems used in greenhouses can reduce the water required to irrigate a crop by reducing losses during water conveyance to the crop, evaporation from the root media, and losses to deep percolation (Mpusia, 2006).

Water use efficiency (*WUE*) is commonly used to describe the relationship between water input and subsequent agricultural production output (Fairweather *et al.*, 2004). The total water applied to a crop is typically compared either to water used by the

plants (Plant water uptake/Total water applied), to crop production outputs (Yield/Total water applied), or to economic returns (Gross return/Water delivered to field). Fresh weight or dry weight yields may be used to calculate *WUE* depending on the application. For crop production systems, fresh weight is most commonly used because it ultimately determines the grower's economic return.

In the San Joaquin Valley of California, where summer conditions are comparable to Tucson, AZ, the water use efficiency (*WUE*: *kg tomato yield/ m³ water applied*) for tomato production was shown to be 10-12 kg m⁻³ for flood irrigation, 11-19 kg m⁻³ for sprinkler irrigation, and 19-25 kg m⁻³ for drip irrigation (Hanson *et al.*, 2006; Hanson and May, 2005; Hanson and May, 2004). Field *WUE* for drip-irrigated tomato production in Israel has been reported as 25 kg m⁻³ in the fall (Ben-Gal and Shani, 2003). Flood irrigation of tomato in India has produced a *WUE* of 5 kg m⁻³ (Mahajan and Singh, 2006).

Many researchers have reported much higher *WUE* values for greenhouse tomato production. Open hydroponic irrigation systems (no recirculation of unused water by plants) in the Netherlands and France have been reported as 45 and 39 kg m⁻³, respectively (Pardossi *et al.*, 2004). Closed irrigation systems (recirculated irrigation water) have been shown to achieve *WUE* values of 66 kg m⁻³ in the Netherlands, and 25 and 30 kg m⁻³ in the warmer climates of Spain (Reina-Sanchez, 2005) and Italy (Incrocci *et al.*, 2006), respectively.

However, none of those projects included water use by the evaporative cooling system needed to maintain the greenhouse climate. Evaporative cooling reduces the air temperature and raises the relative humidity inside the greenhouse by converting sensible

heat into latent heat by evaporation. In semi-arid climates, ventilation alone is not always adequate for cooling the greenhouse, especially during the summer and often on summer nights and during sunny, winter days. Therefore, water use by the evaporative cooling system is important to consider when comparing water use of greenhouse and field crop production.

A handful of studies have examined water use by evaporative cooling systems. An early study using a small-scale model of a pad-and-fan system observed water use rates ranging from 18 to 84 g m⁻² s⁻¹ (Al-Massoum *et al.*, 1998). Another study performed in Saudi Arabia (arid climate) observed much lower water use with a full-scale pad-and-fan system, with water use rates ranging from 0.21 to 0.41 g m⁻² s⁻¹ for ventilation rates of 0.0285 and 0.057 m³ m⁻² s⁻¹ (Al-Helal, 2007).

Sabeh *et al.* (2006) demonstrated that increasing the ventilation rate increased water use by the pad-and-fan cooling system, with water use rates ranging from 0.145 to 0.79 g m⁻² s⁻¹ from the lowest (0.017 m³ m⁻² s⁻¹) to highest (0.079 m³ m⁻² s⁻¹) ventilation rate tested, respectively. The same study also demonstrated that if high ventilation rates were mitigated, water use by the pad-and-fan system could be conserved, often without detriment to the greenhouse conditions.

In regions where evaporative cooling is required, naturally ventilated greenhouses can be easily supplemented with high-pressure fog cooling systems. However, only one study to date has evaluated water use by the high-pressure-fog system in conjunction with natural ventilation in a semi-arid climate. In this study, fog injection was controlled by temperature setpoint and ventilation rate was changed to control relative humidity (Sase

et al., 2006). Increasing the ventilation rate increased the fog system operation, producing water use rates of $0.3 - 0.35 \text{ g m}^{-2} \text{ s}^{-1}$, with ventilation rates ranging from 0.0167 to $0.059 \text{ m}^3 \text{ m}^{-2} \text{ s}^{-1}$. No study thus far has evaluated water use by a high-pressure-fog system used with mechanical ventilation.

None of these studies, however, have examined water use by the evaporative cooling systems in terms of water use efficiency (*WUE*). Generally, *WUE* values are recorded in terms of irrigation water use; however, due to the necessity of using evaporative cooling systems in semi-arid climates, knowing the *WUE* based on all greenhouse water systems would improve the comparisons of field and greenhouse crop production systems. It is believed that when high greenhouse yields are combined with water use rates of the evaporative cooling system that greenhouse crop production will prove to be a water-conservation strategy for agricultural food production.

The purpose of this project was to determine the amount of water and water use efficiency of two commonly used evaporative cooling systems: pad-and-fan and high-pressure-fog with fan ventilation. Water use efficiency values were also calculated for a hydroponically-grown tomato crop and compared to *WUE* values reported for field production of tomatoes using flood, sprinkler, and drip irrigation methods.

2. LITERATURE REVIEW

2.1 Energy and Water Balance on the Greenhouse

2.1.1 Energy Balance

Energy transfer into and out of the greenhouse affects the internal environment, and ultimately determines what systems are needed for environmental control. Using the greenhouse air as the control volume of interest, the control surface is composed of the glazing, the ground, components within the greenhouse, and any open points of entry, including vents and gaps in the structure. Therefore, energy transferred across these surfaces involves both sensible and latent heat exchanges (Boulard and Wang, 2000).

The energy balance equation is represented by Figure 2.1 and the following equation:

$$Q_R + Q_G + Q_V + Q_S + Q_P + Q_L + Q_H = 0 \quad (2.1)$$

Q_R represents heat transfer by radiation. Q_G is the heat transfer across the glazing, and depends on the temperature difference between the outside and inside air to transfer energy both by conduction and convection. Q_V is the heat transfer by ventilation, which removes energy from the greenhouse via air exchange. Q_S is the heat transfer between the ground and greenhouse air and depends on their temperature difference. Q_P is the heat transfer by the various greenhouse components, including structural components, working systems, and evapotranspiration of plants, which transfer latent heat energy to the greenhouse air. Q_L is the latent heat transfer of sensible energy in the air to water in the form of fog droplets, when present. Finally, Q_H is the heat added to the greenhouse using a heater.

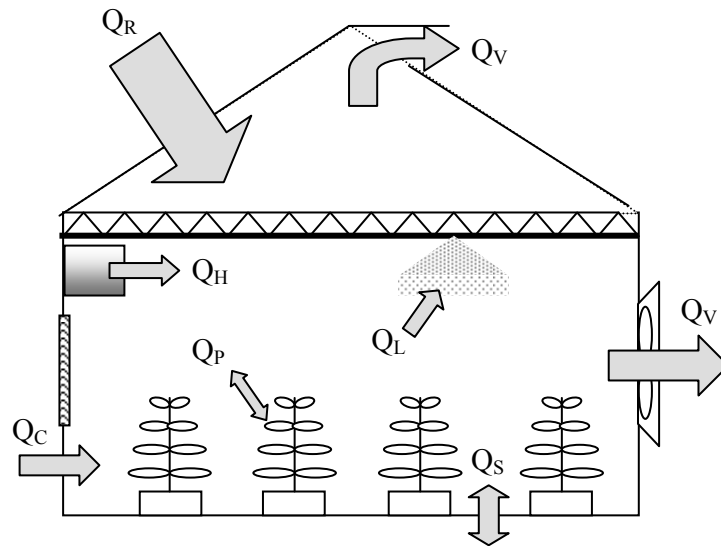


Figure 2.1 Heat transfer in the greenhouse energy balance include radiation (Q_R), conduction and convection across the glazing (Q_G) and the soil (Q_S), ventilation (Q_V), internal greenhouse components such as plants (Q_P), latent heat transfer to water (Q_L), and any operating heating units (Q_H).

2.1.2 Water Vapor Balance

Plants depend on water delivery to their roots (irrigation) to maintain structural form and to deliver water and nutrients throughout the plant via transpiration. Plant transpiration also depends on the concentration of water vapor in the air, which creates a differential in vapor pressure between the plant leaf and the air (Boulard and Wang, 2000). This vapor pressure deficit (VPD) drives moisture from the plant into the air.

The moist air conditions are determined by the transfer of water vapor into and out of the greenhouse. Using the greenhouse air as the control volume, the control surfaces include the glazing, ground, plants, and any open points of entry, including vents and gaps in the structure. Therefore, water vapor transferred across these surfaces will

comprise the water balance equation, which is represented by Figure 2.2 and the following equation:

$$E_V + E_C + E_S + E_T = 0 \quad (2.2)$$

E_V is the water vapor that enters or exits the greenhouse via ventilation, E_C is the water vapor input by the evaporative cooling system, E_S is the water vapor evaporating from the soil and hydroponic components, and E_T is the water vapor input by plant transpiration.

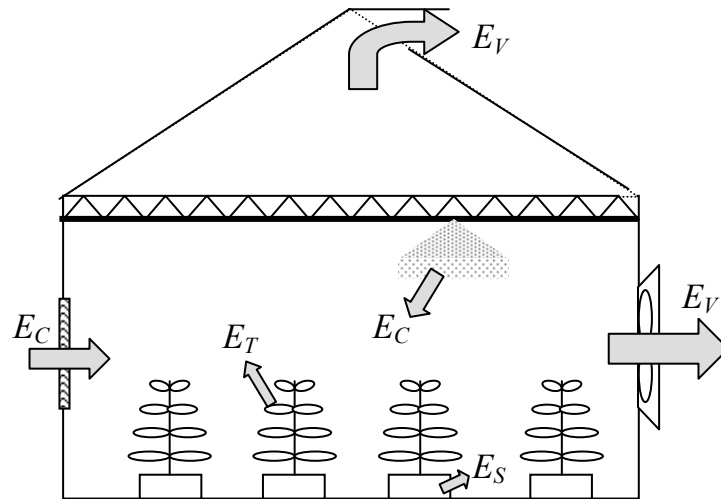


Figure 2.2 Water vapor transfer in the greenhouse include ventilation (E_V), evaporative cooling systems (E_C), evaporation from the soil and hydroponic system (E_S), and plant transpiration (E_T).

2.2 Greenhouse Cooling

When the heat influx produces high greenhouse air temperatures, it is desirable to remove heat quickly and reduce the effects of energy gain on the greenhouse. The two primary methods of doing this are ventilation and evaporative cooling. Ventilation will remove heat from the greenhouse and, if air exchange rates are high enough, can at most

reduce the greenhouse air temperature to the ambient outside condition. Evaporative cooling (Q_L) reduces the inside air temperature to below outside levels by transferring sensible heat from the air (or plants via evapotranspiration) into latent heat energy. The evaporative cooling process may occur by transferring heat from the inside air to water in the greenhouse (eg. high-pressure-fog and mist systems). Evaporative cooling may also cool the outside air before it enters the greenhouse, providing pre-cooled air to the greenhouse (eg. pad-and-fan system). Ventilation provides the air exchange that makes continued evaporative cooling possible, and is necessary for the process to continue. Without ventilation the greenhouse air would reach saturation, stop evaporation, and provide no further cooling

2.2.1 Ventilation

Ventilation is typically the first step taken toward cooling the greenhouse. Ventilation is the process of air exchange that removes heated and humidified air from the greenhouse and replaces it with fresh outside air. The two primary methods of ventilation are mechanical and natural.

2.2.1.1 Mechanical Ventilation

Mechanical ventilation (MV) employs the use of fans to provide air exchange. Typically fans are located along the wall at one long end of the greenhouse. Vent inlets may be located along the opposite wall, along the side walls, or even in the roof (Arbel *et al.*, 2003). One of the primary advantages to using MV is the ability to control ventilation rates. Another advantage is in knowing the direction and speed of airflow in

the greenhouse. The main disadvantages to MV are the use of energy and maintenance, and the creation of non-uniform conditions within the greenhouse (ASABE, 2006).

2.2.1.2 Natural Ventilation

Air exchange by natural ventilation (NV) relies on pressure differences between the outside and inside created by wind (forced convection) and temperature gradients (natural convection) (ASABE, 2006). The major advantage to NV systems is that there is essentially zero operational cost (Willits and Li, 2005). However, because ventilation depends on outside conditions, air exchange rates and direction can be unpredictable. The configuration of vents is a very important consideration for designing natural ventilation systems. Studies have shown that windward vents increase the rate of air exchange but also decrease the uniformity of conditions within the greenhouse (Arbel *et al.*, 2003).

2.2.1.3 Ventilation Effects on Greenhouse Climate

The effects of solar radiation on greenhouse air temperature are reduced by increasing the ventilation rate (Critten and Bailey, 2002). Also, increasing the ventilation rate of both naturally and mechanically ventilated greenhouses has been shown to increase the uniformity of temperature and humidity (Boulard *et al.*, 2004; Willits, 2003a).

However, increasing the ventilation rate has a diminishing return when it comes to lowering the greenhouse air temperature, and little advantage has been shown to using ventilation rates greater than $0.035 \text{ m}^3 \text{ m}^{-2} \text{ s}^{-1}$ (Critten and Bailey, 2002) and $0.05 \text{ m}^3 \text{ m}^{-2} \text{ s}^{-1}$ (Willits, 2003a). Furthermore, without evaporative cooling in semi-arid climates, high

ventilation rates used to reduce greenhouse temperature may have the unwanted effect of removing too much moisture from the air (Boulard *et al.*, 2004). A study using computational fluid dynamics (CFD) supported this finding for arid climates ($T_{Out} = 45^{\circ}\text{C}$, $RH_{Out} = 10\%$), demonstrating that lower ventilation rates maintain higher relative humidities (Al-Helal and Short, 1999).

2.2.2 Evaporative Cooling

When used in conjunction with evaporative cooling, ventilation provides the means for latent energy transfer that cools and humidifies the air when outside conditions are too hot and too dry to provide the desired greenhouse climate. Several methods of evaporative cooling have been tested, including pad-and-fan, high-pressure-fog, low-pressure-mist, wetting the plants (Arbel *et al.*, 2003), and using a wet shade cloth both internally to evaporatively cool the air (Giacomelli *et al.*, 1985) and externally to evaporatively cool the roof (Ghosal *et al.*, 2003). This section will focus on pad-and-fan and high-pressure-fog systems, which are the two most common methods of evaporatively cooling the greenhouse and which were used in this study.

2.2.2.1 Pad-and-Fan Cooling

Pad-and-fan cooling uses fans to pull outside air through a wet pad. The air is cooled when sensible heat is transferred to the water, which evaporates and humidifies the air. Pad materials vary widely, from the common corrugated cellulose and aspen fiber (ASABE, 2006), to the experimental date-fronds leaves (Al-Massoum, 1998) and PVC sponges (Liao and Chiu, 2002).

Pad-and-fan cooling is often appraised in terms of its cooling efficiency, which is defined as:

$$\eta_{Cool} = \frac{T_{DB,Out} - T_{DB,In}}{T_{DB,Out} - T_{WB,Out}} \times 100\% \quad (2.3)$$

Where $T_{DB,Out}$ is the drybulb temperature of the air just outside the pad, $T_{DB,In}$ is the drybulb temperature just inside the pad, and $T_{WB,Out}$ is the wetbulb temperature of the air outside the pad, which is the minimum temperature the air could be cooled for its given moisture content.

The cooling efficiency of the pad-and-fan system has been shown to decrease with increased ventilation rates (Sabeh *et al.*, 2006; Liao and Chui, 2002). This reduction in η_{Cool} at higher ventilation rates was shown to be associated with reductions in the moisture content of the air leaving the pad, presumably due to shorter contact time with the wet pad (Liao and Chui, 2002).

The performance of the pad-and-fan system, and thus η_{Cool} , is greatly affected by the outside air conditions. For a freely transpiring crop, Landsberg *et al.* (1979) showed that the inside air temperature was 3°C less for dry conditions ($T_{Out} = 40^\circ\text{C}$, $RH_{Out} = 30\%$, $VPD_{Out} = 5.2$ kPa) than for more humid conditions ($T_{Out} = 30^\circ\text{C}$, $RH_{Out} = 50\%$, $VPD_{Out} = 2.1$ kPa). Another recent modeling study showed the temperature reduction across the pad increases from 5°C under warm, humid outside conditions ($T_{Out} = 35^\circ\text{C}$, $RH_{Out} = 70\%$, $VPD_{Out} = 1.7$ kPa) to 15°C for warm, dry outside conditions ($T_{Out} = 35^\circ\text{C}$, $RH_{Out} = 25\%$, $VPD_{Out} = 4.2$ kPa) when the same ventilation rate is used (Kittas *et al.*, 2003).

Increasing the ventilation rate can improve cooling by removing more sensible heat from the greenhouse and introducing evaporatively cooled air more quickly (Al-Helal, 2007; Sabeh *et al.*, 2006; Willits, 2003a; Kittas *et al.*, 2003; Al-Jamal, 1994). Higher ventilation rates also reduce the temperature rise from pad to fan (Sabeh *et al.*, 2006; ASABE, 2006; Willits, 2003a; Kittas *et al.*, 2003; Landsberg *et al.*, 1979). However, for a mature tomato crop, good temperature uniformity around the plant canopy area may be observed (Sabeh *et al.*, 2006).

Research has also shown that increasing the ventilation rate reduces the amount of water evaporated from the pad per unit of air, and if airflow across the pad is high enough, cooling and humidification of the air will actually be compromised (Sabeh *et al.*, 2006; Liao and Chui, 2002). When pad-and-fan system is used with a freely transpiring crop, ventilation rates around $0.035 \text{ m}^3 \text{ m}^{-2} \text{ s}^{-1}$ have been shown to optimize temperature reduction without over-dehumidifying the greenhouse regardless of outside conditions or greenhouse type and size (Critten and Bailey, 2002; Landsberg *et al.*, 1979).

Models have also been developed to predict changes in air temperature and moisture levels with distance from the cooling pad. One model was developed that predicted reductions in air and leaf temperature at ventilation rates greater than $0.05 \text{ m}^3 \text{ m}^{-2} \text{ s}^{-1}$ (Willits, 2003b). However, the model only considered outside humidity ratios greater than 9 g kg^{-1} , and most data were reported for levels greater than 14 g kg^{-1} . Another model predicted a 10°C rise across a 60 m-long unshaded greenhouse, and a 7°C rise for a shaded greenhouse with roses (Kittas *et al.*, 2003). This model was developed for an outside air temperature of 35°C and humidity ratio of 8.8 g kg^{-1} ($RH_{Out} = 25\%$).

2.2.2.2 High-Pressure-Fog Cooling

High-pressure-fog cooling is usually accomplished by delivering very fine water droplets (0.5 to 50 μm diameter) to the air inside the greenhouse (ASABE, 2006). Fog nozzles can be distributed throughout the greenhouse, giving the system great potential to produce the most uniform greenhouse conditions (Arbel *et al.*, 2003; Arbel *et al.*, 1999).

Mechanical or natural ventilation can be used in conjunction with fogging. Good uniformity of greenhouse conditions has been attained with both mechanical ventilation (Arbel *et al.*, 2003) and natural ventilation (Ozturk, 2003). Mechanical ventilation has been shown to create more uniform conditions when the ventilation rate is higher (Giacomelli *et al.*, 1985).

Ventilation rate is important to facilitate evaporative cooling and maintain desired moisture levels. Many studies have demonstrated that evaporation is enhanced, and thus cooling, when the relative humidity inside the greenhouse is low (Ozturk, 2003; Arbel *et al.*, 1999). Sase *et al.* (2006) proposed that ventilation rate be used to control the humidity levels in the greenhouse, and thus mitigate the use of fog. It is also important to consider that higher levels of outside relative humidity will require greater ventilation rates to promote the evaporation of fog (Arbel *et al.*, 2003). However, reductions in dry bulb temperature may be limited by these higher outside moisture levels.

Finally, greater decreases in air temperature than leaf temperature have been observed during fogging (Willits, 2005; Critten and Bailey, 2002).

2.2.3 Shading

Reducing the incoming solar radiation by use of internal or external shade cloths or whitewashing has been shown to effectively reduce the greenhouse air temperature, both with and without evaporative cooling. For external shade cloths, white materials tend to reduce the energy gain and air temperature rise of the greenhouse more than the black shade materials (Willits, 2001). The same study, however, showed that black materials reduced the leaf temperature more than white materials. Reducing light transmission into the greenhouse from 60% to 40% by whitewashing the roof was also shown to reduce the temperature gradient from pad to fan by 2°C without a change in ventilation rate (Kittas *et al.*, 2003).

2.3 Water Use for Tomato Crop Production

2.3.1 Water Use for Field Tomato Crop Production

The only source of water use in field crop production is for irrigation. There are three primary methods of irrigation, including flood, sprinkler, and drip,

In the San Joaquin Valley of California, where summer conditions are comparable to Tucson, AZ, the *WUE* for tomato production was shown to be 10-12 kg m⁻³ for flood irrigation, 11-19 kg m⁻³ for sprinkler irrigation, and 19-25 kg m⁻³ for drip irrigation (Hanson *et al.*, 2006; Hanson and May, 2005; Hanson and May, 2004). Field *WUE* for drip-irrigated tomato production in Israel has been reported as low as 8 kg m⁻³ in the spring and up to 25 kg m⁻³ in the fall (Ben-Gal and Shani, 2003). And in India flood irrigation has produced a *WUE* of 5 kg m⁻³ (Mahajan and Singh, 2006).

2.3.2 Water Use for Greenhouse Crop Production

2.3.2.1 Irrigation Water Use

When greenhouse plants are grown in a soilless, hydroponic system, the water is delivered to each plant with a drip tube and the excess water not used by the plants is drained away from the media. This drained water may either be discarded as waste water or be recycled for subsequent irrigations or used for another purpose. An irrigation system that discards all of the drained water is called an “open” irrigation system, and one that recycles all or a portion of the drained water is called a “closed” irrigation system. The amount of water that is used for irrigation largely depends on whether an open or closed irrigation system is used in the greenhouse.

Water use efficiency (*WUE*), the ratio of yield to irrigation water use, is often used as a measure of water use for greenhouse irrigation systems. Open irrigation systems have been shown to produce *WUE* values of 29-33 kg m⁻³ in Italy (Incrocci *et al.*, 2006), and as high as 39 and 45 kg m⁻³ in France and the Netherlands, respectively (Pardossi *et al.*, 2004). The *WUE* values of closed irrigation systems have been reported as 25 kg m⁻³ in Spain (Reina-Sanchez *et al.*, 2005) and as high as 66 kg m⁻³ in the Netherlands (Pardossi *et al.*, 2004).

Deficit irrigation practices have demonstrated increases in *WUE* due to reductions in water use (Kirda *et al.*, 2004), and in some cases increases in yield (Mahajan and Singh, 2006). However, these *WUE* values were still low relative to non-deficit irrigation practices, with values ranging between 10 and 20 kg m⁻³. Finally, flood irrigation can be used in the greenhouse when plants are grown in soil, and *WUE* values have been

reported as low as 7 kg m^{-3} , a value similar to flood irrigation in the field (Mahajan and Singh, 2006).

2.3.2.2 *Evaporative Cooling Water Use*

Information about water use by evaporative cooling systems has been limited. One study used a $0.65 \text{ m} \times 0.7 \text{ m}$ pad model in a tunnel system to test the water consumption efficiency of different wet pad materials, defined as the percentage of water delivered to the pad that was evaporated and used for cooling (Al Massoum *et al.*, 1998). These efficiencies ranged from 54 – 81% depending on material (Cel-Dek® vs. Date Fronds Mat), air flow rate, and water flow rate. From these reported efficiencies, the water use rates of the Cel-Dek® pad (corrugated cellulose) could be deduced as 0.0286 and $0.0176 \text{ L m}^{-2} \text{ s}^{-1}$ for an air speed across the pad of 1.39 m s^{-1} and water flow rates to the pad of 0.083 and $0.042 \text{ L m}^{-2} \text{ s}^{-1}$, respectively. For a lower air speed across the pad (0.9 m s^{-1}) the water use rates were 37.3 and $17.7 \text{ g m}^{-2} \text{ s}^{-1}$ for the same water flow rates of 0.083 and $0.042 \text{ L m}^{-2} \text{ s}^{-1}$, respectively.

A more recent study used a single-span, gutter-connected greenhouse in semi-arid conditions ($T_{Out,Avg} = 38.5^\circ\text{C}$, $RH_{Out,Avg} = 15\%$) to measure water use and cooling efficiency under different ventilation rates (Sabeh *et al.*, 2006). The study found that water use per floor area increased linearly with increasing ventilation rate, with values of 0.145 , 0.182 , 0.51 , 0.67 , and $0.79 \text{ g m}^{-2} \text{ s}^{-1}$ for ventilation rates of 0.017 , 0.037 , 0.051 , 0.067 , and $0.079 \text{ m}^3 \text{ m}^{-2} \text{ s}^{-1}$, respectively. When the pad-and-fan cooling system was

controlled for daytime (24°C) and nighttime (18°C) air temperatures, it used 14.8 L m⁻² day⁻¹.

Another recent study looked at water use by a pad-and-fan cooling system (Cel-Dek®) in a Quonset-style greenhouse filled with cucumber plants under arid conditions ($T_{Out,Avg}=38.7^{\circ}\text{C}$, $RH_{Out,Avg}=11\%$) (Al-Helal, 2007). The study found the maximum daily water use per floor area occurred during the hottest time of day (12:00-13:00) and was 0.21 and 0.41 g m⁻² s⁻¹ for ventilation rates of 0.0285 and 0.057 m³ m⁻² s⁻¹, which represented 0.5 and 1.0 air exchange rates per minute, respectively.

Water use by the high-pressure-fog system has been more limited than for pad-and-fan cooling. A recent study found that increasing the vent area opening, and thus the air exchange rate, increased the fogging rate when the high-pressure-fog system was controlled for air temperature (Sase *et al.*, 2006). When the natural ventilation rate was increased from 0.0167 to 0.059 m³ m⁻² s⁻¹, the rate of fog water use increased from 0.3 to 0.33 g m⁻² s⁻¹.

2.4 Plant Responses to Greenhouse Climate

Transpiration rate (E_T) and leaf temperature (T_{Leaf}) are the two most common parameters used to study plant responses to their greenhouse climate. Other plant responses that can be measured are leaf water potential (Ψ_L), stomatal conductance (g_s), and CO₂ exchange rate. This section will focus on measurements of E_T and T_{Leaf} .

2.4.1 Plant Responses

2.4.1.1 Environmental Effects on E_T

VPD is a major driving component of E_T . Many studies have shown that E_T decreases with increasing VPD and decreasing relative humidity (Prenger *et al.*, 2002; Jolliet and Bailey, 1992). Though it has also been observed that plants grown in greenhouses do not respond as much to changes in VPD , presumably because VPD fluctuations are small (Jarvis, 1985). Also, several studies have demonstrated that increasing the relative humidity with fog or mist systems have reduced E_T (Katsoulas *et al.*, 2001; Urban and Langelez, 2001).

When VPD changes are small, solar radiation becomes an increasingly important factor driving E_T . Some studies have shown a linear relationship between E_T and solar radiation (Baille *et al.*, 1994; Jolliet and Bailey, 1992), whereas other studies have shown very poor correlation (0.1-0.2) between the two variables (Willits, 2003b). This poor correlation seems to be especially true when solar irradiance is greater than 300 W m^{-2} , and E_T has been shown to level off (Prenger *et al.*, 2002). This result supports other studies that plants grown in greenhouses tend to adjust their E_T until reaching a stable equilibrium dictated by the net radiation received (Boulard and Wang, 2000). When the VPD is low due to misting (and other evaporative cooling techniques), a reduction in stomatal conductance has been observed, regardless of solar radiation levels, which may signal a reduction in E_T (Baille *et al.*, 1994). Solar radiation alone seems to be a poor predictor of E_T throughout the day, where VPD and relative humidity conditions always provide a good correlation with E_T (Prenger *et al.*, 2002; Kittas *et al.*, 2001).

Plant E_T has also been positively correlated with high airspeeds as air movement reduces stomatal resistance (Jolliet and Bailey, 1992). Other studies, however, have demonstrated that ventilation rates up to $0.13 \text{ m}^3 \text{ m}^{-2} \text{ s}^{-1}$ have little effect on E_T (Willits, 2003).

Finally, studies have shown that the smallest internal resistance to E_T occurs at 23-25°C for several varieties of tomato plants, which may indicate the temperature range where plants transpire best (Papadakis *et al.*, 1994). However, other studies have contradicted that deduction, showing no correlation between E_T and air temperature (Jolliet and Bailey, 1992).

2.4.1.2 Environmental Effects on T_{Leaf}

When only ventilation is used, T_{Leaf} of rose and tomato plants have been measured as 1-2°C lower than T_{Air} (Kittas *et al.*, 2001; Papadakis *et al.*, 1992). Furthermore, mechanical ventilation may reduce T_{Leaf} more than natural ventilation due to greater airspeeds across the surface of leaves (Willits, 2005). Evaporative cooling has been shown to reduce T_{Leaf} more than ventilation. Two separate studies have shown greater reductions in T_{Leaf} of tomato plants during pad-and-fan cooling than during high-pressure-fog cooling (Handarto *et al.*, 2005; Willits, 2005).

T_{Leaf} is greatly influenced by E_T , which is influenced by VPD , solar radiation, and air movement. A negative linear relationship has been found between T_{Leaf} and E_T (Kacira *et al.*, 2002), as well as between the difference in canopy and air temperature ($T_c - T_a$) and E_T (Tubaileh, 1986; Inoue *et al.*, 1990). Those results were supported by another study that found that T_{Leaf} decreased as VPD increased, a condition which would cause E_T

to increase (Kittas *et al.*, 2001). Interestingly, several studies have demonstrated that increasing the relative humidity with fog or mist systems have reduced T_{Leaf} even though E_T did not increase (Willits and Li, 2005; Katsoulas *et al.*, 2001; Urban and Langelez, 2001).

Studies have also demonstrated that the negative correlation between T_{Leaf} and E_T remained when E_T was normalized for solar radiation was subtracted from the E_T term, demonstrating that the plant effectively cools itself by removing more energy through E_T than it receives through radiation (Saha *et al.*, 1986, Inoue *et al.*, 1990).

T_{Leaf} has been shown to decrease with increasing ventilation rate up to $0.5 \text{ m}^3 \text{ m}^{-2} \text{ s}^{-1}$ under both hot (30°C , 20%) and mild (25°C , 62%) outside conditions (Seginer, 2002). Another study demonstrated that when evaporative cooling was used, T_{Leaf} was reduced for airflow rates up to $0.13 \text{ m}^3 \text{ m}^{-2} \text{ s}^{-1}$, but without evaporative cooling reductions in T_{Leaf} were only observed for ventilation rates up to $0.05 \text{ m}^3 \text{ m}^{-2} \text{ s}^{-1}$ (Willits, 2003b). Although these studies showed differences relative to air movement, the results were coupled to differences in VPD (eg. evaporative cooling vs. no evaporative cooling).

2.4.2 Measuring Plant Responses

2.4.2.1 E_T Measurement Methods

E_T can be directly measured by measuring sap flow, irrigation water drained away from plant, and changes in plant weight.

Lysimeters are one of the most common methods of measuring E_T because they are considered very accurate at precise time intervals (Prenger *et al.*, 2002). They

measure transpiration by calculating the difference between the amount of water that is delivered to the plants and the amount of water that drains from the plant. Therefore, the lysimeter equation is:

$$E_T = E_{Drip} - E_{Drain} \quad [g, mL] \quad (2.4)$$

Other researchers have used Equation 2.4 as a measure of plant water uptake, rather than an estimate of E_T (Reina-Sanchez *et al.*, 2005).

Several greenhouse researchers have used lysimeters to measure E_T , often times with the goal of validating E_T models. Measurement practices by these researchers have ranged from measuring output every 10 minutes (Kittas *et al.*, 2001) to calculating a 60-minute average of 1-minute measurements (Boulard and Wang, 2000).

Sap flow measurements require gauges to be placed within the stems of plants (Nagler, et al., 2003). This method is not ideal because it is an invasive measure of E_T . Another method of measuring E_T is to use a weighing device such as a balance or load cell (Takakura *et al.*, 2005; Prenger *et al.*, 2002; Boulard *et al.*, 2002; Jolliet and Bailey, 1992).

2.4.2.2 T_{Leaf} Measurement Methods

T_{Leaf} can be measured with contact or non-contact sensors. The most common method of measuring T_{Leaf} is by inserting a very fine thermocouple (TC) wire into the veins of several leaves of a plant or several plants within the crop (Willits and Li, 2005; Fatnassi *et al.*, 2004; Boulard et al., 2002; Kittas *et al.*, 2001; Prenger et al., 2002; Papadakis *et al.*, 1994).

T_{Leaf} can be remotely measured using an Infrared (IR) thermometer, avoiding direct contact, and thus physical damage to the plant. Peñuelas *et al.* (1992) compared T_{Leaf} measured by IR thermometer and thermocouples placed in leaf veins of strawberry plants grown in greenhouses. A very high correlation was found between IR and TC measurements of T_{Leaf} ($r=0.986$, $n=108$, $P=0.001$). Therefore, it was determined that IR thermometry was an acceptable measurement of T_{Leaf} .

2.5 Wind Tunnel Modeling with Particle Image Velocimetry (PIV) Measurements

Obtaining results for a scaled-down greenhouse can improve the design of vent configurations, height, fog nozzle placement, etc. prior to building the full-scale structure. Low-speed wind tunnels have been shown to provide a rapid, economical, and accurate measure of fluid flow characteristics for structures such as greenhouses (Lee *et al.*, 2003). The wind tunnel can provide valuable information regarding the aerodynamics of fluid flow within and around the naturally-ventilated greenhouse structure because it can provide large quantities of information based on the true complexity of fluid flow. Using particle image velocimetry (PIV) in conjunction with wind tunnel procedures has been shown to provide useful quantitative visualization results.

Wind tunnel studies have been performed on several types of greenhouses with different vent configurations. One study demonstrated different circulating patterns of airflow in a two-span greenhouse with fully opened roof and a venlo-type roof (Lee *et al.*, 2003). Air entered the fully-opened roof at the leeward end and then traveled down the leeward sidewall, across the greenhouse, and up and out the windward roof. For the

venlo-type roof, air entered at the windward end and then developed a clockwise pattern of airflow within the greenhouse.

The same study also tested 6-span greenhouses with the same vent configurations (Lee *et al.*, 2003). The same pattern of airflow was observed for the fully-opened roof, with air entering through the roof of the sixth span and then circling around to travel across the greenhouse and out of the windward roof. The venlo-type roof produced clockwise circular patterns within pairs of spans and indicated that air entered the roof of spans 2, 4, and 6. Furthermore, the airflow near the gutter for the venlo-type roof was very weak.

Another wind tunnel study examined the effect of roof and side vent configuration on temperature distribution inside a multi-span greenhouse (Kacira *et al.*, 2005). The study showed that temperatures in a multi-span greenhouse were more uniform when both roof and side vents were used. The study also showed that higher wind speeds decreased the internal temperature.

2.6 State of the Art

In many semi-arid climates around the world, the availability of water in semi-arid climates tends to be low. Yet due to the high evapotranspiration potential in these climatic regions, irrigation rates for crop production tend to be very high, often with 90% of fresh water sources used for agriculture. Therefore, reducing water use and increasing the water use efficiency of crop production in these regions is of utmost importance. Greenhouse crop production has been shown to reduce irrigation water requirements and produce yields that are typically 5 – 10 times greater than in the field. These results

suggest that greenhouse crop production may provide an agricultural water-use solution for semi-arid regions.

Evaporative cooling systems are essential for growing greenhouse crops through the summer season and throughout the year in semi-arid climates, as they provide the latent heat transfer to reduce greenhouse temperatures below outside levels. The few studies that have evaluated water use by evaporative cooling systems have not compared it to water use for irrigation. Furthermore, no reported study has demonstrated the water use efficiency of greenhouse crop production.

3. OBJECTIVES

The overall goal of this project was to determine water use by greenhouse evaporative cooling systems operated in semi-arid climate conditions. Two evaporative cooling systems were studied: pad-and-fan and high-pressure fog. The results of this project will be used to recommend improved operational procedures for the two systems that will achieve desired greenhouse conditions using the least amount of water. These results will also aid in design improvements of evaporative cooling systems that use less water to control the greenhouse climate. Finally, the water use data will be used to define and compare the overall water use and water use efficiency (*WUE*) of greenhouse tomato production and compared to field crop production systems.

To achieve this goal, the following objectives were pursued:

1. Measure the water use of a pad-and-fan cooling system for several ventilation rates, and measure the resulting greenhouse conditions and plant responses (water use and leaf temperature).
2. Measure the water use of a high-pressure-fog cooling system for several ventilation rates with water injection controlled by temperature setpoint, and measure the resulting greenhouse conditions and plant responses (water use and leaf temperature).
3. Calculate a total system water use efficiency value for greenhouse tomato production, which includes the using water use by the pad-and-fan and irrigation systems and tomato crop yields, when greenhouse air temperature is controlled with the pad-and-fan cooling system under semi-arid summer conditions.

4. Estimate water use and predict greenhouse inside air temperatures by the pad-and-fan and high-pressure-fog systems using energy balance equations.
5. Study the airflow patterns and temperature distributions within the naturally ventilated greenhouse using a $1/15$ scale model in a wind tunnel and the full-scale greenhouse.

4. METHODS AND MATERIALS

4.1 Greenhouse used for Experiments

All experiments used one of two identical single-span, arched-roof greenhouses (Poly-Tex, Inc., Castle Rock, MN, USA) located in Tucson, AZ, USA (32.3°N, 110.9°W), with the north end oriented 30° west of north (Figure 4.1). The arched roof was comprised of air-inflated, double-polyethylene film (6 mil) glazing (Green-tek, Edgerton, WI, USA). Double-wall acrylic-coated polycarbonate structured sheets (Green-tek, Edgerton, WI, USA) covered the end walls and sidewalls, except for the sidewall roll-up curtains, which were reinforced, translucent double-polyethylene material. Thrip-grade exclusion screens with 0.25 opening ratio and 0.28 mm diameter covered the sidewall vent openings (25 m x 1.5 m), which were 0.61 above the ground and 1.52 m below the gutter.

An internal, movable 50% shade screen (Ludvig Swensson Inc., Charlotte, NC, USA) was mounted 3.4 m above the floor. It spanned from gutter to gutter (9.8 m) and was deployed from truss to truss (4 m). A computer control system (Argus Control Systems Ltd., White Rock, BC, Canada) was used to operate all cooling-related systems in the greenhouse. The greenhouse floor area was 278 m², with a volume of 1092 m³ below the shade curtain, and a total volume of 1688 m³. The two greenhouses were 9.8 m apart from each other, and could be used for side-by-side tests.

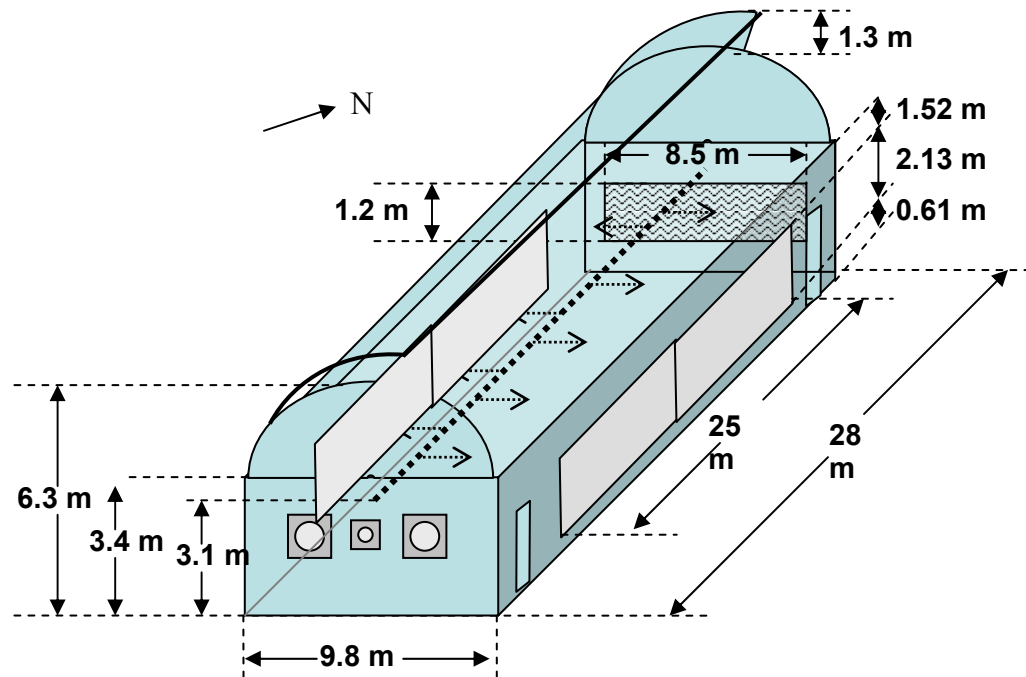


Figure 4.1 Schematic of greenhouse used for cooling experiments shows the location of the evaporative cooling pad (north wall), central, overhead high-pressure-fog line (center of greenhouse), exhaust fans (south wall), and natural ventilation openings (east and west walls, and roof).

4.1.1 Evaporative Cooling Pad

The pad-and-fan system (Val-Co, Bird In Hand, PA, USA) used a 15-cm thick cellulose pad (8.5 m x and 1.2 m), with the bottom edge 1.3 m above ground level (Figure 4.2). The pad was located at the north end of the greenhouse. During tests, water was pumped continuously to an overhead distribution trough, which gravity-fed water to the pad. Once the pad was saturated, all water that was not evaporated from the pad was returned to the sump tank. Water that was evaporated from the pad was continually replenished with a makeup water line that maintained a constant sump tank volume. All pad-and-fan tests were completed with both the roof and sidewall natural vent inlets fully closed.

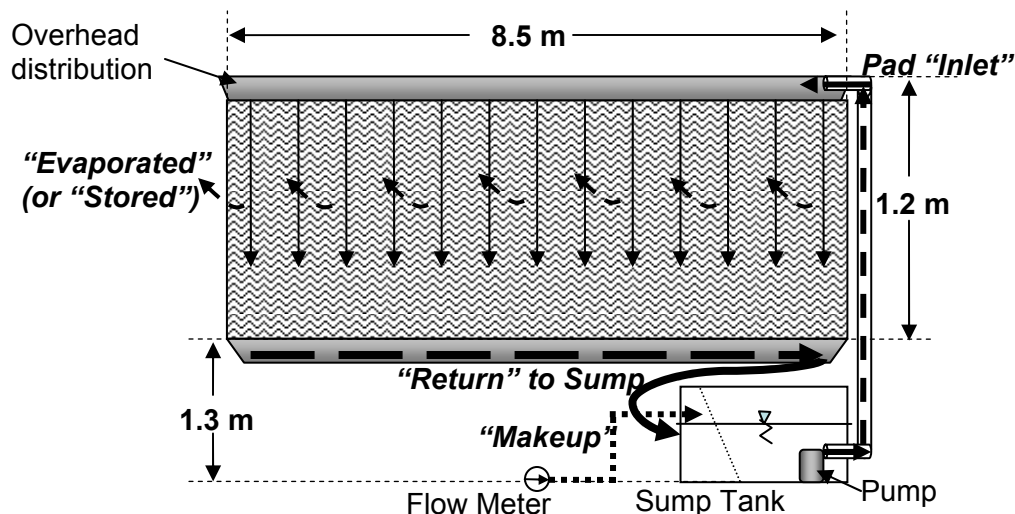


Figure 4.2 Schematic of the pad for the pad-and-fan system, including a 15-cm thick cellulose pad, inlet water, sump return, storage tank, and pump.

4.1.2 High-Pressure-Fog System

The high-pressure-fog system (Val-Co, Bird In Hand, PA, USA) operated at 8960 kPa (1300 psi) and injected fog droplets with less than 50 μm diameter. Several locations of fog injection were studied, including at the vent inlet (north wall), along the east and west walls near to the height of the gutters, and along the center of the greenhouse from inlet to exhaust at 3.1 m above the ground. All high-pressure-fog system tests were completed with both the roof and sidewall natural vents inlets fully closed, except during airflow validation tests of the wind tunnel experiments.

4.1.2.1 Multiple Inlet Fog Nozzle Lines

Four 8.5 m-long fog lines were hung horizontally inside the greenhouse 1.2 m away from the inlet (Figure 4.3). The bottom line was 1.2 m above the floor with each additional line spaced 0.46 m vertically above the line below it. Each line had 36 nozzles

spaced 0.23 m apart that were pointed away from the inlet and toward the plants. Fog delivery rates were 0.219, 0.429, 0.622, and 0.808 g m⁻² s⁻¹ for operation of one line, two lines, three lines, and four lines, respectively.

4.1.2.2 Single Inlet Fog Nozzle Line

The single inlet fog line of nozzles was placed 0.1 m distance from the inside surface of the pad inlet near its bottom edge 1.3 m above the floor (Figure 4.3). Twenty-six nozzles were spaced 0.30 m apart and pointed upwards. When used in conjunction with the central, overhead line, this single inlet fog line delivered 0.16 g m⁻² s⁻¹.

4.1.2.3 Central, Overhead Fog Nozzle Line

The central, overhead fog line was mounted in the center of the greenhouse, from inlet to exhaust, at a height of 3.1 m above the floor. Forty-eight nozzles were spaced 0.5 m apart and alternated in east and west directions (Figure 4.3). To minimize the free water droplets in the exhaust air, no fog nozzles were placed beyond the southern plant zone edge (8 m from the fan). To reduce exhaust of free water droplets through the fans, no fog nozzles were operated beyond the southern plant zone edge.

When operated with the single inlet fog line, each nozzle injected water at a rate of 0.007 g m⁻² s⁻¹, with a total continuous delivery rate of 0.36 g m⁻² s⁻¹. When operated by itself, each nozzle injected water at a rate of 0.008 g m⁻² s⁻¹, producing a total water delivery rate by the central, overhead line of 0.41 g m⁻² s⁻¹ during continuous operation.

4.1.2.4 Side Wall Gutter Fog Nozzle Lines

The side wall gutter fog line of nozzles mounted along the length of the east and west walls near to the gutters was also tested. Both lines were mounted 3.1 m above the floor, or 0.3 m below the actual gutter height, and 0.3 m from the side wall of the greenhouse. They were each 22 m long, starting 1.2 m from the inlet end of the greenhouse and ending 4 m from the fan end of the greenhouse. Each line had a total of 80 nozzles, spaced 0.30 m apart and each delivering $0.005 \text{ g m}^{-2} \text{ s}^{-1}$ of fog when both lines were operated simultaneously. Together both lines delivered a total of $0.90 \text{ g m}^{-2} \text{ s}^{-1}$ of fog water to the greenhouse.

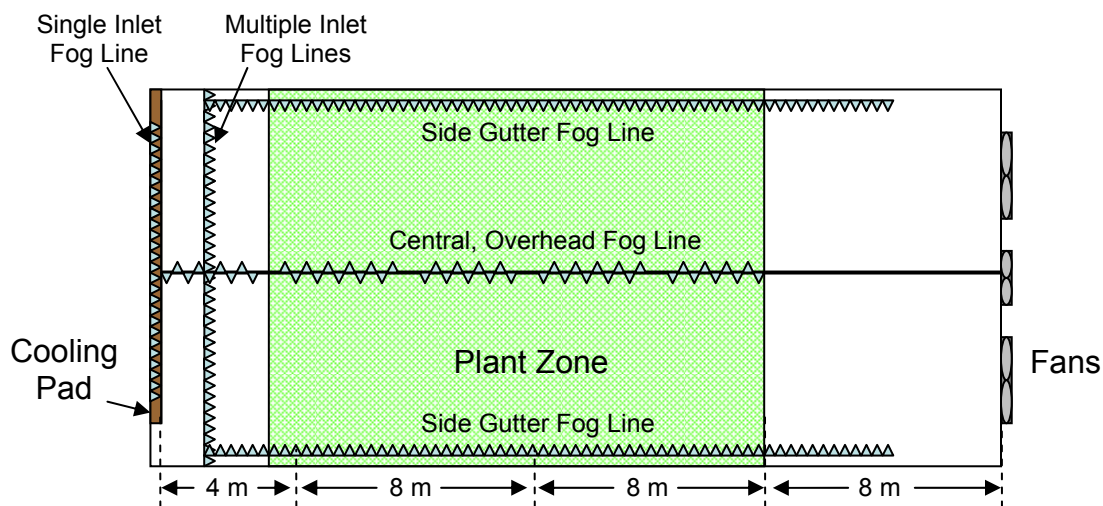


Figure 4.3 Location of the fog lines – multiple inlet, single inlet, side gutter, and central, overhead fog lines – used during high-pressure-fog tests in relation to the plant zone, inlet vent/cooling pad, and exhaust fans.

4.1.3 Ventilation System

Three exhaust fans were used to produce the selected ventilation rates and were located at the south wall of the greenhouse (Figure 4.1). Four ventilation rates were

tested to determine the water use by the pad-and-fan and high-pressure-fog cooling systems. There were two fixed speed, belt driven fans, “FSF” (Model#GS48G600MGA, Val-Co, Bird In Hand, PA, USA, fan diameter = 1.2 m, 0.746 kW electric motor) and one variable speed, direct drive fan, “VSF” (Model #GS36G280MGA, Val-Co, Bird In Hand, PA, USA, fan diameter = 0.9 m, 0.373 kW electric motor).

Ventilation rates were calculated by measuring the face velocity of the air entering the greenhouse from the pad with a hot-wire anemometer (A004, Kanomax Inc., Andover, NJ, USA). Velocity measurements were taken at seven locations across the pad while conducting each experiment during continuous fan operation was employed. The mean velocity was then multiplied by the pad face area (10.2 m^2) to calculate the ventilation rate.

Initial studies of the pad-and-fan system in Summer of 2005 determined ventilation rates of 0.017, 0.037, 0.051, 0.067, and $0.078 \text{ m}^3 \text{ m}^{-2} \text{ s}^{-1}$, which represented 100% VSF, 1 FSF, 1 FSF + 100%VSF, 2 FSF, and 2 FSF + 100%VSF. Due to build up of salts on the pad during the year between initial and final experiments, the same fan operation produced lower ventilation rates of 0.016, 0.034, 0.047, and $0.060 \text{ m}^3 \text{ m}^{-2} \text{ s}^{-1}$ during the final experiments in Summer 2006 (Table 4.1).

Water use by the high-pressure-fog system was tested for ventilation rates of 0.011, 0.016, and $0.034 \text{ m}^3 \text{ m}^{-2} \text{ s}^{-1}$ (Table 4.1). Additional experiments that tested the effect of fog location on inside climate conditions also tested ventilation rates of 3.7 and $20.3 \text{ m}^3 \text{ s}^{-1}$.

Table 4.1 Ventilation rates as determined by the number of fans in operation. Fan operation and subsequent ventilation rates for the pad-and-fan and high-pressure fog systems are denoted by superscripts “P” and “F,” respectively.

Fan Operation	Ventilation Rate, \dot{Q} ($\text{m}^3 \text{ s}^{-1}$)	Ventilation Rate, q ($\text{m}^3 \text{ m}^{-2} \text{ s}^{-1}$)	Ventilation Rate (CFM)	Ventilation Rate (Air Exchanges per minute)
50% VSF ^F	3.0	0.011	6,552	0.1
100% VSF ^{P,F}	4.5	0.016	9,530	0.2
1 FSF ^{P,F}	9.4	0.034	20,341	0.4
100% VSF + 1FSF ^P	13.0	0.047	27,545	0.5
2 FSF ^P	16.7	0.060	35,385	0.7

For the crop *WUE* tests the VSF was allowed to ramp up from 0-100% of maximum operating speed with a maximum ventilation rate of $0.016 \text{ m}^3 \text{ m}^{-2} \text{ s}^{-1}$. Sample ventilation rates measured during the cropping season are shown in Table 4.2.

Table 4.2 Ventilation rates produced by the variable speed fan under several percentages of maximum operating speed.

VSF Operation (% max speed)	Ventilation Rate, \dot{Q} ($\text{m}^3 \text{ s}^{-1}$)	Ventilation Rate, q ($\text{m}^3 \text{ m}^{-2} \text{ s}^{-1}$)
10%	0.01	3.6×10^{-5}
30%	2.1	7.5×10^{-3}
50%	3.0	1.1×10^{-2}
75%	3.8	1.4×10^{-2}
100%	4.5	1.6×10^{-2}

4.1.4 Statistics

All correlations and tests of significance were performed with JMP statistical software (Release 6.0.0, SAS Institute Inc., Cary, NC, USA). Tukey-Kramer HSD tests were performed to test the levels of significance and multivariate analyses were used to test correlations.

4.2 Experimental Procedures for Pad-and-Fan and High-Pressure-Fog Tests

Water use, greenhouse climate, tomato plant transpiration, and leaf temperature were monitored during operation of pad-and-fan and high-pressure-fog cooling systems using continuous mechanical ventilation. Early experiments with both evaporative cooling systems guided the procedural methods for the final tests that would include tomato plant data, such as yield, E_T and T_{Leaf} measurements. These initial experiments tested pad-and-fan water use and the resulting greenhouse conditions only during the hottest, most stable time of the day, typically 11:00 – 14:00. Initial experiments also tested the effect of different fog nozzle locations on inside greenhouse air conditions.

4.2.1 Operation of the Evaporative Cooling Systems

4.2.1.1 Operation of the Pad-and-Fan System – Initial 30-minute tests

Initial studies of the pad-and-fan cooling system included testing the effects of five ventilation rates on water use and inside greenhouse conditions. One set of experiments tested water use with ventilation rates of 4.8, 10.2, 14.1, 18.6, and 21.8 m³ s⁻¹ in the two identical, side-by-side greenhouses. One greenhouse had 472 mature tomato plants, and the second greenhouse was empty. Each ventilation rate was tested for a 30-minute time period during the hottest and most consistent time of the day (12:00 – 15:00) on August 29, 2005. Water use measurements were recorded every 10 minutes and averaged for the 30-minute test period. Inside air temperature and relative humidity were measured every minute and also averaged for the 30-minute test period. The internal shade screen was not used.

The other set of experiments examined the difference in water use by the pad-and-fan system on two days that represented hot, dry summer conditions (August 3, 2005) and a typical monsoon weather day in Tucson, AZ (July 29, 2005). Water use was measured every 30 minutes (09:00 – 16:00) using a ventilation rate of $10.3 \text{ m}^3 \text{ s}^{-1}$ on both days.

4.2.1.2 Operation of the Pad-and-Fan System – Final 9-Hour Experiments

The pad-and-fan cooling system was tested for a nine-hour period for each ventilation rate in May 2006. Fans were operated continuously throughout the day, from 08:00 – 17:00. The pad pump was started at 07:00 to ensure pad saturation. The internal shade screen was deployed when the outside solar radiation was greater than 915 W m^{-2} or a greenhouse air temperature greater than 28°C , and was typically deployed from 11:15 – 14:00.

4.2.1.3 Operation of the High-Pressure-Fog System for Initial Studies on Fog Nozzle Locations

Initial studies of the high-pressure-fog nozzle locations were conducted May 2-5, 2006. The high-pressure-fog system using the multiple inlet fog nozzle locations was operated continuously with continuous ventilation. For all other initial fog tests the high-pressure-fog system was operated using computer control to maintain a range of VPD between 0.8 and 1.2 kPa. Fogging duration was proportioned over a modulating period of 140 seconds. To limit the fogging time to 120 seconds the maximum allowable proportion of On:Off time was set to 85%. With this method of control, the proportional

On:Off time increased from 0% for inside VPD levels of 0.8 kPa or less to 85% when the VPD was 1.2 kPa or greater.

Ventilation rates were not controlled and fans were operated continuously for the specific ventilation rate of interest. Fog On and Off cycling was not monitored during these initial tests.

4.2.1.4 Operation of the High-Pressure-Fog System – Final 9-Hour Experiments

Final experiments of the high-pressure-fog system were conducted during May 2006. Unlike the pad-and-fan system, water use by the high-pressure-fog system is not coupled to ventilation rate unless it is controlled to operate in accordance with the ventilation system or respond to greenhouse conditions, which would inherently be affected by ventilation. Therefore, to create a relationship between ventilation and water use (fog injection) the fog system was controlled based on an air temperature setpoint of 25°C.

A total duty cycle of 140 s was employed, where maximum operation time was set for 110 s to prevent over-saturation of the air and minimum Off-time was set for 30 s to limit the high-pressure pump from cycling on and off too frequently. Like the pad-and-fan system, high-pressure-fog tests occurred during 08:00 – 17:00 and the shade curtain was deployed between 11:00 – 14:00.

4.2.2 Tomato Plants and Irrigation

During the final experiments of the pad-and-fan and high-pressure-fog tests, approximately two-thirds of the greenhouse growing area was occupied by 472 mature

tomato plants (comprising the “plant zone”). The plants were grown hydroponically in rockwool, and were top-drip irrigated every 30 minutes without feedback control, starting at 7:30 and ending at 17:30. For the experiments testing plant transpiration and leaf temperature, the plants were ‘topped’ (removal of growing point) so that only minor changes in total biomass would occur due to side shoot and fruit development during these tests.

4.2.3 Measurements and Calculations

4.2.3.1 Environmental Conditions

Greenhouse climate conditions and their uniformity were monitored with air temperature (Type-T thermocouples, 36 ga) and relative humidity sensors (Model 50Y, Vaisala Inc., USA), which were shielded and aspirated. Sensors were located at canopy height (3 m) at 6 greenhouse locations (just outside the pad, just inside the pad, and at 4 m, 12 m, 20 m, and 28 m distances from the pad) along the center-line of the greenhouse (4.9 m from sidewalls) (Figure 4.4). Vapor pressure deficit (VPD) of the air was calculated from its psychrometric relationship to the inside greenhouse T_{DB} and RH . The three sensors within the plant zone were used to calculate the average plant zone conditions. Outside, incoming, and outgoing radiation levels were measured using three pyranometers sensors (LI-200SA, 400-1100 nm, Li-Cor Inc., Lincoln, NE, USA).

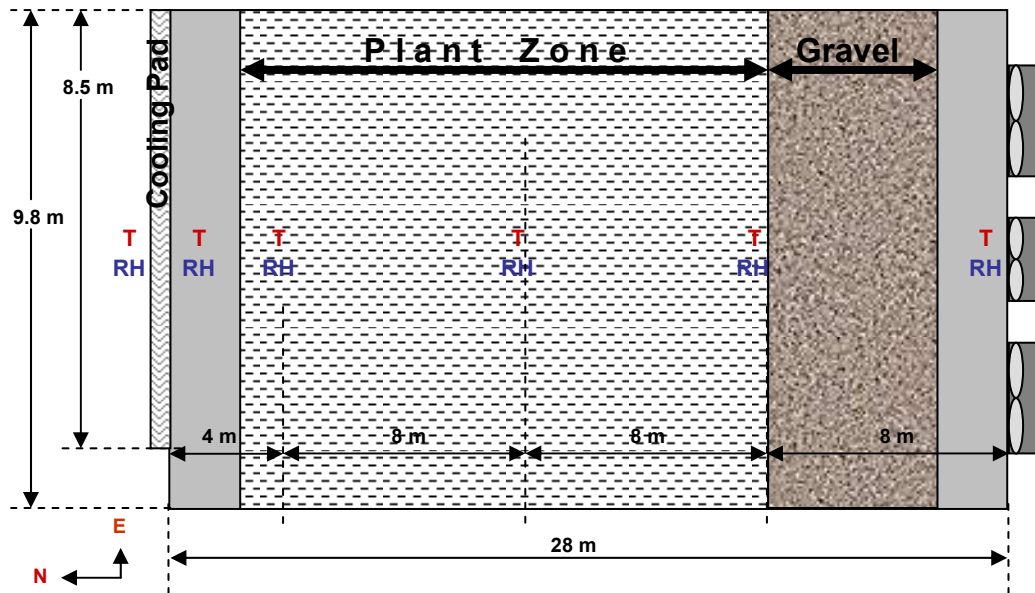


Figure 4.4 Spatial location of air temperature and relative humidity sensors, relative to pad and fan walls. They were placed 3 m above the floor at canopy height. Mature tomato plants were grown in the “plant zone” area.

Outside climate conditions were monitored using a weather station next to the experimental greenhouse. The weather station was located approximately 3 m from the east wall of the greenhouse at a height of 9 m.

All climate data were collected every second and averaged in one-minute intervals using a Campbell 21X datalogger (Campbell Scientific Inc., Logan, UT, USA). Thermocouples and relative humidity sensors were calibrated using an Assman aspirated psychrometer (Model 225-5230).

4.2.3.2 Cooling Efficiency of the Pad

Cooling efficiency of the pad (η_{Cool}) was calculated using data from the air temperature (T_{DB}) and relative humidity (RH) sensors located immediately inside and outside the evaporative cooling pad using Equation 4.1.

$$\eta_{Cool} = \frac{T_{DB,Out} - T_{DB,In}}{T_{DB,Out} - T_{WB,Out}} \times 100\% \quad (4.1)$$

Where $T_{DB,Out}$ is the drybulb air temperature of the air just outside the pad, $T_{DB,In}$ is the drybulb temperature just inside the pad, and $T_{WB,Out}$ is the wetbulb temperature of the air outside the pad, which is the minimum temperature the air could be cooled for its given moisture content. $T_{WB,Out}$ was determined using the psychrometric relationship between drybulb temperature, relative humidity, and wetbulb temperature.

4.2.3.3 Water Use by the Pad-and-Fan System

Water use by the evaporative cooling pad was measured every 30 minutes with an integrated flow meter (1" PMM Series, Precision Meters, Orlando, FL, USA) connected to the makeup water line, which replenished water evaporated from the pad to maintain a constant sump tank volume (Figure 4.2). Based on a water balance on the evaporative cooling pad (Equation 4.2), water delivered to the pad was either evaporated, stored on the pad, or returned to the sump tank (Figure 4.2).

$$V_I = V_E + V_S + V_R \quad (4.2)$$

Where V_I is the volume of water delivered to the pad ($\text{m}^3 \text{s}^{-1}$), V_E is the volume of water evaporated into the greenhouse, V_S is the volume of water stored on the pad, and

V_R is the volume of water returned to the sump. For a saturated cooling pad operating at steady-state, it was assumed that after the pad was initially saturated that the amount of water stored on the pad was constant ($V_S = 0$) and that all V_I was either evaporated or returned to the sump. Under this assumption, the makeup line was only replacing water evaporated into the greenhouse (Equation 4.3).

$$V_R = V_I - V_E \quad (4.3)$$

Therefore, to maintain a constant tank level, the makeup line needed to deliver the same amount of water to the tank that was evaporated from the pad (Equation 4.4).

$$V_M = V_E \quad (4.4)$$

Where V_M is the volume of water delivered to the sump tank by the makeup water line. Water losses due to leaks and evaporation to the outside were measured and were negligible. Therefore, water use by the pad-and-fan system (V_E) was determined by measuring water flow through the makeup line (V_M).

The rate of water use was calculated on the basis of floor area, with the equation:

$$\dot{m}_P = \frac{V_M \times \rho_W}{t \times A_{floor}} \quad (4.5)$$

Where \dot{m}_P is the mass flow rate of water vapor into the greenhouse per greenhouse floor area ($\text{kg m}^{-2} \text{s}^{-1}$) from the pad, ρ_W is the density of water (1000 kg m^{-3}), t is time (1800 s), and A_{floor} is the floor area (278 m^2).

Water use by the pad-and-fan system was also predicted using equations for the psychrometric properties of moist air, as described by Al Helal (2007). Assuming that

the evaporation rate from the pad was uniform across its surface, the following relationships were used to predict water use:

$$\dot{m}_w = \frac{(W_{In} - W_{Out}) \times \rho_{Air,In} \times \dot{Q}}{A_{floor}} \quad (4.6)$$

Where \dot{m}_w is the mass flow rate of water vapor into the greenhouse ($\text{kg s}^{-1} \text{ m}^{-2}$ floor area), $W_{In} - W_{Out}$ is the difference in humidity ratio ($\text{kg H}_2\text{O kg}^{-1}$ dry air) of the outside air and the air exiting the pad, $\rho_{Air,In}$ is the density of air leaving the pad (kg m^{-3}) calculated from the vapor pressure of the air, A_{floor} is the floor area (278 m^2), and \dot{Q} is the volumetric flow rate of air through the pad, or ventilation rate ($\text{m}^3 \text{ s}^{-1}$), estimated as:

$$\dot{Q} = \bar{v} \cdot A_{Pad} \quad (4.7)$$

Where \bar{v} is the face velocity of air through the pad (m s^{-1}), and A_{Pad} is the surface area of the pad (m^2). The face velocity was measured using as an average of seven measurements along the inside surface of the pad. Temperature and relative humidity sensors located along the outside and inside surface of the pad were used to calculate W_{In} and W_{Out} from psychrometric equations as described by ASHRAE (2001).

4.2.3.4 Water Use by the High-Pressure-Fog System

For the final 9-hour experiments, water use by the high-pressure-fog system was calculated by multiplying the water injection rate of the fog nozzles by the operation time of the pump.

$$\dot{m}_F = \frac{V_F \times \rho_W}{t_F \times A_{floor}} \quad (4.8)$$

Where \dot{m}_F is the mass flow rate of water into the greenhouse by the fog system per unit floor area ($\text{kg m}^{-2} \text{s}^{-1}$), V_F is the fog water flow rate (0.113 L s^{-1}), ρ_W is the density of water (kg m^{-3}), t_F is the fog operation time (s), and A_{floor} is the floor area (m^2).

4.2.3.5 Tomato Plant Water Use and Yield

Irrigation water use (WU_I) was measured every 30 minutes with 4 lysimeters, that sampled the drip irrigation water to plants and collected water drained from the plants. Each lysimeter consisted of six total plants located in the center of the greenhouse.

An “open” irrigation system was used to grow the plants, therefore irrigation water not consumed by the plants was drained away (and measured). Therefore, daily WU_I was the total amount of drip water to each plant, and was calculated with the following equation:

$$WU_I = \frac{\text{Drip}_{\text{Mean}} \times 472 \text{ plants} \times 20 \text{ irrigations}}{\text{day}} \quad (4.9)$$

Where $\text{Drip}_{\text{Mean}}$ (mL) is the average amount of irrigation water supplied to each plant, which was measured every 30 minutes. The $\text{Drip}_{\text{Mean}}$ to each plant was 132.5 mL, producing a total WU_I of 1251 L d^{-1} , or $4.5 \text{ L m}^{-2} \text{ d}^{-1}$.

An estimated value of water use by a theoretically 100% closed, recirculating irrigation system ($WU_{I,\text{Closed}}$) was calculated from the amount of drip water that was not drained from the plants:

$$WU_{I,\text{Closed}} = WU_P = (\text{Drip} - \text{Drain}) \times 472 \text{ plants} \times 20 \text{ irrigations} \quad (4.10)$$

Plant water uptake (WU_P , mL) is equal to the amount of water that would be needed in the closed irrigation system to replenish water that was consumed by the plants. Values of WU_P ($W_{I,Closed}$) varied with ventilation rate.

Based on production levels during the month prior to the experiment, the mean yield for the experimental tomato crop was 273 kg per week, which was used to assume a daily yield of 39 kg day⁻¹ for 472 plants.

4.2.3.6 Water Use Efficiency

Water use efficiency (WUE) was calculated from total water use by the irrigation and cooling systems for the period 08:00-17:00, and from the mean daily yield of tomatoes produced in the experimental greenhouse. Water use efficiency based on irrigation water use only (WUE_I) was calculated as:

$$WUE_I = \frac{\text{kg Yield}}{\text{m}^3 H_2O} = \frac{\text{kg Tomato}}{\text{m}^3 (WU_I)} \quad (4.11)$$

Water use efficiency based on pad-and-fan system water use only (WUE_{PF}):

$$WUE_{PF} = \frac{\text{kg Yield}}{\text{m}^3 H_2O} = \frac{\text{kg Tomato}}{\text{m}^3 (WU_{PF})} \quad (4.12)$$

Water use efficiency based on the high-pressure-fog system (WUE_{HPF}):

$$WUE_{HPF} = \frac{\text{kg Yield}}{\text{m}^3 H_2O} = \frac{\text{kg Tomato}}{\text{m}^3 (WU_{HPF})} \quad (4.13)$$

Total system water use efficiency (WUE_S) was calculated for water use by both irrigation (WU_I) and evaporative cooling systems (WU_{EC}):

$$WUE_S = \frac{\text{kg Yield}}{\text{m}^3 H_2O} = \frac{\text{kg Tomato}}{\text{m}^3 (WU_{EC} + WU_I)} \quad (4.14)$$

An estimate of WUE based on a “closed” irrigation system (100% recirculation) was also calculated. This estimate assumed that the amount of irrigation water needed would equal the amount absorbed by the plant (WU_P).

$$WU_I = WU_P \quad (4.15)$$

$$WUE_S = \frac{\text{kg Yield}}{\text{m}^3 \text{ H}_2\text{O}} = \frac{\text{kg Tomato}}{\text{m}^3 (WU_{EC} + WU_P)} \quad (4.16)$$

Additional estimates of WUE were calculated based on typical yearly yields produced by commercial tomato production greenhouses ($65 \text{ kg m}^{-2} \text{ yr}^{-1}$).

4.2.3.7 Plant Transpiration

Lysimeter and drip irrigation data were collected from 4 plants every 30 minutes and used to calculate transpiration rate. Equation 4.17 assumes that 95% of the water taken up by plants is used for transpiration (Hopkins and Huner, 2003):

$$E_T = 0.95 \cdot (\text{Drip} - \text{Drain}) * 472 \text{ plants} \quad (4.17)$$

4.2.3.8 Leaf Temperature

Leaf temperature of three plants was measured at 10:00, 12:00, 14:00, and 16:00 using an infrared thermometer (TN400L, Metris Instruments), with an emissivity of 0.95. The IR hand-held sensor was held 10 cm away from each leaf, providing a view diameter of 0.1 m. Measurements were always taken of the same shaded leaves on each plant at a height of 1.5 m (middle canopy). The plants were at a distance of 5.2 m, 11.0 m, and 17.7 m from the evaporative cooling pad.

4.3 Experimental Procedures for *WUE* of Greenhouse Tomato Production

4.3.1 Tomato Plants and Irrigation

A total of 472 tomato plants were cultivated for 8 months from March 8 to October 4, 2006, with a planting density of 2.94 plants m⁻². The plants occupied 156 m² of floor area and produced a total fruit yield of 48.6 kg m⁻² of growing area for the 8-month growing period. Under typical production practices, approximately 80% of the total greenhouse floor area would be used for production. Therefore, *WUE* values were calculated based on an 80% floor area production area (222 m⁻²) for the same planting density (2.94 plants m⁻²), providing 666 total tomato plants.

Plants were irrigated every 20-40 minutes, depending on the time of year and the solar energy load on the plants and greenhouse. Irrigation frequency and duration were not controlled by temperature or solar radiation levels, but were adjusted daily to produce a desired level of electro-conductivity (EC) in the drainage water. Drainage water was calculated as the difference between drip delivery amounts and the water consumed by plants. Irrigation water use also assumed 666 plants were grown in the greenhouse.

4.3.2 Operation of Pad-and-Fan Cooling System

The pad-and-fan cooling system was utilized throughout the crop production period to maintain a photoperiod setpoint air temperature ($T_{Set,Day}$) of 24°C and a dark period setpoint air temperature ($T_{Set,Night}$) of 18°C. Photoperiod and dark period were determined by the control system as the onset of sunrise and sunset. A two-hour transition phase between each period was utilized to prevent a drastic switch from

photoperiod to dark period cooling requirements. Additionally, to supplement greenhouse air moisture content and to prevent greenhouse *VPD* levels from exceeding 1.8 kPa water was occasionally provided from the high pressure fog evaporative cooling system located at the pad inlet.

The ventilation system utilized the two fixed speed fans (FSF) and the variable speed fan (VSF) to control the air temperature. The VSF was programmed to increase operating speed proportional to the cooling requirement, and it was the first fan to operate when cooling was needed. The FSF operated when cooling demand exceeded the capability of the VSF to attain setpoint temperature.

Proportional-Integral (PI) control was used by the control system (Argus Control Systems Ltd., White Rock, British Columbia, Canada) to operate the fans and activate the pump of the pad-and-fan cooling system. The proportional control setting was 4°C with an offset of 0.5°C. These settings translated into no control activity for air temperatures between 23.5-24.5°C and a proportioned response by the two fans to temperatures greater than 24.5°C. Therefore, if the inside air temperature was 1°C greater than 24.5°C (ie. 25.5°C) the cooling requirement was 25%, and if it was 4°C above 24.5°C the cooling requirement was 100%. The integral response was set so that the system did not react too slowly or quickly to immediate changes in the climate.

Based on this proportional control, the pump delivering water to the pad was set to operate at its full capacity for a cooling requirement exceeding 15% (Table 4.3). The variable speed fan would increase in speed from 0-100% as the cooling requirement increased from 0-50% of maximum cooling demand. The first FSF would then operate

without the VSF when the cooling requirement was between 51-75% of maximum cooling demand. When the cooling requirement exceeded 75%, the VSF was utilized in conjunction with the FSF, again ramping up in operating speed as the cooling requirement increased from 76-100% of maximum cooling demand. The second FSF was never operated.

The ventilation rate at 15% cooling requirement was $0.008 \text{ m}^3 \text{ m}^{-2} \text{ s}^{-1}$, at 50% it was $0.016 \text{ m}^3 \text{ m}^{-2} \text{ s}^{-1}$, between 51-75% it was $0.034 \text{ m}^3 \text{ m}^{-2} \text{ s}^{-1}$, and at 100% cooling demand, was $0.047 \text{ m}^3 \text{ m}^{-2} \text{ s}^{-1}$.

The operation of the pad-and-fan system would not be affected by increasing the production area to 80% of the greenhouse floor area. This expectation is due to the fact that added plants would be located downstream from the control sensor, and therefore not have a significant affect on measured conditions.

Table 4.3 Operation of the components used by the pad-and-fan system (pad pump, variable speed fan (VSF), fixed speed fan (FSF)) using proportional control to provide the cooling capacity demand. The VSF increased speed in proportion to its maximum speed, whereas the pump and FSF were either On or Off. Equivalent ventilation rates produced by the fans are also provided.

Cooling Requirement	0-15%	16-50%	51-75%	76-100%
Pad Pump	Off	On	On	On
VSF (% max)	0 – 30	31 – 100	Off	0 – 100
FSF	Off	Off	On	On
Vent Rate, q ($\text{m}^3 \text{ m}^{-2} \text{ s}^{-1}$)	0.0 – 0.008	0.008 – 0.016	0.034	0.034 – 0.047

4.3.3 Water Use Efficiency (WUE)

Water use by the pad-and-fan system (WU_{PF}) and the irrigation system, both open ($WU_{I,Open}$) and closed ($WU_{I,Closed}$) were measured similarly as discussed in sections 4.2.3. However, for this test WU_{PF} was measured at noon on several days throughout the crop life cycle (March 9, 10, 14, 23; May 9, 10, 11, 12, 19, 31; July 18, 19, 20, 26, 27, 31; October 4). Water use by the open irrigation system was measured by lysimeter on a daily basis (Kroggel *et al.*, unpublished), and water use by the closed irrigation system assumed that water needed for irrigation would be equivalent to the amount of water absorbed by the plants (see Equation 4.2).

Total water use was calculated as the amount of water used by each system for the entire crop cycle (March 8 – October 4). Daily water use rates were divided into 9 categories of seasonal time periods:

- 1) March 8 – March 22 (Late Winter)
- 2) March 23 – May 9 (Early spring)
- 3) May 10 – May 31 (Mid-spring)
- 4) June 1 – July 18 (Dry summer)
- 5) July 19 – July 31 (Peak monsoon)
- 6) August 1 – October 4 (Monsoon/Early autumn)

The water use efficiency (WUE) of both systems was calculated using Equations 4.11 and 4.12 with yield and water use totals for different periods of the crop cycle.

Water use by the irrigation and pad-and-fan systems was also combined to produce a total system water use efficiency value (WUE_S). Open irrigation water use was measured as the total amount of irrigation water provided to the plants.

$$WUE_{S,Open} = \frac{\text{kg Yield}}{\text{m}^3 H_2O} = \frac{\text{kg Tomato}}{\text{m}^3 (WU_{PF} + WU_{I,Open})} \quad (4.18)$$

Closed irrigation water use was an estimate of the minimum amount of water used by the plants (WU_P) without any drainage to waste. It was estimated as the difference between water provided and the water drained.

$$WUE_{S,Closed} = \frac{\text{kg Yield}}{\text{m}^3 H_2O} = \frac{\text{kg Tomato}}{\text{m}^3 (WU_{PF} + WU_P)} \quad (4.19)$$

WUE values were divided into the same categories as water use, starting with May 10 (when tomato harvest began). They were also separated by pre-monsoon and monsoon conditions, defined as:

- 1) Pre-monsoon (WUE_{PM}) calculates WUE from total yield and water use between March 8 and July 18, 2006, and
- 2) Monsoon (WUE_M) calculates WUE from total yields between July 18 and October 4, 2006, and water use from May 10 to October 4, 2006.

It should be noted that although the monsoon season officially started on July 3, 2006 (following 3 consecutive days of dewpoint temperature greater than or equal to 12.2°C), the weather resumed a semi-arid pattern on July 10 and until July 18. Therefore, for this analysis, July 18, 2006 was used as the monsoon start date.

4.3.4 Outside and Greenhouse Conditions

The outside and greenhouse climate data that are presented are those collected by the computer control system (Argus Control Systems Ltd., White Rock, BC, Canada), which used the data to operate the pad-and-fan system. Outside conditions are presented as daytime averages from 08:00 – 16:00. Inside conditions are presented as daytime averages (08:00 – 16:00) and nighttime averages (0:00 – 08:00), when evaporative cooling was likely not to occur.

4.4 Energy Balance Equations Used to Estimate Evaporative Cooling Water Use and Inside Air Temperatures for a Greenhouse in Semi-Arid Conditions

4.4.1 Energy Balance Equations

When evaporative cooling is used, the greenhouse climate is affected by energy and moisture balances, which contribute to both sensible and latent heat transfers. Moisture gains in the greenhouse from evaporative cooling (E_{Cool}), plant transpiration (E_T), and surfaces of the soil, plants, or other objects in the greenhouse (E_{Surf}) are denoted by E ($\text{kg m}^{-2} \text{s}^{-1}$).

$$E = E_{Cool} + E_T + E_{Surf} \quad (4.20)$$

The moisture balance on the greenhouse can be described by:

$$E = \rho \cdot q \cdot (W_{In} - W_{Out}) \quad (4.21)$$

where ρ is the density of air (kg m^{-3}), q is the ventilation rate ($\text{m}^3 \text{m}^{-2} \text{s}^{-1}$), and $(W_{In} - W_{Out})$ is the difference in humidity ratio ($\text{kg H}_2\text{O kg}^{-1} \text{dry air}$) between the inside and outside air. Note that *Equation 4.21* is equivalent to *Equation 4.6*, which was used to estimate the daily water use consumption by the pad-and-fan system.

The heat balance of the greenhouse includes both sensible and latent heat transfers, with the generalized equation:

$$S_n = H_V + H_C + L_V \quad (4.22)$$

where S_n is the net solar radiation inside the greenhouse, H_V is the sensible heat transfer via ventilation, H_C is the sensible heat transfer via convection-conduction through the greenhouse cover, and L_V is the latent heat transfer due to ventilation. In more detail, the steady-state energy balance can be described by:

$$R_n = (C_p \cdot \rho \cdot q + k \cdot w) \cdot (T_{In} - T_{Out}) + h_{fg} \cdot E \quad (4.23)$$

where R_n is the net solar radiation inside the greenhouse (W m^{-2}), C_p is the heat capacity of the moist air ($\text{J kg}^{-2} \text{C}^{-1}$), k is the overall heat transfer coefficient of the greenhouse ($\text{J m}^{-2} \text{s}^{-1}$), w is the ratio of glazing to floor area (constant), $(T_{In} - T_{Out})$ is the difference in inside and outside temperature, and h_{fg} is the latent heat transfer coefficient (J kg^{-1}).

The amount of water vapor in the greenhouse air can be estimated by rearranging the terms in the above equation to obtain:

$$E = \left(\frac{R_n - (C_p \cdot \rho \cdot q + k \cdot w) \cdot (T_{In} - T_{Out})}{h_{fg}} \right) \quad (4.24)$$

Furthermore, air temperature inside the greenhouse can also be estimated by:

$$T_{In} = T_{Out} + \frac{R_n - h_{fg} \cdot E}{\rho \cdot C_p \cdot q + k \cdot w} \quad (4.25)$$

4.4.2 Estimating Evaporative Cooling Water Use

Water use by the pad-and-fan and high-pressure-fog cooling systems were estimated using the moisture and energy balance equations described above. All calculations were performed in 30-minute increments, using the 30-minutes averages from 1-minute data collected during the all-day water use experiments described in *Sections 4.2.1.2 and 4.2.1.4*.

Pad-and-fan system water use was calculated using Equation 4.21 for psychrometric properties measured at the outside and inside surfaces of the wet pad. Calculations assumed no contribution to water vapor input by plant transpiration or surface evaporation. Note that Equation 4.21 is equivalent to Equation 4.24 when energy terms related to solar radiation (R_n) and heat transfer through the cover (k, w) are excluded.

High-pressure-fog water use was more complicated due to the introduction of water at multiple locations throughout the greenhouse. Equations 4.21 and 4.24 were calculated to test the accuracy of both the moisture and energy balance equations for estimating water use. Because all of the water vapor input by fog and plant transpiration would have occurred between the inlet and 20 m locations, air conditions measured at 20 m were used to calculate water use. To estimate fog water use, E_{Surf} was assumed to be equal to zero and E_T measurements were assumed accurate and subtracted from the right side of Equations 4.21 and 4.24 to obtain:

$$E = \rho \cdot q \cdot (W_{In} - W_{Out}) - E_{ET} \quad (4.26)$$

and

$$E = \left(\frac{R_n - (C_p \cdot \rho \cdot q + k \cdot w) \cdot (T_{In} - T_{Out})}{h_{fg}} \right) - E_T \quad (4.27)$$

4.4.3 Estimating Inside Air Temperature

Equation 4.25 was used to estimate inside air temperature at the three plant zone measurement locations (4 m, 12 m, and 20 m), so $T_{In} = T_4$, T_{12} , and T_{20} . For both the pad-and-fan and high-pressure-fog cooling systems, T_4 , T_{12} , and T_{20} were calculated using the measured outside temperature for T_{Out} in Equation 4.25. Air temperatures were also calculated using the inside air temperatures measured at the previous locations (T_{x-1}), so that $T_{Out} = T_0$, $T_{Out} = T_4$, and $T_{Out} = T_{12}$, for calculations at T_4 , T_{12} , and T_{20} , respectively.

Furthermore, the value of E_{Cool} and E_T was modified according to the test location. For the pad-and-fan system E_{Cool} was constant at all locations and equal to the measured value. For the high-pressure-fog system the value of E_{Cool} increased from 4 m to 20 m location, based upon the number of nozzles present prior to each location. Assuming that each nozzle delivered water at the same flow rate, E_{Cool} was equal to 21%, 60%, and 100% of total measured fog water use at 4 m, 12 m, and 20 m locations, respectively. The same logic was used to estimate the contribution of E_T to each location. Therefore, 10%, 50%, and 100% of the total measure E_T was used for calculations at 4 m, 12 m, and 20 m locations, respectively.

Based upon the above assumptions, the following equations were used for each test location:

*Pad-and-fan*Location

$$4 \text{ m} \quad T_{In} = T_{Out} + \frac{R_n - h_{fg} \cdot (100\%E_{Cool} + 10\%E_T)}{\rho \cdot C_p \cdot q + k \cdot w} \quad (4.28)$$

$$\text{and} \quad T_{In} = T_0 + \frac{R_n - h_{fg} \cdot (100\%E_{Cool} + 10\%E_T)}{\rho \cdot C_p \cdot q + k \cdot w} \quad (4.29)$$

$$12 \text{ m} \quad T_{In} = T_{Out} + \frac{R_n - h_{fg} \cdot (100\%E_{Cool} + 50\%E_T)}{\rho \cdot C_p \cdot q + k \cdot w} \quad (4.30)$$

$$\text{and} \quad T_{In} = T_4 + \frac{R_n - h_{fg} \cdot (100\%E_{Cool} + 50\%E_T)}{\rho \cdot C_p \cdot q + k \cdot w} \quad (4.31)$$

$$20 \text{ m} \quad T_{In} = T_{Out} + \frac{R_n - h_{fg} \cdot (100\%E_{Cool} + 100\%E_T)}{\rho \cdot C_p \cdot q + k \cdot w} \quad (4.32)$$

$$T_{In} = T_{12} + \frac{R_n - h_{fg} \cdot (100\%E_{Cool} + 100\%E_T)}{\rho \cdot C_p \cdot q + k \cdot w} \quad (4.33)$$

*High-Pressure-Fog*Location

$$4 \text{ m} \quad T_{In} = T_{Out} + \frac{R_n - h_{fg} \cdot (21\%E_{Cool} + 10\%E_T)}{\rho \cdot C_p \cdot q + k \cdot w} \quad (4.34)$$

$$\text{and} \quad T_{In} = T_0 + \frac{R_n - h_{fg} \cdot (21\%E_{Cool} + 10\%E_T)}{\rho \cdot C_p \cdot q + k \cdot w} \quad (4.35)$$

$$12 \text{ m} \quad T_{In} = T_{Out} + \frac{R_n - h_{fg} \cdot (60\%E_{Cool} + 50\%E_T)}{\rho \cdot C_p \cdot q + k \cdot w} \quad (4.36)$$

$$\text{and} \quad T_{In} = T_4 + \frac{R_n - h_{fg} \cdot (60\%E_{Cool} + 50\%E_T)}{\rho \cdot C_p \cdot q + k \cdot w} \quad (4.37)$$

$$20 \text{ m} \quad T_{In} = T_{Out} + \frac{R_n - h_{fg} \cdot (100\%E_{Cool} + 100\%E_T)}{\rho \cdot C_p \cdot q + k \cdot w} \quad (4.38)$$

$$\text{and} \quad T_{In} = T_{12} + \frac{R_n - h_{fg} \cdot (100\%E_{Cool} + 100\%E_T)}{\rho \cdot C_p \cdot q + k \cdot w} \quad (4.39)$$

Although using the measurements from previous locations does not provide the most realistic application of the model, the comparisons between these methods of temperature predictions will provide academic value for model validation. Furthermore, due to the dynamic characteristic of the high-pressure-fog system, the steady-state energy balance has limitations and does not provide the most accurate estimate of water use or air temperature.

4.5 Experimental Procedures for Testing the Effects of Buoyancy and Wind Direction on Airflow and Temperature Distribution in the Naturally-Ventilated Greenhouse Using a Wind Tunnel Model and Using the Full-Scale Greenhouse

Airflow and temperature distributions within the greenhouse using natural ventilation were studied using $1/15$ scale model in a wind tunnel and further examined with experiments in the full-scale greenhouse.

Wind tunnel experiments were performed on a $1/15$ scale model of the experimental greenhouse to study the effects of natural ventilation and surface floor heating on airflow and temperature distribution during natural ventilation conditions. The wind tunnel at the National Institute for Rural Engineering (NIRE) in Tsukuba, Ibaraki, Japan was used for the model experiments during Fall 2005. A series of airflow experiments in the full-scale experimental greenhouse during 2004 were also performed

and tested the validity of the model results. By understanding the movement of air inside the greenhouse, the high-pressure-fog system can be better designed to maximize evaporation, and thus minimize excessive water use, when combined with natural ventilation.

4.5.1 Description of Wind Tunnel and Model Greenhouse

The total length of the wind tunnel was 68 m, and the test section was 3H x 4W x 20L m (Figure 4.5). A 4 m diameter fan was located at one end of the wind tunnel and the air was passed through diffusion, strainer, and compression sections to produce uniform, laminar airflow before entering the test section.

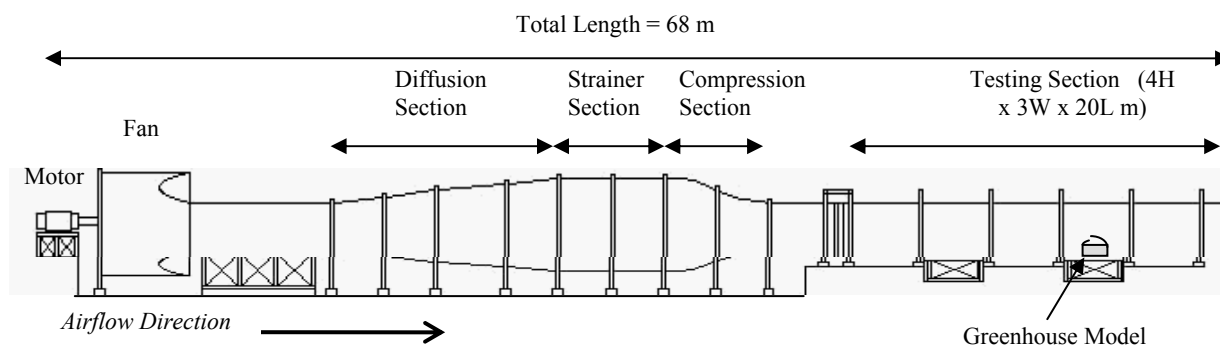


Figure 4.5 Schematic diagram of the wind tunnel used at the National Institute for Rural Engineering in Tsukuba, Japan.

A $1/15$ scale model of the experimental greenhouse was used for the wind tunnel experiments, with dimensions of 1.9L x 0.65W m, with gutter height of 0.27 m and 0.42 m height to the center of the arch (Figure 4.6). The model was fabricated from aluminum prism (10 mm x 10 mm) and acrylic board (2 mm thickness). To simulate the physical conditions of the full-scale Arizona greenhouse, the sidewalls had insect screening (open

ratio = 0.248) and the roof had no screen. Two silicon rubber heating pads (Sakaguchi E.H. Voc Corp., Japan), each 1.9L x 0.325W x 0.02H m, were placed side-by-side on the floor of the greenhouse model structure to simulate the effect of a solar heated floor inside the greenhouse. Pad temperature was maintained by connecting a thermocouple to a temperature controller.

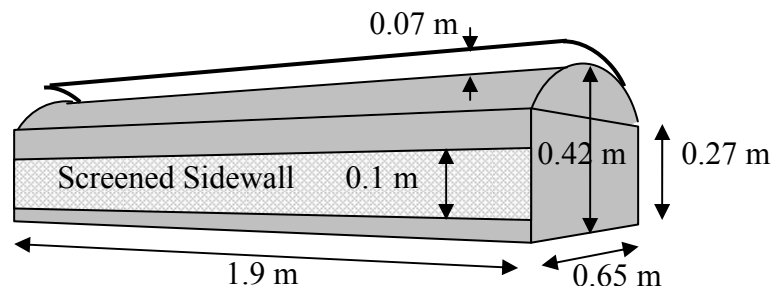


Figure 4.6 A $1/15$ scale model of arched-roof, single-span greenhouse used for wind tunnel experiments.

4.5.2 Temperature Distribution

To study temperature distribution, 20 Type-T thermocouples were placed in a horizontal cross-section of the greenhouse model (Figure 4.7). It was assumed that there would be no significant difference in temperature distribution along the length of the model since the predominant direction of airflow would be along its width. The distance between thermocouples was smaller near the floor of the model because the largest temperature gradient was expected near the heated floor.

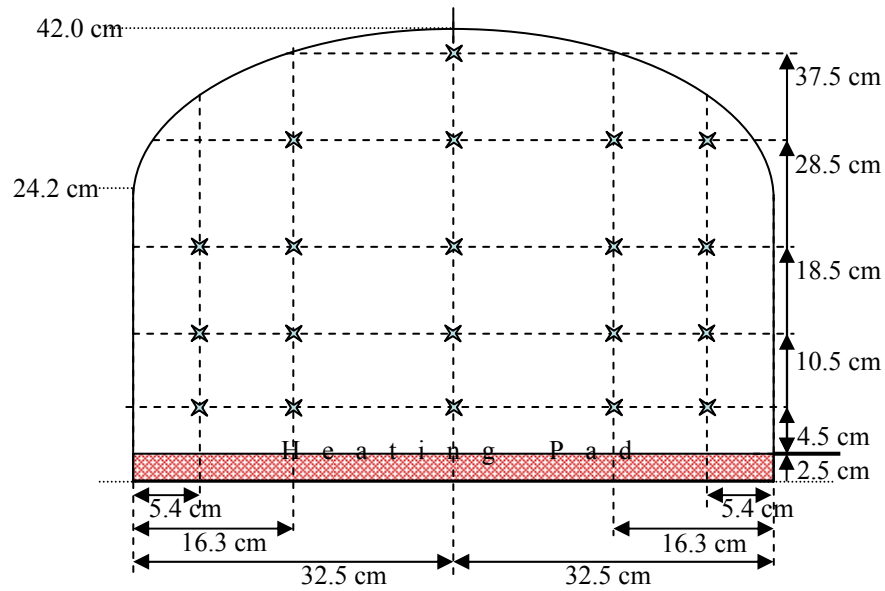


Figure 4.7 Locations of thermocouples along horizontal cross-section of greenhouse model inside wind tunnel.

4.5.3 Particle Image Velocimetry

Airflow patterns were visualized and analyzed using a Particle Image Velocimetry (PIV) system (TSI, Inc., Shoreview, MN, USA). The PIV system used double-pulsed lasers to illuminate smoke particles that were injected into the air upstream from the model. The double-pulsed laser was directed into the test area with a reflector and spread into two laser sheets with a convex lens to illuminate a wide cross-sectional area. The illuminated smoke particles within this interrogation area were then photographed using a charge-coupled device (CCD) video camera. The images were then processed using a series of cross-correlations, which calculated the travel distance of the smoke over 1 ms time increments. A velocity vector map was produced from these cross-correlations, providing a graphical visualization of air speed and direction.

The Nd:YAG laser energy was 120 mJ with a 532 nm wavelength. The thickness of the laser sheet was very important and was maintained around 1 mm for this study. Smoke particles were produced from non-toxic Dioctyl Sebacate liquid using a smoke generator (LAS-N, Seika Co., Osaka, Japan) and air compressor (GK-55, Meiji Air Compressor Mfg. Co., Osaka, Japan). The mean diameter of smoke particles was 1 μm . Insight software (SAS/Insight, SAS Institute Inc., Cary, NC, USA) was used to perform the cross-correlation analysis and display the velocity vector map.

4.5.4 Experimental Procedure

The effect of buoyancy on airflow and temperature distribution was studied for several wind and floor temperature conditions. Because the wind and temperature conditions inside the wind tunnel were different from those of the actual greenhouse, the wind tunnel conditions needed to be scaled to simulate true conditions.

4.5.4.1 Archimedes Similarity Calculations

To accurately simulate real conditions, many parameters needed to be scaled to the $1/15$ scale model. Archimedes number (Ar) was used to determine the required wind tunnel air velocity and surface temperature of the heating pad located on the floor of the greenhouse model. Archimedes number can be calculated from the following equation:

$$Ar = \frac{g \cdot \beta \cdot \Delta T \cdot L}{U^2} \quad (4.40)$$

where g is the gravity constant (9.8 m s^{-2}), β is the coefficient of volume expansion ($1/T_{\text{In}} = 0.0032 \text{ K}^{-1}$), ΔT is the temperature difference between the floor temperature and outside

temperature ($T_{GH,Floor} - T_{Out}$, K), L is a representative length, so that the width, length, height, or other parameter of the full-scale greenhouse is 15 times that of the model scale, and U is the wind velocity (m s^{-1}).

To determine the required wind tunnel velocity and heating pad temperature, Archimedes similarity was assumed to produce the following relationship:

$$Ar_{FullGH} = Ar_{ModelGH} \quad (4.41)$$

$$\frac{g \cdot \beta_F \cdot (T_{Floor,F} - T_{Out}) \cdot 1}{U_F^2} = \frac{g \cdot \beta_M \cdot (T_{Floor,M} - T_{Tunnel}) \cdot \left(\frac{L_F}{L_M}\right)}{U_M^2} \quad (4.42)$$

Where $T_{Floor,F}$ is the temperature of the floor surface in the full-scale greenhouse, T_{Out} is the ambient temperature outside the full-scale greenhouse, $T_{Floor,M}$ is the temperature of the heated pad in the model greenhouse, T_{Tunnel} is the ambient temperature outside the model and in the wind tunnel test section, and L_F/L_M is the characteristic length scaling constant ($L_F = 15$, $L_M = 1$, $L_F/L_M = 15$). Subscript F is for full-scale greenhouse and subscript M is for the model-scale greenhouse.

By knowing all values for the full-scale greenhouse and defining ΔT , the required wind tunnel air speed can be calculated with the equation:

$$U_M = U_F \left[\frac{(T_{Floor,F} - T_{Out})_M}{(T_{Floor,F} - T_{Out})_F} \cdot \frac{L_M}{L_F} \right]^{1/2} \quad (4.43)$$

with the assumption $\beta_F = \beta_M$.

4.5.4.2 Simulated Conditions

Three temperature differences between the greenhouse floor and ambient air conditions were simulated and tested ($\Delta T_{Floor,F - Ambient} = 10, 20, 30^\circ\text{C}$). These values were chosen based on preliminary infrared temperature measurements of the greenhouse gravel floor, as well as the experience of NIRE researchers who have observed $\Delta T = 30^\circ\text{C}$ (Table 4.4). The required wind tunnel velocity was calculated using the Archimedes number and similarity principle (Table 4.5).

Table 4.4 Infrared temperature measurements made of the greenhouse floor and on the ground outside (both gravel) when the ambient outside temperature was 31°C .

Surface	Temperature (IR)
Gravel Floor (no shade, no cooling)	41°C
Gravel Floor (under plant canopy, no cooling)	30°C
Gravel Outside (full sun)	51°C

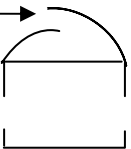
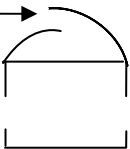
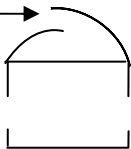
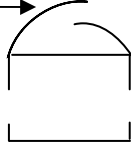
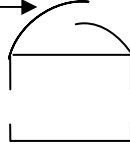
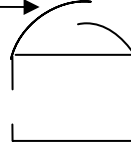
Table 4.5 Wind tunnel requirements for temperature difference and wind velocity calculated from the similarity principle using Archimedes number and full-scale greenhouse conditions.

Full-Scale Conditions		Model GH	Calculated Wind Tunnel Requirements	
$T_{Surf} - T_{Out}$	Wind Velocity	Model Scale	$T_{Surf} - T_{Out}$	Wind Tunnel Velocity
$\Delta T_F (C)$	$U_F (m\ s^{-1})$	L_F/L_M	$\Delta T_M (C)$	$U_M (m\ s^{-1})$
10	1	15	40	0.534
20	1	15	50	0.422
30	1	15	50	0.345

The ΔT_M was produced by adjusting the heated floor temperature according to the outside air temperature inside the wind tunnel. Wind velocity in the wind tunnel was controlled by adjusting the fan RPM. Wind direction was changed by rotating the model 180 degrees on a turntable.

A wind velocity of 1.0 m s^{-1} was simulated to emphasize the effect of buoyancy in the wind tunnel tests. Two wind directions were tested, 90° and 270° , so that air moved perpendicular to the ridge of the greenhouse (Table 4.6). The sidewall vents were tested with screens (100% Screen) and without the screens (100% Open) (0.19 m^2 vent area per side). The screens were the same as those used on the full-scale greenhouse (opening diameter = 28 mm, open ratio = 25). The roof vent was fully opened without screens (0.20 m^2 total roof vent area).

Table 4.6 Wind tunnel treatments testing the effects of wind direction and ΔT ($T_{\text{Floor}} - T_{\text{out,ambient}}$) on air movement and temperature distribution.

	$\Delta T = 10^\circ\text{C}$	$\Delta T = 20^\circ\text{C}$	$\Delta T = 30^\circ\text{C}$
Wind Direction = 90°	Treatment 1	Treatment 2	Treatment 3
Vents			
Side = 100%, Screen			
Roof = 100% Open			
Wind Direction = 270°	Treatment 4	Treatment 5	Treatment 6
Vents			
Side = 100%, Screen			
Roof = 100% Open			

4.5.4.3 Dimensionless Temperature and Air Velocity

To translate the results of the wind tunnel model into the full-scale greenhouse, dimensionless temperature and air velocity were calculated and used for analysis.

Dimensionless temperature (θ_T) was calculated by:

$$\theta_T = \frac{T_{In} - T_{Tunnel}}{T_{Pad} - T_{Tunnel}} \quad (4.44)$$

T_{In} is the air temperature measured inside the model, T_{Tunnel} is the ambient air temperature outside the model and in the wind tunnel test section, and T_{Pad} is the surface temperature of the heated pad.

Similarly, dimensionless velocity (U, V) was calculated by:

$$\text{x-velocity: } U = \frac{U_{In}}{U_{Out}} \quad (4.45)$$

$$\text{y-velocity: } V = \frac{V_{In}}{V_{Out}} \quad (4.46)$$

where subscript *In* is the air velocity measured inside the model and subscript *Out* is for the air velocity produced by the wind tunnel.

4.5.5 Greenhouse Validation Experiments

Airflow measurements were taken within the full-scale greenhouse in Arizona and were used to validate the results of the wind tunnel experiments. A three-dimensional ultrasonic anemometer (Model 8100, R.M. Young Company, Traverse City, MI, USA) was used to measure air velocity and direction. A total of nine measurement points were monitored along the cross-sectional width, in the center of the greenhouse (Figure 4.8).

Data were collected in one-second intervals and averaged every one minute. The experiments were performed in the morning (10:00 – 12:00), when outside wind conditions were most stable.

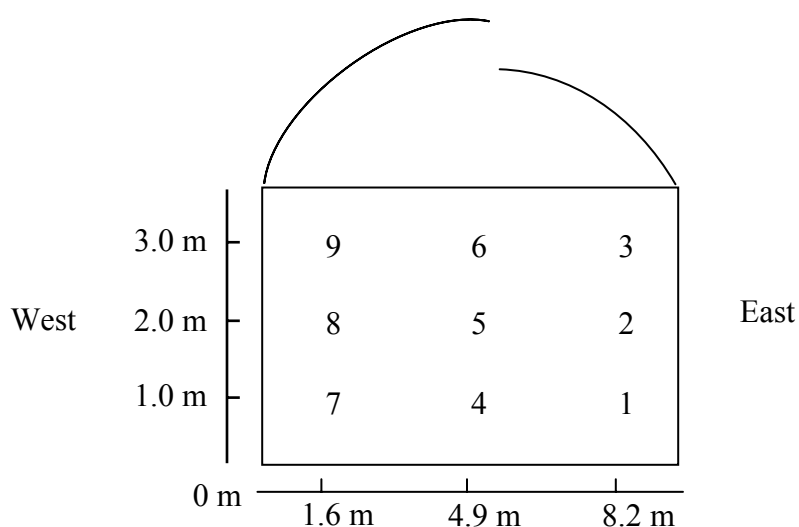


Figure 4.8 Locations where 3-D airflow measurements were monitored in the full-sclae greenhouse in Arizona.

Outside wind conditions were also monitored during the experiments with the weather station. Wind directions from the North, East, South, and West were represented by conventional azimuth degree values of 0° , 90° , 180° , and 270° , respectively.

The following four conditions were tested with the open roof and 100% open, screened sidewalls: i) without plants, without fog; ii) without plants, with fog; iii) with plants, without fog; and iv) with plants, with fog.

5. RESULTS

5.1 Initial Water Use Studies of the Pad-and-Fan Cooling System

5.1.1 Effect of Ventilation Rate on Water Use

The 30-minute averages of water use for pad-and-fan evaporative cooling under five ventilation rates increased linearly ($R^2 = 0.99$) with increasing ventilation rate up to $21.8 \text{ m}^3 \text{ s}^{-1}$ (Figure 5.1). Large fluctuations in water use by the pad-and-fan system were observed at the initial 10-minute measurement as evaporation rates adjusted to the change in ventilation rate. These temporal fluctuations are reflected in the large standard deviation values observed during the short monitoring intervals. However, after 20 minutes the pad-and-fan system reached a steady-state condition and subsequently the evaporation rate stabilized.

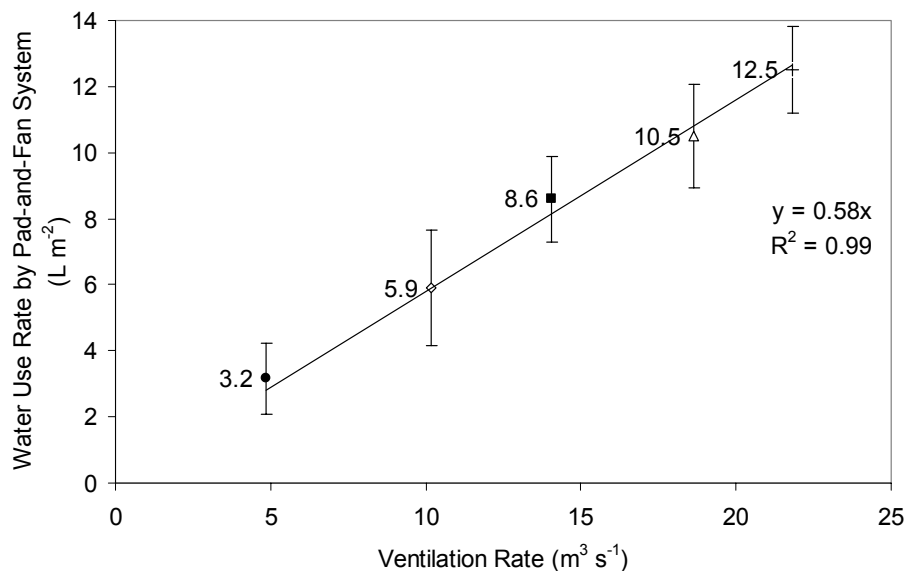


Figure 5.1 Thirty-minute averages and standard deviations of water use by two equivalent pad-and-fan systems operating simultaneously for five ventilation rates (4.8 , 10.2 , 14.1 , 18.6 , and $21.8 \text{ m}^3 \text{ s}^{-1}$).

5.1.2 Effect of Ventilation Rate on Greenhouse Conditions

For both the empty and plant-filled greenhouses the air temperature decreased from greater than 30°C at 4.8 m³ s⁻¹ to about 28°C at 14.1 m³ s⁻¹, with no further air temperature reduction at higher ventilation rates. The relative humidity for the empty greenhouse increased from 40% at 4.8 m³ s⁻¹ to 48-50% at 14.1 m³ s⁻¹ and higher. In the plant-filled greenhouse the relative humidity decreased with increasing ventilation rate, and stabilized to the same level (50%) as the greenhouse without plants for ventilation rates of 14.1 m³ s⁻¹ and greater.

Although greater amounts of water vapor were added to the greenhouse air with increased ventilation rate, the air temperature, and the relative humidity, stabilized at 14.1 m³ s⁻¹ and above (Figure 5.2). This stabilization indicated that a ventilation rate of 14.1 m³ s⁻¹ provided the maximum rate of sensible heat removal from this greenhouse for the outside conditions. Furthermore, the decreased relative humidity for increasing ventilation rate in the plant-filled greenhouse provided evidence that plant transpiration contributed more to latent heat transfer at lower ventilation rates, where air temperature was less than in the greenhouse without plants. A ventilation rates of 14.1 m³ s⁻¹ and above air temperatures and relative humidity levels were the same in both greenhouses, suggesting that latent heat transfer from transpiration was offset by the high rate of air exchange produced at those ventilation rates.

It is unlikely that these ranges of greenhouse conditions produced significantly different rates of plant transpiration and thus produce different rates of latent heat transfer. It is more likely that the stabilization of conditions occurred due to the

maximized rate of sensible heat removal. However, because plant transpiration was not measured, the mechanism for this stabilization was uncertain.

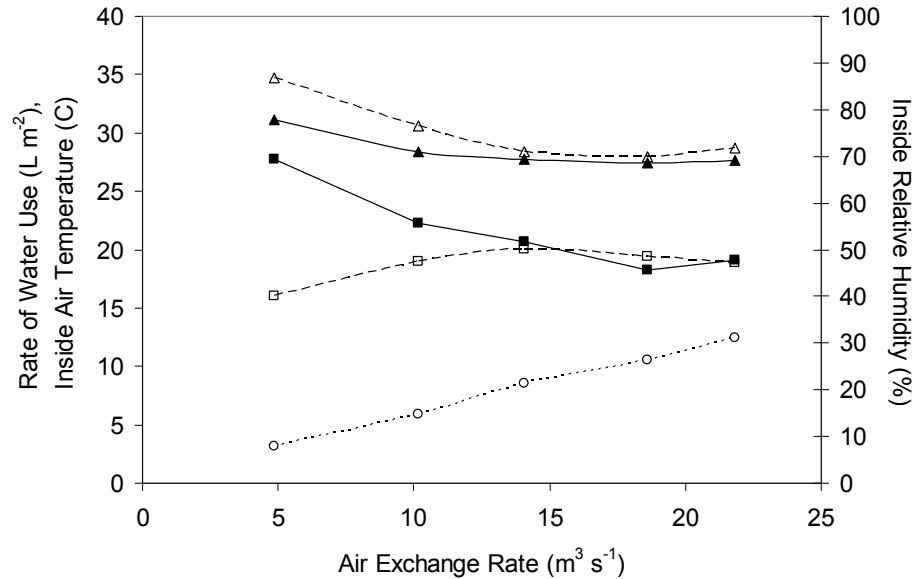


Figure 5.2 Average plant zone air temperatures (▲) and average plant zone relative humidity (■) levels measured during the simultaneous operation of pad-and-fan cooling for a greenhouse without plants (open symbols) and an identical plant-filled greenhouse (solid symbols) for five ventilation rates (4.8, 10.2, 14.1, 18.6, and $21.8 \text{ m}^3 \text{s}^{-1}$). Pad-and-fan water use ($\cdots\circ\cdots$) was the average for the two greenhouses with outside conditions $T_{Air,Out} = 38^\circ\text{C}$, $RH_{Out} = 15\%$.

5.1.3 Effect of Outside Climate Conditions on Water Use Rate

Water use by the pad-and-fan system was also examined for days that represented dry summer conditions and more humid monsoon conditions using a single ventilation rate ($10.3 \text{ m}^3 \text{s}^{-1}$). Figure 5.3 demonstrates that the outside vapor pressure deficit greatly affected water use by the pad-and-fan system. Incremental increases in water use occurred for changes in outside VPD of 1.0 kPa . Water use rates were approximately 0.05 , 0.10 , 0.15 , and $0.2 \text{ g m}^{-2} \text{s}^{-1}$ for outside vapor pressure deficits between 1.0 - 2.0 , 2.0 - 3.0 , and 3.0 - 4.0 kPa , respectively. During monsoon conditions, when the outside VPD

was low, less water was evaporated from the pad, both reducing water use and limiting the pad-and-fan to evaporatively cool the air. These results agree with previous modeling studies (Kittas *et al.*, 2003; Willits, 2003b).

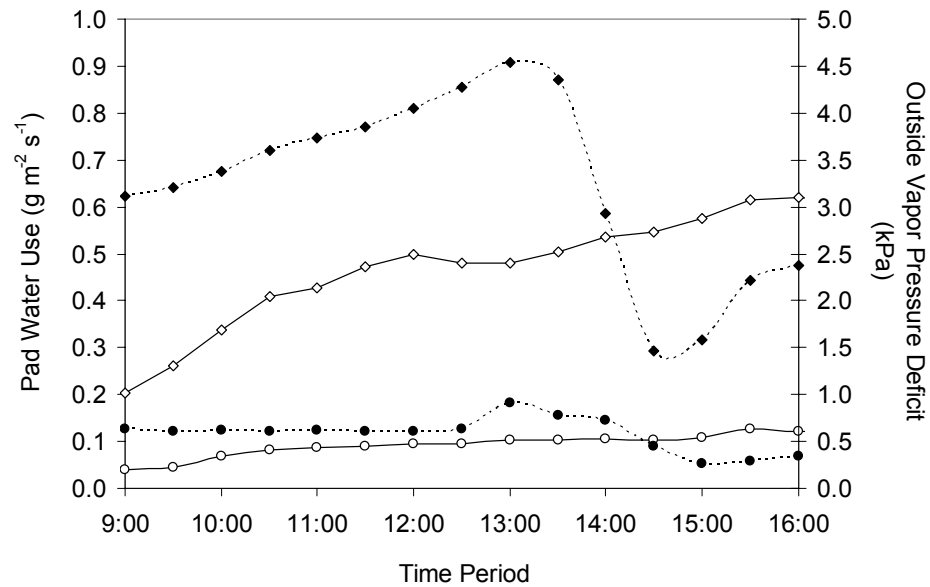


Figure 5.3 Outside VPD (◆) during dry summer conditions (—) and more humid, monsoon summer conditions (···) throughout a typical day, and corresponding water use rates by the pad-and-fan system (●) when operated at one ventilation rate ($10.3 \text{ m}^3 \text{ s}^{-1}$).

5.2 Effect of Pad-and-Fan Cooling on Greenhouse Water Use, Climate Conditions, Plant Transpiration and Leaf Temperatures for a Semi-Arid Climate

5.2.1 Outside Environmental Conditions

The outside temperature and relative humidity levels were very similar for all test days (Figure 5.4). Morning temperature and relative humidity (08:00) were approximately 25°C and 15-20%, respectively, and stabilized to approximately 36°C and 7-10% after 14:00. The mean outside temperature, relative humidity, and vapor pressure deficit for these tests during the 08:00 – 17:00 was 33.8°C ($\pm 0.4^\circ\text{C}$), 10.4% ($\pm 1.8\%$), and 4.8 kPa (± 0.2 kPa), respectively (Table 5.1).

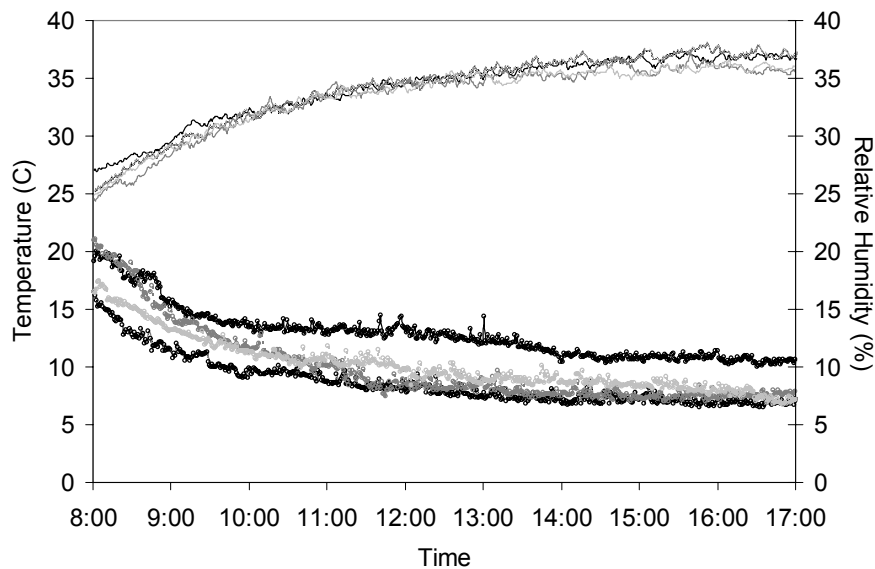


Figure 5.4 Outside temperature (—) and relative humidity (○) during full day tests of the pad-and-fan system for four ventilation rates: 4.5 m³ s⁻¹ (—), 9.4 m³ s⁻¹ (—), 13 m³ s⁻¹ (—), and 16.7 m³ s⁻¹ (—).

Table 5.1 Mean outside climate conditions (temperature, relative humidity, and vapor pressure deficit) for the entire experimental period (08:00 – 17:00) and during the part of the day when outside conditions were relatively stable (11:00 – 17:00) for the full day tests of the pad-and-fan system for four ventilation rates.

\dot{Q} ($\text{m}^3 \text{s}^{-1}$)	T_{Out} ($^{\circ}\text{C}$)	RH_{Out} (%)	VPD_{Out} (kPa)	T_{Out} ($^{\circ}\text{C}$)	RH_{Out} (%)	VPD_{Out} (kPa)
08:00 – 17:00				11:00 – 17:00		
4.5	34.1 ± 2.9	12.8 ± 2.3	4.6 ± 0.8	35.8 ± 1.1	11.7 ± 1.1	5.0 ± 0.3
9.4	34.1 ± 3.3	8.6 ± 2.1	5.0 ± 0.9	36.1 ± 1.1	7.5 ± 0.6	5.5 ± 0.4
13.0	33.4 ± 3.2	9.9 ± 3.4	4.7 ± 0.9	33.4 ± 0.6	9.9 ± 0.8	4.7 ± 0.2
16.7	33.4 ± 3.0	10.1 ± 2.3	4.7 ± 0.8	35.2 ± 0.8	8.9 ± 0.9	5.2 ± 0.3
Mean \pm SD	33.8 ± 0.4	10.4 ± 1.8	4.8 ± 0.2	35.6 ± 0.4	9.0 ± 1.9	5.2 ± 0.2

Outside solar radiation followed a smooth parabolic curve during tests for 4.5 and $9.4 \text{ m}^3 \text{s}^{-1}$, when skies were clear for the entire day (Figure 5.5). Outside solar radiation was less consistent for $13.0 \text{ m}^3 \text{s}^{-1}$ and most variable during the test for $16.7 \text{ m}^3 \text{s}^{-1}$, which caused the shade curtain to stow and the resulting incoming radiation to increase between 13:15–13:45.

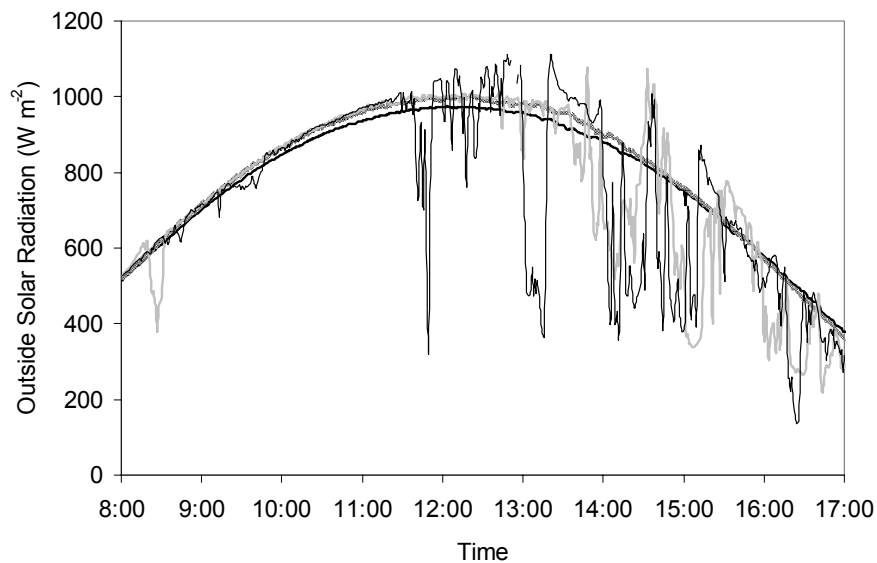


Figure 5.5 Outside solar radiation during pad-and-fan cooling under four ventilation rates: $4.5 \text{ m}^3 \text{s}^{-1}$ (—), $9.4 \text{ m}^3 \text{s}^{-1}$ (—), $13 \text{ m}^3 \text{s}^{-1}$ (---), and $16.7 \text{ m}^3 \text{s}^{-1}$ (---).

5.2.2 Cooling Efficiency of the Pad-and-Fan Cooling System

Increasing the ventilation rate decreased the cooling efficiency of the pad-and-fan cooling system (Table 5.2). The mean cooling efficiency was 83.2, 80.6, 77.4, and 73.5% for ventilation rates of 4.5, 9.4, 13.0, and 16.7 m³ s⁻¹, respectively. Statistically significant differences in η_{Pad} were found between all the ventilation rates according to a Tukey-Kramer HSD analysis ($p < 0.01$).

Moisture gain of the air passing through the pad affected cooling efficiency. Table 5.2 shows an inverse relationship between cooling efficiency and ventilation rate. As more moisture was gained by the air at lower ventilation rates, indicated by a larger difference in humidity ratio, the drybulb air temperature was reduced more and approached closer to wetbulb air temperature, effectively increasing cooling efficiency. Liao and Chiu (2002) also observed decreased cooling efficiency associated with increased ventilation rates, resulting from lower air humidity ratios and greater drybulb temperature depressions. Typically, pad-and-fan system manufacturers, such as ACME©, recommend an airflow rate across the pad of 1.27 m s⁻¹, which is equivalent to 13.0 m³ s⁻¹ for this greenhouse.

Table 5.2 Mean cooling efficiency (η_{Pad}) for the pad-and-fan system calculated using the equation $\eta_{Pad} = (T_{DB,Out} - T_{DB,PadIn}) / (T_{DB,Out} - T_{WB,Out})$. Standard deviations represent the variability observed during the testing period (08:00-17:00) for each ventilation rate tested (4.5, 9.4, 13.0, and 16.7 m³ s⁻¹). Letters represent significantly different values from a Tukey-Kramer HSD test ($p < 0.01$). Mean changes in humidity ratio ($W_{In} - W_{Out}$) and differences in $T_{DB,In}$ and $T_{WB,Out}$ are also presented.

\dot{Q} (m ³ s ⁻¹)	η_{Pad} (%)	$W_{In} - W_{Out}$ (g H ₂ O kg ⁻¹ Dry Air)	$T_{DB,In} - T_{WB,Out}$ (°C)
4.5	83.2 ^a ± 3.0	8.4	2.8
9.4	80.6 ^b ± 2.7	6.3	3.9
13	77.4 ^c ± 2.4	5.8	4.4
16.7	73.5 ^d ± 2.2	5.3	5.0

5.2.3 Water Use by the Pad-and-Fan Cooling System

Measuring water use over time confirmed the results of the preliminary study, which had indicated that it takes time for the system to reach a steady-state condition. Water use by the pad-and-fan system steadily increased until about 13:00 for all ventilation rates, before stabilizing for the remainder of the test period (Figure 5.6). However, regardless of time of day, the water use was consistently greater for higher ventilation rates.

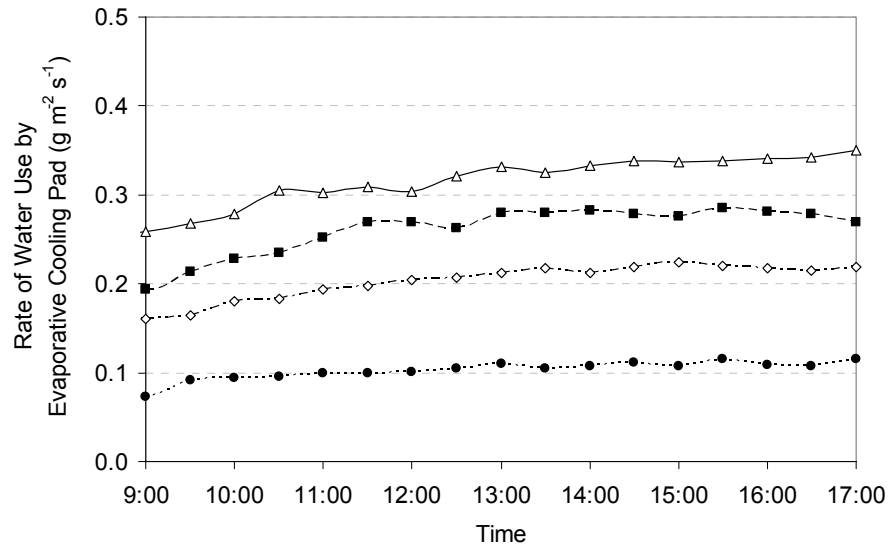


Figure 5.6 Rate of water use by the pad-and-fan evaporative cooling system for 09:00-17:00 for four ventilation rates: $4.5 \text{ m}^3 \text{ s}^{-1}$ (·····●·····), $9.4 \text{ m}^3 \text{ s}^{-1}$ (-·◇·-), $13 \text{ m}^3 \text{ s}^{-1}$ (--■--), and $16.7 \text{ m}^3 \text{ s}^{-1}$ (-△-).

Water use by the pad-and-fan system increased with increasing ventilation rate (Figure 5.7). During the period of 08:00 – 17:00, the total water use per unit floor area for the pad-and-fan system was 3.2 L m^{-2} of water for the lowest ventilation rate tested ($4.5 \text{ m}^3 \text{ s}^{-1}$) and 10.1 L m^{-2} , or 300% greater, under the highest ventilation rate ($16.7 \text{ m}^3 \text{ s}^{-1}$). For the 9-hour period the average water use rates were 0.10 , 0.19 , 0.26 , $0.31 \text{ g m}^{-2} \text{ s}^{-1}$, which are comparable to preliminary studies and values found by other studies for similar ventilation rates (El Helal, 2007). When considered on the basis of per area of pad, all of the water use rates are much less than the values (2.6 , 4.9 , 6.8 , $8.5 \text{ g s}^{-1} \text{ m}^{-2}$) found in a pad-and-fan model study by Al Massoum *et al.* (1998).

Total water use predicted by psychrometric equations overestimated by 12-25% the amount of water that would be used by the pad-and-fan system (Figure 5.7). This overestimation most likely occurred due to the sensor location, which was at the center of

the pad where a higher stream of water was observed. Section 5.6 will present more analysis on the estimation of water use by the pad-and-fan system.

For the ventilation rates tested, both the measured and modeled water use increased linearly with increased ventilation rates, agreeing with the initial studies presented in Section 5.1.1 (Figure 5.1), which included an even higher ventilation rate of $21.8 \text{ m}^3 \text{ s}^{-1}$. It is expected that water use would peak and stabilize at some higher ventilation rate, when the rate of evaporation from and delivery to the pad would be equivalent.

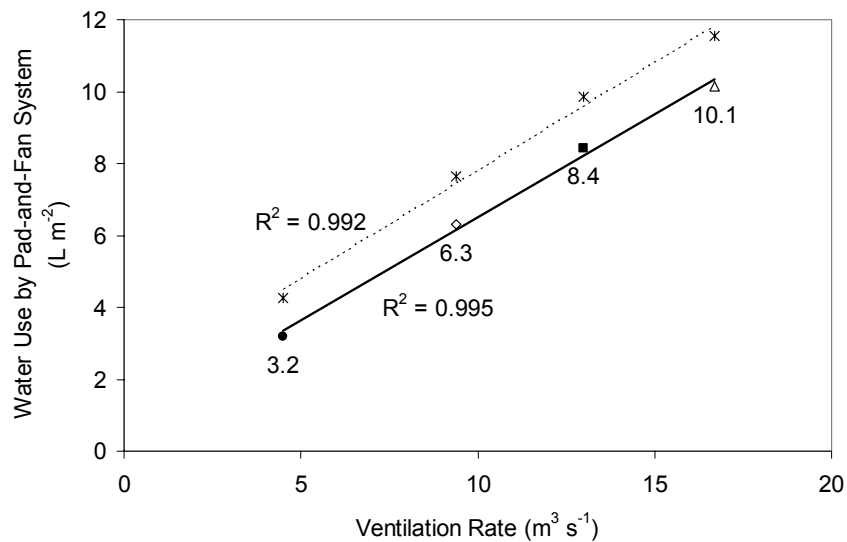


Figure 5.7 Total pad-and-fan cooling water use measured (—) and modeled using psychrometrics (···) for four ventilation rates: $4.5 \text{ m}^3 \text{ s}^{-1}$ (●), $9.4 \text{ m}^3 \text{ s}^{-1}$ (◇), $13 \text{ m}^3 \text{ s}^{-1}$ (■), and $16.7 \text{ m}^3 \text{ s}^{-1}$ (△) for the period 08:00-17:00.

When all the WU_{PF} data were analyzed together, ventilation rate dominated WU_{PF} results ($r = 0.95$) and outside conditions were not as influential (Table 5.3). However, the moisture conditions of the outside air did affect WU_{PF} , with moderate negative correlations associated with RH ($r = -0.54$) and W ($r = -0.68$). The effect of moist air

conditions on WU_{PF} became even clearer when the data were grouped by ventilation rate.

Within a given ventilation rate, strong positive correlations were found between WU_{PF} and $T_{Air,Out}$ ($r > 0.90$) and VPD_{Out} ($r > 0.90$) and negative correlations were found with relative humidity ($r < -0.83$).

Table 5.3 Correlations (r) between WU_{PF} and ventilation rate using multivariate analysis, and outside climate conditions including temperature (T_{Out}), relative humidity (RH_{Out}), vapor pressure deficit (VPD_{Out}), and absolute humidity (W_{Out}). Correlations were also calculated for each ventilation rate: 4.5, 9.4, 13.0, and 16.7 $\text{m}^3 \text{s}^{-1}$.

Parameter	r	r (4.5)	r (9.4)	r (13.0)	r (16.7)
<i>Vent Rate</i>	0.95	--	--	--	--
T_{Out}	0.19	0.92	0.98	0.89	0.98
RH_{Out}	-0.54	-0.83	-0.94	-0.84	-0.97
VPD_{Out}	0.30	0.93	0.98	0.89	0.97
W_{Out}	-0.68	0.73	-0.30	-0.88	-0.78

5.2.4 Water Use by Tomato Plants

The irrigation schedule for the tomato plants was the same throughout the experimental period; therefore, the total irrigation water use was the same for all ventilation rates tested. Water uptake was the least at 4.5 $\text{m}^3 \text{s}^{-1}$, but there was no observable increase in trend with increasing ventilation rate (Table 5.4). The total water use by the plants (ΣWU_P) during the test period (08:00 – 17:00) was 632, 806, 739, and 756 L for ventilation rates of 4.5, 9.4, 13.0, and 16.7 $\text{m}^3 \text{s}^{-1}$, respectively. Values for $\overline{WU_P}$ were 0.065, 0.084, 0.077, and 0.079 $\text{g m}^{-2} \text{s}^{-1}$ for ventilation rates of 4.5, 9.4, 13.0, and 16.7 $\text{m}^3 \text{s}^{-1}$, respectively.

Table 5.4 Total water use for irrigation (WU_I), total plant water uptake (ΣWU_P), and mean plant water uptake rates ($\overline{WU_P}$) during the test period (08:00-17:00) for four ventilation rates: 4.5, and 9.4, 13.0, and 16.7 $\text{m}^3 \text{s}^{-1}$.

\dot{Q} ($\text{m}^3 \text{s}^{-1}$)	ΣWU_I (L)	ΣWU_P (L)	$\overline{WU_P}$ ($\text{g m}^{-2} \text{s}^{-1}$)
4.5	1251	632	0.065 ^a
9.4	1251	806	0.084 ^b
13.0	1251	739	0.077 ^{ab}
16.7	1251	756	0.079 ^{ab}

5.2.5 Total Greenhouse Water Use

Together the irrigation and pad-and-fan cooling systems used a total of 7.7, 10.8, 12.9, and 14.6 $\text{L m}^{-2} \text{d}^{-1}$ for ventilation rates of 4.5, 9.4, 13.0, and 16.7 $\text{m}^3 \text{s}^{-1}$, respectively (Table 5.5). At 4.5 $\text{m}^3 \text{s}^{-1}$, the irrigation system used 30% more water than the pad-and-fan system (3.2 $\text{L m}^{-2} \text{d}^{-1}$). For all other ventilation rates, the pad-and-fan system used more water than the irrigation system. Water use by the pad-and-fan system was 140%, 180%, and 225% more than the irrigation system for ventilation rates of 9.4, 13.0, and 16.7 $\text{m}^3 \text{s}^{-1}$, respectively.

A 100% “closed” irrigation system would have reduced the irrigation system water use, only adding new water to the system to replace water consumed by the plants. Therefore, the total amount of water used by the irrigation system would equal WU_{PU} . The total daytime water use with a “closed” irrigation system would be 5.5, 9.2, 11.1, and 12.9 $\text{L m}^{-2} \text{d}^{-1}$ for ventilation rates of 4.5, 9.4, 13.0, and 16.7 $\text{m}^3 \text{s}^{-1}$, respectively. If a 100% closed system was used, water use by the pad-and-fan system would have represented 58%, 74%, 76%, and 79% of all greenhouse water use for ventilation rates of 4.5, 9.4, 13.0 and 16.7 $\text{m}^3 \text{s}^{-1}$, respectively.

Table 5.5 Total daily water use per floor area by the open irrigation system (WU_I), pad-and-fan system (WU_{PF}), and closed irrigation system (ΣWU_{PU}) for the 9-hour test day (08:00-17:00) for ventilation rates of 4.5, 9.4, 13.0 and 16.7 m³ s⁻¹. Total greenhouse water use with the pad-and-fan system and open irrigation ($\Sigma WU_{S,Open}$) and closed irrigation ($\Sigma WU_{S,Closed}$) systems also presented.

\dot{Q} (m ³ s ⁻¹)	ΣWU_{PF} (L m ⁻² d ⁻¹)	ΣWU_I (L m ⁻² d ⁻¹)	ΣWU_{PU} (L m ⁻² d ⁻¹)	$\Sigma WU_{S,Open}$ (L m ⁻² d ⁻¹)	$\Sigma WU_{S,Closed}$ (L m ⁻² d ⁻¹)
4.5	3.2	4.5	2.3	7.7	5.5
9.4	6.3	4.5	2.9	10.8	9.2
13.0	8.4	4.5	2.7	12.9	11.1
16.7	10.1	4.5	2.7	14.6	12.9

5.2.6 Water Use Efficiency

The overall system water use efficiency (WUE_S) decreased with increasing ventilation rate as the pad-and-fan system used more water at higher ventilation rates (Table 5.6). Based only upon “open” irrigation system water use and tomato yields in the test greenhouse, the WUE_I was 31 kg m⁻³, a smaller but comparable value to those obtained in the Netherlands (45 kg m⁻³) and France (39 kg m⁻³) (Pardossi *et al.*, 2004).

The WUE_{PF} decreased with increasing ventilation rate, as more water was evaporated from the pad. The WUE_{PF} was 44, 22, 17, and 14 kg m⁻³ for ventilation rates of 4.5, 9.4, 13.0, and 16.7 m³ s⁻¹, respectively. Therefore, the total WUE_S , based on open irrigation and pad-and-fan water use, was 18, 13, 11, and 10 kg m⁻³ for ventilation rates 4.5, 9.4, 13.0, and 16.7 m³ s⁻¹, respectively, which range from field production WUE values from flood (10-12 kg m⁻³) to sprinkler (11-19 kg m⁻³) irrigation (Hanson *et al.*, 2006; Hanson and May, 2005; Hanson and May, 2004).

Using a “closed” irrigation system would have increased WUE_I by 100% to 62 kg m⁻³ for 4.5 m³ s⁻¹, and by 70% to greater than 50 kg m⁻³ for the other ventilation rates (Table 5.6). WUE_I for the “closed” system were approximately the same for ventilation

rates above $9.4 \text{ m}^3 \text{ s}^{-1}$ because transpiration rates were about the same. These WUE_I levels compare well to the 66 kg m^{-3} reported for greenhouses in the Netherlands (Pardossi *et al.*, 2004), and were better than the 25 and 30 kg m^{-3} reported for a closed-loop systems in Spain (Reina-Sanchez, 2005) and Italy (Incrocci *et al.*, 2006).

Unfortunately, these marked improvements in WUE_I were diminished greatly by low WUE_{PF} , and resulted in only modest increases in WUE_S overall. For a “closed” irrigation system, the WUE_S values would be 26, 16, 13, and 11 kg m^{-3} for ventilation rates of 4.5, 9.4, 13.0, and $16.7 \text{ m}^3 \text{ s}^{-1}$, respectively, ranging from low field sprinkler WUE ($11\text{-}19 \text{ kg m}^{-3}$) to greater than high drip ($19\text{-}25 \text{ kg m}^{-3}$) irrigation (Hanson *et al.*, 2006; Hanson and May, 2005; Hanson and May, 2004).

Finally, the WUE_S for a commercial tomato yield of 65 kg m^{-2} grown in a “closed” irrigation system would have been 33, 20, 16, and 14 kg m^{-3} for ventilation rates of 4.5, 9.4, 13.0, and $16.7 \text{ m}^3 \text{ s}^{-1}$, respectively. Also, it is likely that yields would have differed based on long-term use of the above ventilation rates, creating different values for WUE for the different ventilation rates. The effect of outside conditions and pad-and-fan operation on tomato yield will be discussed further in Section 5.5

Table 5.6 Water use efficiency (WUE) of the greenhouse water systems, including irrigation for open ($WUE_{I,Open}$) and closed ($WUE_{I,Closed}$) systems and the pad-and-fan system (WUE_{PF}) for four ventilation rates, and the resulting system water use efficiency (WUE_S) when water use by both systems is considered. Results are divided for tomato yields obtained in the experimental greenhouse (39 kg day^{-1}) and those that might be expected in commercial tomato production (49.5 kg day^{-1}).

\dot{Q} $\text{m}^3 \text{ s}^{-1}$	Test Greenhouse Yield = $39 \text{ kg} = 0.14 \text{ kg m}^{-2} \text{ d}^{-1}$				
	WUE_{PF}	$WUE_{I,Open}$	$WUE_{I,Closed}$	$WUE_{S,Open}$	$WUE_{S,Closed}$
4.5	44	31	62	18	26
9.4	22	31	52	13	16
13.0	17	31	53	11	13
16.7	14	31	51	10	11
\dot{Q}	Commercial Yield = $49.5 \text{ kg} = 0.18 \text{ kg m}^{-2} \text{ d}^{-1}$				
	WUE_{PF}	$WUE_{I,Open}$	$WUE_{I,Closed}$	$WUE_{S,Open}$	$WUE_{S,Closed}$
4.5	56	39	78	23	33
9.4	28	39	66	16	20
13.0	21	39	67	14	16
16.7	18	39	65	12	14

5.2.7 Greenhouse Environmental Conditions

5.2.7.1 Mean Greenhouse Conditions

The mean daytime (08:00 – 17:00) plant zone air temperatures decreased as the ventilation rate increased up to $13.0 \text{ m}^3 \text{ s}^{-1}$, with no further reduction at higher ventilation rates. The mean daytime plant zone air temperatures were 26.2, 22.6, 21.3, and 21.4°C for ventilation rates of 4.5, 9.4, 13.0, and $16.7 \text{ m}^3 \text{ s}^{-1}$, respectively (Figure 5.8).

Increasing the ventilation rate also decreased the mean plant zone relative humidity, with values of 71.3, 64.1, 62.3, and 56.4%, for 4.5, 9.4, 13.0, and $16.7 \text{ m}^3 \text{ s}^{-1}$, respectively.

Vapor pressure deficit increased slightly with increasing ventilation rate, but never exceeded 1.2 kPa.

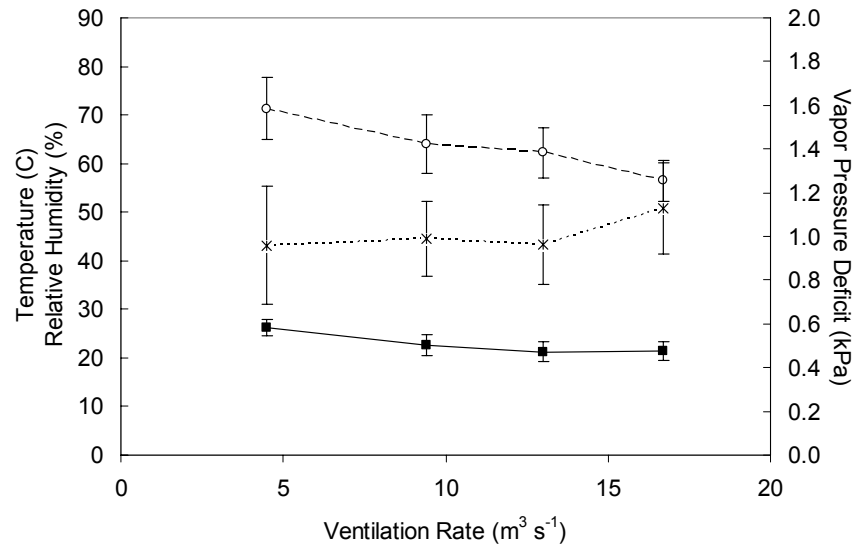


Figure 5.8 Mean daytime (08:00 – 17:00) plant zone air temperature ($\text{—}\blacksquare\text{—}$), relative humidity ($\text{---}\circ\text{---}$), and vapor pressure deficit ($\cdots\times\cdots$).

Ventilation rates of 13.0 and $16.7 \text{ m}^3 \text{ s}^{-1}$ produced the greatest air temperature difference between inside and outside, with mean reductions of 12.1 and 12.0°C , respectively (Table 5.7). The mean air temperature difference was 7.9 and 11.5°C for 4.5 and $9.4 \text{ m}^3 \text{ s}^{-1}$, respectively. The smallest increase in relative humidity ($+46.7\%$) occurred at $16.7 \text{ m}^3 \text{ s}^{-1}$, and was less than the increase at other ventilation rates, which all provided increases greater than 50% . All ventilation rates lowered the VPD by more than 3.5 kPa , with the greatest difference observed for the $9.4 \text{ m}^3 \text{ s}^{-1}$ ventilation rate.

Table 5.7 Mean plant zone air temperature, relative humidity, vapor pressure deficit, and incoming radiation during one day of testing (08:00 – 17:00) with standard deviations (*italics*). The values ΔT ($T_{\text{GH-Out}}$), ΔRH ($RH_{\text{GH-Out}}$), and ΔVPD ($VPD_{\text{GH-Out}}$) represent their differences relative to outside conditions averaged over the same period.

\dot{Q} ($\text{m}^3 \text{s}^{-1}$)	T_{GH} ($^\circ\text{C}$)	RH_{GH} (%)	VPD_{GH} (kPa)	Rad_{In} (W m^{-2})	ΔT ($^\circ\text{C}$)	ΔRH (%)	ΔVPD (kPa)
4.5	$26.2^a \pm 1.7$	$71.3^a \pm 6.4$	$0.96^{ab} \pm 0.27$	$431^a \pm 121$	-7.9	+58.5	-3.6
9.4	$22.6^b \pm 2.2$	$64.1^b \pm 6.0$	$0.97^{ab} \pm 0.17$	$404^a \pm 153$	-11.5	+55.5	-4.0
13.0	$21.3^b \pm 2.1$	$62.3^b \pm 5.1$	$0.94^b \pm 0.18$	$358^a \pm 156$	-12.1	+52.4	-3.7
16.7	$21.4^b \pm 1.9$	$56.4^c \pm 4.1$	$1.1^a \pm 0.21$	$311^a \pm 96$	-12.0	+46.3	-3.6

5.2.7.2 Temporal Trends in Greenhouse Conditions

With incoming solar radiation levels measured just above the plant tops and below the shade curtain, Figure 5.9 shows that the double polyethylene cover itself reduced incoming solar radiation by about 30%. When the shade curtain was deployed (11:30-14:00), the incoming solar radiation was reduced a total of 70%, from outside levels greater than 1000 W m^{-2} and radiation intensity at the canopy top was approximately 300 W m^{-2} .

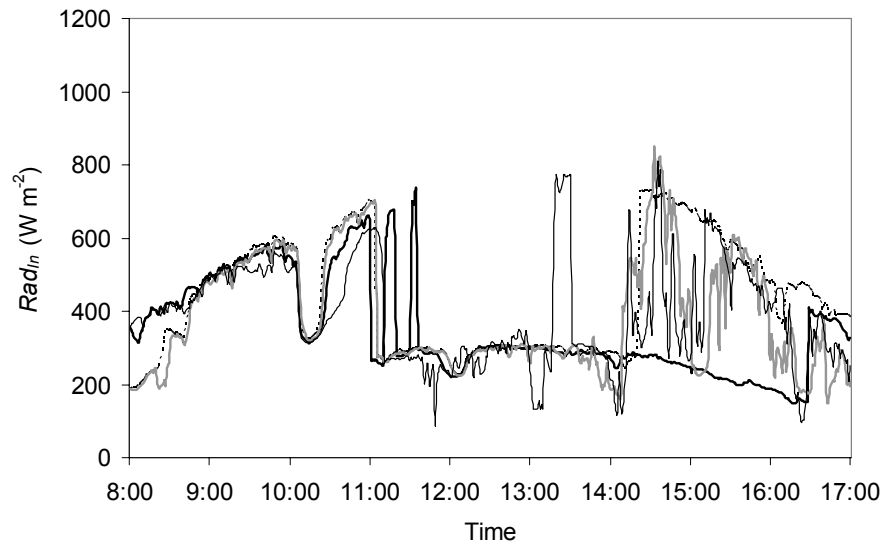


Figure 5.9 Incoming solar radiation intensity during the pad-and-fan cooling tests for four ventilation rates: $4.5 \text{ m}^3 \text{ s}^{-1}$ (—), $9.4 \text{ m}^3 \text{ s}^{-1}$ (···), $13.0 \text{ m}^3 \text{ s}^{-1}$ (—), and $16.7 \text{ m}^3 \text{ s}^{-1}$ (—).

In general, mean plant zone air temperatures increased until 11:00, and then stabilized when the shade curtain was deployed (Figure 5.10). For 4.5 and $9.4 \text{ m}^3 \text{ s}^{-1}$ the mean plant zone air temperature increased after the shade curtain was removed at 14:00. At 13.0 and $16.7 \text{ m}^3 \text{ s}^{-1}$, the temperature did not increase following the removal of shade, indicating that the ventilation rates were high enough to offset the solar energy gain.

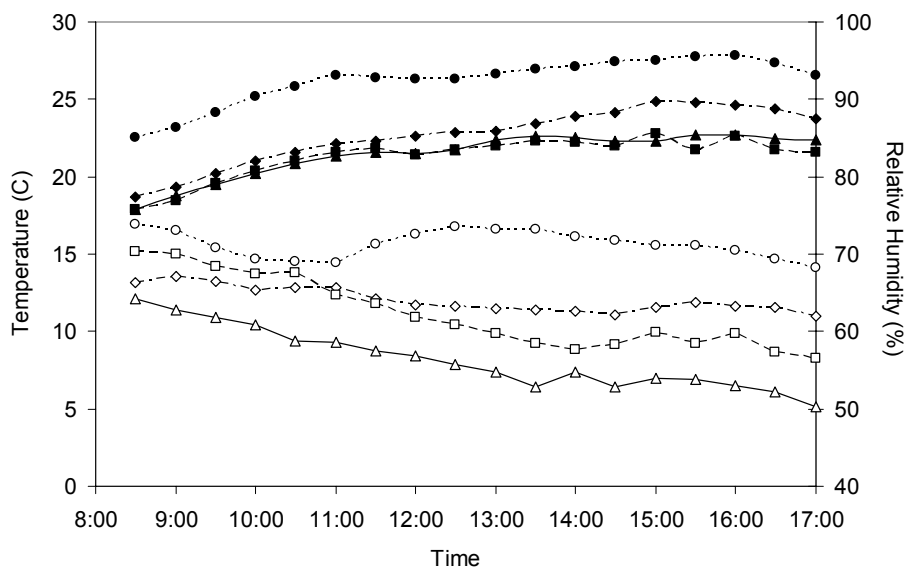


Figure 5.10 Mean plant zone air temperatures (solid symbols) and relative humidity levels (open symbols) calculated every 30 minutes for four ventilation rates: $4.5 \text{ m}^3 \text{ s}^{-1}$ ($\cdots\bullet\cdots$), $9.4 \text{ m}^3 \text{ s}^{-1}$ ($--\blacklozenge--$), $13 \text{ m}^3 \text{ s}^{-1}$ ($--\blacksquare--$), and $16.7 \text{ m}^3 \text{ s}^{-1}$ ($-\blacktriangle-$).

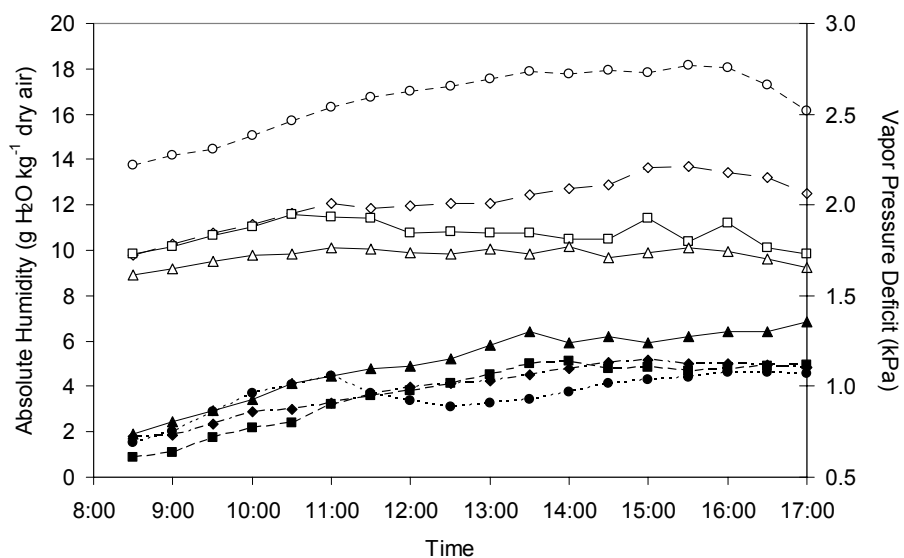


Figure 5.11 Mean plant zone absolute humidity (open symbols) and vapor pressure deficit (solid symbols) were calculated every 30 minutes for four ventilation rates: $4.5 \text{ m}^3 \text{ s}^{-1}$ ($\cdots\bullet\cdots$), $9.4 \text{ m}^3 \text{ s}^{-1}$ ($--\blacklozenge--$), $13 \text{ m}^3 \text{ s}^{-1}$ ($--\blacksquare--$), and $16.7 \text{ m}^3 \text{ s}^{-1}$ ($-\blacktriangle-$).

In general, relative humidity decreased until 14:00 and then stabilized for the remainder of the day. At $4.5 \text{ m}^3 \text{ s}^{-1}$ the relative humidity increased when the shade curtain was deployed regardless of the increased air temperature, most likely because moist air was prevented from rising into the roof space above the plant canopy. Relative humidity levels at the other ventilation rates tended to increase during shading and were proportional to the decreases in air temperature. At $9.4 \text{ m}^3 \text{ s}^{-1}$ relative and humidity ratio gradually increased after 14:00 (Figure 5.11).

VPD increased during the day and for 4.5 , 13.0 , and $16.7 \text{ m}^3 \text{ s}^{-1}$ ventilation rates followed the trends observed in relative humidity (Figure 5.11). For $9.4 \text{ m}^3 \text{ s}^{-1}$, the VPD more closely followed trends in temperature, which increased over the day, unlike relative humidity, which was stable for most of the day. At $4.5 \text{ m}^3 \text{ s}^{-1}$ the VPD decreased markedly after the shade was deployed, from 11:00-12:30, and then gradually increased.

5.2.7.3 Spatial Uniformity of Greenhouse Conditions

Figures 5.12, 5.13, 5.14, and 5.15 plot the changes in air temperature, relative humidity, vapor pressure deficit, and humidity ratio (absolute humidity) as the air traveled from the pad to the fans. Climate conditions were relatively uniform within the plant zone itself. However, as expected, air temperature increased from pad-to-fan and the absolute humidity of the air increased. Also, relative humidity decreased and *VPD* slightly increased.

The magnitude of increasing air temperature from pad to fan declined with increasing ventilation rate, with increases of 8.6 , 5.1 , 3.9 , and 4.0°C for ventilation rates of 4.5 , 9.4 , 13.0 , and $16.7 \text{ m}^3 \text{ s}^{-1}$, respectively (Table 5.8). For 4.5 and $9.4 \text{ m}^3 \text{ s}^{-1}$ the

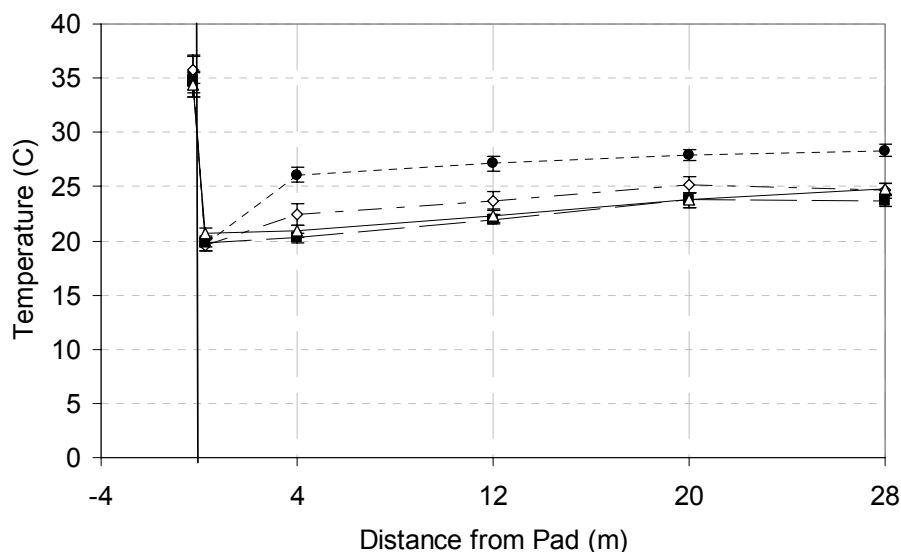


Figure 5.12 Mean temperatures observed outside the pad and at several greenhouse locations (0, 4, 12, 20, and 28 m from the pad inlet) during pad-and-fan cooling for four ventilation rates: $4.5 \text{ m}^3 \text{ s}^{-1}$ ($\cdots\bullet\cdots$), $9.4 \text{ m}^3 \text{ s}^{-1}$ ($--\diamond--$), $13 \text{ m}^3 \text{ s}^{-1}$ ($--\blacksquare--$), and $16.7 \text{ m}^3 \text{ s}^{-1}$ ($—\triangle—$). Means were calculated from values measured when outside conditions were most stable (11:00 – 17:00). The solid vertical line represents the cooling pad location.

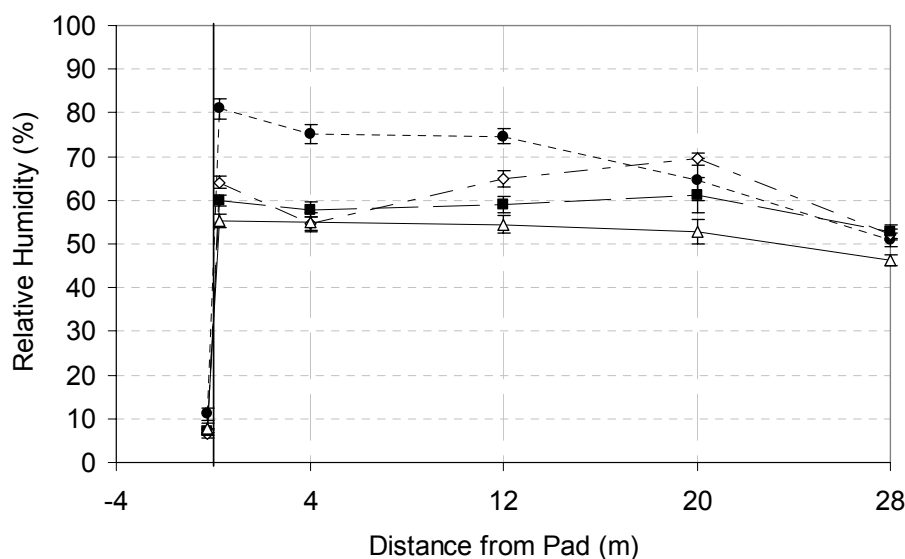


Figure 5.13 Mean relative humidity levels observed outside and at several greenhouse locations (0, 4, 12, 20, and 28 m from the pad inlet) during pad-and-fan cooling for four ventilation rates: $4.5 \text{ m}^3 \text{ s}^{-1}$ ($\cdots\bullet\cdots$), $9.4 \text{ m}^3 \text{ s}^{-1}$ ($--\diamond--$), $13 \text{ m}^3 \text{ s}^{-1}$ ($--\blacksquare--$), and $16.7 \text{ m}^3 \text{ s}^{-1}$ ($—\triangle—$). Means were calculated from values measured when outside conditions were most stable (11:00 – 17:00). The solid vertical line represents the cooling pad location.

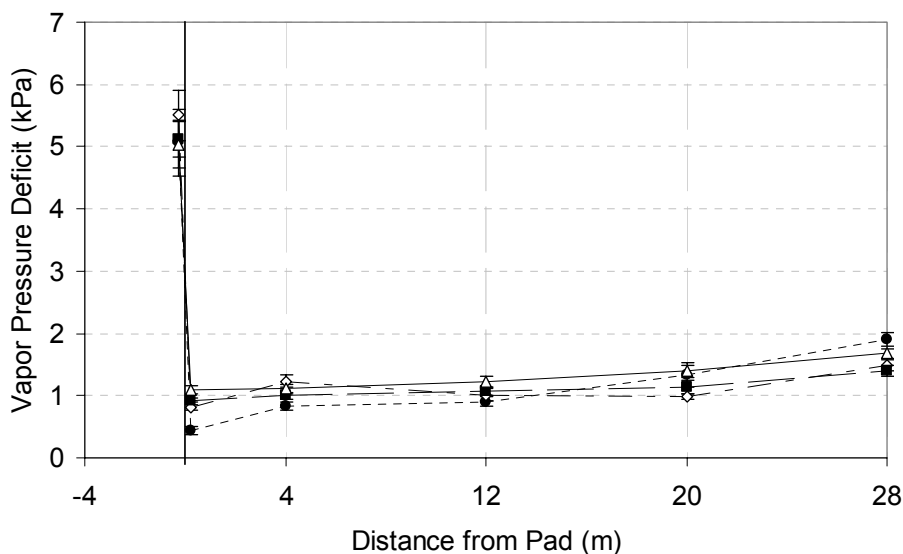


Figure 5.14 Mean vapor pressure deficit values observed outside and at several greenhouse locations (0, 4, 12, 20, and 28 m from the pad inlet) during pad-and-fan cooling for four ventilation rates: $4.5 \text{ m}^3 \text{ s}^{-1}$ ($\cdots\bullet\cdots$), $9.4 \text{ m}^3 \text{ s}^{-1}$ ($--\diamond--$), $13 \text{ m}^3 \text{ s}^{-1}$ ($--\blacksquare--$), and $16.7 \text{ m}^3 \text{ s}^{-1}$ ($-\triangle-$). Means were calculated from values measured when outside conditions were most stable (11:00 – 17:00). The solid vertical line represents the cooling pad location.

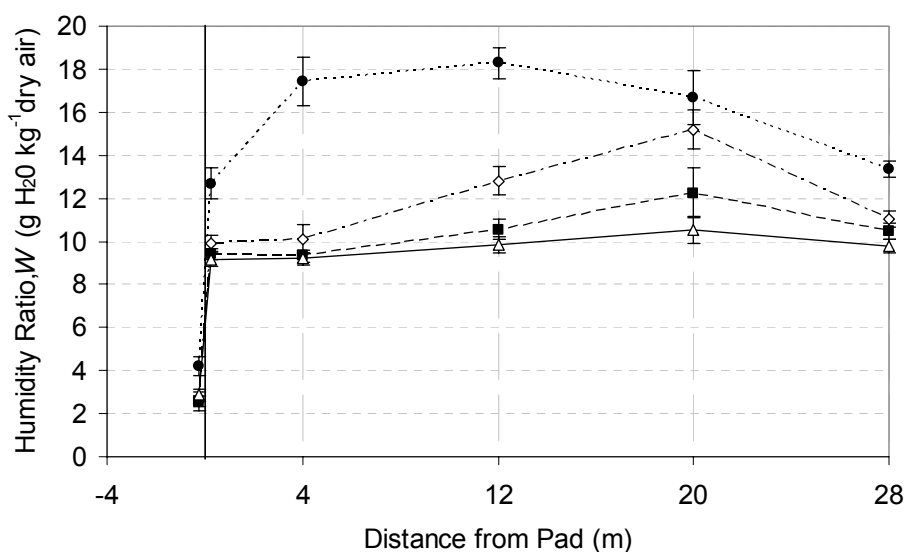


Figure 5.15 Mean humidity ratio (W) of the air observed at several greenhouse locations (0, 4, 12, 20, and 28 m from the pad inlet) during pad-and-fan cooling for four ventilation rates: $4.5 \text{ m}^3 \text{ s}^{-1}$ ($\cdots\bullet\cdots$), $9.4 \text{ m}^3 \text{ s}^{-1}$ ($--\diamond--$), $13 \text{ m}^3 \text{ s}^{-1}$ ($--\blacksquare--$), and $16.7 \text{ m}^3 \text{ s}^{-1}$ ($-\triangle-$). Means were calculated from values measured when outside conditions were most stable (11:00 – 17:00). The solid vertical line represents the cooling pad location.

greatest rise in air temperature occurred between the pad and the plant zone (4 m from the pad), as the air had more exposure time to radiation and convective heat transfer before reaching the plants (Figure 5.10). For 13.0 and 16.7 m³ s⁻¹ most of the rise in air temperature occurred within the plant zone itself, possibly due to less latent heat transfer, as implied by lower humidity ratio (Figure 5.15). In general, air temperatures either increased very little or not at all from the plants (20 m from pad) to the fans (28 m from pad).

Table 5.8 Uniformity of greenhouse air temperature, relative humidity, and vapor pressure deficit during pad-and-fan cooling for four ventilation rates (4.5, 9.4, 13.0, and 16.7 m³ s⁻¹) is presented as the mean difference between measurements made at different greenhouse locations during the most stable part of the day (11:00-17:00).

\dot{Q} (m ³ s ⁻¹)	Pad-to-Fan Difference (0-28 m)	Pad-To-Plants Difference (0-4 m)	Max Plant Zone Difference (Locations w/Max Difference)
<i>Air Temperature (°C)</i>			
4.5	8.6 ± 0.4	6.3 ± 0.5	1.9 ± 0.4 (4-20 m)
9.4	5.1 ± 0.4	2.9 ± 0.6	2.7 ± 0.3 (4-20 m)
13.0	3.9 ± 0.3	0.4 ± 0.1	3.5 ± 0.4 (4-20 m)
16.7	4.0 ± 0.3	0.2 ± 0.1	2.9 ± 0.2 (4-20 m)
<i>Relative Humidity (%)</i>			
4.5	-30.1 ± 1.7	-5.8 ± 2.2	-10.5 ± 3.8 (12-20 m)
9.4	-11.8 ± 1.1	-9.3 ± 0.8	14.6 ± 1.5 (4-20 m)
13.0	-7.4 ± 1.3	-2.2 ± 0.9	3.3 ± 3.1 (4-20 m)
16.7	-9.0 ± 0.7	-0.2 ± 0.8	-2.4 ± 1.4 (12-20 m)
<i>Vapor Pressure Deficit (kPa)</i>			
4.5	1.4 ± 0.1	0.4 ± 0.0	0.5 ± 0.1 (4/12-20 m)
9.4	0.7 ± 0.1	0.4 ± 0.1	-0.3 ± 0.1 (4-12/20 m)
13.0	0.5 ± 0.1	0.1 ± 0.0	0.1 ± 0.1 (4-12/20 m)
16.7	0.6 ± 0.1	0.0 ± 0.0	0.3 ± 0.0 (4/12-20 m)
<i>Humidity Ratio, W (g H₂O kg⁻¹ dry air)</i>			
4.5	0.69 ± 0.82	4.7 ± 1.2	-1.6 ± 1.3 (12-20 m)
9.4	1.1 ± 0.27	0.21 ± 0.44	5.1 ± 0.5 (4-20 m)
13.0	1.1 ± 0.35	-0.09 ± 0.13	2.9 ± 1.1 (4-20 m)
16.7	0.65 ± 0.28	0.06 ± 0.11	1.3 ± 0.5 (4-20 m)

Relative humidity decreased from 0-4 m as the air temperature increased (Figure 5.13), and decreased from 20-28 m as the humidity ratio decreased (Figure 5.15). Overall relative humidity decreased from pad-to-fan, with greater decreases occurring at lower ventilation rates. Pad-to-fan reductions in relative humidity were 30.1, 11.8, 7.4, and 9.0% for ventilation rates of 4.5, 9.4, 13.0, and 16.7 m³ s⁻¹, respectively (Table 5.8). At the 4.5 m³ s⁻¹ ventilation rate the relative humidity was stable through the first half of the plant zone, and then decreased to the fans, corresponding to the decreasing trend in humidity ratio (Figure 5.15). The lack of increasing humidity ratio at 4.5 m³ s⁻¹ likely resulted from the low transpiration rates observed during that test (see Section 5.2.8). However, the cause for the negative average value of humidity ratio is uncertain and should only occur if the plants, ground, or other greenhouse materials acted as a sink for moisture.

At 9.4 m³ s⁻¹ the relative and humidity ratio levels increased along the plant zone, reflecting the higher transpiration rates and possibly an airflow that did not exhaust air too quickly. At 13.0 and 16.7 m³ s⁻¹ the relative humidity was nearly constant as the air passed across the plant zone, although a slight increase in humidity ratio observed. Therefore, it's likely that the small increase in temperature and humidity ratio were enough to offset a decrease in relative humidity.

The VPD tended to increase as the air passed across the plant zone, as the temperature increased and relative humidity decreased or stayed the same. However, at 9.4 m³ s⁻¹ the VPD actually decreased slightly, reflecting the large increase in humidity ratio of the air.

Although relative humidity decreased and vapor pressure increased from pad-to-fan, the overall water vapor content of the air increased as it traveled across the plants (Figure 5.15), indicating that the air collected water from the transpiring plants. Similar increases in humidity ratio from pad-to-fan were observed for 4.5 and 16.7 m³ s⁻¹ ventilation rates, with increases of 0.69 and 0.65 g H₂O kg⁻¹ dry air for 4.5 and 16.7 m³ s⁻¹, respectively. Ventilation rates of 9.4 and 13.0 m³ s⁻¹ both had increases in water vapor content of 1.1 g H₂O kg⁻¹ dry air. Finally, humidity ratio increased as the air traveled along the plant zone for all ventilation rates except 4.5 m³ s⁻¹, which decreased at distances beyond 12 m.

5.2.8 Transpiration Rate and Water Use by Tomato Plants

The transpiration rates (E_T) of plants calculated before 11:00 were erroneously high due to an initial hydration period of rockwool media and plants. After this initial period (post-11:00), E_T became relatively stable; therefore, only data collected after 11:00 are presented in Figure 5.16. E_T peaked during the period between 15:00 – 16:00, as plants responded to increased solar energy load. Finally, E_T declined until 17:00 as structural shading increased due to the low sun angle.

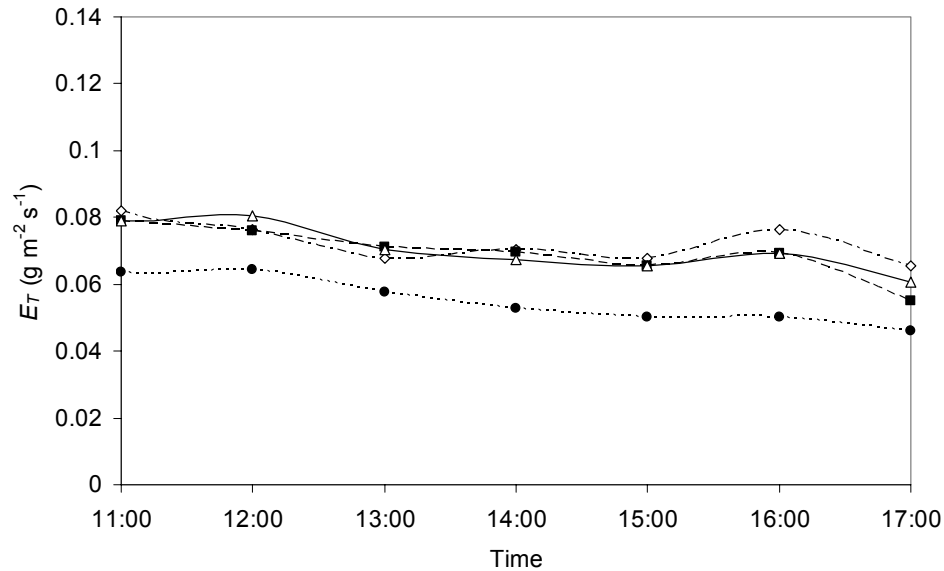


Figure 5.16 Transpiration rates of tomato plants for pad-and-fan cooling for four different ventilation rates: $4.5 \text{ m}^3 \text{s}^{-1}$ ($\cdots\bullet\cdots$), $9.4 \text{ m}^3 \text{s}^{-1}$ ($--\diamond--$), $13 \text{ m}^3 \text{s}^{-1}$ ($--\blacksquare--$), and $16.7 \text{ m}^3 \text{s}^{-1}$ ($—\triangle—$). Each value represents the one-hour mean of transpired water ($\text{g m}^{-2} \text{s}^{-1}$) from 30-minute measurements using a lysimeter.

A low correlation was found between E_T and incoming solar radiation during the 11:00 – 17:00 period of testing (Figure 5.17). Plant E_T was more closely correlated to the psychrometric properties of the air than to incoming solar radiation. E_T was negatively correlated to inside air temperature ($r = -0.76$), VPD ($r = -0.67$), and W ($r = -0.52$). Because E_T and water uptake rates were similar among ventilation rates, their correlation was very low ($r = 0.22$). When shade (13:00-14:00) and post-shade (15:00-16:00) periods are isolated from the data the correlations increase, with $r = -0.81$, 0.74 , -0.72 , and -0.69 for inside air temperature, relative humidity, vapor pressure deficit, and absolute humidity, respectively.

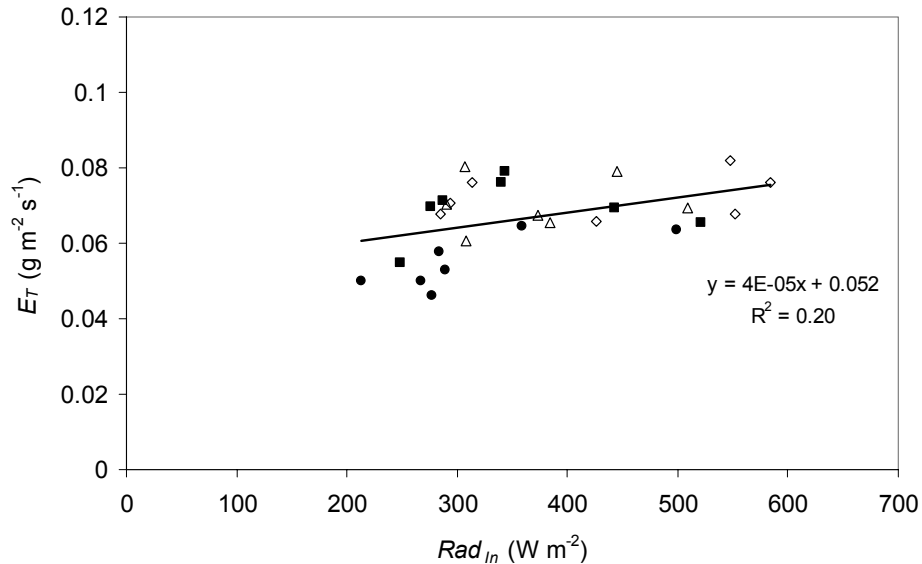


Figure 5.17 Transpiration rate (E_T) of tomato plants versus incoming solar radiation (Rad_{in}) during pad-and-fan cooling for four ventilation rates: 4.5 $m^3 s^{-1}$ (●), 9.4 $m^3 s^{-1}$ (◇), 13 $m^3 s^{-1}$ (■), and 16.7 $m^3 s^{-1}$ (△). Linear regression performed on data points (11:00 – 17:00) for all three ventilation rates.

Transpiration rate has been demonstrated to follow a positive linear relationship with solar radiation (Jolliet and Bailey, 1992), and the results of this study during the more stable period of the day (11:00 – 17:00) generally support that relationship. Although E_T did tend to be higher during non-shading periods, overall the E_T tended to decrease throughout the day (Figure 5.17). Furthermore, the correlation between E_T and Rad_{in} increased from $r = 0.24$, when all data were considered, to $r = 0.54$, when shade and post-shade periods were evaluated separately from the data.

Between 11:00-17:00 the mean plant water uptake (WU_{PU}) was 0.056, 0.072, 0.071, and 0.072 $g m^{-2} s^{-1}$ for ventilation rates of 4.5, 9.4, 13.0 and 16.7 $m^3 s^{-1}$, respectively (Table 5.9). A Tukey-Kramer HSD test revealed that water uptake rate at 4.5 $m^3 s^{-1}$ was significantly less ($p < 0.05$) than at the other three ventilation rates.

Table 5.9 Mean plant water uptake rates (WU_{PU}) from 11:00-17:00 for different ventilation rates for pad-and-fan evaporative cooling. Means with significant difference ($p < 0.05$) according to Tukey-Kramer HSD are represented by different letters.

\dot{Q} ($\text{m}^3 \text{s}^{-1}$)	WU_{PU} ($\text{g m}^{-2} \text{s}^{-1}$)
4.5	0.056 ^a
9.4	0.073 ^b
13.0	0.070 ^b
16.7	0.071 ^b

5.2.9 Leaf Temperature

In general, leaf temperature (T_{Leaf}) decreased with increasing ventilation rate, but with similar values measured at 13.0 and 16.7 $\text{m}^3 \text{s}^{-1}$ after 12:00 (Figure 5.18). The mean T_{Leaf} values measured at 4.5 $\text{m}^3 \text{s}^{-1}$ were significantly greater than those measured at all other ventilation rates ($p < 0.01$), with no significant difference between T_{Leaf} for the other ventilation rates.

Assuming that leaf temperatures did not change between two-hour measurement intervals, leaf temperature was always less than the mean plant zone air temperature during the 2-hour period leading up to T_{Leaf} measurements (Table 5.10). The greatest $T_{Air}-T_{Leaf}$ differences occurred at 12:00 and 14:00, when the plants were shaded. There was also little change in T_{Leaf} from 12:00 to 14:00, except at 4.5 $\text{m}^3 \text{s}^{-1}$, which increased nearly 4°C in the 2-hour period. This T_{Leaf} increase corresponded to the small increase in water vapor conditions.

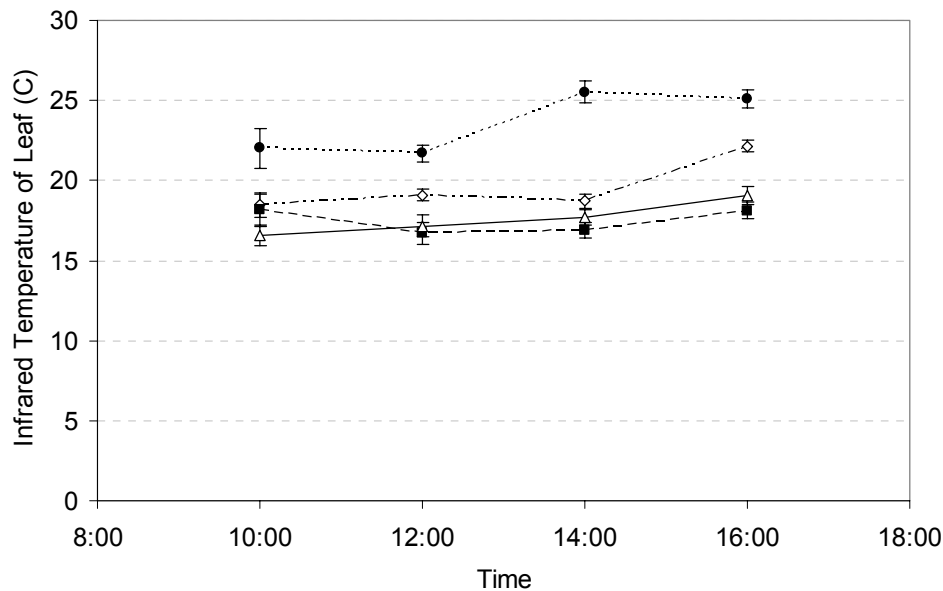


Figure 5.18 Mean leaf temperatures and standard deviations of 3 shaded leaves measured with an infrared thermometer during pad-and-fan evaporative cooling for four ventilation rates: $4.5 \text{ m}^3 \text{ s}^{-1}$ ($\cdots\bullet\cdots$), $9.4 \text{ m}^3 \text{ s}^{-1}$ ($--\diamond--$), $13 \text{ m}^3 \text{ s}^{-1}$ ($--\blacksquare--$), and $16.7 \text{ m}^3 \text{ s}^{-1}$ ($—\triangle—$). The shade curtain was used between 11:00-14:00.

T_{Leaf} had a strong positive correlation with air temperature ($r = 0.92$), relative humidity ($r = 0.73$), and humidity ratio ($r = 0.93$), and a negative correlation with E_T ($r = -0.64$). However, no correlation was found in association with VPD ($r = 0.003$) or Rad_{In} ($r = -0.03$). These correlations demonstrate the relationship between greenhouse conditions and plant response. At the lowest ventilation rate, the air temperatures were high but so was the humidity, ultimately causing significantly low transpiration rates. During low transpiration rates, the leaves were unable to evaporatively cool themselves to the lower temperatures observed at the higher ventilation rates.

T_{Leaf} also tended to increase with increasing distance from the cooling pad (Table 5.10), with the greatest increases occurring in the morning at 08:00. Greatest variability occurred during the morning and uniformity generally improved as the day progressed,

with T_{Leaf} differences at 10:00, 12:00, 14:00, and 16:00 ranging from 1.3-2.3°C, 0.8-1.3°C, 0.9-1.2°C, and 0.7-1.1°C, respectively. The improvements in T_{Leaf} uniformity corresponded to shading periods, which began at 11:00 and continued until 14:00.

Table 5.10 Leaf temperature (T_{Leaf}) at three locations, and average plant zone air conditions for four ventilation rates during specific times of the day. T_{Leaf} was measured with an Infrared thermometer on three plants at different distances from the cooling pad (5.2, 11, 17.7 m) during pad-and-fan cooling. Numbers in italics refers to maximum T_{Leaf} differences observed. Tests of significance performed with Tukey-Kramer HSD. Values with similar letters are not significantly different at $p < 0.01$.

\dot{Q} ($m^3 s^{-1}$)	Leaf Temperature (°C)				Mean Plant Zone Conditions		
	5.2 m	11 m	17.7 m	Mean	Temp (°C)	RH (%)	VPD (kPa)
10:00					08:00-10:00		
4.5	20.6	22.5	22.9	22.0 ^a	23.8 ± 1.2	71.8 ± 8.5	0.8 ± 0.3
9.4	17.7	18.5	19.2	18.5 ^b	19.8 ± 1.8	66.3 ± 4.2	0.8 ± 0.1
13	17.1	18.3	19.1	18.2 ^b	19.1 ± 2.1	69.0 ± 3.0	0.7 ± 0.1
16.7	15.8	16.8	17.1	16.6 ^c	19.1 ± 1.7	62.4 ± 2.0	0.8 ± 0.1
12:00					10:00-12:00		
4.5	21.1	21.9	22.1	21.7 ^a	26.3 ± 1.0	70.5 ± 6.6	1.0 ± 0.3
9.4	18.7	19.1	19.5	19.1 ^b	22.1 ± 1.6	64.8 ± 5.7	0.9 ± 0.1
13	15.9	17.1	17.1	16.7 ^c	21.5 ± 1.8	64.4 ± 4.1	0.9 ± 0.1
16.7	16.4	17.7	17.4	17.2 ^c	21.3 ± 1.4	58.0 ± 1.3	1.1 ± 0.1
14:00					12:00-14:00		
4.5	25.1	25.2	26.3	25.5 ^a	26.8 ± 0.9	73.1 ± 3.6	0.9 ± 0.2
9.4	18.2	18.8	19.1	18.7 ^b	23.3 ± 1.3	62.9 ± 6.4	1.1 ± 0.1
13	16.4	17.3	17.0	16.9 ^c	22.1 ± 1.5	59.2 ± 1.6	1.1 ± 0.1
16.7	17.3	17.5	18.2	17.7 ^{bc}	22.3 ± 1.3	54.5 ± 1.6	1.2 ± 0.1
16:00					14:00-16:00		
4.5	24.5	25.2	25.6	25.1 ^a	27.6 ± 0.7	71.1 ± 6.3	1.0 ± 0.3
9.4	21.8	22.1	22.5	22.1 ^b	24.6 ± 1.1	63.0 ± 6.8	1.1 ± 0.1
13	17.8	18.7	17.9	18.1 ^c	22.3 ± 1.6	59.1 ± 2.8	1.1 ± 0.0
16.7	18.4	19.4	19.4	19.1 ^c	22.5 ± 1.2	53.4 ± 1.2	1.3 ± 0.1

5.3 Initial Studies on the Effect of Nozzle Location for a High-Pressure-Fog Cooling System in a Single-Span Greenhouse in a Semi-Arid Climate

5.3.1 Fog Nozzle Location at Vent Inlet

Fogging at the inlet produced very different results in cooling depending on the combination of fog injection rate (E_{Fog}) and greenhouse ventilation rate (q). The low fogging rate of $0.219 \text{ g m}^{-2} \text{ s}^{-1}$ combined with low ventilation rate of $4.5 \text{ m}^3 \text{ s}^{-1}$ produced both non-uniform and fluctuating greenhouse conditions, with differences of nearly 1.0 kPa from 4 m to 20 m (Figure 5.19). As the fog injection and ventilation rates were increased, the VPD at 4 m was reduced to nearly zero (saturated air) and its uniformity from 12 m to 28 m was improved. The most uniform and temporally-stable conditions occurred at a ventilation rate of $13.0 \text{ m}^3 \text{ s}^{-1}$ and fog injection rate of $0.622 \text{ g m}^{-2} \text{ s}^{-1}$. The fog injection rate of $0.808 \text{ g m}^{-2} \text{ s}^{-1}$ produced VPD variation of greater than 1 kPa from the 12 to 28 m location for both ventilation rates tested.

Adding all fog water near the inlet produced very saturated conditions around the plants that were closest to the inlet. Also, large gradients in VPD from inlet (0 m) to exhaust (28 m) were observed, with increases exceeding 0.5 kPa at ventilation rates of $16.7 \text{ m}^3 \text{ s}^{-1}$ and higher and increases of 1.5 kPa at $13.0 \text{ m}^3 \text{ s}^{-1}$ and lower ventilation rates. Due to this large variability in VPD that was created and the fact that gradients were larger than those observed for the pad-and-fan system (Section 5.2.7.3), it was concluded that locating all the fog nozzles at the inlet vent was not a design improvement and no further tests were made on this fog configuration.

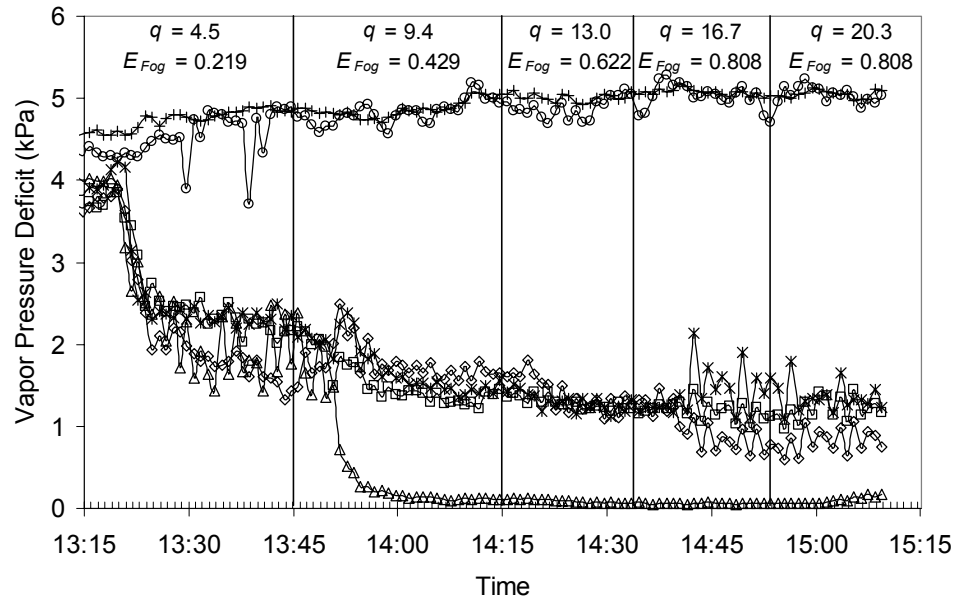


Figure 5.19 Vapor pressure deficit levels over time during continuous high-pressure-fog cooling, with all fog nozzles located inside the greenhouse at the vent inlet, for five mechanical ventilation rates ($q = 4.5, 9.4, 13.0, 16.7,$ and $20.3 \text{ m}^3 \text{ s}^{-1}$) and four fog injection rates, ($E_{Fog} = 0.219, 0.249, 0.622,$ and $0.808 \text{ g m}^{-2} \text{ s}^{-1}$). VPD measurements were taken at the following five distances from the inlet: 0 m (\circ), 4 m (Δ), 12 m (\diamond), 20 m (\square), and 28 m ($*$), and outside ($—$).

5.3.2 Fog Nozzle Location on Central, Overhead Line

When operated to control VPD between 0.8 and 1.2 kPa, the central, overhead fog line produced more uniform VPD conditions in the greenhouse than the multiple fog lines at the vent inlet (Figure 5.20). Although variability in VPD did occur from inlet to exhaust, within the plant zone itself, variability was very low (less than 0.3 kPa) for all ventilation rates tested. At $4.5 \text{ m}^3 \text{ s}^{-1}$ the VPD measured within the plant zone was nearly 1.0 kPa. The VPD was about 0.8 kPa at $3.7 \text{ m}^3 \text{ s}^{-1}$ and 0.6 kPa at $3.0 \text{ m}^3 \text{ s}^{-1}$.

Regardless of the initial VPD levels or the ventilation rate tested, approximately 7 minutes were required for the VPD to stabilize and attain a constant value within the greenhouse. When the ventilation rate of $4.5 \text{ m}^3 \text{ s}^{-1}$ was repeated, the VPD values

recorded were lower than the initial test, especially at the 4 m location. This result likely occurred as a result of fog condensate accumulating on plants and other surfaces during the low ventilation rate tests, and later evaporating during tests of the higher ventilation rate. As a result, the greenhouse was ventilated without fog between each ventilation treatment for all future fog configuration tests.

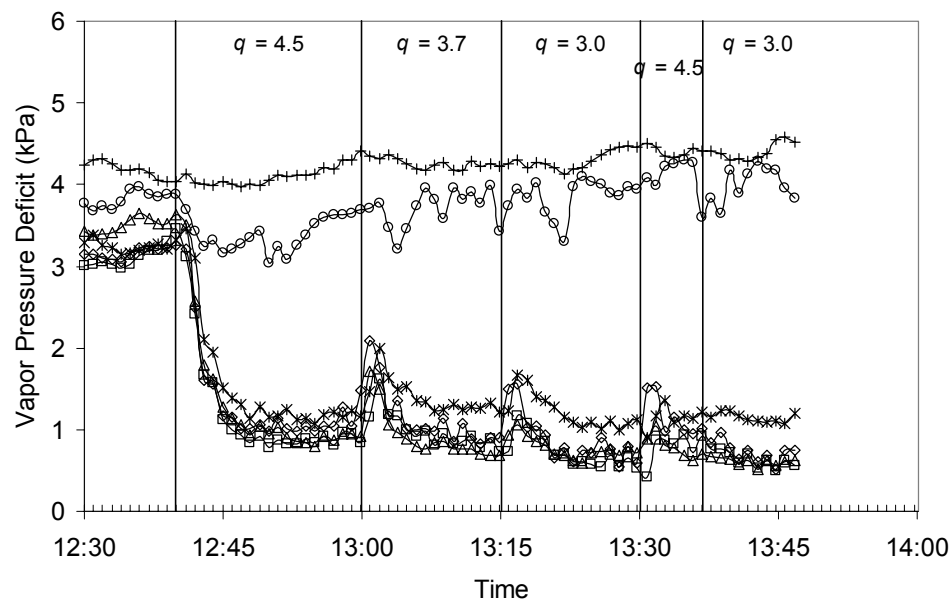


Figure 5.20 Vapor pressure deficit levels during *VPD*-control of high-pressure-fog cooling ($E_{Fog} = 0.287 \text{ g m}^{-2} \text{ s}^{-1}$), with nozzles located along a central, overhead line running from inlet to exhaust, and using mechanical ventilation rates of 3.0, 3.7, and 4.5 $\text{m}^3 \text{ s}^{-1}$. *VPD* measurements were taken at the following five distances from the inlet: 0 m (\circ), 4 m (Δ), 12 m (\diamond), 20 m (\square), and 28 m ($*$), and outside ($+$).

As indicated by this series of tests, the central, overhead fog nozzle line could produce uniform greenhouse air conditions with the mechanical ventilation rates tested. Additionally, because the *VPD* in the plant zone nearest the inlet (4 m) was low ($VPD < 1.0 \text{ kPa}$), the fog injected by nozzles on the overhead line between the inlet vent and plants was enough to condition the air prior to reaching the plants. Finally, this test also

demonstrated that *VPD* control of the high-pressure-fog system produced temporally-stable greenhouse conditions.

5.3.3 Fog Nozzle Location on Central, Overhead Line and at Pad Inlet

Adding one line of fog nozzles across the vent inlet to operate simultaneously with the central, overhead fog line produced lower *VPD* levels within the plant zone than when the central, overhead line was used alone for the same ventilation rates. For all three plant zone locations, ventilation rates of 3.0 and 4.5 m³ s⁻¹ produced *VPD* values that were less than 0.3 kPa, which were below the desired range (Figure 5.21). At 9.4 m³ s⁻¹ the *VPD* was close to 1.0 kPa for all greenhouse locations except 4 m, which was still less than 0.5 kPa. And at 16.7 m³ s⁻¹, the *VPD* was both non-uniform and temporally-variable.

Similar to the results found for only using the central, overhead line, 7 minutes were required for *VPD* levels to stabilize to a constant value. Therefore, producing equal *VPD* levels prior to each test did not affect the rate of changing conditions. However, ventilation of the greenhouse between tests would still allow condensation water to evaporate between tests, reducing the risk of measuring erroneously low *VPD* levels during subsequent tests.

Good spatial uniformity throughout the greenhouse could be obtained when the inlet vent fog line was operated with the central, overhead line for ventilation rates of 4.5 m³ s⁻¹ and below. However, *VPD* values (less than 0.5 kPa) were lower than what is typically desired, and much lower than the minimum control value (0.8 kPa). Therefore, the inlet vent fog line was an unnecessary addition to the evaporative cooling system for

this greenhouse layout and outside environmental conditions because the central, overhead fog line had nozzles located between the inlet vent and plants, thereby allowing it to condition the entering air prior to the air reaching the plants.

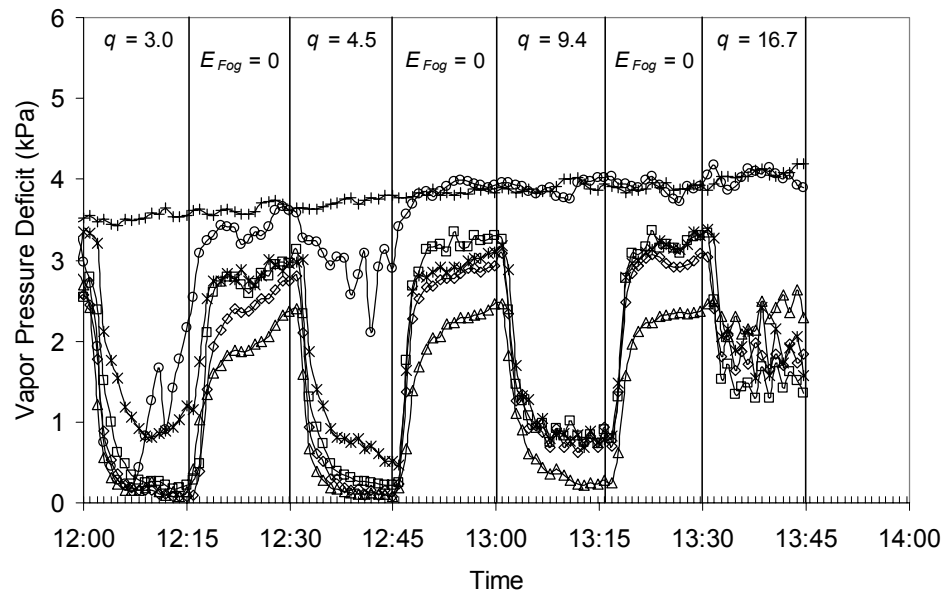


Figure 5.21 Vapor pressure deficit levels during *VPD* -control of high-pressure-fog cooling, with nozzles located along the pad inlet and in a central, overhead line running from inlet to fans ($E_{Fog} = 0.523 \text{ g m}^{-2} \text{ s}^{-1}$), and using mechanical ventilation rates of 3.0, 4.5, 9.4, and $16.7 \text{ m}^3 \text{ s}^{-1}$. *VPD* measurements were taken at the following five distances from the inlet: 0 m (\circ), 4 m (Δ), 12 m (\diamond), 20 m (\square), and 28 m ($*$), and outside ($+$).

5.3.4 Fog Nozzle Location on Side Wall Gutter Lines

The side wall gutter fog line of nozzles mounted along the length of the east and west side walls near to the gutters produced extremely uniform environmental conditions from 4 m to 28 m for ventilation rates ranging from 4.5 to $13.0 \text{ m}^3 \text{ s}^{-1}$ (Figure 5.22). However, due to large number of nozzles (160) and subsequently high fogging rate ($0.9 \text{ g m}^{-2} \text{ s}^{-1}$) *VPD* was very close to 0.0 kPa. The *VPD* levels also reached a constant value

within five minutes of initiating the fog, two minutes sooner than the other tests using the central, overhead fog line with and without the single fog line at the inlet.

The very good uniformity of environmental conditions produced by the side gutter fog lines demonstrate that they could be a better design option to using only the central, overhead line. Furthermore, uniformity was better at the high ventilation rate of $4.5 \text{ m}^3 \text{ s}^{-1}$ with the side gutter fog lines than for the central, overhead line. Finally, this greenhouse was also designed for use with natural ventilation through the roof and sidewalls, thus these side gutter lines may provide the fogging needs for use under both mechanical and natural ventilation.

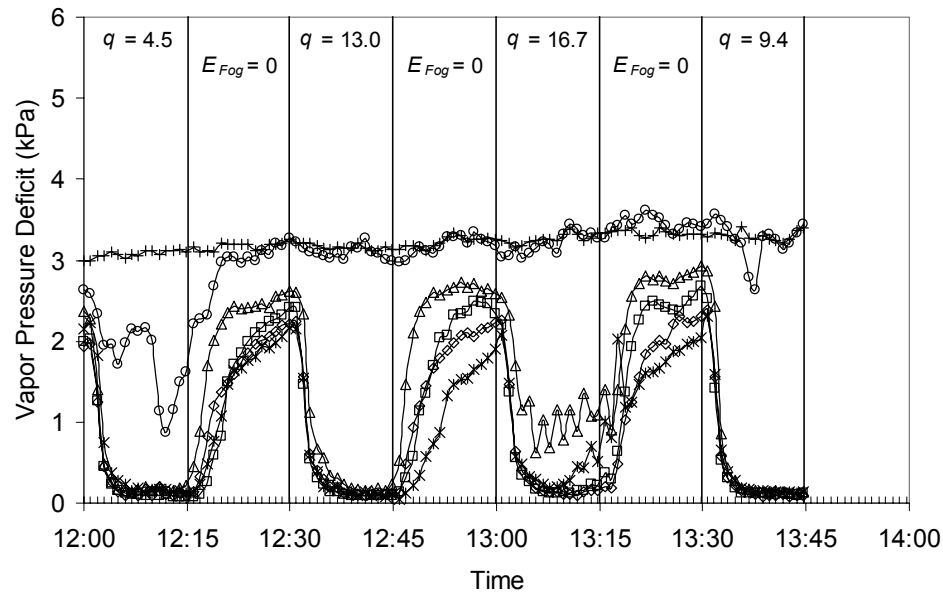


Figure 5.22 Vapor pressure deficit versus time during *VPD*-control of high-pressure-fog cooling, with side wall gutter fog line of nozzles mounted along the length of the east and side walls near to the gutters ($E_{Fog} = 0.90 \text{ g m}^{-2} \text{ s}^{-1}$), and with mechanical ventilation. *VPD* was measured at 0 m (—○—), 4 m (—△—), 12 m (—◇—), 20 m (—□—), and 28 m (—*—) distances from the inlet, and outside (—+—).

5.4 Effect of High-Pressure-Fog Cooling on Greenhouse Water Use, Climate Conditions, Plant Transpiration and Leaf Temperatures for a Semi-Arid Climate

5.4.1 Outside Environmental Conditions

The outside environmental conditions were similar for all test days, except for a 2-5% lower relative humidity levels during the test of $3.0 \text{ m}^3 \text{ s}^{-1}$ (Figure 5.23). In general, the temperature increased from about 25-27°C at 08:00 and leveled off to about 35°C around 14:00. The relative humidity was between 15-20% in the morning, and less than 10% in the afternoon. The mean outside temperature, relative humidity, and vapor pressure deficit for these tests between 08:00 – 17:00 was 33.7°C ($\pm 0.6^\circ\text{C}$), 10.6% ($\pm 1.3\%$), and 4.7 kPa ($\pm 0.2 \text{ kPa}$), respectively (Table 5.11). The outside solar radiation was the same for all test days (Figure 5.24).

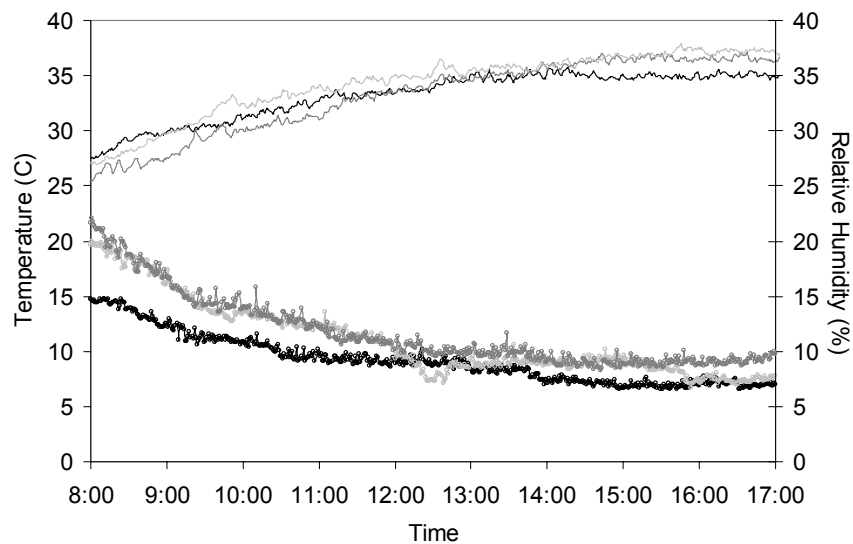


Figure 5.23 Outside temperature (—) and relative humidity (∘) during full day tests of the high-pressure-fog system for four ventilation rates: $3.0 \text{ m}^3 \text{ s}^{-1}$ (—), $4.5 \text{ m}^3 \text{ s}^{-1}$ (—), and $13 \text{ m}^3 \text{ s}^{-1}$ (—).

Table 5.11 Mean outside conditions and standard deviations of air temperature, relative humidity, and vapor pressure for the entire experimental period (08:00 – 17:00) and when outside conditions were relatively stable (11:00 – 17:00).

\dot{Q} ($\text{m}^3 \text{s}^{-1}$)	T_{Out} ($^{\circ}\text{C}$)	RH_{Out} (%)	VPD_{Out} (kPa)	T_{Out} ($^{\circ}\text{C}$)	RH_{Out} (%)	VPD_{Out} (kPa)
08:00 – 17:00				11:00 – 17:00		
3.0	33.3 ± 2.2	9.2 ± 2.2	4.7 ± 0.6	34.5 ± 0.7	7.9 ± 1.0	5.1 ± 0.2
4.5	33.3 ± 3.4	11.7 ± 3.3	4.6 ± 1.0	35.3 ± 1.5	9.7 ± 0.8	5.2 ± 0.5
9.4	34.4 ± 2.9	11.0 ± 3.5	4.9 ± 0.9	36.0 ± 1.1	9.0 ± 1.3	5.4 ± 0.4
Mean \pm SD	33.7 ± 0.6	10.6 ± 1.3	4.7 ± 0.2	35.3 ± 0.7	8.9 ± 0.9	5.2 ± 0.2

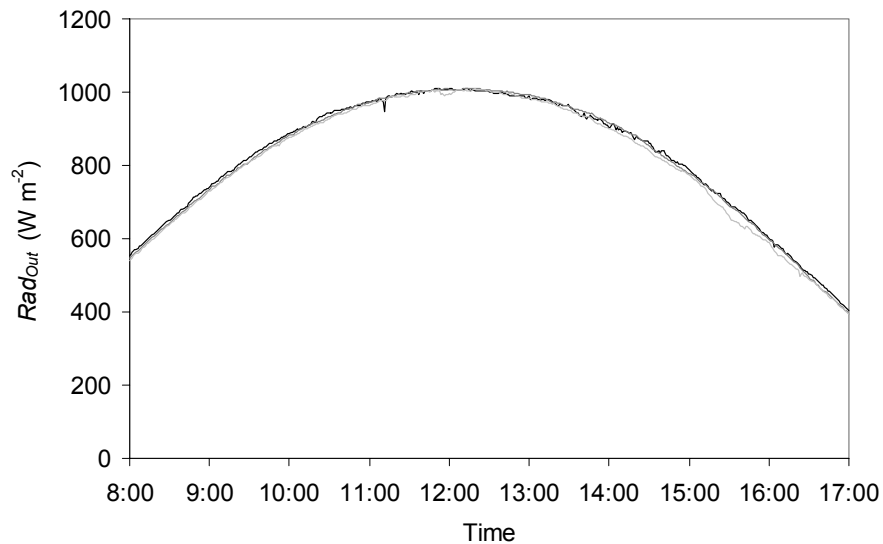


Figure 5.24 Outside solar radiation levels during full day tests of the high-pressure-fog system for four ventilation rates: $3.0 \text{ m}^3 \text{s}^{-1}$ (—), $4.5 \text{ m}^3 \text{s}^{-1}$ (---), and $13 \text{ m}^3 \text{s}^{-1}$ (···).

5.4.2 High-Pressure-Fog Operation

The fog system was programmed to cycle in 140 s duty cycles to maintain a setpoint air temperature of 25°C (Section 4.2.1.4). Fog On-time exceeded Off-time for all ventilation rates tested. However, the fraction On-time varied with ventilation rate. For each day, the mean percentage of fog On-time was 60%, 55%, and 71% for ventilation rates of 3.0 , 4.5 and $9.4 \text{ m}^3 \text{s}^{-1}$, respectively (Table 5.12). At $4.5 \text{ m}^3 \text{s}^{-1}$ the

On-time was only 20% greater than the amount of Off-time, whereas at the highest ventilation rate the On-time exceeded Off-time by 60%.

Table 5.12 Mean fraction of fog operation On-time and mean On-time calculated over a 420 s time interval for three ventilation rates (3.0, 4.5, 9.4 m³ s⁻¹). The total fogging time during 08:00-17:00 is also included. Significance tests performed with Tukey-Kramer HSD. Data followed by same letter are not significantly different.

\dot{Q} (m ³ s ⁻¹)	Fraction Fog On-time	Mean Fog On-time (s)	Total Fog Time (s)
3.0	0.60 ± 0.16	253 ^a ± 67	19,169
4.5	0.55 ± 0.20	235 ^a ± 84	17,981
9.4	0.71 ± 0.18	297 ^b ± 74	22,590

In the morning, when the outside air temperature was near the greenhouse setpoint temperature, the fog system was Off more than it was On for all ventilation rates (Figure 5.25). As the day progressed and outside air temperatures increased, the cooling requirement increased and longer fog operation times were needed until the On-time duration exceeded Off-time for all ventilation rates.

At the highest ventilation rate of 9.4 m³ s⁻¹, the required On-time surpassed the Off-time at around 09:00, which was 60 minutes sooner than at 3.0 m³ s⁻¹ and 90 minutes sooner than at 4.5 m³ s⁻¹. Also, the On-time duration during 3.0 tended to be longer than at 4.5 m³ s⁻¹ before 12:30, after which cycling frequencies were about the same.

The maximum On-time duration was achieved much sooner under 9.4 m³ s⁻¹ than the other two ventilation rates (Figure 5.25). At 9.4 m³ s⁻¹ the maximum On-time first occurred before 11:00, where the other ventilation rates did not require the maximum On-time until about 14:30, when shading ended. Furthermore, the maximum On-time (and minimum Off-time) was a constant requirement for 9.4 m³ s⁻¹ after 13:00 until the end of

the test period (17:00). The other two ventilation rates only required continuous maximum On-time from 14:30-16:00, and at $4.5 \text{ m}^3 \text{ s}^{-1}$, Off-times exceeded the minimum requirement for most of this maximum On period.

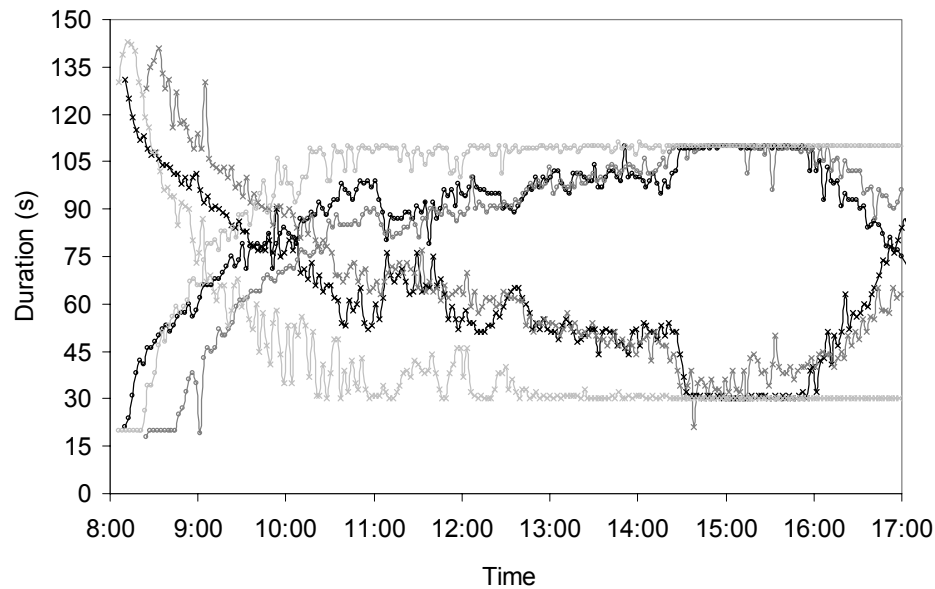


Figure 5.25 On (○) and Off (×) duration versus time of day for the high-pressure-fog system operated with three ventilation rates: $3.0 \text{ m}^3 \text{ s}^{-1}$ (—), $4.5 \text{ m}^3 \text{ s}^{-1}$ (—), and $13 \text{ m}^3 \text{ s}^{-1}$ (—). The shade curtain was used between 11:00 – 14:30.

5.4.3 Water Use by the High-Pressure-Fog System

Total water use by the high-pressure-fog system for one day (08:00-17:00) of operation was 7.8, 7.3, and 9.2 L m^{-2} for ventilation rates of 3.0, 4.5, and $9.4 \text{ m}^3 \text{ s}^{-1}$, respectively (Figure 5.26). These values are equivalent to a mean water use rate of 14.4, 13.5, and $17 \text{ g m}^{-2} \text{ min}^{-1}$, which are rates lower than the $18 - 21 \text{ g m}^{-2} \text{ min}^{-1}$ found by a previous study (Sase *et al.*, 2006). Also, if the high-pressure-fog system was not operated to control for the inside air temperature setpoint (T_{Set}) and continuous fogging had been

employed, 13.2 L m^{-2} of water would have been used, an increase of 30% relative to the water use at the highest ventilation rate tested ($9.4 \text{ m}^3 \text{ s}^{-1}$).

Water use was directly related to the cycling of the high-pressure-fog system, producing a perfect linear relationship between the On time and water use ($r = 1.0$).

Water use by the high-pressure-fog system was greatest for a ventilation rate of $9.4 \text{ m}^3 \text{ s}^{-1}$ (Figure 5.26), which had the longest fog operating time of all ventilation rates (Table 5.12). Water use at a ventilation rate of $3.0 \text{ m}^3 \text{ s}^{-1}$ was greater than $4.5 \text{ m}^3 \text{ s}^{-1}$ due to its longer operating times before 11:00 and shorter Off times after 14:30.

Consequently, a poor linear relationship was found between the ventilation rates tested and water use due to the non-linear operating times produced by the control system (Figure 5.26), which was programmed to control greenhouse air temperature. However, as will be discussed in Section 5.4.7, the high humidity created by the low air exchange rate of $3.0 \text{ m}^3 \text{ s}^{-1}$ reduced the evaporation potential, thereby limiting air temperature reduction. Furthermore, at $9.4 \text{ m}^3 \text{ s}^{-1}$ the air exchange rate was too high for the high-pressure-fog system to sufficiently retain the evaporatively cooled air inside the greenhouse, and may have also exhausted some of the fog droplets prior to evaporation. Therefore, creating the desired greenhouse air conditions would be more effectively (and efficiently) achieved if both fog injection rate *and* ventilation rate were controlled.

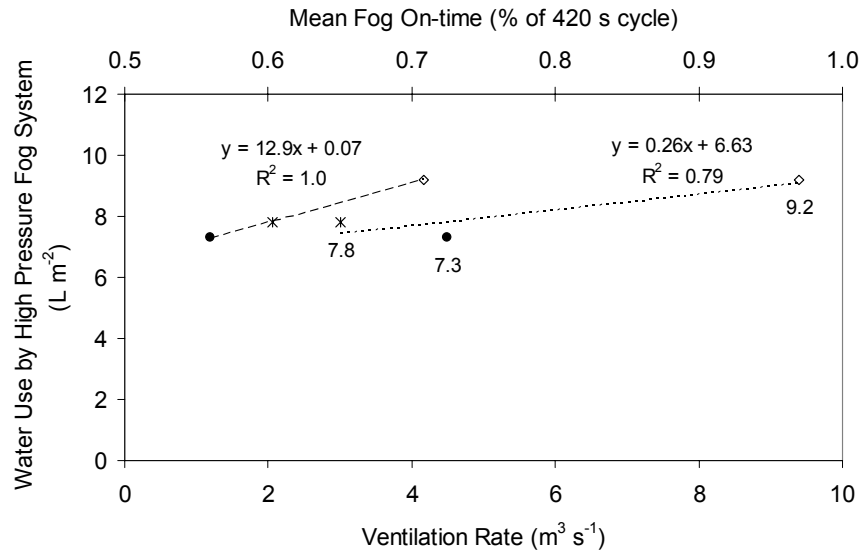


Figure 5.26 Total water use by the high-pressure-fog cooling system versus ventilation rate ($3.0 \text{ m}^3 \text{s}^{-1}$ (*), $4.5 \text{ m}^3 \text{s}^{-1}$ (●), and $9.4 \text{ m}^3 \text{s}^{-1}$ (◇)), and linear relationship between water use and On-time (—) and ventilation rate (....) during 08:00 – 17:00 test period.

Water use and outside environmental conditions were highly correlated (Table 5.13), including temperature ($r > +0.90$) and moist air conditions such as relative humidity ($r > -0.90$). These correlations support the increasing WU_{HPF} observed in the first part of the day (pre-12:00), when outside temperatures increased and relative humidity decreased.

Table 5.13 Correlations (r) between fog water use (WU_{HPF}) and ventilation rate, and outside climate conditions including temperature (T_{Out}), relative humidity (RH_{Out}), vapor pressure deficit (VPD_{Out}), and absolute humidity (W_{Out}); and multivariate correlations were also calculated for each ventilation rate (3.0 , 4.5 , and $9.4 \text{ m}^3 \text{s}^{-1}$).

Parameter	r	r (3.0)	r (4.5)	r (9.4)
Vent Rate	0.29			
T_{Out}	0.91	0.90	0.94	0.91
RH_{Out}	-0.83	-0.91	-0.98	-0.90
VPD_{Out}	0.89	0.88	0.94	0.88
W_{Out}	-0.46	-0.83	-0.94	-0.72

The rate water use was about the same for all ventilation rates between 08:00 and 09:00, while at $4.5 \text{ m}^3 \text{ s}^{-1}$ there was a 30-minute delay. This was likely due to the 2°C lower outside air temperatures before 09:00 (Figure 5.27). After 09:00 the rate of water use remained the same for $9.4 \text{ m}^3 \text{ s}^{-1}$ but diminished significantly for $3.0 \text{ m}^3 \text{ s}^{-1}$ and slightly less for the $4.5 \text{ m}^3 \text{ s}^{-1}$. After 11:00, when the shade curtain was pulled, the rate of water use increased more slowly and was about the same for 3.0 and $4.5 \text{ m}^3 \text{ s}^{-1}$.

Maximum fog operation and water use was achieved by 13:00 for $9.4 \text{ m}^3 \text{ s}^{-1}$, and at 15:00 for 3.0 and $4.5 \text{ m}^3 \text{ s}^{-1}$ (Figure 5.27). The rate of water use was always greatest at $9.4 \text{ m}^3 \text{ s}^{-1}$, except at 15:00, when the solar heat gain in the greenhouse was greatest and maximum water use was required regardless of ventilation rate. Between 15:00-16:00, longer Off-time intervals for $4.5 \text{ m}^3 \text{ s}^{-1}$ decreased water use. Finally, after 16:00 water use decreased quickly for 3.0 and $4.5 \text{ m}^3 \text{ s}^{-1}$, but did not for $9.4 \text{ m}^3 \text{ s}^{-1}$, indicating that the ventilation rate was too great for the outside environmental conditions and the design of the fog system (ie. the number of nozzles in the system).

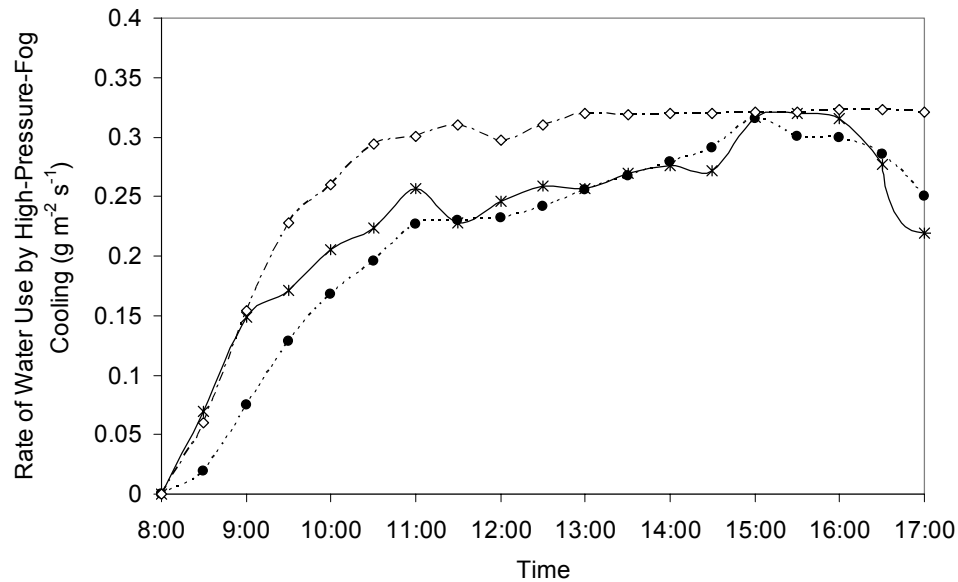


Figure 5.27 Rate of water use by the high-pressure-fog evaporative cooling system from 08:00-17:00 for three ventilation rates: $3.0 \text{ m}^3 \text{ s}^{-1}$ ($-*-$), $4.5 \text{ m}^3 \text{ s}^{-1}$ ($\cdots\bullet\cdots$), and $9.4 \text{ m}^3 \text{ s}^{-1}$ ($- \diamond -$).

5.4.4 Water Use by Tomato Plants

The total water use by the tomato plants (ΣWU_p) during the test period (08:00 – 17:00) was 774, 821, and 925 L, for ventilation rates of 3.0 , 4.5 , and $9.4 \text{ m}^3 \text{ s}^{-1}$, respectively (Table 5.14). The total plant water uptake increased with increasing ventilation rate and fog water use. However, the mean daytime values ($\overline{WU_p}$) were not significantly different ($p > 0.05$). The $\overline{WU_p}$ from 08:00-17:00 was 0.077 , 0.082 , and 0.094 L m^{-2} for ventilation rates of 3.0 , 4.5 , and $9.4 \text{ m}^3 \text{ s}^{-1}$, respectively.

Table 5.14 Total water use for irrigation (W_I), total plant water uptake (ΣWU_P), and mean plant water uptake rates ($\overline{WU_P}$) during the test period (08:00-17:00) for three ventilation rates: 3.0, 4.5, and 9.4 m³ s⁻¹. Mean $\overline{WU_P}$ values were calculated from 30-minute measurements during the test period. Letters represent significantly different values ($p < 0.05$).

\dot{Q} (m ³ s ⁻¹)	W_I (L)	ΣWU_P (L)	$\overline{WU_P}$ (g m ⁻² s ⁻¹)
3.0	1251	774	0.077 ^a
4.5	1251	821	0.082 ^a
9.4	1251	925	0.094 ^a

5.4.5 Total Greenhouse Water Use

The high-pressure-fog system in this greenhouse and under the tested operating procedures always used more water than the open irrigation system. The highest ventilation rate (9.4 m³ s⁻¹) used 9.2 L m⁻² d⁻¹ for cooling, which was twice the amount of water was used for open irrigation, and represented two-thirds of the total water used in the greenhouse that day. Water use by ventilation rates of 3.0 and 4.5 m³ s⁻¹ represented closer to 60% of the total greenhouse water use. Together the “open” irrigation and high-pressure-fog systems produced a total greenhouse system water use ($\Sigma WU_{S,Open}$) of 12.3, 11.8, and 13.7 L m⁻² d⁻¹ during the 08:00-17:00 test period for ventilation rates of 3.0, 4.5, and 9.4 m³ s⁻¹, respectively (Table 5.15).

By using a 100% closed irrigation system that adds water only to replace water use by plants (WU_{PU}), the closed system would have utilized 2.8, 3.0, and 3.3 L m⁻² d⁻¹ for ventilation rates of 3.0, 4.5, and 9.4 m³ s⁻¹. Had a closed system been used, WU_{HPF} would have represented 74%, 71%, and 73% of all the water used in the greenhouse for ventilation rates of 3, 4.5, and 9.4 m³ s⁻¹, respectively.

Table 5.15 Water use by the high-pressure-fog system (WU_{HPF}), open irrigation system (WU_I), closed irrigation system (ΣWU_P), and the resulting total greenhouse system water use for open ($\Sigma WU_{S,Open}$) and closed ($\Sigma WU_{S,Closed}$) irrigation with high-pressure-fog cooling during 08:00-17:00 test period for ventilation rates of 3.0, 4.5, and 9.4 m³ s⁻¹.

\dot{Q} (m ³ s ⁻¹)	ΣWU_{HPF} (L m ⁻² d ⁻¹)	ΣWU_I (L m ⁻² d ⁻¹)	ΣWU_{PU} (L m ⁻² d ⁻¹)	$\Sigma WU_{S,Open}$ (L m ⁻² d ⁻¹)	$\Sigma WU_{S,Closed}$ (L m ⁻² d ⁻¹)
3.0	7.8	4.5	2.8	12.3	10.6
4.5	7.3	4.5	3.0	11.8	10.3
9.4	9.2	4.5	3.3	13.7	12.5

5.4.6 Water Use Efficiency

For the yields obtained in the experimental greenhouse, the WUE_{HPF} was 18, 19, and 15 kg m⁻³ for ventilation rates of 3.0, 4.5, and 9.4 m³ s⁻¹, respectively. When only considering water use for open irrigation, $WUE_{I,Open}$ was 31 kg m⁻³ (Table 5.16), a smaller value than what has been obtained in the Netherlands (45 kg m⁻³) and France (39 kg m⁻³) (Pardossi *et al*, 2004), but similar to values obtained in Spain (Reina-Sanchez, 2005) and Italy (Incrocci *et al*, 2006), which have more similar climates to the location of our experimental greenhouse. Combining $WU_{I,Open}$ and WU_{HPF} produced total $WUE_{S,Open}$ values of 11, 12, and 10 kg m⁻³ for ventilation rates of 3.0, 4.5, and 9.4 m³ s⁻¹, respectively, which are within the range of flood irrigation WUE values (10-12 kg m⁻³) reported for field tomato production (Hanson *et al*, 2006; Hanson and May, 2005; Hanson and May, 2004).

Although, the WUE_I was greater overall for a closed irrigation system, WU_P increased with increasing ventilation rate, causing $WUE_{I,Closed}$ to decrease with increasing ventilation rate, with values of 50, 47, and 42 kg m⁻³ for ventilation rates of 3.0, 4.5, and 9.4 m³ s⁻¹, respectively. These $WUE_{I,Closed}$ values were still lower than the 66 kg m⁻³ reported for greenhouses in the Netherlands (Pardossi *et al*, 2004), but were greater than

the 25 and 30 kg m⁻³ reported for the closed-loop systems in the more similar climates of Spain (Reina-Sanchez, 2005) and Italy (Incrocci *et al*, 2006), respectively.

Unfortunately, these marked improvements in WUE_I for the closed system were diminished greatly by low WUE_{HPF} vales, resulting in only modest increases of WUE_S overall. The “closed” irrigation system produced $WUE_{S,Closed}$ values of 13, 14, and 11 kg m⁻³ for ventilation rates of 3.0, 4.5, and 9.4 m³ s⁻¹, respectively, which are within the WUE values reported for field sprinkler irrigation (11-19 kg m⁻³) (Hanson *et al*, 2006; Hanson and May, 2005; Hanson and May, 2004).

Finally, the WUE_S for a tomato yield of 65 kg m⁻² grown in a closed irrigation system would have been 17, 17, and 14 kg m⁻³ for ventilation rates of 3.0, 4.5, and 9.4 m³ s⁻¹, respectively.

Table 5.16 Water use efficiency (WUE) of the greenhouse water systems, including irrigation for open ($WUE_{I,Open}$) and closed ($WUE_{I,Closed}$) systems and the high-pressure-fog system (WUE_{HPF}) for three ventilation rates, and the resulting system water use efficiency (WUE_S) when water use by both systems is considered. Results are divided for tomato yields obtained in the experimental greenhouse (39 kg day⁻¹) and those that might be expected in commercial tomato production (49.5 kg day⁻¹).

\dot{Q} m ³ s ⁻¹	Test Greenhouse Yield = 39 kg = 0.14 kg m ⁻² d ⁻¹				
	WUE_{HPF}	$WUE_{I,Open}$	$WUE_{I,Closed}$	$WUE_{S,Open}$	$WUE_{S,Closed}$
3.0	18	31	50	11	13
4.5	19	31	47	12	14
9.4	15	31	42	10	11
\dot{Q}	Commercial Yield = 49.5 kg = 0.18 kg m ⁻² d ⁻¹				
	WUE_{HPF}	$WUE_{I,Open}$	$WUE_{I,Closed}$	$WUE_{S,Open}$	$WUE_{S,Closed}$
3.0	23	39	64	14	17
4.5	24	39	60	15	17
9.4	19	39	54	13	14

5.4.7 Greenhouse Environmental Conditions

5.4.7.1 Mean Greenhouse Conditions

The greenhouse air temperature setpoint (25°C) was achieved under all ventilation rates with the high-pressure-fog system. Mean daytime (08:00 – 17:00) plant zone temperatures were 25.2, 24.8, and 25.1°C for ventilation rates of 3.0, 4.5, and 9.0 m³ s⁻¹, respectively (Table 5.17). There were statistically significant decreases in mean plant zone relative humidity ($p < 0.05$) as ventilation rate was increased, with values of 73.6, 64.1, and 55.2% for 3.0, 4.5, and 9.4 m³ s⁻¹, respectively. The reduction in moisture content of the air was also reflected in significant increases in *VPD* with increasing ventilation rate, from 0.8 kPa at 3.0 m³ s⁻¹ to 1.4 kPa at 9.4 m³ s⁻¹, which is approaching undesirably dry conditions.

Increasing the ventilation rate reduced the overall difference in relative humidity between outside and the greenhouse. There was a 30% drop in ΔRH_{GH-Out} from the lowest ventilation rate to the highest ventilation rate (Table 5.17).

Table 5.17 Mean plant zone air temperature, relative humidity, vapor pressure deficit, and incoming radiation calculated over the entire test period (08:00 – 17:00) with standard deviations (*italics*). The values ΔT (T_{GH-Out}), ΔRH (RH_{GH-Out}), and ΔVPD (VPD_{GH-Out}) represent their differences relative to outside conditions averaged over the same period. Letters represent significantly different values from a Tukey-Kramer HSD test ($p < 0.01$).

\dot{Q} (m ³ s ⁻¹)	T_{GH} (°C)	RH_{GH} (%)	VPD (kPa)	Rad_{in} (W m ⁻²)	ΔT (°C)	ΔRH (%)	ΔVPD (kPa)
3.0	25.2 ^a ± 0.7	73.8 ^a ± 1.2	0.8 ^a ± 0.35	436 ^a ± 144	-8.0	+64.4	-3.8
4.5	24.8 ^a ± 0.7	63.7 ^b ± 8.3	1.1 ^b ± 0.22	432 ^a ± 132	-8.5	+52.4	-3.5
9.4	25.1 ^a ± 1.0	59.0 ^c ± 4.2	1.4 ^c ± 0.13	441 ^a ± 130	-9.3	+44.1	-3.5

5.4.7.2 Fog duration and Greenhouse Conditions

Figure 5.28 represents the relationship between plant zone air temperature and high-pressure-fog water use. Fog injection rate and greenhouse air temperature directly influenced each other. However, with fog injection rate presented in the y-axis, the influence of air temperature on operation of the high-pressure-fog system is emphasized.

The high-pressure-fog system was controlled by an air temperature setpoint of 25°C, therefore fog injection rate increased with increasing air temperature. Plant zone air temperatures generally remained between 23 and 27°C, with 4.5 m³ s⁻¹ producing the most air temperatures below 24°C. Air temperature often exceeded 26°C at a ventilation rate of 9.4 m³ s⁻¹, resulting in frequent maximum fog injection rates.

When maximum fogging (0.329 g m⁻² s⁻¹) was not required, increasing the ventilation rate produced lower plant zone air temperatures for a given fog injection rate. In general, 4.5 m³ s⁻¹ maintained temperatures below 26°C for all fogging rates and closest to 25°C without requiring maximum fog injection rates. At 9.4 m³ s⁻¹, however, maximum fog injection rates were required most often but were not always able to maintain setpoint air temperatures. In fact, maximum fogging at 9.4 m³ s⁻¹ either produced air temperatures that were less than 24°C or was unable to prevent air temperatures from exceeding 26°C. At 3.0 m³ s⁻¹ air temperatures were highest for a given fog injection rate.

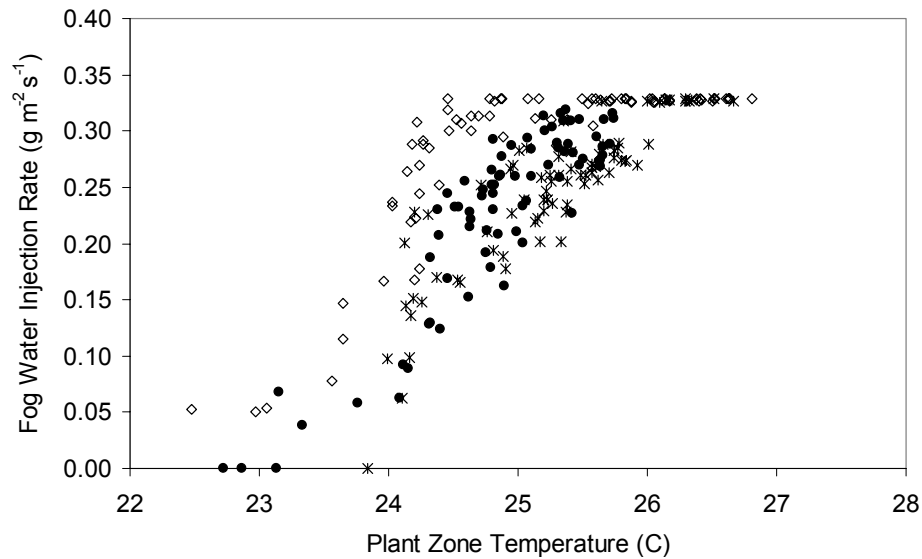


Figure 5.28 Fog water injection rates as influenced by greenhouse air temperature for three ventilation rates: $3.0 \text{ m}^3 \text{ s}^{-1}$ (*), $4.5 \text{ m}^3 \text{ s}^{-1}$ (●), and $9.4 \text{ m}^3 \text{ s}^{-1}$ (◇). Seven-minute intervals (420 s) were used to calculate the mean plant zone air temperature values and fog injection rates for the three ventilation rates tested.

Like air temperature, relative humidity and fog injection rate directly influenced each other. However, fog injection rate was not controlled by relative humidity values, therefore *RH* is presented as the dependent variable in Figure 5.29. In general, there was a linear increase in relative humidity with increasing fog injection rate, with regression coefficients of 0.90, 0.88, and 0.45 for ventilation rates of 3.0 , 4.5 and $9.4 \text{ m}^3 \text{ s}^{-1}$, respectively (Figure 5.29). Relative humidity was less than 50% when fogging represented 30% or less of the total cycle interval ($0.10 \text{ g m}^{-2} \text{ s}^{-1}$). When fog injection rates were greater than $0.30 \text{ g m}^{-2} \text{ s}^{-1}$ the relative humidity was greater than 80% at $3.0 \text{ m}^3 \text{ s}^{-1}$, around 70% at $4.5 \text{ m}^3 \text{ s}^{-1}$, and 50-60% at $9.4 \text{ m}^3 \text{ s}^{-1}$.

As expected, greater fog injection rates raised the relative humidity, but by increasing the ventilation rate the humidity of the greenhouse was reduced. For

maximum fog injection rates ($0.33 \text{ g m}^{-2} \text{ s}^{-1}$), the relative humidity approached 85%, 70%, and 55% for ventilation rates of 3.0 , 4.5 , and $9.3 \text{ m}^3 \text{ s}^{-1}$, respectively.

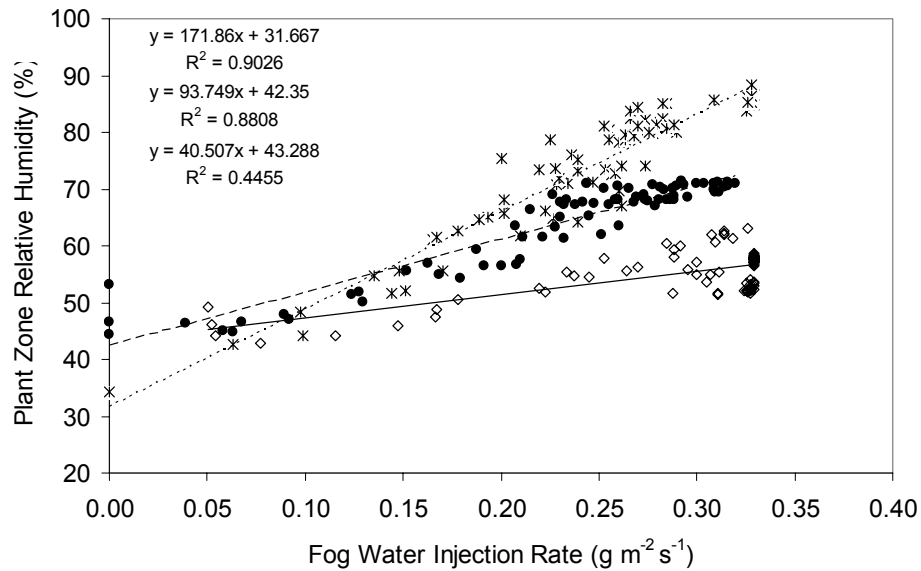


Figure 5.29 Plant zone air relative humidity as a function of fog water injection rate. Equations represent the linear regressions of ventilation rates $3.0 \text{ m}^3 \text{ s}^{-1}$ (*), $4.5 \text{ m}^3 \text{ s}^{-1}$ (●), and $9.4 \text{ m}^3 \text{ s}^{-1}$ (◇) from top to bottom. Seven-minute intervals (420 s) were used to calculate the mean plant zone relative humidity levels and fog injection rates for the three ventilation rates tested.

5.4.7.3 Temporal Trends in Greenhouse Environmental Conditions

The trends in incoming solar radiation (Rad_{In}) were the same during all test days for the fog evaporative cooling tests (Figure 5.30). Between 10:00 – 10:30 the reduction of Rad_{In} was due to structural shading, and between 11:00 – 14:30 the reduction was due to the shade curtain having been deployed.

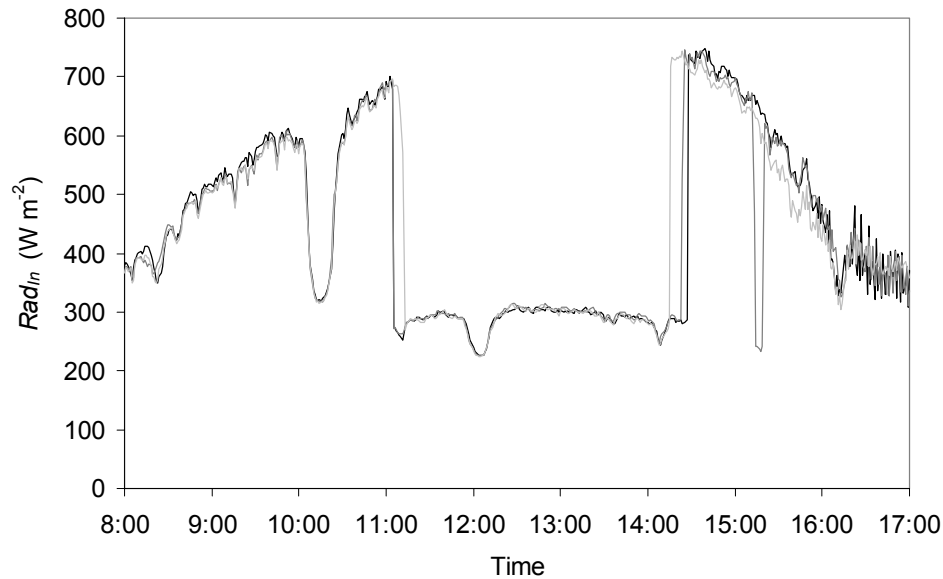


Figure 5.30 Incoming solar radiation (Rad_{in}) versus time of day during high-pressure-fog cooling for three ventilation rates: $3.0 \text{ m}^3 \text{ s}^{-1}$ (—), $4.5 \text{ m}^3 \text{ s}^{-1}$ (---), and $9.4 \text{ m}^3 \text{ s}^{-1}$ (···).

In general, the inlet air temperature and relative humidity followed the trends of outside conditions (Figure 5.31), with inlet temperatures rising and relative humidity levels declining until outside conditions stabilized around 13:00 (Figure 5.31). Shading affected inlet air conditions at $3.0 \text{ m}^3 \text{ s}^{-1}$, reducing the temperature from 34°C to 28°C and raising the relative humidity from 10% to 70% for a 1-hour period (Figure 5.26a). Later, removal of the shade curtain also lowered inlet air temperature from 32° to 28°C and raised relative humidity from a mean of 30% to 50%.

Greenhouse air temperatures generally increased throughout the day for all ventilation rates (Figure 5.31). Temperatures at 12 and 20 m from the inlet vent (plant zone) were similar throughout the day. The air temperature at 4 and 28 m from the inlet vent were most affected by changes in Rad_{in} , especially following the removal of the shade curtain at 14:30.

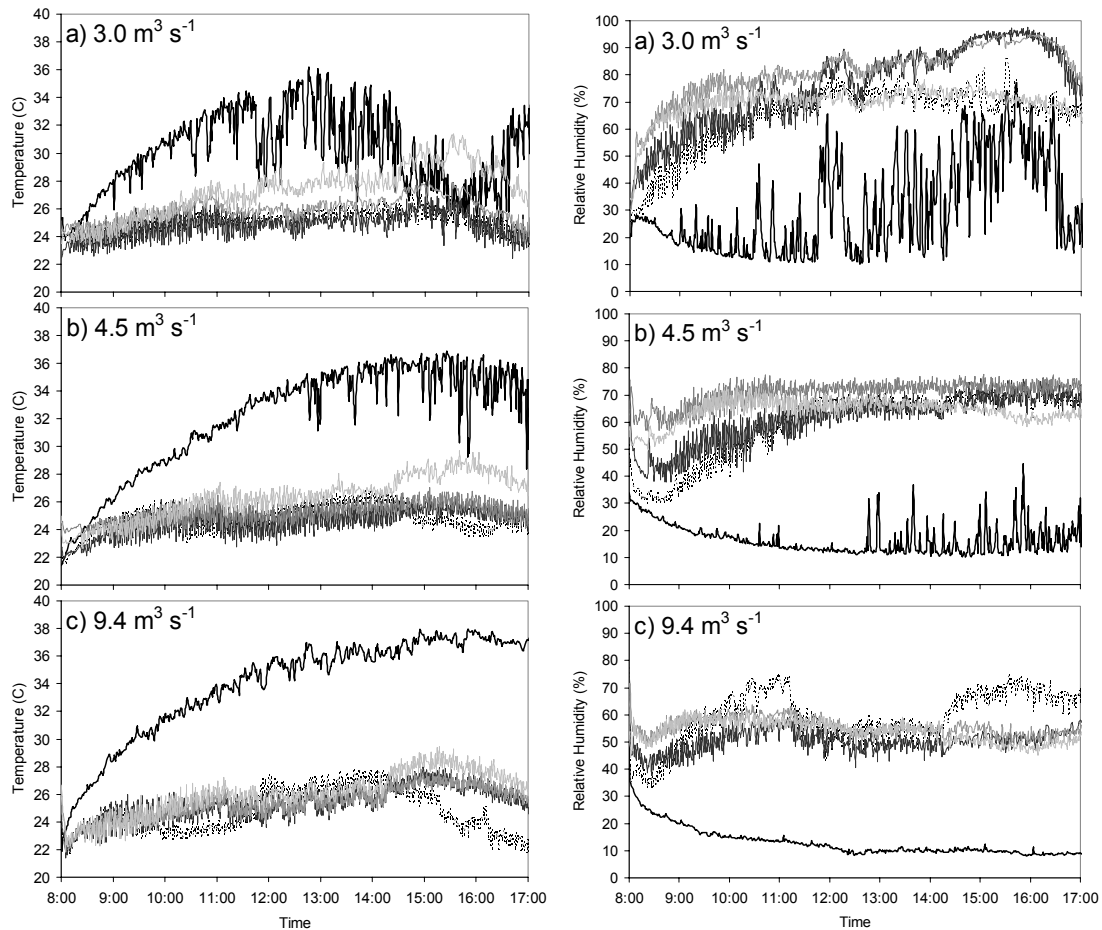


Figure 5.31 Greenhouse temperatures and relative humidity versus time of day during high-pressure-fog for three ventilation rates: a) $3.0 \text{ m}^3 \text{ s}^{-1}$, b) $4.5 \text{ m}^3 \text{ s}^{-1}$, and c) $9.4 \text{ m}^3 \text{ s}^{-1}$. Locations at five distances from the inlet were monitored: 0 m (—), 4 m (....), 12 m (—), 20 m (—), and 28 m (—).

At $3.0 \text{ m}^3 \text{ s}^{-1}$, the relative humidity increased throughout most of the day at 12 and 20 m locations, peaking above 90% after 14:30, when the air temperature was greatest and more fog water was required (Figure 5.31a). At 4 m and 28 m *RH* stabilized near 70% by 12:00. At $4.5 \text{ m}^3 \text{ s}^{-1}$, the relative humidity at 20 and 28 m stabilized more quickly (10:00) than at 4 and 12 m locations (12:00), with values between 60-70%. At $9.4 \text{ m}^3 \text{ s}^{-1}$ the relative humidity rose at all locations until the shade curtain was deployed,

and then decreased slightly to near 50% for the remainder of the day. The exception occurred at 4 m location, where the relative humidity increased to about 70% after shading was removed probably as a result of greater evaporation in that location (5.31c).

Figures 5.32 and 5.33 smooth the fluctuations of plant zone air temperature and relative humidity by presenting 7-minute averages, and including the On-time percentage of the fog system. Ventilation rates of 3.0 and 9.4 m³ s⁻¹ maintained approximately the same range in greenhouse air temperature throughout the day (24-26.5°C). At 3.0 m³ s⁻¹ the air temperature did not peak at 26.5°C until 15:00, after which it declined steadily. At 9.4 m³ s⁻¹, however, 26.5°C was first reached at 13:00 and eventually peaked at 27°C at approximately 15:00 before finally decreasing. At 4.5 m³ s⁻¹ the smallest range of air temperatures were maintained (24-25.5°C) with very few and small fluctuations.

With respect to relative humidity, 9.4 m³ s⁻¹ produced the smallest range but also the lowest values (50-60%). At 3.0 m³ s⁻¹, the relative humidity was greater than 60% after 09:00 and between 70 and 90% after 10:30. The 4.5 m³ s⁻¹ ventilation rate did not produced a relative humidity greater than 60% until nearly 11:00, however it consistently remained at 65% after 12:00.

Shading affected the trends in both air temperature and relative humidity. Although air temperature was controlled with fogging, it still increased during shading under all ventilation rates (Figure 5.32). Shading produced different trends in humidity values, with an increase at 3.0 m³ s⁻¹, stabilization at 4.5 m³ s⁻¹, and a reduction at 9.4 m³ s⁻¹. Furthermore, removing the shade curtain caused an increase in relative humidity at 9.4 m³ s⁻¹, likely resulting from an increase in transpiration rate since fog On-time was

maximized earlier. The small increases in relative humidity after shading observed at the other ventilation rates were likely caused by higher fog injection rates.

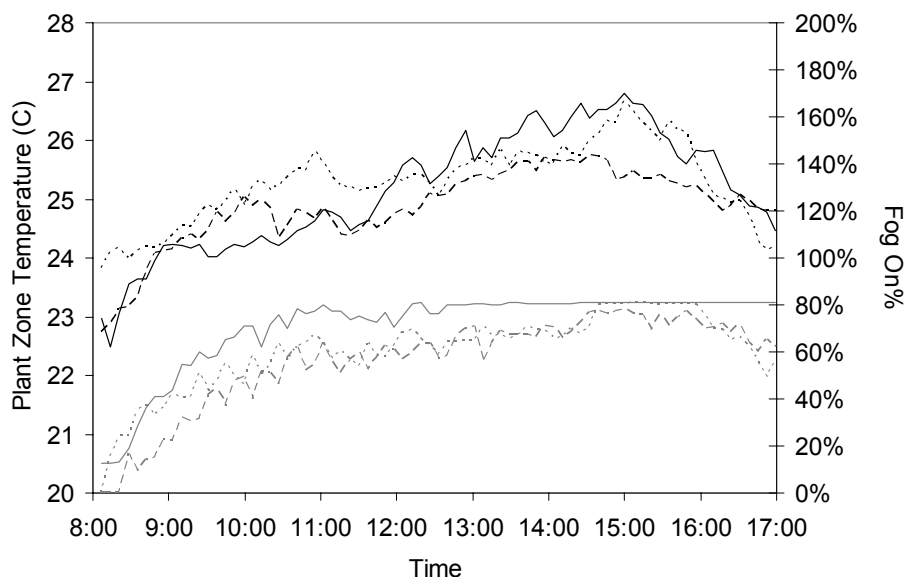


Figure 5.32 Seven-minute mean plant zone air temperatures and fog On-time percentages versus time of day for three ventilation rates: $3.0 \text{ m}^3 \text{ s}^{-1}$ (....), $4.5 \text{ m}^3 \text{ s}^{-1}$ (---), and $9.4 \text{ m}^3 \text{ s}^{-1}$ (—). Black lines represent plant zone temperatures and gray lines represent Fog On%.

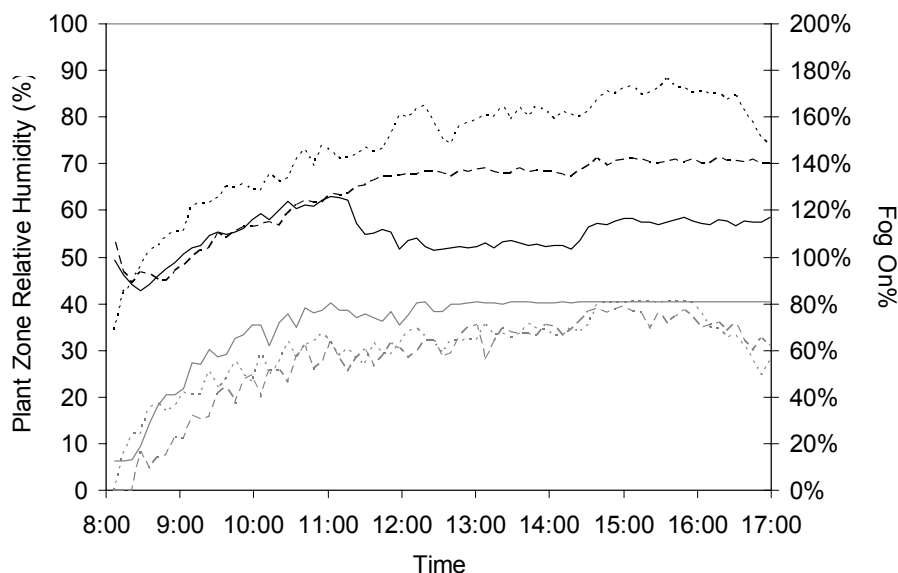


Figure 5.33 Seven-minute mean plant zone relative humidity levels and fog On-time percentages versus time of day for three ventilation rates: $3.0 \text{ m}^3 \text{ s}^{-1}$ (....), $4.5 \text{ m}^3 \text{ s}^{-1}$ (---), and $9.4 \text{ m}^3 \text{ s}^{-1}$ (—). Black lines represent plant zone relative humidity and gray lines represent Fog On%.

The largest magnitudes of temporal fluctuations were observed at the inlet (0 m) and in the center of the plant zone (12 m) (Figure 5.34). At $9.4 \text{ m}^3 \text{ s}^{-1}$ greater variability in air temperature was observed near the fans (28 m) than near the inlet (0 m). Relative humidity was also more variable at all locations within the plant zone at $9.4 \text{ m}^3 \text{ s}^{-1}$ than at the other ventilation rates.

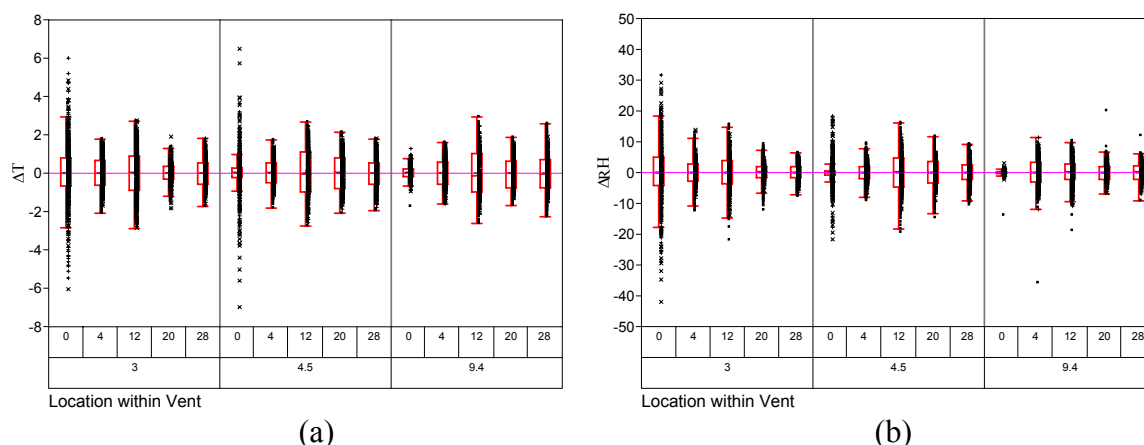


Figure 5.34 Box plots of temporal variability in (a) air temperature (ΔT) and (b) relative humidity (ΔRH) during the test period at several greenhouse locations (0, 4, 12, 20, and 28 m distance from inlet), presented as differences between each 1-minute measurement for three ventilation rates (3, 4.5, and $9.4 \text{ m}^3 \text{ s}^{-1}$).

5.4.7.4 Spatial Uniformity of Greenhouse Environmental Conditions

Mean air temperatures within the plant zone were very uniform and about 25°C for all ventilation rates (Figure 5.35). There was about a 1°C and 0.5°C increase from 12 m to 20 m for ventilation rates of 3.0 and $4.5 \text{ m}^3 \text{ s}^{-1}$, respectively. The temperature at the inlet was greatest for all ventilations rates and closest to outside values at $9.4 \text{ m}^3 \text{ s}^{-1}$. At $3.0 \text{ m}^3 \text{ s}^{-1}$ the inlet temperature was 7°C less than the outside temperature resulting from greater evaporation of fog near the inlet.

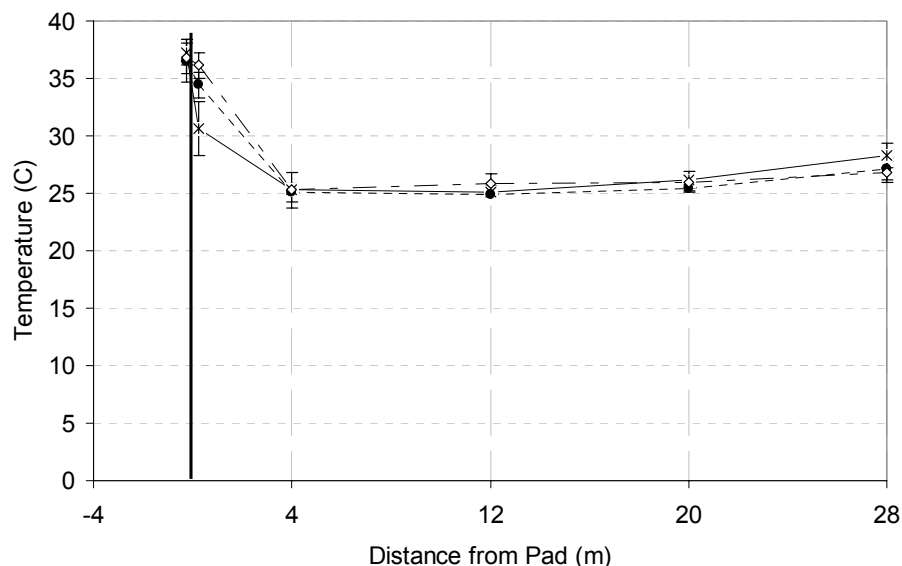


Figure 5.35 Air temperature (mean and s.d. for 11:00-17:00) versus distance from the inlet vent representing spatial uniformity during high-pressure-fog cooling for three ventilation rates: $3.0 \text{ m}^3 \text{ s}^{-1}$ ($-*-$), $4.5 \text{ m}^3 \text{ s}^{-1}$ ($\cdots\bullet\cdots$), and $9.4 \text{ m}^3 \text{ s}^{-1}$ ($--\diamond--$). The solid vertical line represents the cooling pad location.

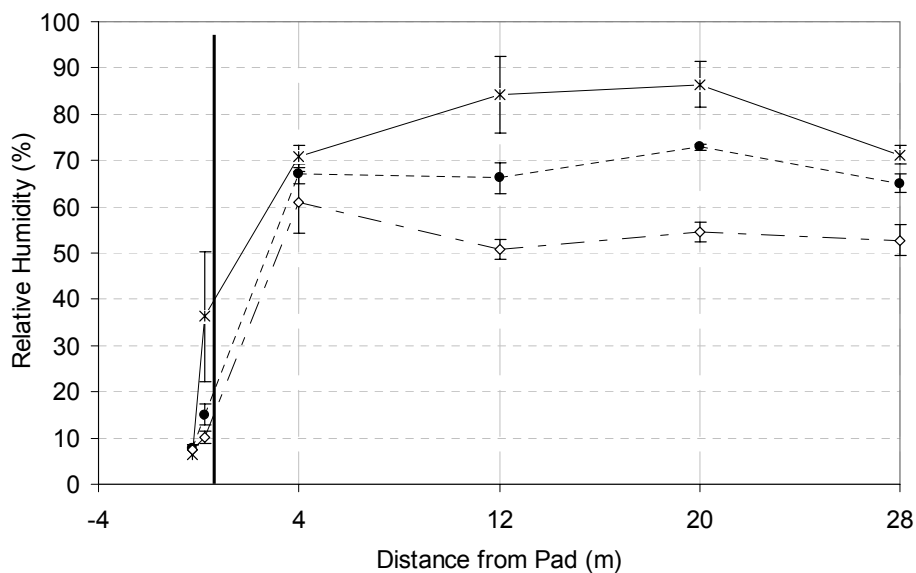


Figure 5.36 Relative humidity (mean and s.d. for 11:00-17:00) versus distance from inlet vent representing spatial uniformity during high-pressure-fog cooling for three ventilation rates: $3.0 \text{ m}^3 \text{ s}^{-1}$ ($-*-$), $4.5 \text{ m}^3 \text{ s}^{-1}$ ($\cdots\bullet\cdots$), and $9.4 \text{ m}^3 \text{ s}^{-1}$ ($--\diamond--$). The solid vertical line represents the cooling pad location.

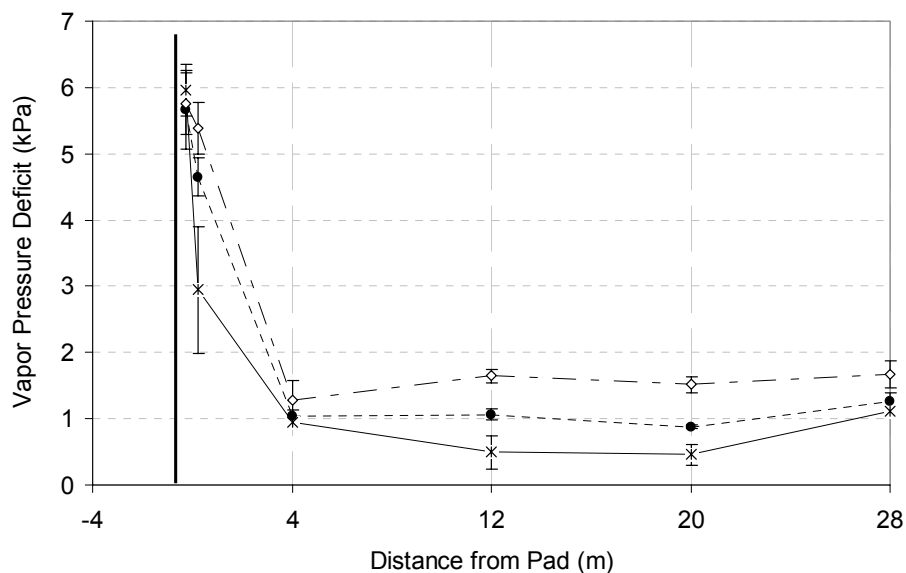


Figure 5.37 Vapor pressure deficit (mean and s.d. for 11:00-17:00) versus distance from vent inlet representing spatial uniformity during high-pressure-fog cooling for three ventilation rates: $3.0 \text{ m}^3 \text{ s}^{-1}$ ($-*-$), $4.5 \text{ m}^3 \text{ s}^{-1}$ ($\cdots\bullet\cdots$), and $9.4 \text{ m}^3 \text{ s}^{-1}$ ($--\diamond--$). The solid vertical line represents the cooling pad location.

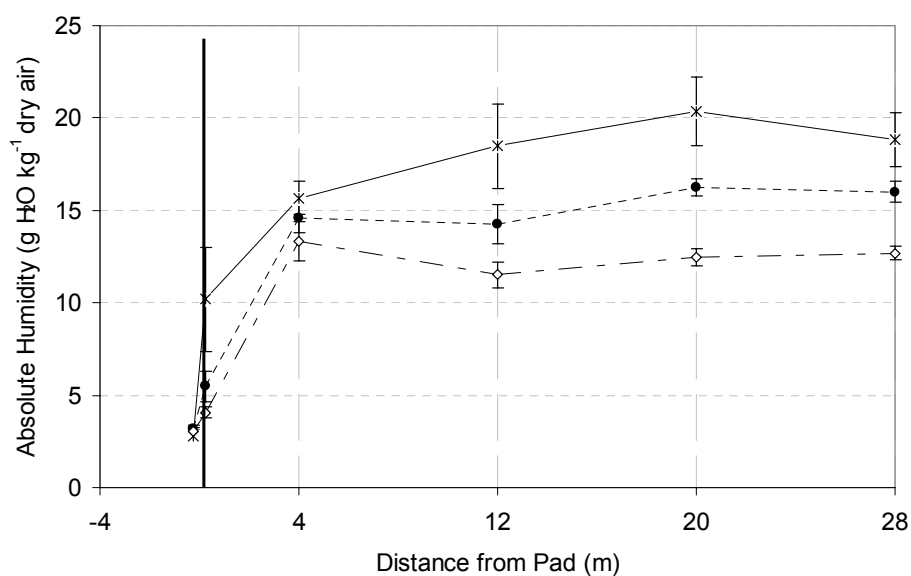


Figure 5.38 Absolute humidity (mean and s.d. for 11:00-17:00) versus distance from inlet vent representing spatial uniformity during high-pressure-fog cooling for three ventilation rates: $3.0 \text{ m}^3 \text{ s}^{-1}$ ($-*-$), $4.5 \text{ m}^3 \text{ s}^{-1}$ ($\cdots\bullet\cdots$), and $9.4 \text{ m}^3 \text{ s}^{-1}$ ($--\diamond--$). The solid vertical line represents the cooling pad location.

Relative humidity was less uniform within the greenhouse compared to air temperature at any ventilation rate (Figure 5.36) and generally followed the spatial trends of absolute humidity (Figure 5.38). The relative and absolute humidity of the air near the inlet was much greater and more variable at $3.0 \text{ m}^3 \text{ s}^{-1}$ than at 4.5 and $9.3 \text{ m}^3 \text{ s}^{-1}$, likely due to greater evaporative activity allowed near the inlet under slower airspeeds.

The relative humidity doubled from the inlet to 4 m location at $3.0 \text{ m}^3 \text{ s}^{-1}$, and increased by 400% at the other two ventilation rates. The relative humidity of the air increased with distance from the pad at $3.0 \text{ m}^3 \text{ s}^{-1}$, from a value of 70% at 4 m to 87% at 20 m. The moisture content of the air remained constant between 4 m and 12 m at $4.5 \text{ m}^3 \text{ s}^{-1}$, and slightly decreased at $9.4 \text{ m}^3 \text{ s}^{-1}$. An increase in moisture was then observed from 12 m to 20 m at these two ventilation rates. Finally, the absolute humidity did not change from 20 m to 28 m location at the outlet for 4.5 and $9.4 \text{ m}^3 \text{ s}^{-1}$, but decreased slightly for $3.0 \text{ m}^3 \text{ s}^{-1}$. Overall, the moisture content of the air at every location was always greater with decreasing ventilation rate.

A constant level of absolute humidity would be expected between the plant zone and fan outlet because there was no additional source of water vapor supply in that region. The absolute humidity did remain constant at 4.5 and $9.4 \text{ m}^3 \text{ s}^{-1}$, but a small decrease was observed at $3.0 \text{ m}^3 \text{ s}^{-1}$ (Figure 5.38). The decreased absolute humidity values may have occurred due to the reduced resistance to airflow between the plant zone and fans, relative to that within the plant zone. At the very low air speeds produced by $3.0 \text{ m}^3 \text{ s}^{-1}$, a large boundary layer may have developed above the plant canopy and around the sensors, causing relatively high measures of vapor content in the air. Near the fan

outlet, however, the increased airspeed would be expected to produce a much smaller boundary layer near the sensors, thereby improving their sensitivity, and causing measured humidity levels to be lower than those measured within a boundary layer.

VPD levels were also different among the three ventilation rates due to the different moisture content levels of air they produced (Figure 5.37). However, *VPD* was more uniform than relative and absolute humidity. In general, *VPD* was less than 1.0 kPa at $3.0 \text{ m}^3 \text{ s}^{-1}$, approximately 1.0 kPa at $4.5 \text{ m}^3 \text{ s}^{-1}$, and greater than 1.0 kPa at $9.4 \text{ m}^3 \text{ s}^{-1}$ at all locations within the plant zone.

5.4.8 Transpiration and Water Uptake Rates by the Tomato Plants

Based on the results observed with the pad-and-fan system that became relatively constant after 11:00 (Section 5.2.8), transpiration rates (E_T) were also plotted during the period of 11:00 – 17:00 for the high-pressure-fog cooling system tests (Figure 5.39). Similar to the E_T results found for the pad-and-fan system, E_T during high-pressure-fogging also declined, especially when the shade curtain was used. After the shade period ended (14:30), E_T for ventilation rates of 4.5 and $9.4 \text{ m}^3 \text{ s}^{-1}$ increased and peaked at 16:00. The E_T at $3.0 \text{ m}^3 \text{ s}^{-1}$ did not, however, decrease, but continued to decline even during the highest solar load and without shade. The low *VPD* ($< 0.5 \text{ kPa}$) of the air after shade removal also likely suppressed transpiration. Furthermore, if more fog water accumulated on the surfaces of plants with low ventilation conditions ($3.0 \text{ m}^3 \text{ s}^{-1}$), the boundary layer resistance between leaves and air would increase, thereby suppressing E_T .

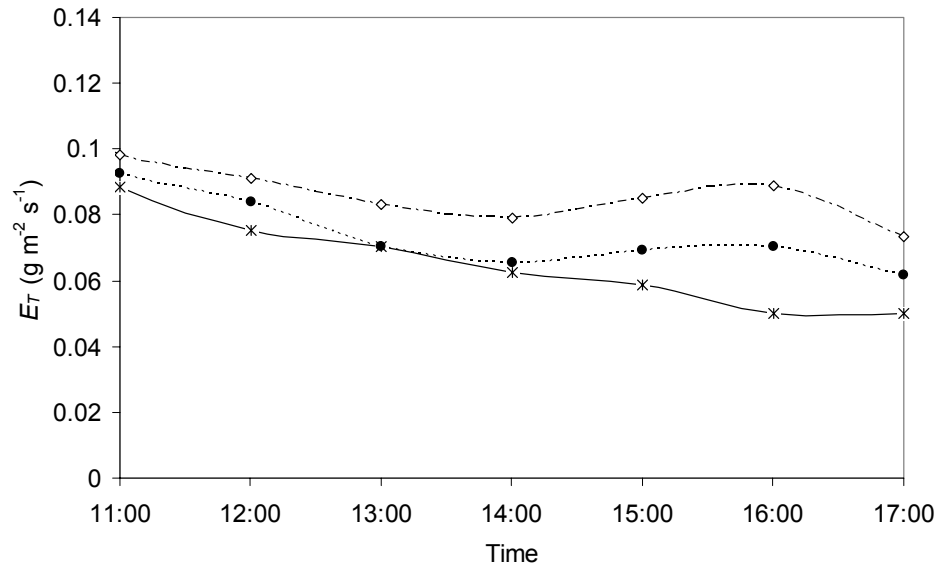


Figure 5.39 Transpiration rate of tomato plants versus time of day for high-pressure-fog cooling between 11:00 – 17:00 for three ventilation rates: $3.0 \text{ m}^3 \text{s}^{-1}$ ($-*-$), $4.5 \text{ m}^3 \text{s}^{-1}$ ($\cdots\bullet\cdots$), and $9.4 \text{ m}^3 \text{s}^{-1}$ ($--\diamond--$).

Positive relationships between E_T and solar radiation (Rad_{in}) have been reported (Joliet and Bailey, 1992); however this study found a weak linear relationship between the two variables (Figure 5.40). E_T measurements at $3.0 \text{ m}^3 \text{s}^{-1}$ weaken the relationship, due to the low E_T values observed even during increased levels of Rad_{in} following the removal of shade curtain (Figure 5.39). However, when data points from $3.0 \text{ m}^3 \text{s}^{-1}$ are removed from the plot, the linear relationship did not improve (data not shown).

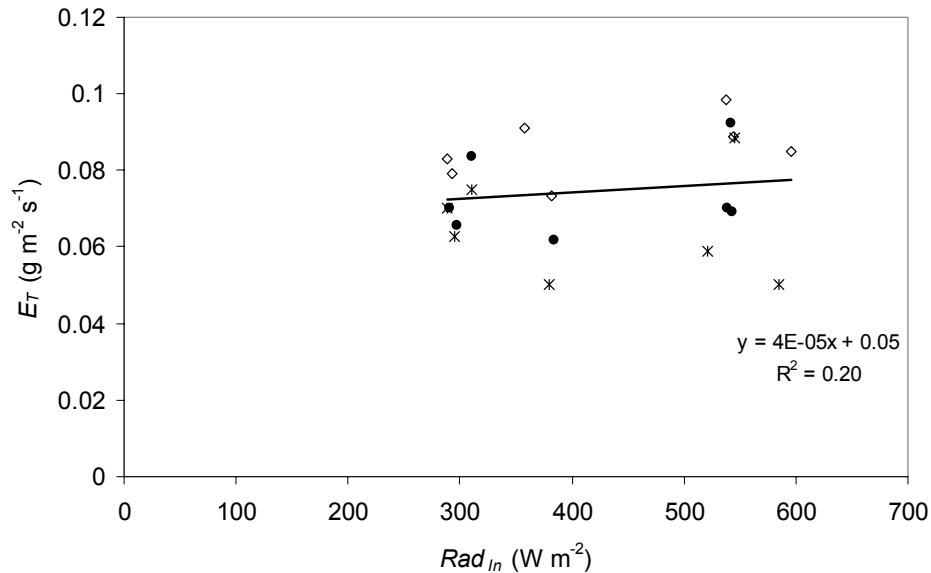


Figure 5.40 Transpiration rate (E_T) of tomato plants versus incoming solar radiation (Rad_{in}) during high-pressure-fogging for three ventilation rates: 3.0 $\text{m}^3 \text{s}^{-1}$ (*), 4.5 $\text{m}^3 \text{s}^{-1}$ (●), and 9.4 $\text{m}^3 \text{s}^{-1}$ (◇). Linear regression performed on data points (11:00 – 17:00) for all three ventilation rates.

Plant water uptake was found to be highly correlated with the psychrometric properties of the air regardless of time of day, including RH ($r = -0.82$), VPD ($r = +0.74$), and W ($+0.85$), less so with air temperature ($r = -0.66$), but poorly correlated with Rad_{in} ($r = 0.20$). Ventilation rate was highly correlated to WU_{PU} and produced significantly different WU_{PU} values after 11:00. Therefore, the significant effect that ventilation rate had on the moist air properties (Table 5.18) indirectly affected WU_{PU} .

By isolating and comparing the moist air conditions of the final hour of shading (13:00-14:00) and the following hour without shade in the afternoon (15:00-16:00), the correlations with moist air conditions became even stronger, with $r = -0.86$, $r = +0.87$, and $r = -0.86$ for RH , VPD , and W , respectively (Table 5.18). However, the correlation to incoming solar radiation became much lower ($r = -0.03$).

Although lysimeter data do not provide the most accurate measure of E_T in short time intervals (less than 1 hour), the greenhouse climate conditions were found to have significant effects on the lysimeter measurements. Specifically, the high air moisture conditions with low VPD seemed to reduce plant transpiration.

Table 5.18 Mean plant water uptake rates (WU_{PU}) for the full test period (11:00-17:00), after initial hydration of the plants (11:00-17:00), during shading (13:00-14:00), and after shading (15:00-16:00) for different ventilation rates for high-pressure-fog evaporative cooling. Means with significant difference ($p < 0.05$) according to Tukey-Kramer HSD are represented by different letters.

\dot{Q} ($\text{m}^3 \text{s}^{-1}$)	Mean $\overline{WU_{PU}}$ ($\text{g m}^{-2} \text{s}^{-1}$)			
	8:00-17:00	11:00-17:00	13:00-14:00	15:00-16:00
3.0	0.077 ^a	0.063 ^a	0.066 ^b	0.052 ^a
4.5	0.082 ^a	0.072 ^a	0.066 ^b	0.071 ^b
9.4	0.094 ^a	0.087 ^b	0.079 ^a	0.087 ^c

5.4.9 Leaf Temperature

In general, the lowest mean leaf temperature (T_{Leaf}) occurred at 12:00, after about one hour of shading, and the highest T_{Leaf} occurred at 16:00, after approximately 2 hours without shading (Figure 5.41). After 12:00 T_{Leaf} gradually increased until the final measurement at 16:00. Also, the mean T_{Leaf} was significantly greater ($p < 0.01$) for $3.0 \text{ m}^3 \text{s}^{-1}$ than the other two ventilation rates, possibly due to the lower E_T observed at $3.0 \text{ m}^3 \text{s}^{-1}$.

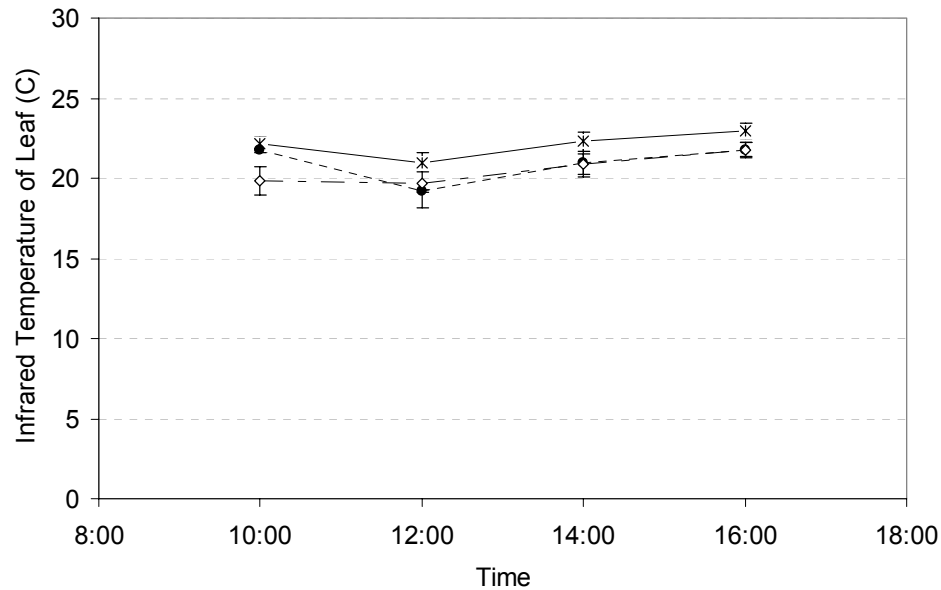


Figure 5.41 Mean and standard deviation of leaf temperature versus time of day of three shaded leaves measured with an infrared thermometer during high-pressure-fog cooling for four ventilation rates: $3.0 \text{ m}^3 \text{ s}^{-1}$ (—*—), $4.5 \text{ m}^3 \text{ s}^{-1}$ (···•···), and $9.4 \text{ m}^3 \text{ s}^{-1}$ (---◇---). The shade curtain was used between 11:00 – 14:30.

Overall, T_{Leaf} remained between 20–24°C for all ventilation rates (Table 5.19).

Measured leaf temperatures were always lower than the mean plant zone air temperature during the 2-hour period leading up to T_{Leaf} measurements. The greatest $T_{Air} - T_{Leaf}$ differences ($\approx 5^\circ\text{C}$) occurred at 12:00 when T_{Leaf} measurements were the lowest.

Between 12:00 and 14:00 T_{Leaf} increased more than mean T_{Air} , creating smaller differences. At 16:00 the $T_{Air} - T_{Leaf}$ difference was smallest at $4.5 \text{ m}^3 \text{ s}^{-1}$ due to the capability of the fog and ventilation systems to maintain setpoint air temperature.

The difference in leaf temperatures (T_{Leaf}) between the three locations was used to determine spatial uniformity. T_{Leaf} decreased with increasing distance from the inlet, with the greatest decreases occurring at 14:00 for all ventilation rates. The greatest spatial uniformity was at 16:00, when T_{Leaf} values were highest. Leaf temperature differences at

10:00, 12:00, 14:00, and 16:00 ranged from 0.2-2.0°C, 0.1-3.6°C, 0.1-2.2°C, and 0.2-2.2°C, respectively. Spatial uniformity was best at 16:00 for 3.0 m³ s⁻¹, in the morning for 4.5 m³ s⁻¹ (10:00 and 12:00), and in the afternoon for 9.4 m³ s⁻¹ (14:00 and 16:00).

Leaf temperature did not have a strong correlation to any of the environmental parameters measured. The greatest correlation was found between T_{Leaf} and absolute humidity ($r = +0.53$). Weak correlations were found between air temperature ($r = +0.50$), relative humidity ($r = +0.47$), VPD ($r = -0.43$), and incoming radiation ($r = +0.22$). Low correlation was also found between E_T and leaf temperature ($r = -0.36$).

Table 5.19 Leaf temperatures (T_{Leaf}) and mean plant zone environmental conditions versus time of day of three plants at different distances from the cooling pad (5.2, 11, 17.7 m) during high-pressure-fog cooling at three ventilation rates. T_{Leaf} was measured with an infrared thermometer. The difference in T_{Leaf} between the three locations determined uniformity. Numbers in italics refers to maximum temperature differences observed. Tests of significance performed with Tukey-Kramer HSD. Values with similar letters for a given time are not significantly different at $p < 0.01$.

\dot{Q} (m ³ s ⁻¹)	Leaf Temperature (°C)				Mean Plant Zone Conditions			
	5.2 m	11 m	17.7 m	Mean	T (°C)	RH (%)	VPD (kPa)	Rad_{In} (W m ⁻²)
10:00					08:00-10:00			
3.0	22.6	22.2	21.8	22.2 ^a	24.5±0.4	55.7±9.8	1.3±0.3	500±87
4.5	21.8	21.6	21.8	21.7 ^a	24.0±0.8	50.3±4.3	1.5±0.1	493±83
9.4	21.0	19.7	18.8	19.8 ^b	23.8±0.5	50.5±5.0	1.5±0.1	489±84
12:00					10:00-12:00			
3.0	21.8	20.9	20.3	21.0 ^a	25.3±0.2	71.7±3.7	0.9±0.1	427±162
4.5	19.3	19.2	19.1	19.2 ^b	24.7±0.1	62.7±3.9	1.2±0.1	426±161
9.4	21.6	19.4	18.0	19.7 ^b	24.6±0.3	58.8±3.0	1.3±0.1	447±147
14:00					12:00-14:00			
3.0	23.1	22.1	21.7	22.3 ^a	25.5±0.2	79.8±1.7	0.7±0.05	292±14
4.5	22.0	21.2	19.8	21.0 ^b	25.3±0.3	68.2±0.2	1.0±0.01	294±13
9.4	21.8	20.4	20.5	20.9 ^b	25.9±0.3	55.6±0.4	1.6±0.02	291±13
16:00					14:00-16:00			
3.0	22.7	22.6	23.6	23.0 ^a	26.1±0.2	84.4±2.6	0.5±0.1	553±173
4.5	22.3	21.8	21.1	21.7 ^b	25.5±0.2	70.0±1.3	1.0±0.0	541±136
9.4	21.6	22.4	21.4	21.8 ^b	26.3±0.4	56.5±2.2	1.5±0.1	570±102

5.5 Water Use Efficiency for Hydroponic Greenhouse Tomato Production Using Pad-and-Fan Cooling in a Semi-Arid Climate

5.5.1 Outside and Greenhouse Environmental Conditions

The outside environmental conditions observed during the 2006 crop production season followed a very typical weather pattern of air temperature and relative humidity for Tucson, Arizona (Figure 5.42). As the daytime outside air temperature increased from January to mid-July, the *VPD* increased from about 1.0 kPa to greater than 6.0 kPa in May (Figure 5.43). The monsoon season officially began July 3, and at that time the *VPD* was reduced to 3.0 kPa. However, the *VPD* increased above 7.0 kPa again until mid-July, which is not typical for the monsoon season. The *VPD* remained below 5.0 kPa for the remainder of the study, with fluctuations near 1.0 kPa. The average daytime solar radiation increased from 650 W m^{-2} at the start of the test to 900 W m^{-2} in May, and back to near 650 W m^{-2} by the end of the study.

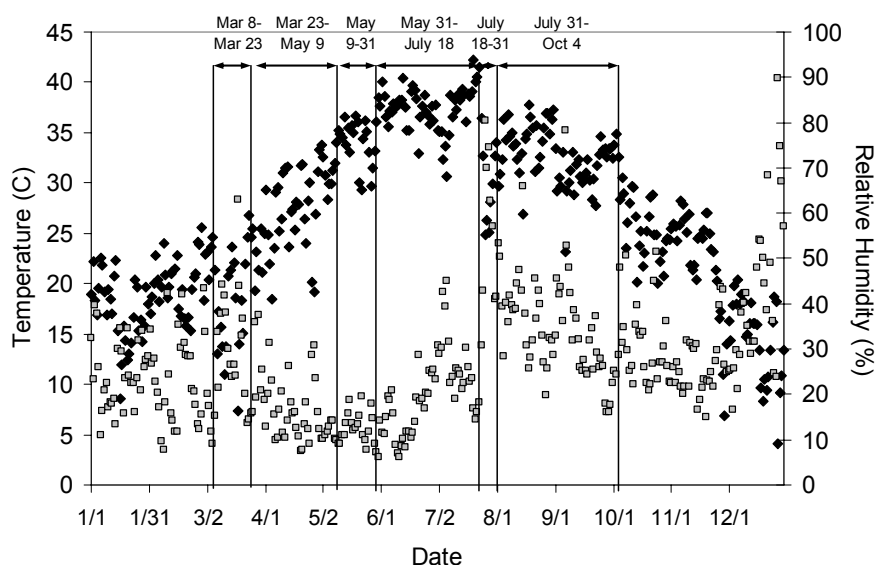


Figure 5.42 Mean daytime (08:00 – 16:00) outside air temperature (♦) and relative humidity (■) during 2006. Test periods during the 8-month study period are delineated.

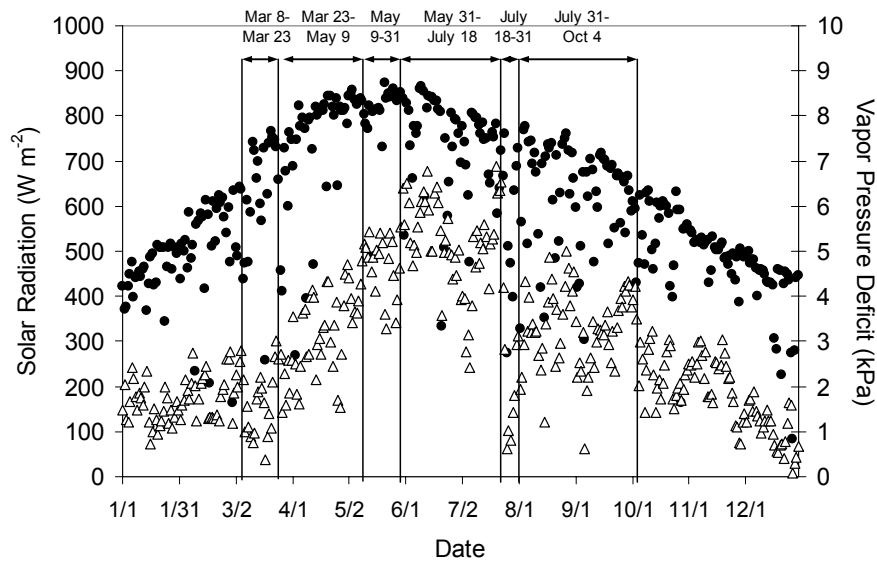


Figure 5.43 Mean daytime (08:00 – 16:00) outside VPD (Δ) and solar radiation (\bullet) during 2006. Test periods during the 8-month study period are delineated.

The average daytime and nighttime air temperatures in the greenhouse were controlled between 23-30°C and 18-24°C, respectively, and depended largely on the season (Figure 5.44). In general, the pad-and-fan system was able to control both daytime and nighttime inside temperatures better when outside conditions were drier ($VPD > 5.0$ kPa), as observed from March to approximately July 18. The greenhouse VPD was always maintained below 2.0 kPa, with the lowest VPD levels occurring at night and after the onset of the monsoon season.

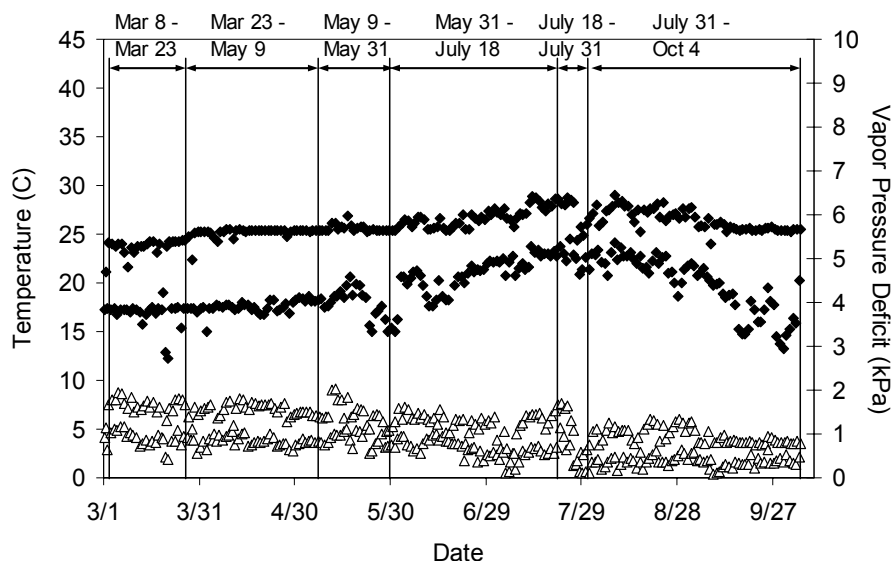


Figure 5.44 Mean daytime (08:00 – 16:00) and nighttime (0:00 – 08:00) inside air temperature (♦) and *VPD* (Δ) during the crop season (March 8 – October 4, 2006).

5.5.2 Seasonal Greenhouse Water Use

Figure 5.45 represents the daily rate of water use by the pad-and-fan and irrigation systems during the crop seasonal time period (March to October). The daily water use rate of the pad-and-fan system increased from March to July 18 as outside conditions became warmer and drier (Figure 5.45). This increased water use resulted from the increased ventilation rates used to maintain the setpoint air temperature. With the onset of monsoon season (July 18), less water was used by the pad-and-fan system because outside temperatures were 5-10°C cooler and the air moisture content was greater ($VPD < 5.0$ kPa). These markedly different outside conditions reduced both the cooling load (lower ventilation rate) and the effectiveness of the pad-and-fan system to add water vapor to the air from the pad.

Water use by the open irrigation system increased throughout the study as more water was needed to meet the plant water demand, and maintain oxygen and electroconductivity levels in the root zone. The water uptake rate of the plants followed the trend of changing irrigation practices.

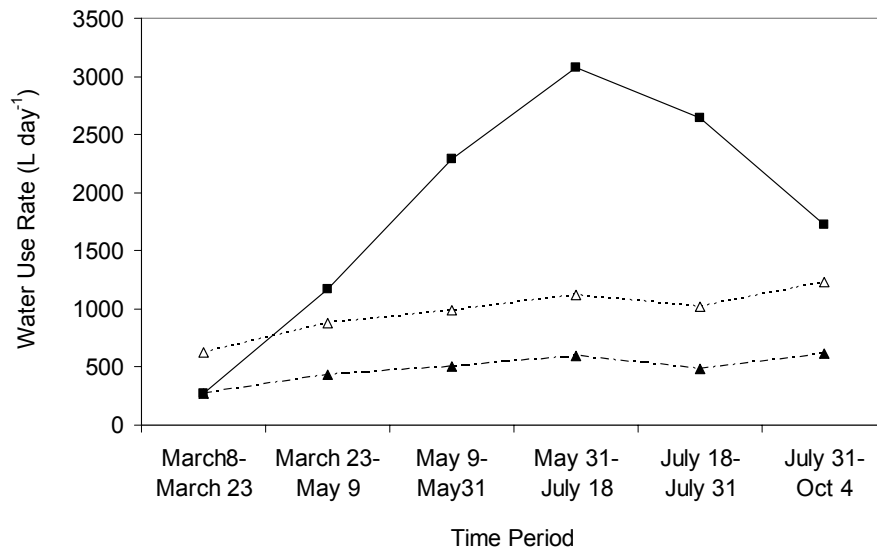


Figure 5.45 Daily 24-hr water use rates by the pad-and-fan system (—■—), open irrigation system (···△···), and closed irrigation systems (---▲---) from March 8 to October 4, 2006.

The seasonal change of outside environmental conditions had a direct effect on pad-and-fan system performance (Figure 5.46). The cooling efficiency (η_{Cool}) of the pad-and-fan system was about 25% lower during the monsoon conditions of August than during the dry, summer conditions of May. Therefore, although lower ventilation rates have been shown to produce higher η_{Cool} (Section 5.2.2), the low values of η_{Cool} observed during monsoon conditions occurred from higher outside wet bulb air temperatures, which reduced the absorption of water vapor from the pad.

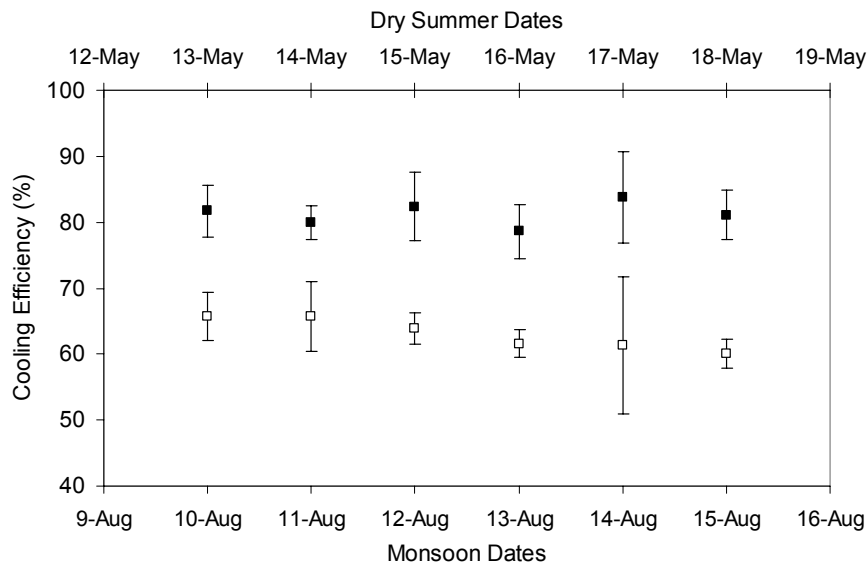


Figure 5.46 Mean and standard deviation of pad-and-fan cooling efficiency (η_{Cool}) during May 12 – 19, 2006, representing dry, summer conditions (■) (upper data) and during August 10 – 15, 2006, representing summer monsoon conditions (□) (lower data).

5.5.3 Greenhouse Water Use Efficiency

5.5.3.1 Tomato Yields and Greenhouse Water Use

Based on the 222 m² production floor area, the cumulative yield in the greenhouse was 36 kg m⁻² for the 209-day crop life cycle (Table 5.20). The large 90 kg d⁻¹ yield obtained in May occurred because the first harvest was delayed, allowing more fruit to develop and be harvested. Following this initial harvest, yields were regularly around 50 kg d⁻¹. When comparing the mean pre-monsoon and monsoon yields, the effect of monsoon conditions becomes less prominent, as the 6 weeks leading up to first harvest yielded no tomatoes but water was still required to grow the plants.

The total water use by the pad-and-fan system (WU_{PF}) during the 209-day crop cycle was 1.8 m³ m⁻². WU_{PF} increased from 0.33 m³ day⁻¹ in March to 3.1 m³ day⁻¹ in

July, as more water was needed to cool the greenhouse as outside conditions became warmer and drier. After July 18, WU_{PF} decreased to nearly half of its July peak to $1.7 \text{ m}^3 \text{ d}^{-1}$ with the onset of monsoon.

The tomato plants were irrigated with a total of $1.2 \text{ m}^3 \text{ m}^{-2}$ of water, about 25% less than what was needed to evaporatively cool the greenhouse. $WU_{I,Open}$ increased from less than $1.0 \text{ m}^3 \text{ d}^{-1}$ during the pre-harvest season, when outside conditions were not too hot to May 10 when $WU_{I,Open}$ remained near $1.2 - 1.5 \text{ m}^3 \text{ d}^{-1}$ for the remainder of the growing season.

The tomato plants utilized $0.6 \text{ m}^3 \text{ m}^{-2}$ of water during the full 209-day crop period, a value that was half the total irrigation amount (Table 5.20). Based on $WU_{I,Closed}$ values, the plants used more irrigation water after the start of monsoon season, when the evaporative cooling was operated less and VPD was less than 1.0 kPa .

Table 5.20 Mean daily tomato yields and water use rates by the pad-and-fan system and the open and closed irrigation systems. Crop totals presented are based on a 222 m^2 production floor area for a 209-day crop life cycle.

	<i>Yield</i> (kg day^{-1})	WU_{PF} ($\text{m}^3 \text{ day}^{-1}$)	$WU_{I,Open}$ ($\text{m}^3 \text{ day}^{-1}$)	$WU_{I,Closed}$ ($\text{m}^3 \text{ day}^{-1}$)
Mar8 – Mar22	---	0.33	0.63	0.27
Mar23 – May9	---	1.2	0.87	0.43
May10 – May31	90	2.3	1.2	0.63
June1 – July18	51	3.1	1.4	0.74
July19 – July31	49	2.5	1.3	0.61
Aug1 – Oct4	42	1.7	1.5	0.77
Pre-Monsoon	39	2.3	1.4	0.70
Monsoon	35	1.6	1.6	0.84
Total	38	1.9	1.3	0.66
$\Sigma_{Mar-Oct}$	36 kg m^{-2}	$1.8 \text{ m}^3 \text{ m}^{-2}$	$1.2 \text{ m}^3 \text{ m}^{-2}$	$0.6 \text{ m}^3 \text{ m}^{-2}$

5.5.3.2 Water Use Efficiency

The total WUE_{PF} was less than both $WUE_{I,Open}$ and $WUE_{I,Closed}$. The overall WUE_S for the entire life of the crop was 11.7 kg m^{-3} and 14.6 kg m^{-3} for the open and closed irrigation systems, respectively. Monsoon conditions reduced water consumption used by the pad-and-fan system, subsequently increasing the WUE_{PF} from 17.1 to 22.5 kg m^{-3} . However, the overall $WUE_{S,Open}$ and $WUE_{S,Closed}$ remained the same due to the lower yields and higher water use rates of the irrigation system during that period.

The high yields harvested in May helped produce the highest WUE values observed during the cropping season, which were 38.9 , 73.1 , and 143 kg m^{-3} for WUE_{PF} , $WUE_{I,Open}$, and $WUE_{I,Closed}$, respectively (Table 5.21). However, those values are misleading due to the delayed harvest that allowed a large first yield. As the season progressed, yields decreased to consistent values (approximately 50 kg d^{-1}) and the outside conditions became hotter and drier, causing higher water rates for cooling and irrigation and reducing the WUE_{PF} and $WUE_{I,Open}$ by about one-half to 16.5 and 36.2 kg m^{-3} , respectively. The greater use of water by the plants ($WU_{I,Closed}$) in May, June, and July, coupled with a reduction in yield, caused the $WUE_{I,Closed}$ to decrease to 68.6 kg m^{-3} . The lower yields and higher irrigation water use after the onset of monsoon produced $WUE_{I,Open}$ and $WUE_{I,Closed}$ values of 28.1 and 54.7 kg m^{-3} , respectively. However, the reduced water use by the pad-and-fan system during monsoon increased the WUE_{PF} to 24.4 kg m^{-3} .

The $WUE_{S,Open}$ in May was 25.4 kg m^{-3} , which was the highest value found for the crop and corresponded to the highest yields and low water use by both the pad-and-fan

and open irrigation system. During the dry summer season (June 1 – July 18, 2006)

$WUE_{S,Open}$ was reduced to 11.3 kg m^{-3} due to the lower yields and high water use rates by both systems.

Theoretically, using a 100% closed-irrigation system would greatly improve the water use efficiency of the greenhouse (irrigation + evaporative cooling) from values similar to flood irrigation ($10\text{-}12 \text{ kg m}^{-3}$) up to values within the range of sprinkler irrigation ($11\text{-}19 \text{ kg m}^{-3}$) (Hanson *et al*, 2006; Hanson and May, 2005; Hanson and May, 2004). Only the closed irrigation had WUE values greater than those obtained in the Netherlands (45 kg m^{-3}) and France (39 kg m^{-3}) (Pardossi *et al*, 2004), and the WUE of $25 - 30 \text{ kg m}^{-3}$ in the warmer climates of Spain (Reina-Sanchez, 2005) and Italy (Incrocci *et al.*, 2006). However, together with the pad-and-fan water use, the WUE for producing a full-term greenhouse tomato crop was much less than all the irrigation-based greenhouse WUE values reported.

Table 5.21 Seasonal and total WUE_{PF} , WUE_I , and WUE_S based on 222 m^2 growing area for the 209-day production period.

	WUE_{PF} (kg m^{-3})	$WUE_{I,Open}$ (kg m^{-3})	$WUE_{I,Closed}$ (kg m^{-3})	$WUE_{S,Open}$ (kg m^{-3})	$WUE_{S,Closed}$ (kg m^{-3})
May10 – May31	38.9	73.1	143	25.4	30.6
June1 – July18	16.5	36.2	68.6	11.3	13.3
July19 – July31	19.8	38.3	80.3	13.0	15.9
Aug1 – Oct4	24.4	28.1	54.7	13.0	16.9
Pre-Monsoon	17.1	27.7	55.3	10.5	13.0
Monsoon	22.5	21.3	41.5	10.9	14.6
Total	19.6	29.0	57.5	11.7	14.6

5.6 Using the Energy Balance Equation to Estimate Evaporative Cooling Water Use and Inside Air Temperatures for a Greenhouse in Semi-Arid Conditions

5.6.1 Evaporative Cooling Water Use

5.6.1.1 Pad-and-Fan Cooling Water Use

A comparison between measured and model-predicted (*Equation 4.21*) water use by the pad-and-fan system is shown in Figure 5.47. The energy balance equation produced a good prediction for water use ($R^2 = 0.98$), with values slightly greater than those measured. Much of this over-prediction can be attributed to the location of the temperature and relative humidity sensors, which were at the center of the pad, where the heaviest streams of water were observed during experiments. With higher rates of evaporation expected in the high-stream location, it is reasonable that the energy balance would over-predict total water use.

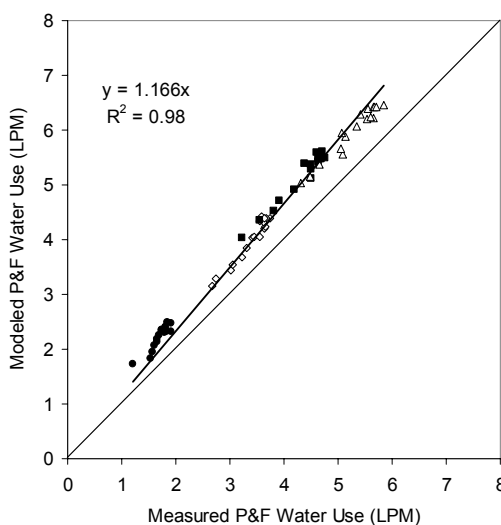


Figure 5.47 Modeled versus measured water use by the pad-and-fan cooling system using data from 11:00 – 17:00 for four ventilation rates: $4.5 \text{ m}^3 \text{ s}^{-1}$ (●), $9.4 \text{ m}^3 \text{ s}^{-1}$ (◇), $13 \text{ m}^3 \text{ s}^{-1}$ (■), and $16.7 \text{ m}^3 \text{ s}^{-1}$ (Δ).

5.6.1.2 High-Pressure-Fog Cooling Water Use

Water use predicted by the energy balance and moisture balance models is shown in Figure 5.48. Both models predicted lower water use rates than was actually used by the high-pressure-fog system. These results suggest that not all of the water introduced into the greenhouse was evaporated or was needed to produce the air temperatures observed at the 20 m location in the greenhouse for the three ventilation rates tested. Much of the delivered water that was not used to produce the greenhouse climate, would have either landed on surfaces, such as plants, or extracted from the greenhouse by the fans prior to evaporation. Therefore, the difference in predicted and measured could be used as an estimate of the amount of water that could have been saved during the high-pressure-fog cooling tests.

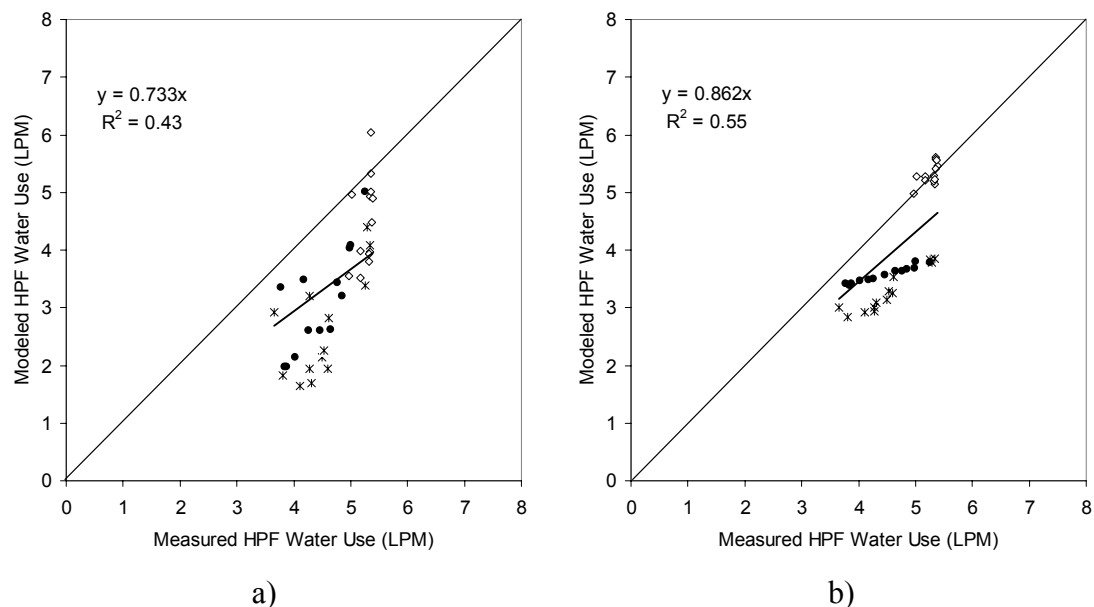


Figure 5.48 Modeled versus measured water use by the high-pressure-fog cooling system using a) the energy balance model (*Equation 4.27*) and b) the moisture balance (*Equation 4.26*) for data from 11:00 – 17:00 at 20 m location for three ventilation rates: 3.0 m³ s⁻¹ (*), 4.5 m³ s⁻¹ (•), and 9.4 m³ s⁻¹ (◊).

Using the difference between measured and predicted values of fog water use at the south-end of the plant zone (20 m from the inlet vent), where all fog water input should be accounted for, it is clear in Table 5.22 that a considerable amount of fog water could be saved for all three ventilation rates. However, the amount of potential savings decreases with increasing ventilation rate. For example, although more water was used for $9.4 \text{ m}^3 \text{ s}^{-1}$ than for the other two ventilation rates, nearly 85% of the water was evaporated to produce the observed greenhouse climate conditions, compared to only 58% and 70% at 3.0 and $4.5 \text{ m}^3 \text{ s}^{-1}$, respectively. Therefore, as might be expected, the higher ventilation rate maintained a high level of evaporative potential in the greenhouse by introducing a larger amount of outside air relative to the other ventilation rates, and thus precluded large amounts of surface wetting.

However, at $9.4 \text{ m}^3 \text{ s}^{-1}$ fog water droplets were observed being ejected from the greenhouse, demonstrating that even greater water savings could be made with a better design of the high-pressure-fog system. Also, at $4.5 \text{ m}^3 \text{ s}^{-1}$ more desirable relative humidity levels were observed than at $9.4 \text{ m}^3 \text{ s}^{-1}$. Thus, although more water may have evaporated in the air at $9.4 \text{ m}^3 \text{ s}^{-1}$, the water vapor was exhausted from the greenhouse more quickly than water was injected (and evaporated) through fogging.

Table 5.22 Total water use measured ($E_{Measured}$) and predicted ($E_{Predicted}$) by the energy balance model for high-pressure-fog cooling at the 20 m greenhouse location between 11:00-17:00, and the total potential savings in water ($E_{Meas} - E_{Pred}$) during the test of three ventilation rates (3.0, 4.5, and $9.4 \text{ m}^3 \text{ s}^{-1}$).

\dot{Q} ($\text{m}^3 \text{ s}^{-1}$)	Σ Water Use		Potential Savings
	$E_{Measured}$ (L m^{-2})	$E_{Predicted}$ (L m^{-2})	$E_{Meas} - E_{Pred}$ (L m^{-2})
3.0	6.3	3.7	2.6
4.5	6.3	4.4	1.9
9.4	7.4	6.3	1.1

The potential savings in water use changed over time and depends on the total energy input into the greenhouse (Figure 5.49). In general, the potential water savings were increased when the greenhouse was shaded because the solar energy input was low, which reduced the available energy for evaporating the fog. After removal of the shade (after 2:00), water use increased by 50-60 L for all three ventilation rates and the injected fog water evaporated more readily with the added solar energy input.

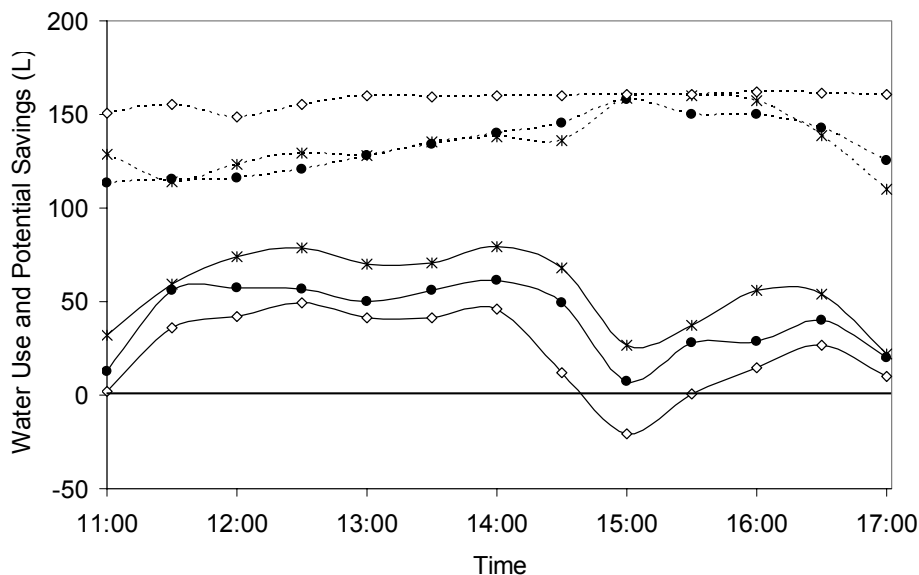


Figure 5.49 Water use by the high-pressure-fog system (---) from 11:00-17:00 and the potential water savings (—) calculated as the difference in predicted and measured water use ($E_{Meas} - E_{Pred}$) in 30-minute increments for three ventilation rates: $3.0 \text{ m}^3 \text{ s}^{-1}$ (*), $4.5 \text{ m}^3 \text{ s}^{-1}$ (●), and $9.4 \text{ m}^3 \text{ s}^{-1}$ (◇).

The negative value of potential savings (-20 L) at $9.4 \text{ m}^3 \text{ s}^{-1}$ occurred because more water was needed to produce the observed conditions than was actually provided by the fog system. Referring to the plant transpiration trends in Figure 5.34, E_T increased following the removal of shade. In fact, the 30-minute total of E_T between 14:30 and 15:00 was measured as 42 L. Therefore, 22 L of fog water theoretically could have been saved under the post-shade condition at 15:00 during $9.4 \text{ m}^3 \text{ s}^{-1}$.

Similar but lower increases in E_T were observed at $4.5 \text{ m}^3 \text{ s}^{-1}$, again indicating the decreased need for fog water following shading. No increase in E_T was observed for $3.0 \text{ m}^3 \text{ s}^{-1}$ after shading, though a reduction in potential water savings was found. Therefore, at $3.0 \text{ m}^3 \text{ s}^{-1}$ the greater solar energy allowed for more evaporation of the fog in the air. Finally, it is likely that evaporation of surface water from the plants, ground, and other greenhouse components contributed to the greenhouse climate and the high potential water savings near the end of the day, even as fog water use declined.

Improved operation control and system design of the high-pressure-fog system is required for managing water use. A single ventilation rate cannot be expected to produce the desired greenhouse climate and simultaneously minimize water use. Furthermore, improving the layout and distribution of the fog nozzles will reduce ejection through exhaust fans and facilitate more evaporation within the air before internal greenhouse surface wetting can occur.

5.6.2 Greenhouse Air Temperatures

5.6.2.1 Pad-and-Fan System

A linear regression between the measured and predicted air temperatures was performed to validate the T_{Out} and T_{x-l} models for the pad-and-fan cooling system. In Figure 5.50a (T_{Out} model) a linear relationship between predicted and measured values of air temperature was found, but with decreasing confidence with increasing distance from the pad. Furthermore, the greatest over-prediction for the T_{Out} model occurred for $3.0 \text{ m}^3 \text{ s}^{-1}$ during the period after the shade curtain was removed (15:00 – 15:30) for all three locations. In fact, the over-predicted values for all four ventilation rates occurred during 15:00 – 15:30, suggesting this result occurred from erroneously high measurements of R_n .

Using the temperatures measured at the location upstream from the prediction location (T_{x-l}) greatly improved the predictive ability of the energy balance model for air temperature (Figure 5.50b). Furthermore, the r-squared value of the linear regression was greater at the 12 and 20 m locations than at the 4 m location, suggesting that the air temperatures measured at 4 m and 12 m were relatively accurate. However, as described above, the conditions at the pad inlet may not been as accurate. Also, the R_n value at the 4 m location may have been less accurate than the other locations due to the proximity of the opaque pad and concrete walkway between the pad and 4 m location, as well as the presence of overhead systems, such as heaters.

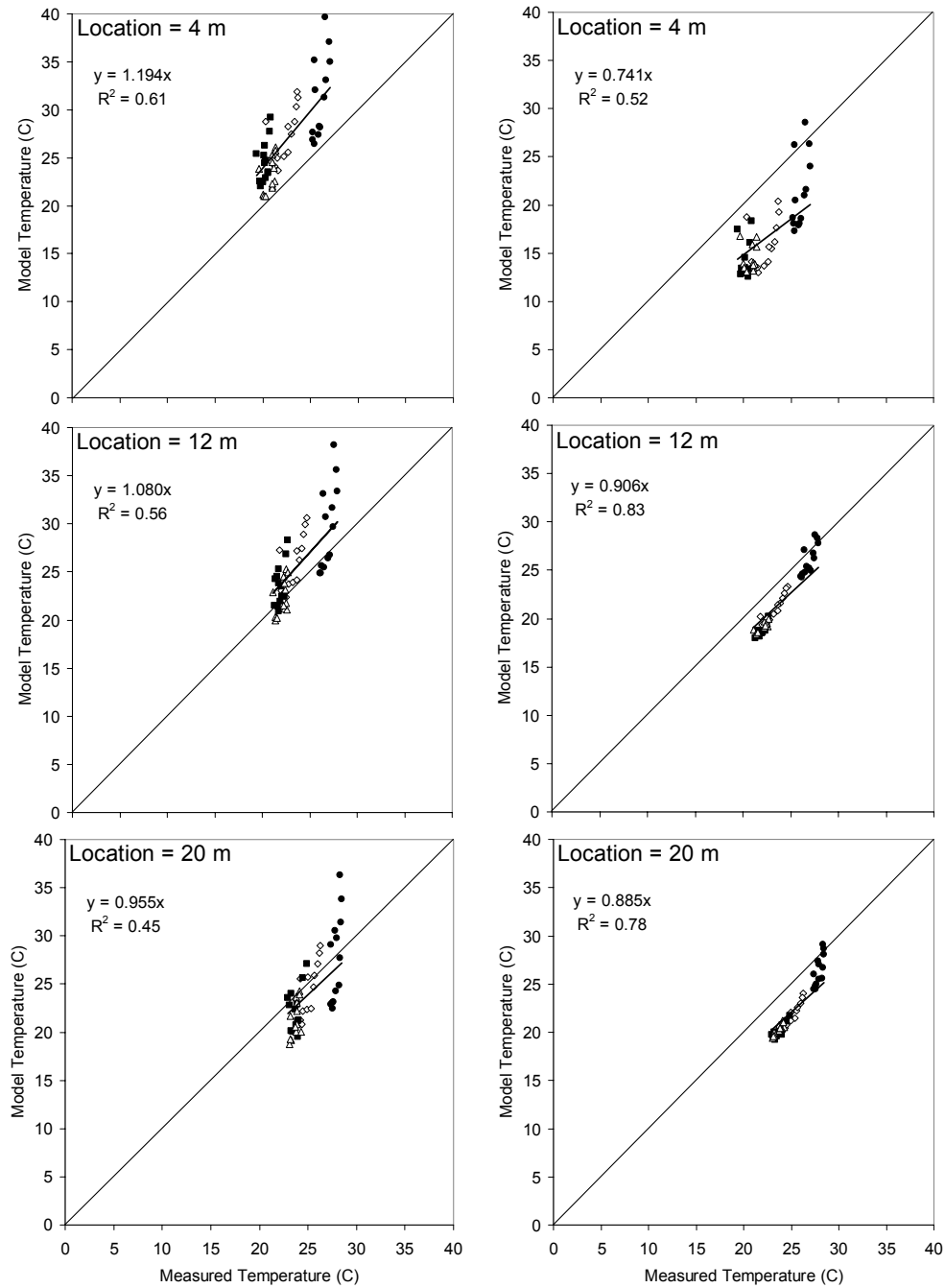
a) T_{Out} b) T_{x-l}

Figure 5.50 Modeled versus measured inside air temperatures with pad-and-fan cooling at 4 m, 12 m, and 20 m locations using a) T_{Out} and b) T_{x-l} in the energy balance equation for ventilation rates $4.5 \text{ m}^3 \text{ s}^{-1}$ (●), $9.4 \text{ m}^3 \text{ s}^{-1}$ (◇), $13 \text{ m}^3 \text{ s}^{-1}$ (■), and $16.7 \text{ m}^3 \text{ s}^{-1}$ (Δ).

Although knowing the climate conditions at several locations was convenient for validating the energy balance model, the purpose of the model in practice would be to predict the greenhouse conditions with only limited information about the inside climate. This model demonstrates that by knowing the greenhouse conditions at one location (such as the center of plant zone, 12 m) the grower could estimate the conditions at other greenhouse locations, both downstream and upstream from the measurement location during the plug-flow condition of the pad-and-fan cooling system.

5.6.2.2 High-Pressure-Fog System

Measured air temperature variations during the day were small during high-pressure-fog cooling, in part because 25°C was the target control temperature. However, the model air temperatures did tend to vary greatly (Figure 5.51) about the 25°C target. Therefore, the energy balance model for the high-pressure-fog system was validated by comparing the means of modeled and measured air temperatures, rather than using a linear regression.

The means and standard deviations for air temperatures both measured and then modeled with the energy balance are given in Table 5.23. The modeled air temperature for both T_{Out} and T_{x-1} agree most with measurements at the center plant zone location (12 m from vent inlet), verifying the results in Figure 5.51. This result is noteworthy because this location corresponds exactly to the control sensor location. Therefore, if conditions at the 12 m location were used for the models, they would provide accurate feedback for control purposes.

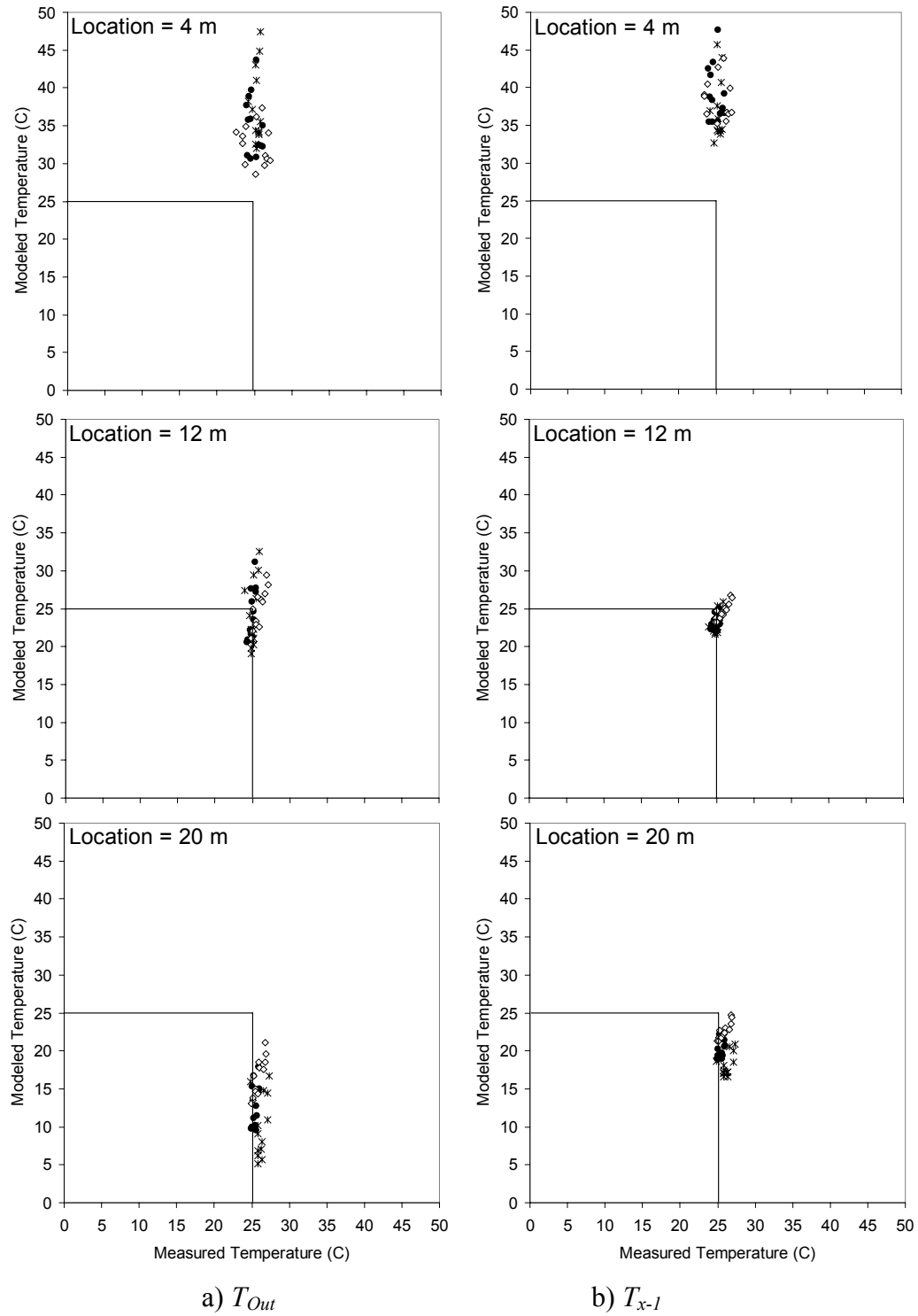


Figure 5.51 Modeled versus measured inside air temperatures with high-pressure-fog at 4 m, 12 m, and 20 m locations using a) T_{Out} and b) T_{x-1} in the energy balance equation for ventilation rates of $3.0 \text{ m}^3 \text{ s}^{-1}$ (*), $4.5 \text{ m}^3 \text{ s}^{-1}$ (●), and $9.4 \text{ m}^3 \text{ s}^{-1}$ (○).

Table 5.23 Comparison of measured and modeled mean air temperatures for the time period 11:00 – 17:00 at each plant zone location for a given ventilation rate using the energy balance with both the outside air temperature (T_{Out}) and the previous measured air temperature (T_{x-1}) in Equation 4.25. Letters represent values that are significantly different ($p < 0.01$) for a given location based on Tukey-Kramer HSD.

Location	\dot{Q} ($\text{m}^3 \text{ s}^{-1}$)	$T_{Air, Measured}$		$T_{Air, Model}, T_{Out}$		$T_{Air, Model}, T_{x-1}$	
		Mean ($^{\circ}\text{C}$)	S.D.	Mean ($^{\circ}\text{C}$)	S.D.	Mean ($^{\circ}\text{C}$)	S.D.
4 m	3.0	25.3 ^a	± 0.5	37.6 ^b	± 5.0	37.1 ^{b,d}	± 4.1
	4.5	25.0 ^a	± 0.8	35.1 ^{b,d}	± 4.0	39.1 ^d	± 3.7
	9.4	25.2 ^a	± 1.6	32.6 ^b	± 2.7	38.5 ^{b,d}	± 2.7
12 m	3.0	25.1 ^{a,b}	± 0.5	24.3 ^{a,b}	± 4.4	23.0 ^b	± 1.4
	4.5	24.9 ^{a,b}	± 0.4	24.2 ^{a,b}	± 3.4	23.3 ^{a,b}	± 0.9
	9.4	25.8 ^a	± 0.8	24.8 ^{a,b}	± 2.6	24.6 ^{a,b}	± 1.1
20 m	3.0	26.2 ^a	± 0.7	10.1 ^f	± 4.1	18.2 ^{c,d}	± 1.5
	4.5	25.5 ^a	± 0.4	12.6 ^c	± 2.9	20.0 ^c	± 1.0
	9.4	25.9 ^a	± 0.7	16.5 ^d	± 2.6	22.6 ^b	± 1.1

Both models over-estimated the air temperature at 4 m and under-estimated the air temperature at 20 m location for all three ventilation rates tested. Also, both models predicted that air temperature at 4 m would decrease with increasing ventilation rate, and would increase with increasing ventilation rate at 20 m. However, these trends were not observed for the measurements taken.

The over-estimation at 4 m corresponds to the combination of low fog input rate prior to that location (21% of total) and the assumption that solar energy gain was constant from location to location. In reality, the solar energy gain from the inlet to 4 m would most likely be lower than that between 4 m and 12 m, both due to the difference in distance and greater shading near the inlet due to the opaque pad and overhead heaters.

The under-estimation of air temperatures at the 20 m location is significant because it demonstrates that the assumption of 100% evaporation of fog was incorrect for these tests. Furthermore, air temperatures predicted by the T_{Out} model were significantly

lower than those for the T_{x-1} model because it assumed that all the water introduced into the greenhouse was evaporated at that sensor point (20 m). Although the T_{x-1} model also assumed that all water evaporated at that point, it also took into account the greenhouse air conditions prior to that location. Therefore, due to the lower air temperatures and higher humidity levels at 12 m relative to the outside conditions, the T_{x-1} model predicted more modest temperature reductions due to lower evaporation capacity of the inside air.

Finally, the energy balance model used for these analyses assumed steady-state conditions. However, the high-pressure-fog system is highly dynamic, with rapidly changing greenhouse environmental conditions as fog is injected, evaporated, and exhausted through the fans. Therefore, using a dynamic, time-dependent model would potentially have improved model accuracy.

5.7 Using a Wind Tunnel to Test the Effects of Buoyancy and Wind Direction on Airflow and Temperature Distribution in a Naturally-Ventilated Greenhouse

5.7.1 Air Movement in the Wind Tunnel Model

5.7.1.1 Wind Direction

Wind direction had a significant effect on the air movement inside the greenhouse model. The 90° wind direction produced a circular airflow pattern (Figure 5.52). Air entered through the roof and vertically traveled down the leeward sidewall ($V = -0.232$). The air then move in the x-direction across the floor and opposite to the outside wind direction ($U = -0.141$), before turning upward along the windward wall ($V = 0.200$) (Table 5.24). The strong horizontal airflow inside the model most likely impeded the entrance of air through the windward wall.

The 270° wind direction had a more horizontal airflow pattern as air entering the windward wall dominated air movement in the model (Figure 5.52). Air entered the model through the sidewall ($U = 0.158$) and moved across the model ($U = 0.152$) before reaching the leeward sidewall and rising ($V = 0.174$) to exit the roof. Before the air could enter the roof it had to turn 180 degrees, causing a reduction in momentum and speed and decreasing its effect on air movement inside the model.

5.7.1.2 Buoyancy (ΔT)

Buoyancy did not significantly affect air movement inside the greenhouse model. Therefore, even at the simulated low wind speed of 1 m s^{-1} , convection caused by wind dominated airflow in the wind tunnel experiments.

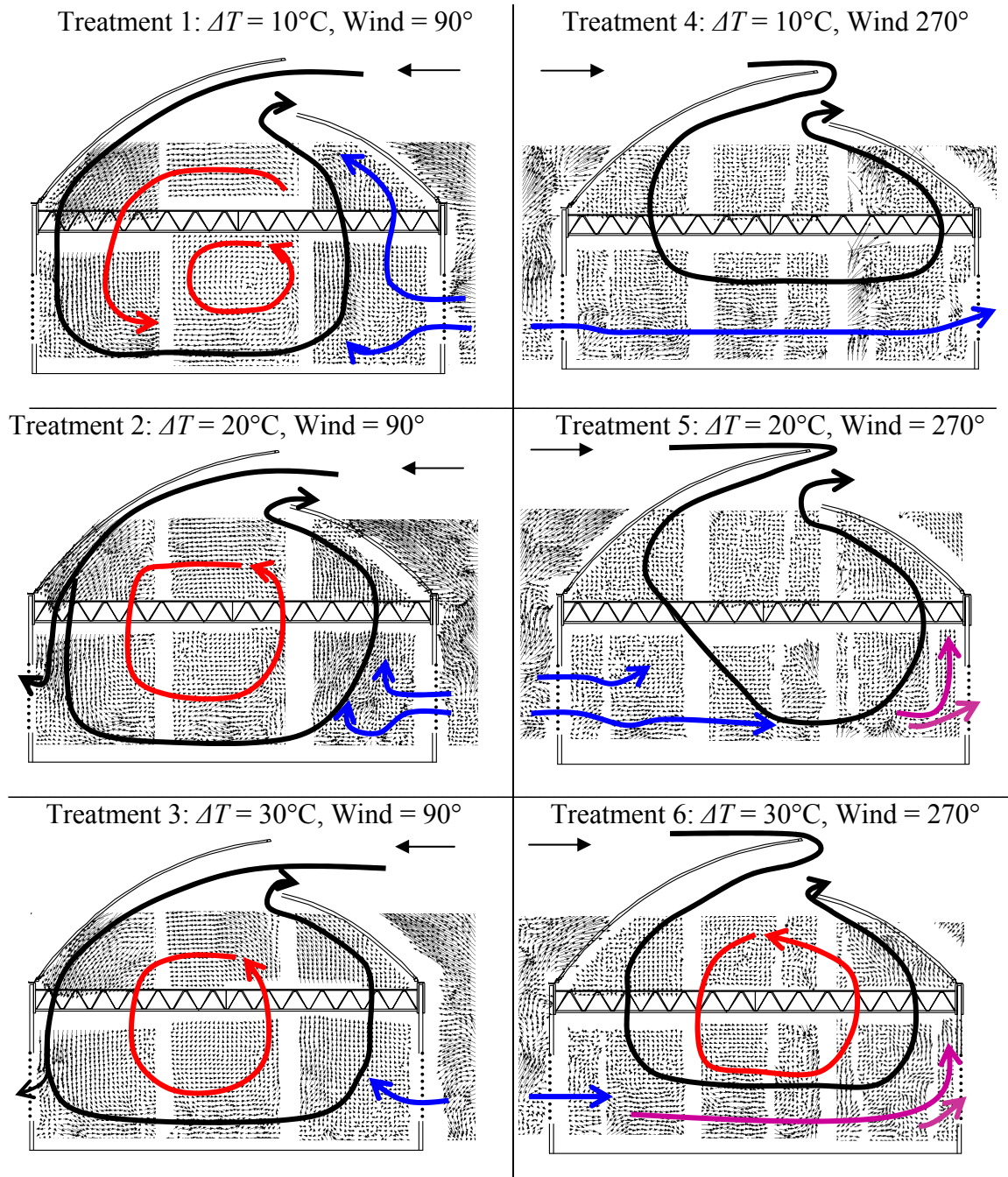
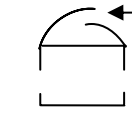
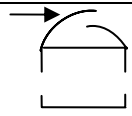


Figure 5.52 Velocity vector maps, produced by Particle Image Velocimetry (PIV), demonstrate the general airflow patterns observed in the wind tunnel greenhouse model.

Table 5.24 Values for dimensionless velocity in the x-direction, $U(x)$, and y-direction, $V(y)$, calculated from the particle image velocimetry (PIV) system during wind tunnel experiments.

		$U(x)$			$V(y)$		
Treatment		Windward	Center	Leeward	Windward	Center	Leeward
 90°	T=10°C	-0.025	-0.141	-0.116	0.196	0.006	-0.253
	$\Delta T=20^\circ\text{C}$	-0.161	-0.197	-0.046	0.292	0.099	-0.288
	$\Delta T=30^\circ\text{C}$	0.005	-0.085	-0.039	0.113	0.035	-0.156
	Mean	-0.063	-0.141	-0.067	0.200	0.047	-0.232
 180°	$\Delta T=10^\circ\text{C}$	0.195	0.203	0.083	-0.009	0.043	0.116
	$\Delta T=20^\circ\text{C}$	0.199	0.109	0.123	-0.008	-0.007	0.318
	$\Delta T=30^\circ\text{C}$	0.079	0.145	0.055	0.047	0.062	0.089
	Mean	0.158	0.152	0.087	0.010	0.033	0.174

5.7.2 Temperature Distribution in the Wind Tunnel Model

5.7.2.1 Wind Direction

Wind direction affected the air temperature distribution inside the greenhouse model. In general, the temperature nearest the side vents had the lowest mean θ_T (Table 5.25). For the 90° wind direction, the air moving along the leeward side of the model and the fresh air entering the windward vent caused the mean θ_T at the leeward and windward sides to be nearly the same. However, for the 270° wind direction, most of the fresh air entered the model through the windward side vent, causing the θ_T at the windward side of the model to be significantly lower than the leeward side. The mean θ_T at the center of the model was always high, most likely due to the low air movement observed there.

In general, the mean θ_T measured nearest the floor of the model was lower than those measured at other heights. This result probably occurred because fresh air entering the windward wall dropped toward the floor, filling the space created by the hot air

rising. However, the 90° wind direction produced a more vertically uniform temperature distribution, with no significant difference in mean θ_T between heights tested. The mean θ_T near the floor for the 270° wind direction was significantly lower than those measured in the center of the model due to the large influx of air through the windward side vent.

5.7.2.2 Buoyancy (ΔT)

The value of ΔT did not significantly affect temperature distribution in the wind tunnel model. Although the mean of θ_T was larger for $\Delta T = 30^\circ\text{C}$ and 270° wind direction, there was no significant difference in the vertical temperature distribution between those ΔT tested.

Table 5.25 Values for θ_T calculated from temperatures measured at various locations inside the greenhouse model during the tested wind tunnel treatments. $\theta_T = (T_{in} - T_{tunnel}) / (T_{pad} - T_{tunnel})$

Treatment	θ_T for Side-to-Side Location			θ_T for Measurement Height (cm)					Mean θ_T
	Windward	Center	Leeward	4.5	10.5	18.5	23.5	37.5	
1	0.228 ^{a,b}	0.296 ^c	0.238 ^b	0.215 ^d	0.254	0.268	0.266	0.256	0.254
2	0.236 ^{a,b}	0.294 ^c	0.236 ^b	0.219 ^d	0.257	0.265	0.265	0.255	0.255
3	0.238 ^{a,b}	0.290 ^c	0.229 ^b	0.225 ^d	0.250	0.260	0.260	0.249	0.252
4	0.229 ^a	0.264 ^c	0.261 ^c	0.203 ^d	0.254	0.290	0.280	0.254	0.251
5	0.223 ^a	0.259 ^c	0.258 ^c	0.201 ^d	0.245	0.286	0.274	0.245	0.246
6	0.238 ^a	0.282 ^c	0.283 ^c	0.217 ^d	0.275	0.304	0.300	0.270	0.268

5.7.3 Full-Scale Greenhouse Validation Study

Figure 5.53 shows the airflow patterns, including wind speed and direction, at the nine measurement locations for all four treatments: i) no plants, no fog; ii) no plants, with fog; iii) with plants, no fog; and iv) with plants, with fog. Outside air temperature and IR temperature measurements of the greenhouse floor measured at 11:00 on July 31, 2005,

produced a ΔT of only 2°C ($T_{\text{Floor},F} = 30^{\circ}\text{C}$, $T_{\text{Out}} = 32^{\circ}\text{C}$). None of the wind tunnel treatments closely resembled the full-scale measurements of ΔT . Therefore, the wind tunnel treatment using the smallest ΔT ($\Delta T = 10^{\circ}\text{C}$) was used for comparison with the full-scale experiments. Furthermore, the full-scale Treatment of no plants, no fog (i) was most similar to the wind tunnel experiments conducted. Also, the wind direction of 81° for Treatment i (full-scale) (Figure 5.53i) closely resembled the wind conditions tested in Treatment 1 of the wind tunnel experiment (Figure 5.52).

5.7.3.1 No Plants, No Fog

The airflow pattern of the full-scale Treatment with no plants, no fog (i) strongly validated the results found in the wind tunnel experiments. A strong circular pattern was found in both experiments and was dominated by the momentum of air entering the greenhouse through the roof opening. As the air approached the east sidewall (right-hand side), the air both decreased greatly in speed and turned in an upward direction. According to the results of the wind tunnel experiments, the decreased airspeed and changed direction was caused by a combination of reduced momentum and the entrance of air through the screen moving in opposite direction to the internal airflow. Furthermore, the full-scale experiment also showed weak air movement in the center of the greenhouse near the gutter (3 m height) as the model predicted.

These results provide indication for where fog should be injected into the greenhouse. To maximize evaporation, the fog should be delivered to locations with the greatest evaporative potential, which are along the west sidewall where outside air travels quickly into the greenhouse, as well as along the east sidewall due to the additional influx

of outside air. Furthermore, fog injected at the center of the greenhouse at gutter height would evaporate most poorly due to the slow air movement and circulating pattern of mostly inside air observed there.

5.7.3.2 With Fog and With Plants

Using the high-pressure-fog system concurrently with natural ventilation caused the air to initially move in the same pattern as without plants by traveling down the west sidewall (Figure 5.53ii). However, air movement was stifled when it reached the floor, likely due to fog settling and restricting horizontal air movement. Similar to the experiment without fog, the air tended to travel from west to east in the greenhouse. With the added momentum of the fog, this eastward movement of inside air was enhanced to restrict airflow entering the greenhouse through the sidewall. A film of water may have also developed on the screen from the fog, further restricting air from entering through the sidewall. Finally, during this test, the outside wind direction was less perpendicular to the screen wall, thereby limiting the force of outside air on the screen and limiting its entry.

The addition of plants in the greenhouse greatly restricted internal air movement. Without fog (Figure 5.53iii) the air entering the greenhouse still traveled down the west sidewall with great momentum. However, very little horizontal movement was observed through the plants and across the greenhouse. Operating the high-pressure-fog system under natural ventilation, when plants were present, most significantly restricted the circular airflow pattern, even when the outside wind speeds were high, creating favorable conditions for producing a strong internal airflow.

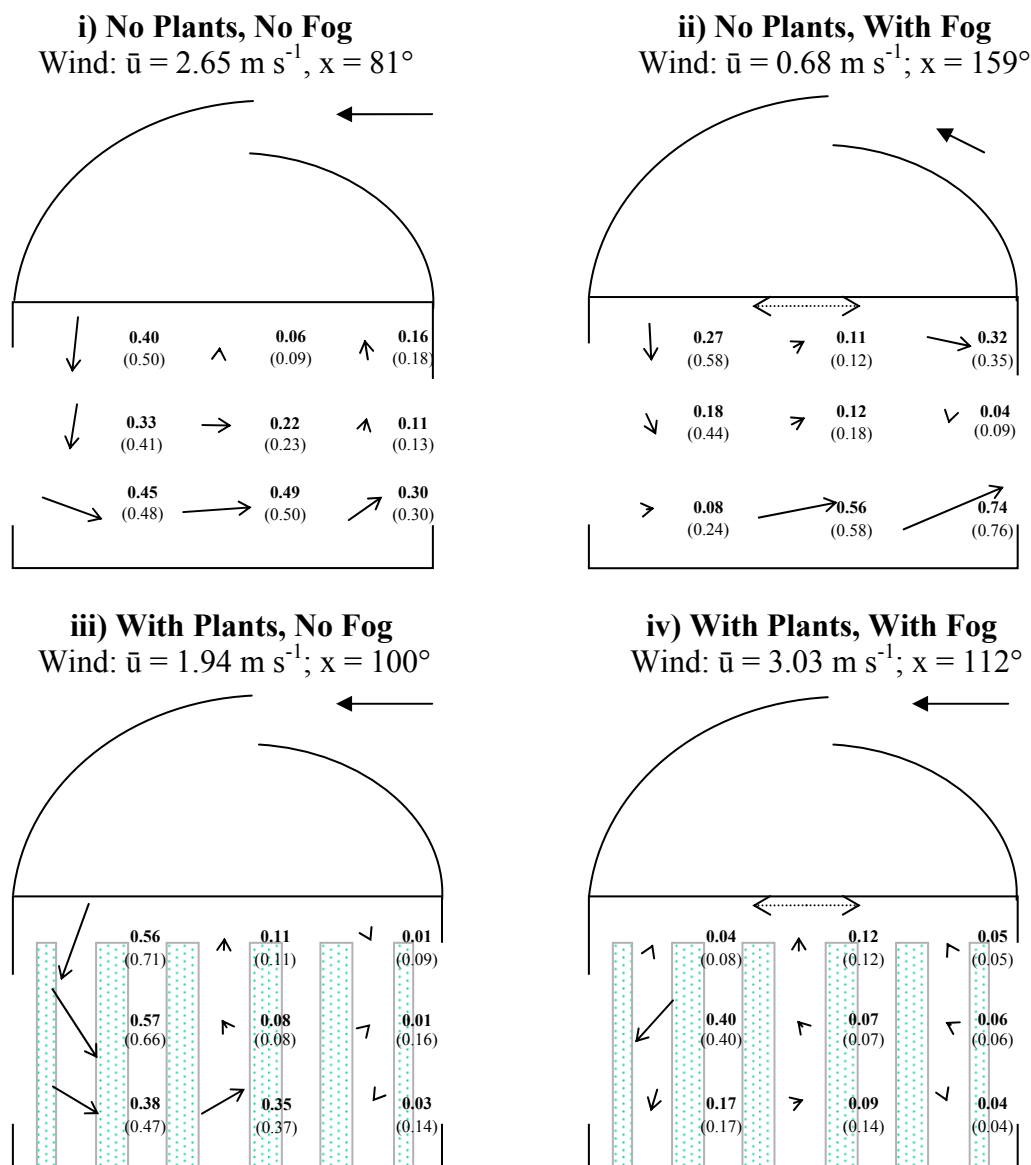


Figure 5.53 Air velocity and direction within the airflow experiments in the full-scale greenhouse for four treatments: i) no plants, no fog; ii) no plants, with fog; iii) with plants, no fog; and iv) with plants, with fog. Bold numbers represent the measured air West-East vertical plane velocity (m s^{-1}), and numbers in parentheses represent three-dimensional air velocity (m s^{-1}). Wind direction measured in a clockwise rotation (azimuth degree angle, $^\circ$).

6. DISCUSSION

6.1 Greenhouse Water Use and Water Use Efficiency

6.1.1 Pad-and-Fan Cooling

Increasing the ventilation rate reduced the cooling efficiency of the pad-and-fan system. This inverse relationship between ventilation rate and cooling efficiency has been observed by other researchers (Liao and Chui, 2002) and were caused by the lower rate of water uptake by the air as it passed through the pad, as measured by smaller increases in humidity ratio levels at the pad's exit. For an evaporative cooling system to be 100% efficient, the air must become saturated and reach the wet bulb temperature. Therefore, at high air speeds, the shorter contact time with the wet pad would be expected to decrease moisture gain and effectively reduce the air temperature reduction and the cooling efficiency.

Although each parcel of air contained more moisture at lower ventilation rates, higher ventilation rates used more water overall as greater volumes of dry air passed across the wet pad at higher speeds. The preliminary pad-and-fan experiments also demonstrated linear increases in water use with increasing ventilation rate up to the maximum ventilation rate tested of $0.079 \text{ m}^3 \text{ m}^{-2} \text{ s}^{-1}$. Water use efficiency of the pad-and-fan system (WU_{PF}) averaged during the daily 9-hour period were comparable to values found within other studies for similar ventilation rates (Al Helal, 2007). Finally, the WU_{PF} rates were more than ten times less than those found in a model-scale study of a pad-and-fan system using psychrometric equations to calculate water use (Al Massoum *et*

al., 1998). Part of the discrepancy may be explained by the use of psychrometrics to estimate WU_{PF} , which was shown in this study to overestimate water use. Also, the model-scale study would be more prone to edge effects due to its small size.

Strong correlations were found between outside environmental conditions and WU_{PF} , reflecting how regional and seasonal climate can directly affect the performance of the pad-and-fan system. As air temperature increased and relative humidity decreased, either during the day or from Spring to Summer in the 6-month crop period, the evaporation potential (VPD) of the outside air increased, resulting in greater WU_{PF} .

Overall greenhouse water use, which was composed of water from irrigation and evaporative cooling, was dominated by the pad-and-fan cooling system, especially when the 100% closed irrigation system was considered. For the ventilation tests, total greenhouse water use efficiency (WUE_S) was higher at lower ventilation rates. WUE_S values ranged from 10-26 kg m⁻³, which were comparable to field WUE values for flood (10-12 kg m⁻³) and drip (19-25 kg m⁻³) irrigation (Hanson *et al.*, 2006; Hanson and May, 2005; Hanson and May, 2004). Using a 100% recirculating irrigation system always improved WUE , and at the lowest ventilation rate (4.5 m³ s⁻¹) produced WUE values (26 kg m⁻³) greater than the best reported drip-irrigated values (19-25 kg m⁻³) (Hanson *et al.*, 2006; Hanson and May, 2005; Hanson and May, 2004). For the 6-month tomato crop study, the WUE depended on the time of year (outside environmental conditions) and ranged from 10-17 kg m⁻³, which are comparable to flood (10-12 kg m⁻³) and high-range sprinkler (11-19 kg m⁻³) WUE values. The highest WUE was obtained during May when yields were high and cooling demand was still relatively low.

6.1.2 High-Pressure-Fog Cooling

Ventilation rates with the high-pressure-fog system affected its ability to cool greenhouse air temperatures to the control setpoint. When the high-pressure-fog system was coupled to the ventilation systems via setpoint temperature control strategy, water use did not increase linearly with ventilation rate, but was lowest at the middle ventilation rate tested of $4.5 \text{ m}^3 \text{ s}^{-1}$. High ventilation rates caused too much air exchange for adequate evaporative cooling and water use rates increased. At low ventilation rates, the high moisture levels in the air inhibited the evaporation of water and reductions in air temperature, ultimately causing the high-pressure-fog system to provide more water. Furthermore, higher fog injection rates increased the relative humidity overall, but overall humidification was reduced by increasing the ventilation rate. These results demonstrate the potential for using ventilation to control greenhouse humidity levels, as has been tested by Sase *et al.* (2006).

Ventilation rate and outside environmental conditions both contributed to the operating procedures of the high-pressure-fog system, resulting in different fog injection requirements. Fog requirements increased as more outside air was introduced into the greenhouse, supporting the findings of other studies (Sase *et al.*, 2006). Fog requirements were also high for the lowest ventilation rate because of limited air exchange, which also increased the inside air's absolute humidity. This effect ultimately inhibited evaporation, raised greenhouse air temperature, and triggered a false need for more fog.

Outside conditions also affected the operation of the high-pressure-fog system. Fogging requirements increased as the outside temperature increased and relative

humidity decreased. Although these conditions would improve the evaporation potential of the air, they also increased the fogging required to cool those outside temperatures to the setpoint air temperature in the greenhouse. Therefore, the On-time portion of the cycle was maximized by 12:00 noon at the highest ventilation rate, but the lower air exchange rates at 3.0 and $4.5 \text{ m}^3 \text{ s}^{-1}$ reduced the cooling load on the high-pressure-fog system, and did not maximize operation until after 14:00.

Water use was directly related to the operating frequency of the high-pressure-fog system, which differed based on ventilation rate, outside conditions, and its overall ability to meet and maintain setpoint air temperature (T_{Set}). The lower water use at a ventilation rate of $4.5 \text{ m}^3 \text{ s}^{-1}$ demonstrated that the high-pressure-fog system controlled setpoint air temperature more easily than the lowest ventilation rate ($3.0 \text{ m}^3 \text{ s}^{-1}$), which caused the air to approach saturation, or the highest ventilation rate tested ($9.4 \text{ m}^3 \text{ s}^{-1}$), which discharged fog droplets from the greenhouse before they could evaporate. If the high-pressure-fog system was not operated to control T_{Set} and continuous fogging had been employed, nearly twice the amount of fog water would have been used. Furthermore, if the ventilation rate had been controlled in conjunction with controlled fogging rates, excessive and erroneous uses of fog could have been avoided.

For the high-pressure-fog system, increasing the ventilation rate from $3.0 \text{ m}^3 \text{ s}^{-1}$ would have helped evaporate the extra fog delivered to the greenhouse. Decreasing the ventilation rate from $9.4 \text{ m}^3 \text{ s}^{-1}$ would have reduced the cooling load and allowed the evaporatively cooled air to remain within the greenhouse with sufficient time to benefit the plants. At $4.5 \text{ m}^3 \text{ s}^{-1}$, however, the plant zone air temperature only exceeded the

setpoint temperature by 0.5°C at its peak, suggesting that adequate evaporative cooling was maintained when the mean plant zone relative humidity was 65%.

The water use efficiency for high-pressure-fog cooling alone was 19-24 kg m⁻³, with the lowest efficiency observed at a ventilation rate of 9.4 m³ s⁻¹. The *WUE* of the open irrigation was 40 kg m⁻³ for open irrigation. The total greenhouse water use efficiency (*WUE_S*), combining water use by high-pressure-fog and 100% closed irrigation systems, ranged from 11-13 kg m⁻³, which were similar to field sprinkler irrigation (11-19 kg m⁻³) (Hanson *et al.*, 2006; Hanson and May, 2005; Hanson and May, 2004).

6.2 Greenhouse Environment

6.2.1 Pad-and-Fan Cooling

Unlike relative humidity, which continuously declined with increasing ventilation rate, reductions in air temperature greatly diminished above ventilation rates of 9.4 m³ s⁻¹ (0.035 m³ m⁻² s⁻¹). The healthy plants in this experiment were able to match the solar demand and reduce the need for high inputs of water vapor (greater than 0.194 g m⁻² s⁻¹) into the greenhouse air provided by ventilation rates greater than 0.035 m³ m⁻² s⁻¹. These results agree with previous studies that found no improvement in air temperature and humidity conditions in a greenhouse with freely transpiring plants when ventilation rates exceeded 0.035 m³ m⁻² s⁻¹ (Critten and Bailey, 2002; Landsberg *et al.*, 1979). Finally, these results are of particular interest because manufacturers typically recommend an airflow rate through the pad of 1.27 m s⁻¹, which is equivalent to the ventilation rate of 13.0 m³ s⁻¹ (0.046 m³ m⁻² s⁻¹) tested for this greenhouse.

Air temperature and relative humidity both increased from pad-to-fan regardless of ventilation rate. Increasing the ventilation rate did reduce the air temperature rise from the pad to fan from 8.6°C at 4.5 m³ s⁻¹ to 4.0°C at 16.7 m³ s⁻¹, as the faster-moving air likely gained less sensible heat. The temperature gradient of 5°C observed at 9.4 m³ s⁻¹ (0.033 m³ m⁻² s⁻¹) compare best to a study with roses that found a 5°C increase over a 30 m distance at a ventilation rate of 0.027 m³ m⁻² s⁻¹ (Kittas *et al.*, 2001). Other studies with tomato plants have not tested pad-and-fan systems in climates that have daytime absolute humidity levels less than 9 g kg⁻¹, possibly explaining why their results did not compare well to the results of this project.

Unfortunately, the smaller temperature gradients with higher ventilation rates were accompanied by mean relative humidity levels that were less than 60%. This reduction in relative humidity with increased ventilation rate occurred due to less moisture gain at the pad and less moisture gain through the plant zone. Such low relative humidity levels are not desired for good tomato plant growth and productivity.

VPD also increased from pad-to-fan. However, the humidity ratio increased as the air traveled across the plants and gained plant-transpired water vapor. Therefore, the rise in *VPD* occurred as a result of the increased temperature from pad-to-fan, not a reduction in water content, demonstrating the plants continued to provide water to the air. Kittas *et al.* (2003) also observed an increase in *VPD* from pad-to-fan resulting from increasing air temperature.

At 4.5 m³ s⁻¹, the moisture content of the air at 4 m from the pad was greater than at the pad. At the other ventilation rates, only a rise in air temperature, with no increase

in humidity ratio, was observed from the pad to 4 m, indicating sensible heat gain only across the empty space between pad and plants. It is possible that at the lowest ventilation rate the air speed across the canopy was so low that a thick boundary layer developed over the top of the plant canopy and around the sensors located at the 4 m distance from the pad. Because a thicker boundary layer would limit mixing of air close to the plant tops, water vapor from transpiration could have accumulated in the air around the sensors, resulting in relatively high measurements of absolute humidity.

Likewise, the absolute humidity at the 20 m location was unexpectedly lower than at the other plant zone locations for $4.5 \text{ m}^3 \text{ s}^{-1}$. At all other ventilation rates, the absolute humidity increased as the air gained moisture from evapotranspiration. Because the 20 m location is along the edge of the plant zone closest to the fans, less resistance to airflow, and therefore more mixing, would be expected at the location nearest the pad. If the boundary layer thickness was less at the 20 m location than the 4 m location, then the sensors at 20 m may have measured conditions *outside* the boundary layer.

If this hypothesis is true, then the same result would be expected for air temperature (or heat gain) measurements. However, there was still an increase in air temperature across the plant zone at the lowest ventilation rate. Nevertheless, it is interesting to note that at $4.5 \text{ m}^3 \text{ s}^{-1}$ the temperature increase across the plant zone was *smallest* and from pad to 4 m it was *highest*.

For these experiments, the sensors were placed just above the canopy at the same height to measure the environmental conditions directly experienced by the plants. This location is typically considered superior to eye-level height or other heights too far below

(or above) where the plants develop and grow (apical meristem). However, it is possible that the differences in boundary layer thickness caused inconsistent measurements and erroneous comparisons between conditions that were inside and outside the boundary layer. Additionally, the boundary resistance to airflow created by the plants would be greater at lower airspeeds, possibly trapping incoming air within the space between pad and plants and increasing sensible heat gain. For these experiments, the ventilation rate of $4.5 \text{ m}^3 \text{ s}^{-1}$ produced the most unexpected results in greenhouse environmental conditions, likely due to differences in internal air profiles.

6.2.2 High-Pressure-Fog Cooling

6.2.2.1 Fog Nozzle Location

Location of the fog nozzles within the greenhouse during mechanical ventilation had a great effect on the greenhouse climate. Injecting all fog water near the inlet produced very saturated conditions around the plants closest to the inlet, with a gradient in moisture conditions from inlet to fans. The central, overhead line with *VPD*-control produced uniform greenhouse conditions. Addition of an inlet fog line to the central, overhead line did not necessarily improve greenhouse uniformity; however, very low *VPD* levels were produced most everywhere within the greenhouse (less than 0.5 kPa). Therefore, the inlet vent fog line was an unnecessary addition to the central, overhead line for producing the desired environmental conditions for tomato plants. Using fog lines at the side gutters produced the most uniform greenhouse conditions. However, due to the large number of nozzles, the *VPD* levels were near 0.0 kPa. If the number of

nozzles were reduced in the side gutter fog lines, more desirable levels of *VPD* would be expected. Furthermore, their placement would be advantageous for use with the natural ventilation airflow patterns produced in this greenhouse.

6.2.2.2 Ventilation Tests with Central, Overhead Line

During ventilation tests with the central, overhead fog line, the fog system maintained a mean daytime plant zone air temperature within a range of 24-26°C. The highest ventilation rate (9.4 m³ s⁻¹) had the most difficulty maintaining desired greenhouse conditions (T_{set} =25°C, RH = 70%) and the air temperature continued to increase above 26°C in the afternoon even as fogging frequency increased. The relative humidity in the greenhouse decreased and *VPD* increased with increasing ventilation rate regardless of fogging rate. Increasing the fogging rate did increase relative humidity, but RH was always higher at lower ventilation rates. Air exchange was the most important mechanism affecting air moisture conditions in the greenhouse, agreeing with the work by Sase *et al.* (2006), who modified ventilation rates to control relative humidity.

Fluctuations in greenhouse air conditions were greatest in the morning, when On- and Off-times of the high-pressure-fog system frequently varied, especially compared to the afternoon when On-times were maximized and Off-times were minimized. The temperature reduction and relative humidity increase observed at the inlet after 14:00 for 3.0 m³ s⁻¹ occurred after the internal shade curtain was removed, indicating that evaporative cooling increased as a direct result of increased energy input from solar radiation. When radiation heat transfer was low during shade (less than 300 W m⁻²), the low ventilation rates were insufficient to evaporate all the fog water, allowing

unevaporated fog water to accumulate in the region between the inlet and plants during shading. When shade was removed and solar energy levels increased (greater than 700 W m^{-2}), this water evaporated, decreasing the temperature and raising the relative humidity.

A similar rise in relative humidity was observed at the 4 m location with $9.4 \text{ m}^3 \text{ s}^{-1}$. This may have occurred due to free water accumulating on plants and surfaces when high quantities of fog water were delivered during shading. This surface water was then evaporated from plants and surfaces nearest the inlet of fresh air, causing an increase in relative humidity and a reduction in air temperature. An overall increase in air temperature was observed at the other greenhouse locations after the shade was removed, with no change in relative humidity. This result suggests evaporative cooling was offset by the heat gain of solar radiation.

The greatest variability in moist air properties occurred at the vent inlet where the majority of latent heat transfer occurred. Air temperatures were very uniform within the plant zone, and confirmed the results of previous studies that used mechanical ventilation in conjunction with high-pressure-fogging (Arbel *et al.*, 2003; Giacomelli *et al.*, 1985). The lowest inlet air temperature and highest inlet relative humidity occurred at $3.0 \text{ m}^3 \text{ s}^{-1}$ as a result of low air velocities through the vent, which allowed fog to evaporate and remain near the inlet for a longer duration, rather than being carried away downstream. This effect reduced the air temperature 7°C and increased the relative humidity by 30% relative to outside conditions, and thus provided better air conditions for plants closest to the inlet. At the highest ventilation rate, fog droplets injected near the 4 and 12 m

locations may have been combined, pulled toward the fans, and then evaporated closer to the 20 m sensor, producing the lower VPD levels observed there.

6.3 Plant Responses

6.3.1 Pad-and-Fan Cooling

Plant transpiration was erroneously determined to be higher in the morning, as a result of the measurement technique, which was an indirect measure of transpiration. Much water thought to have been utilized by the plant was used to hydrate the rockwool media after the previous night period with no irrigation (12 hours). The 6-hour period (11:00 – 17:00) of plant transpiration (E_T) data produced a linear relationship with Rad_{in} , though it remained relatively weak ($r = 0.54$). E_T was found to have a negative correlation with humidity ratio ($r = 0.65$), but poor correlations to relative humidity and VPD ($r < 0.5$), disagreeing with previous studies (Kittas *et al.*, 2001; Boulard *et al.*, 2000; Jolliet and Bailey, 1992; Bakker, 1991). However, those studies looked at VPD levels ranging from 0 to 3 kPa, where the present study did not observe values greater than 1.5 kPa. As suggested by Seginer (1994), changes in E_T and WU_P may be averted when evaporative cooling provides a more humid climate and low stress conditions. Furthermore, measuring the actual water vapor content of the air may provide an even stronger relationship to E_T , and may be a valuable consideration for the development of future E_T models. Finally, the low airspeeds produced at $4.5 \text{ m}^3 \text{ s}^{-1}$ likely contributed to the significantly lower E_T values observed at that ventilation rate (Jolliet and Bailey, 1992).

A negative correlation ($r = 0.75$) was found between air temperature and E_T . Therefore, the high temperatures observed at the lowest ventilation rate (26°C) may have caused the tomato plants to transpire less. Previous studies have shown different varieties of tomato plants having the smallest internal resistance to transpiration at 23-25°C (Papadakis *et al.*, 1994). Therefore, it is possible that the tomato plants in this study increased their resistance at some temperature greater than 23°C, which was observed when the ventilation rate was $9.4 \text{ m}^3 \text{ s}^{-1}$.

Leaf temperature (T_{Leaf}) decreased with increasing ventilation rate. Two hours after the shade screen was removed (16:00) T_{Leaf} increased at all ventilation rates except the lowest. These increases in T_{Leaf} coincided with relatively stable T_{Air} measurements, suggesting that the plants themselves shaded the greenhouse structural components and ground by absorbing incoming solar radiation that entered at a lower sun angle. Plant self-shading explains why low *air* temperatures were observed concurrently with elevated T_{Leaf} at 16:00. Furthermore, this result occurred despite concurrently higher E_T levels, further substantiating the effect that increased solar absorption had on plant responses.

A negative relationship between VPD and E_T was found ($r \approx 0.7$) and no correlation was observed for VPD and T_{Leaf} ($r = 0.0$). An inverse relationship was also found between E_T and T_{Leaf} ($r = -0.67$), demonstrating that plants were able to self-cool by increasing their rate of transpiration. Correlations were also found between E_T and T_{Leaf} and the greenhouse air temperature and humidity ratio, which depended on the ventilation rates tested. The plants responded most to a ventilation rate of $4.5 \text{ m}^3 \text{ s}^{-1}$, which resulted in significantly lower E_T and significantly higher T_{Leaf} than at the other ventilation rates.

Finally, although more water was evaporated into the greenhouse at higher ventilation rates, neither climate conditions nor plant functions were necessarily improved. Above $9.4 \text{ m}^3 \text{ s}^{-1}$ there was no increase in transpiration rate or reduction in leaf temperature, demonstrating that those higher ventilation rates were unnecessary for this greenhouse and tomato crop.

6.3.2 High-Pressure-Fog Cooling

Plant transpiration (E_T) generally increased with increasing ventilation rate, though not necessarily with significant differences. A weak relationship between E_T and Rad_{In} was observed ($r^2 = 0.20$), although higher correlations were found between E_T and greenhouse air temperature ($r = -0.66$) and relative humidity ($r = -0.82$). Furthermore, E_T was highly correlated to ventilation rate, which produced a very large range of VPD levels in the greenhouse, from 0.6 kPa at $3.0 \text{ m}^3 \text{ s}^{-1}$ to nearly 1.5 kPa at $9.4 \text{ m}^3 \text{ s}^{-1}$. Therefore, it is likely that E_T responded most directly to the larger differences in VPD and relative humidity produced by the different ventilation rates rather than the smaller changes observed for a given ventilation rate (Prenger *et al.*, 2002; Katsoulas *et al.*, 2002; Urban and Langelez, 2002; Jolliet and Bailey, 1992; Jarvis, 1985). Furthermore, higher airspeeds across the plants likely occurred with increased ventilation rate, further contributing to the overall increase in E_T and plant water uptake with increasing ventilation rate (Jolliet and Bailey, 2002).

Leaf temperatures (T_{Leaf}) were highest at the lowest ventilation rate, possibly due to lower transpiration rates (Seginer, 2002; Kacira *et al.*, 2002), though a strong correlation between T_{Leaf} and E_T was not observed ($r = -0.43$). The difference between

T_{Leaf} and T_{Air} was greatest during shading, though both increased from 12:00 to 14:00.

During shading T_{Leaf} also decreased with increasing distance from the inlet, though this trend was not observed without shading.

Overall, low correlations were found between greenhouse air conditions and T_{Leaf} . It is possible that low values of T_{Leaf} during shading occurred due to the wetting of leaves by an accumulation of unevaporated fog, which would be expected during shading, when solar radiation was low, and further from the inlet, where higher moisture levels were observed. Latent heat transfer on the leaf surface, would have subsequently reduced leaf temperature without corresponding reductions in T_{Air} .

Finally, lower T_{Leaf} values were observed under higher VPD conditions, although they were weakly correlated ($r = -0.43$). However, other studies have found strong relationship between T_{Leaf} and VPD , though typically under larger variations in VPD (Kittas *et al.*, 2001).

6.4 Greenhouse Modeling Studies

6.4.1 Energy Balance Model

The energy balance model was used to calculate the predicted water requirements to achieve the observed greenhouse climate conditions. Predictions of pad-and-fan water use by the energy balance were greater than those measured because higher water-flow rates were observed on the pad where the sensors were located. To improve water use predictions by the pad-and-fan system, water flow across the pad should be uniform.

These results also indicate that higher water flow rates across the pad would increase pad-and-fan water use under semi-arid conditions. However, the pad-and-fan ventilation studies produced marginal reductions in air temperature with increasing ventilation rate and water use. Therefore, it is uncertain if increasing the flow rate, and thus increasing water use, for a given ventilation rate would produce significantly cooler and more humid greenhouse air conditions.

Using the energy balance model to estimate water use by the high-pressure-fog system demonstrated that more fog water was delivered to the greenhouse than was actually needed to produce the given greenhouse conditions for outside environmental conditions at a given time. The excess fog water not evaporated in the air would have either landed on surfaces or been ejected from the greenhouse by the fans, which would represent “wasted” water not used for evaporative cooling. Although all of the fog water landing on surfaces within the greenhouse would have been expected to evaporate at some time in the future, there is loss of control when fog does not evaporate in the air,

not only from the reduced ability to control the greenhouse conditions, but also from an increased risk for pathogenic. Certainly, evaporation within the air itself is cited as the primary advantage of the high-pressure-fog system relative to its low-pressure-misting counterpart. Therefore, the model extends the argument for improving the design and control of the high-pressure-fog system to eliminate surface wetting and the ejection of fog through vents, to both conserve water *and* improve growing conditions.

The energy balance model predicted air temperatures that were close to those values measured, especially when using known inside air temperatures, rather than the outside air temperature, to calculate T_{Air} at other locations. However, this modeling study demonstrated that knowing the condition at one location (such as the center of plant zone, 12 m) would allow the grower to estimate the conditions in the greenhouse at locations other than the one measured. For the pad-and-fan system, very good estimates would be expected for locations both downstream and upstream from the measurement location.

For the high-pressure-fog system, using the T_{x-l} model for the high-pressure-fog system was better than the T_{Out} model for predicting inside air temperatures because it took into account the lower evaporation potential of the inside air relative to the outside. However, it still assumed that 100% of the fog injected upstream from the sensor location evaporated exactly at that point within the greenhouse, and didn't account for water evaporating upstream or landing on surfaces. Therefore, the air temperature model could be improved by using the quantity of water expected to evaporate upstream from that location to calculate the expected temperature reduction due to the modified evaporation potential of the air. Better measurements of R_n using a net radiometer that is sensitive to

larger radiation bandwidths would further improve the results of the model. There is a need to develop a more accurate model for the fog system to be used for design and operation of the high-pressure-fog system.

The energy balance models used for this study reveal the inaccuracies of the model and, therefore, offer opportunities for improvement. Modeling inaccuracies include, but are not limited to, measurement error, steady-state assumptions, and the use of average greenhouse conditions to produce instantaneous values.

For the pad-and-fan system, water use predicted by the energy balance model (*Equation 4.26*) was very close to the measured value. The slight over-estimation resulted from the inlet sensors being located in a less than optimum position adjacent to the pad.

For the high-pressure-fog system, the greatest source of error came from the assumption that all fog evaporated instantaneously. This assumption caused a tendency for water use to be under-predicted by both models, demonstrating that not all the water introduced by the fog system was evaporated, or was even needed to produce the measured results. Therefore, the difference in model and measured water use provided a crude estimation of how much water could have been saved had all the fog been evaporated with a 100% instantaneous cooling efficiency.

6.4.2 Wind Tunnel Model

Understanding airflow patterns and temperature distribution inside naturally ventilated greenhouses can improve the design of the structure and aid in the placement and control of a high-pressure-fog system. As the wind tunnel experiments demonstrated,

natural ventilation can produce robust and predictable airflow patterns, which can be used in conjunction with high-pressure-fog cooling. When the roof was opened, it channeled outside air entering the greenhouse toward the gutter and into a circular pattern.

Furthermore, the limited effect of ΔT (buoyancy) on air movement and temperature distribution inside the greenhouse suggested that even at very low wind speeds ($\leq 1 \text{ m s}^{-1}$) forced convection (wind) can dominate natural convection (buoyancy) in a single-span, arched-roof greenhouse. Therefore, injecting fog water at the location where the majority of outside air will enter the greenhouse, rather than near the plant canopy where the air is cooler and more humid, will increase the amount of water evaporated, produce cooler conditions, and reduce unevaporated water losses.

Airflow studies in the full-scale greenhouse demonstrated the challenge of using fog with natural ventilation to produce the desired greenhouse conditions when plants are present. Because both the plants and the fog affected the airflow patterns, they should not be ignored when designing the greenhouse. Designing a natural ventilation system that produces strong natural airflow patterns will help. Also, the location and configuration of the fog system should be designed to facilitate those airflow patterns. If these two systems are designed together and consider the influence of the plants, the greenhouse can be designed to provide the desired climate.

Finally, by knowing the airflow patterns produced by the ventilation system and the plants (without fog), the high-pressure-fog system can be designed to facilitate evaporation. For instance, a circular pattern with a strong downdraft along the west sidewall developed in all wind tunnel experiments and in the full-scale experiments when

fog wasn't used. Because the strong airflow of outside air will have greater evaporative potential than slow-moving inside air, a good design of the high-pressure-fog system may be to inject water up and into the path of incoming air from the roof. By doing so, more water would be evaporated in the air and less water would be wasted by landing on the plants and floor inside the greenhouse.

7. RECOMMENDATIONS

Water use and water use efficiency values of the evaporative cooling systems were specific to the greenhouse used for these experiments. The best overall greenhouse design for minimizing water use and losses will require additional studies that examine different greenhouse structures (size, covering material, etc.), crops, and variations on the evaporative cooling systems studied here, as well as completely innovative designs of those systems.

Overall, future designs for evaporative cooling system should avoid over-design of the ventilation system, which increased water use with diminishing benefit to the greenhouse conditions and plant responses. By designing the ventilation and evaporative cooling systems specifically for greenhouse type, location, and crop, resource utilization will be more efficient and greenhouse climate conditions more favorable to production.

Some of the variations that may be studied with the pad-and-fan system include pad thickness, material, and size. Increasing the pad thickness and size would increase the overall surface area of the pad and increase cooling potential of the system, but may use more water than is necessary. Several other studies have tested the use of alternative pad materials to corrugated cellulose, including date-fronds leaves and PVC sponges with mixed results. These materials and others may increase the life and improve performance, especially when used with hard water, salt water, or recycled (gray) water resources. It may also be possible to reduce mechanical ventilation requirements by placing pads above the crop and using natural convection properties to create airflow and deliver cool, humidified air to the plants, although this design would have maintenance challenges.

Fog nozzle placement greatly affected uniformity and the overall greenhouse climate conditions. The central, overhead fog line, as well as the side gutter fog lines, provided the most uniform conditions in the single-span greenhouse. Furthermore, as the wind tunnel and full-scale airflow tests demonstrated, the ventilation method, vent configuration, fog operation and the presence of plants will all affect the distribution of air and evaporation of fog. Therefore, additional studies considering all of those factors should be pursued to improve the design of the high-pressure-fog system, ventilation system, cropping system, and greenhouse structure for both mechanical and natural ventilation systems. Ultimately these systems should all be designed together to produce the most uniform greenhouse conditions while minimizing cooling water use.

With mechanical ventilation, future studies may want to examine a distribution of fog nozzles that reduces in number from inlet to exhaust. Furthermore, greater uniformity may be obtained by distributing the nozzles across the width of the greenhouse and pointing them against the flow of air, rather than using one line that runs along the midline of the greenhouse length. Finally, the distribution of fog nozzles should be designed to eliminate the ejection of fog droplets from the greenhouse before they are able to evaporate.

Additional studies on high-pressure-fog control should be performed to improve performance and minimize water use. The water use results and operating patterns of the high-pressure-fog system demonstrated that controlling the system solely based on setpoint temperature can produce undesirable operating procedures, such as delivering more fog when the air was near saturation and evaporative cooling was minimal.

Therefore, using vapor pressure deficit (or relative humidity) as a control parameter for the high-pressure-fog system should also be tested in conjunction with mechanical ventilation as it has begun to be tested with natural ventilation (Sase *et al.*, 2006). Further studies using natural ventilation with high-pressure-fog cooling should be pursued, as natural ventilation systems will reduce energy consumption, in addition to the expected reduction in water consumption.

Open irrigation systems greatly reduce the greenhouse *WUE* and should be avoided in semi-arid climates. Many greenhouse producers use “closed” irrigation systems that do not recycle 100% of the unused irrigation system, but attempt to recycle 60-80% of the drainage water. Although this recycling method will use less water than the fully open irrigation system, true 100% closed irrigation systems should be studied and developed to maximize water conservation.

Another beneficial study would be to cultivate a full tomato crop using high-pressure-fog cooling to determine the full crop water use efficiency. Also, because evaporative cooling often continued through midnight, studies on water use and greenhouse conditions at night would be a valuable addition to our current understanding of greenhouse water use and nighttime control of evaporative cooling system. Plant responses to evaporative cooling methods should also be further examined. Plant transpiration and leaf temperatures for tomato and other crops should be further examined and compared for the pad-and-fan and high-pressure-fog systems.

Predicting evaporative cooling water needs and uses could be improved by using a dynamic energy balance model for the high-pressure-fog system, rather than assuming

steady-state conditions. These models could also be improved by incorporating transpiration models and developing quantitative relationships between plant water use and evaporative cooling water use.

Finally, completely new greenhouse and evaporative cooling designs should be explored, with the objective of conserving water while providing the greenhouse crop with desirable climate conditions. These designs may include closed greenhouse systems, heat exchangers that condense water, or systems integrated with urban HVAC or other industrial systems.

8. CONCLUSIONS

The factors that affect water use efficiency (*WUE*), both in the area of water use and yields, include agronomic management (varieties and cropping strategies), engineering designs that enhance cropping systems, irrigation management such as scheduling, and institutional oversight and incentives that encourage the efficient use of water (Fairweather *et al.*, 2004). This project has demonstrated that greenhouse crop production can achieve *WUE* values that are as good as or better than many of the practices used to grow field tomatoes. Although *WUE* values for the entire greenhouse system were not as high as drip-irrigated field production, the ability to grow high yield, high quality produce all year round in a semi-arid climate is quite important.

With the seemingly inevitable shifts in climate change, air temperature, carbon dioxide, and sea levels, the world's populations may need to migrate to new, possibly infertile lands. Greenhouse crop production could provide the technological means to grow food crops in such an era of overpopulation, minimal resources, and harsh environmental conditions. However, to achieve this objective, greenhouse design will need to be studied in different climates and with different crops – including cereal grains, vegetables, and fruits – and the overall greenhouse design will need to be improved to reduce resource utilization and attain true sustainability.

By eliminating the engineer's propensity to over-design systems, much water (and energy) could be saved by abandoning the 1 air exchange per minute rule-of-thumb and designing ventilation and evaporative cooling systems that are specific to the greenhouse crop, size, and location. Based on the results of this study, this approach to design can

improve greenhouse water use efficiency, while possibly improving climate conditions and plant responses. Implementing a closed irrigation system will further increase the overall water use efficiency of the greenhouse. Numerical and scaled-down physical models can be valuable tools for designing the greenhouse and its systems to provide better growing conditions and reduce the use of limited resources, such as water.

Finally, to attain a fully-sustainable greenhouse crop production system, all “outputs” must be converted into “inputs” somewhere within the greenhouse system. Therefore, if the irrigation system is not designed for 100% recirculation, the drainage water should be utilized for another purpose *within the greenhouse*, such as a water vapor condenser. Water vapor could then be captured from the exhaust air to recover irrigation “losses” (plant water uptake) or evaporative cooling losses (evaporation or bleed-off). Bleed-off water from the cooling pads could also be diverted into the irrigation system and used to control salinity and EC levels. Pruned plant materials could be used for mulching, insulation, or as compost for an adjacent mushroom production facility.

By pursuing these ideas and many others, greenhouse designers, researchers, and growers will become model stewards of the earth, in addition to supplying consumers with good-tasting, high-quality produce all year round. Furthermore, by tackling these design challenges now, we will be better equipped to feed the world of tomorrow’s changed climate conditions, space travel expeditions, and urban vertical communities.

REFERENCES

- Al-Helal, I., T.H. Short. 1999. A CFD study of naturally and fan ventilated greenhouses in extreme arid climates. *ASAE Paper No. 99-5011*.
- Al-Helal, I. 2007. Effects of ventilation rate on the environment of a fan-pad evaporatively cooled, shaded greenhouse in extreme arid conditions. *Appl.Engng. in Agric.* 23(2):221-230.
- Al-Jamal, K. 1994. Greenhouse cooling in hot countries. *Energy*. 19(11): 1187-1192.
- Al Massoum, A., I. Haffar, M.H. Ahmed. 1998. A similitude model for testing greenhouse evaporative cooling pads under the hot-arid conditions of the U.A.E. *Acta Hort.* 456:329-337.
- Arbel, A. O. Yekutieli, M. Barak. 1999. Performance of a fog system for cooling greenhouses. *J.Agric.Engng.Res.* 72:129-136.
- Arbel, A., M. Barak, A. Shklyar. 2003. Combination of forced ventilation and fogging systems for cooling greenhouses. *Biosys Engng.* 84(1):45-55.
- ASABE. 2006. EP406.4: Standards for heating, ventilating, and cooling greenhouses. *American Society for Agricultural and Biological Engineers*. St. Joseph, MI, ASABE.
- ASHRAE Fundamentals. 2001. Ch 6: Psychrometrics. In *American Society for Heating, Refrigeration, and Air Conditioning Engineers*. SI ed. Atlanta, GA: ASHRAE, Inc.
- Baille, M., A. Baille, D. Delmon. 1994. Microclimate and transpiration of greenhouse rose crops. *Agric. Forest Meteorol.* 71:83-97.
- Bakker, J.C. 1991. Leaf conductance of four glasshouse vegetable crops as affected by air humidity. *Agric. Forest Meteorol.* 55:23-36.
- Ben-Asher, J., C.J. Phene, A. Kinarti. 1992. Canopy temperature to assess daily evapotranspiration and management of high frequency drip irrigation systems. *Agric Water Mgmt.* 22:379-390.
- Ben-Gal, A. U. Shani. 2003. Water use and yield of tomatoes under limited water and excess boron. *Plant soil.* 256: 179-186.
- Boulard, T., S. Wang. 2000. Greenhouse crop transpiration simulation from external climate conditions. *Agric. Forest Meteorol.* 100:25-34.

- Boulard, T., M. Mermier, J. Fargues, N. Smits, M. Rougier, J.C. Roy. 2002. Tomato leaf boundary layer climate: implications for microbiological whitefly control in greenhouses. *Agric. Forest Meteorol.* 110:159-176.
- Cook, R., L. Calvin. 2005. Greenhouse tomatoes change the dynamics of the north American fresh tomato industry. *USDA Economic Research Report No. 2.*
- Critten, D.L., B.J. Bailey. 2002. A review of greenhouse engineering developments during the 1990s. *Agric. Forest Meteorol.* 112:1-22.
- Fairweather, H., N. Austin, M. Hope. 2004. Irrigation insights 5 – water use efficiency: an information package. *New South Wales Agriculture Report.*
- Ghosal, M.K., G.N. Tiwari, N.S.L. Srivastava. 2003. Modeling and experimental validation of a greenhouse with evaporative cooling by moving water film over external shade cloth. *Energy and Bldgs.* 35:843-850.
- Giacomelli, G.A., M.S. Giniger, A.E. Krass. 1985. Utilization of the energy blanket for evaporative cooling of the greenhouse. *ASAE Paper No. 85-4047.* 10 pp.
- Handarto, M. Hayashi, T. Kozai. 2005. Air and leaf temperatures and relative humidity in a naturally ventilated single-span greenhouse with a fogging system for cooling and its evaporative cooling efficiency. *Environ. Cont. Biol.* 43(1): 3-11.
- Hanson, B., D. May. 2004. Effect of subsurface drip irrigation on processing tomato yield, water table depth, soil salinity, and profitability. *Agric. Water Mgmt.* 68: 1-17
- Hanson, B.R., D.M. May. 2005. Crop evapotranspiration of processing tomato in the San Joaquin Valley of California, USA. *Irrig Sci.* 24(4): 211-221.
- Hanson, B.R., R.B. Hutmacher, D.M. May. 2006. Drip irrigation of tomato and cotton under shallow saline ground water conditions. *Irrig Drain Systems.* 20: 155-175.
- Hatfield, J.L., R.J. Reginato, S.B. Idso. 1984. Evaluation of canopy temperature-evapotranspiration models over various crops. *Agric. Forest Meteorol.* 32:41-53.
- Hopkins, W.G, N.P.A. Huner. 2003. Introduction to Plant Physiology. 3rd Ed. John Wiley & Sons Inc.
- Idso, S.B., P.J. Pinter Jr., R.J. Reginato. 1990. Non-water stressed baselines: the importance of site selection for air temperature and air vapour pressure deficit measurements. *Agric. Forest Meteorol.* 53:73-80.

- Incrocci, L., F. Malorgio, A.D. Bartola, A. Pardossi. 2006. The influence of drip irrigation or subirrigation on tomato grown in closed-loop substrate culture with saline water. *Scientia horticulturae*. 107:365-372.
- Inoue, Y., B.A. Kimball, R.D. Jackson, P.J. Pinter Jr., R.J. Reginato. 1990. Remote estimation of leaf transpiration rate and stomatal resistance based on infrared thermometry. *Agric. Forest Meteorol.* 51:21-33.
- Jacobs, K., M.A. Worden. 2004. Arizona's Water Future: *Challenges and Opportunities*. 85th Arizona Town Hall (13-20).
- Jarvis, P.G. 1985. Coupling of transpiration to the atmosphere in horticultural crops: the omega factor. *Acta Hort.* 171:187-205.
- Jensen, M.H. 1996. New strategies and alternatives for greening the desert. *Proc. Restoration and Rehabilitation of the Desert Environment*. 149-155. N. Al-Awadhi, M.T. Balba, and C. Kamizawa, eds., The Netherlands: Elsevier Science.
- Jolliet, O., B.J. Bailey. 1992. The effect of climate on tomato transpiration in greenhouses: measurements and models comparison. *Agric. Forest Meteorol.* 58:43-62.
- Jongebreur, A.A. 2000. Strategic themes in agricultural and bio-resource engineering in the 21st Century. *J. agric. Engng Res.* 76: 227-236.
- Kacira M., Sase S., Okushima L. 2004. Optimization of vent configuration by evaluating greenhouse and plant canopy ventilation rates under wind-induced ventilation. *Trans. ASAE* (47): 2059-2067.
- Kacira, M., P.P. Ling, T.H. Short. 2002. Establishing crop water stress index (CWSI) threshold values for early, non-contact detection of plant water status. *Trans. ASAE*. 45(3):775-780.
- Katsoulas, N., A. Baille, C. Kittas. 2001. Effect of misting on transpiration and conductances of a greenhouse rose canopy. *Agric. Forest Meteorol.* 106:233-247.
- Kirda, C. M. Cetin, Y. Dasgan, S. Topcu, H. Kaman, B. Ekici, M.R. Derici, A.I. Ozguven. 2004. Yield response of greenhouse grown tomato to partial root drying and conventional deficit irrigation. *Agric. Water Mgmt.* 69:191-201.
- Kittas, C., N. Katsoulas, A. Baille. 2001. Influence of greenhouse ventilation regime on the microclimate and energy partitioning of a rose canopy during summer conditions. *J. Agric. Engng. Res.* 79(3): 349-360.

- Kittas, C., T. Bartzanas, A. Jaffrin. 2001. Greenhouse evaporative cooling: measurement and data analysis. *Trans. ASAE*. 44(3):683-689.
- Kittas, C., T. Bartzanas, A. Jaffrin. 2003. Temperature gradients in a partially shaded large greenhouse equipped with evaporative cooling pads. *Biosys. Eng.* 85(1):87-94.
- Kroggel, M., K. Dietrich, C. Kubota. Unpublished data on plant water use and tomato yields for studies on the effect of irrigation electro-conductivity on tomato lycopene content.
- Landsberg, J.J., B. White, M.R. Thorpe. 1979. Computer analysis of the efficacy of evaporative cooling for glasshouses in high energy environments. *J.Agric. Engng. Res.* 24:29-39.
- Lee, I., S. Sase, L. Okushima, A. Ikeguchi, K. Choi, and J. Yun. 2003. A wind tunnel study of natural ventilation for multi-span greenhouse scale models using two-dimensional particle image velocimetry (PIV). *Trans. ASAE*. 46(3): 763-772.
- Liao, C.M., K.H. Chiu. 2002. Wind tunnel modeling the system performance of alternative evaporative cooling pads in Taiwan region. *Bldg. Environ.* 37:177-187.
- Mahajan, G. K.G. Singh. 2006. Response of greenhouse tomato to irrigation and fertigation. *Agric. Water Mgmt.* 84:202-206.
- Mpsusia, P.T.O. 2006. Comparison of water consumption between greenhouse and outdoor cultivation. *M.S.Thesis*. Internatl Inst. Geo-Info Sci and Earth Observation. Enschede, Netherlands. 86 pp.
- Nagler, P.L., E.P. Glenn, T.L. Thompson. 2003. Comparison of transpiration rates among saltcedar, cottonwood and willow trees by sap flow and canopy temperature methods. *Agric. Forest Meteorol.* 116: 73-89.
- Ozturk, H.H. 2003. Evaporative cooling efficiency of a fogging system for greenhouses. *Turk.J.Agric.For.* 27:49-57.
- Papadakis, G. A. Frangoudakis, S. Kyritsis. 1994. Experimental investigation and modeling of heat and mass transfer between a tomato crop and the greenhouse environment. *J.Agric.Engng.Res.* 57:217-227.
- Pardossi, A., F. Tognoni, L. Incrocci. 2004. Mediterranean greenhouse technology. *Chron. Hort.* 44(2):28-34.

- Peñuelas, J., R. Save, O. Marfa, L. Serrano. 1992. Remotely measured canopy temperature of greenhouse strawberries as indicator of water status and yield under mild and very mild water stress conditions. *Agric. Forest Meteorol.* 58:63-77.
- Prenger, J.J., R.P. Fynn, R.C. Hansen. 2002. A comparison of four evapotranspiration models in a greenhouse environment. *Trans. ASAE.* 45(6):1779-1788.
- Ragab, R., C. Prodhomme. 2002. Climate change and water resources management in arid and semi-arid regions: prospective and challenges for the 21st Century. *Biosystems Engineering.* 81(1):3-34.
- Reina-Sánchez, A., R. Romero-Aranda, J. Cuartero. 2005. Plant water uptake and water use efficiency of greenhouse tomato cultivars irrigated with saline water. *Agric. Water Mgmt.* 78:54-66.
- Sabeh, N.C., G.A. Giacomelli, C. Kubota. 2006. Water use for pad and fan evaporative cooling of a greenhouse in a semi-arid climate. *Acta Hort.* 719:409-416.
- Saha, S.K., AJAI, A.K.S. Gopalan, D.S. Kamat. 1986. Relations between remotely sensed canopy temperature, crop water stress, air vapour pressure deficit and evapotranspiration in chickpea. *Agric. Forest Meteorol.* 38:17-26.
- Sase, S., M. Ishii, H. Moriyama, C. Kubota, K. Kurata, M. Hayashi, N.C. Sabeh, P. Romero, G.A. Giacomelli. 2006. Effect of natural ventilation rate on relative humidity and water use for fog cooling in a semiarid greenhouse. *Acta Hort.* 719: 385-392.
- Sase S., Reiss E., Both A.J. Roberts W.J. 2002. A natural ventilation model for open-roof greenhouse. *CCEA Newsletter.* 11(3).
- Seginer, I. 2002. The role of transpirational cooling in the design of greenhouse ventilation. *Acta Hort.* 578:55-61.
- Taconet, O., A. Olioso, M.B. Mehrez, N. Brisson. 1995. Seasonal estimation of evaporation and stomatal conductance over a soybean field using surface IR temperatures. *Agric. Forest Meteorol.* 73:321-337.
- Takakura, T., K. Takayama, H. Nishina, K. Tamura, S. Muta. 2005. Evapotranspiration estimate by heat balance equation. *ASAE Paper No. 054151.* 9 pp.
- Tubaileh, A.S., T.W. Sammis, D.G. Lugg. 1986. Utilization of thermal infrared thermometry for detection of water stress in spring barley. *Agric. Water Mgmt.* 12:75-85.

Urban, L., I. Langelez. 1992. Effect of high-pressure mist on leaf water potential, leaf diffusive conductance, CO₂ fixation and production of cultivar 'Sonia' rose plants grown on rockwool. *Scient. Hort.* 50:229-244.

USDA. National Agricultural Statistics Services. 1997. Census of Agriculture. <http://www.nass.usda.gov/census/>.

USDA. National Agricultural Statistics Services. 2002. Census of Agriculture. <http://www.nass.usda.gov/census/>.

USGS. United States Geological Survey. 2004. Estimated use of water in the United States in 2000. <http://water.usgs.gov/watuse/>.

Willits, D.H. 2001. The effect of cloth characteristics on the cooling performance of external shade cloths for greenhouses. *J.Agric.Engng.Res.* 79(3):331-340.

Willits, D.H. 2003a. Cooling fan-ventilated greenhouses: a modeling study. *Biosys. Engrng.* 84(3):315-329.

Willits, D.H. 2003b. The Penman-Monteith equation as a predictor of transpiration in a greenhouse tomato crop. *ASAE Paper No. 034095*. 14 pp.

Willits, D.H., S. Li. 2005. A comparison of naturally ventilated vs. fan ventilated greenhouses in the southeastern U.S. *ASAE Paper No. 054155*. 12 pp.